Calibration study of bivalve shells – implications for paleoenvironmental reconstruction

Dissertation

zur Erlangung des Grades

“Doktor der Naturwissenschaften“

im Promotionsfach Geologie/Paläontologie

am Fachbereich Chemie, Pharmazie und Geowissenschaften

der Johannes Gutenberg-Universität Mainz

von

Lina Yan

geb. in Heilongjiang, China

Mainz, 2013

Berichterstatter:

Berichterstatter:

Datum der mündlichen Prüfung: 16th December 2013

DECLARATION

I hereby declare on my honor that the thesis submitted is my own work

except for quotations which have been listed in the References.

Ich erkläre hiermit, dass ich die vorliegende Arbeit

selbständig verfasst und keine anderen als

die angegebenen Quellen und Hilfsmittel benutzt habe.

Signature: 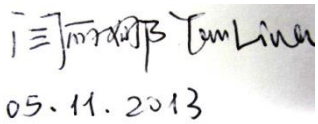

Date: 05.11.2013

Place: Mainz

PREFACE

With curiosity for the world and desire for knowledge, I landed in Frankfurt airport and started my Ph.D. study in Palaeotological group under the supervision of Prof. Dr. ***, in the University of Mainz at 01st September 2010. During the three years, I have been kept working on bivalve mollusk shells, which contain a wealth of environmental, climatic, and life history information, preserved as physical and chemical variations within the shells.

Bivalve mollusk sequentially secrets its shell with periodicity, such as the annual, fortnightly and daily increments, recording the growth histories, metabolism and environmental conditions experienced during the deposition of that shell material. Furthermore, bivalve shells can preserve life history and environmental information during their growth as variations in geochemistry, such as oxygen and stable carbon isotopes ($\delta^{18}O_{shell}$ and $\delta^{13}C_{shell}$). Distinct shell growth structures, i.e. growth increments and growth lines, can enable precise calendar dating of each successive band of shell periodic accretion and estimation of ontogenetic age. Micro-sampling technique of shell cross sections provides a means of high-resolution $\delta^{18}O_{shell}$ and $\delta^{13}C_{shell}$ proxies for bivalve archives, which is essential to better understand processes and mechanisms of environmental changes in seasonal or sub-seasonal time scale.

This Ph.D. dissertation has four main components, with one publication and one submission in high-impact, peer-reviewed journals, one prepared draft and one chapter with the preliminary results. The first paper, which has been published in Palaeogeography, Palaeoclimatology, Palaeoecology, investigates if $\delta^{18}O_{shell}$ of the long-lived marine bivalve *Eurhomalea exalbida* can serve as a faithful proxy of temperature in southern South America. The second paper, a well-prepared draft, focuses on variations in inter-annual (ontogenetic) and intra-annual (seasonal) $\delta^{13}C_{shell}$ to examine if $\delta^{13}C_{shell}$ in *E. exalbida* is a servable indicator of ambient environments on the basis of sclerochronology and environmental comparisons. The third paper, submitted to the Journal of oceanography, presents the detailed analysis of the life history traits, $\delta^{18}O_{shell}$ and $\delta^{13}C_{shell}$ records of the short-lived marine bivalve *Paphia undulata*. The objective is to evaluate if shells of this species can provide reliable, sub-seasonally resolved data on past East Asian summer monsoon strengths, and to exploit the possibility into predictions of future monsoon-related climate extremes in SE Asia. Additionally, preliminary investigations on the freshwater pearlshells *Margaritifera falcata* are presented in the last part, which is meant to provide environmental implications on population age structures and shell growth rates of the freshwater mussel.

This research includes the efforts of some other co-authors, especially Prof. Dr. ***. I would like to express my gratitude to his constructive comments and plenty of time spent on corrections to improve my writing. “Be always critical of your own data” is his famous words, which benefits me a lot in science. Furthermore, I would like to acknowledge the Chinese Scholarship Council (CSC) and the Earth System Research Centre-Geocycles (Johannes Gutenberg-University of Mainz), which makes this research project possible. I would also like to thank the providers of my study material and all the people who contributed to this study here.

Signature: 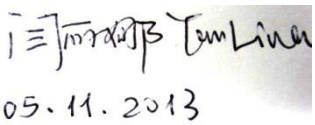

Date: 05.11.2013

Place: Mainz

ABSTRACT

The accretionary shells of bivalve mollusks can provide environmental information, such as water temperature, precipitation, freshwater fluxes, primary productivity and anthropogenic activities in the form of variable growth rates and variable geochemical properties, such as stable oxygen and carbon isotopes. However, paleoenvironmental reconstructions are constrained by uncertainties about isotopic equilibrium fractionation during shell formation, which is generally acknowledged as a reasonable assumption for bivalves, but it has been disputed in several species. Furthermore, the variation in shell growth rates is accepted to rely on multiple environmental variables, such as temperature, food availability and salinity, but can differ from species to species. Therefore, it is necessary to perform species-specific calibration studies for both isotope proxies and shell growth rates before they can be used with confidence for environmental interpretations of the past. **Accordingly, the principal objective of this Ph.D research is to examine the reliability of selected bivalve species, the long-lived *Eurhomalea exalbida* (Dillwyn), the short-lived and fast growing species *Paphia undulata* (Born 1778), and the freshwater mussel *Margaritifera falcata* (Gould 1850), as paleoenvironmental proxy archives.**

The first part (Chapter 2) is focused on $\delta^{18}O_{shell}$ and shell growth history of live-collected *E. exalbida* from the Falkland Islands (Southwest Atlantic). Results indicate that *E. exalbida* likely captures the full seasonal temperature amplitude in its shell. Annual growth line formation occurs between fall and early winter. The most remarkable finding, however, is that *E. exalbida* formed its shell with an offset of -0.48‰ to -1.91‰ from the expected oxygen isotopic equilibrium with the ambient water. If this remained unnoticed, paleotemperature estimates would overestimate actual water temperatures by 2.1-8.3°C. With increasing ontogenetic age, the discrepancy between measured and reconstructed temperatures increased exponentially, irrespective of the seasonally varying shell growth rates. This study clearly demonstrates that, when the disequilibrium fractionation effect is taken into account, *E. exalbida* can serve as a high-resolution paleoclimate archive for the southern South America. The species therefore provides quantifiable temperature estimates, which yields new insights into long-term paleoclimate dynamics for mid to high latitudes on the southern hemisphere.

The stable carbon isotope of biogenic carbonates is generally considered to be useful for reconstruction of seawater dissolved inorganic carbon. The $\delta^{13}C_{shell}$ composition of *E. exalbida* was therefore, investigated in the second part (Chapter 3) of this study. This chapter focuses on inter-annual (ontogenetic) and intra-annual (seasonal) variations in $\delta^{13}C_{shell}$. A decreasing trend in $\delta^{13}C_{shell}$ is observed through ontogeny, as well as evident seasonal cycles in all studied specimens. This decreasing trend and the seasonal cycles in $\delta^{13}C_{shell}$ both appear to be linked to the variations

in shell growth rates, which can be attributed to the inverse correlation between the mantle metabolic activity and shell growth rates. Furthermore, environmental records in $\delta^{13}C_{shell}$ are found to be strongly obscured by changes in shell growth rates, even if removing the ontogenetic decreasing trend. This suggests that $\delta^{13}C_{shell}$ in *E. exalbida* may not be useful as an environmental proxy, but a potential tool for ecological investigations.

In addition to long-lived bivalve species, short-lived species that secrete their shells extremely fast, can also be useful for environmental reconstructions, especially as a high-resolution recorder. Therefore, *P. undulata* from Daya Bay, South China Sea (SCS) was utilized in Chapter 4 to evaluate and establish a potential proxy archive for past variations of the East Asian monsoon (EAM) on shorter time-scales. Results indicate that this species lived for only three years and secreted their shells uninterruptedly between March and mid November near oxygen isotopic equilibrium with the ambient environment. The $\delta^{18}O_{shell}$ can provide qualitative estimates of the amount of monsoonal rain and terrestrial runoff and the $\delta^{13}C_{shell}$ likely reflect the relative amount of isotopically light terrestrial carbon that reaches the ocean during the summer monsoon season. Therefore, shells of *P. undulata* can provide serviceable proxy archives to reconstruct the frequency of exceptional summer monsoons in the past. The relative strength of monsoon-related precipitation and associated changes in ocean salinity and the $\delta^{13}C$ ratios of the dissolved inorganic carbon signature ($\delta^{13}C_{DIC}$) can be estimated from the $\delta^{18}O_{shell}$ and $\delta^{13}C_{shell}$ values as well as shell growth patterns.

In the final part (Chapter 5) of this thesis, the freshwater pearl shell *M. falcata* from four rivers in British Columbia, Canada was preliminarily studied concerning the lifespans and the shell growth rates. Two groups separated by the Georgia Strait can be clearly distinguished. Specimens from the western group (Piercy Creek River and Chase River) exhibit a shorter lifespan, while the eastern group (Salmon River and Little Campbell River) live longer. Moreover, the average lifespan seems to decrease from south to north. The computed growth equations (shell height versus ontogenetic age) from the eastern and western groups differ as well. The western group exhibits a lower growth rate (with a slope of 7.7~7.8), while bivalves from the eastern group grow faster (with a slope of 9.1). The land use history seems to be responsible for the differences in lifespans of the specimens from the two groups. Differences in growth rate may be induced by differences in water temperature or nutrient input also related to the land use activities. However, these speculations have not been proven yet since lacking of the local water data. Future work should conduct field measurements of river hydrology and water chemistry to test these hypotheses.

Overall, this thesis clearly demonstrates the species-specific complexities of environmental proxy archives, both in marine species (*E. exalbida* and *P. undulata*) and in freshwater species (*M. falcata*). The potentially useful proxies, namely $\delta^{18}O_{shell}$ and $\delta^{13}C_{shell}$ were evaluated individually for each marine species, as well as shell growth rates for both the marine and freshwater species. Results reveal that it is not always possible to extract information on environmental conditions from these proxies, especially from $\delta^{13}C_{shell}$. Therefore, it should be emphasized that the calibration study must not be ignored before any archive can be applied in palaeoclimatic and palaeoenvironmental research.

ZUSAMMENFASSUNG

Akkretionär gebildete Muschelschalen können Informationen über die Umwelt, wie z.B. Temperatur, Niederschlag, Süßwassereintrag, Primärproduktivität, sowie anthropogene Einflüsse speichern. Dies geschieht in Form geochemischer Eigenschaften wie der Sauerstoff- und Kohlenstoffisotopie und variablen Wachstumsmustern. Die mögliche Fraktionierung von Isotopen während der Schalenbildung ist jedoch ein erheblicher Unsicherheitsfaktor bei der Rekonstruktion vergangener Umweltbedingungen. Das Auftreten von Fraktionierung ist bei Muscheln anerkannt, jedoch ist sie für viele Arten umstritten. Des Weiteren hängt die Variation der Schalenwachstumsraten von verschiedenen Umweltbedingungen wie Temperatur, Nahrungsverfügbarkeit und Salinität ab. Diese sind jedoch artspezifisch. Daher ist es notwendig, artspezifische Kalibrationsstudien für stabile Isotope sowie das Schalenwachstum durchzuführen, um zuverlässige Aussagen über vergangene Umweltbedingungen treffen zu können. Das wesentliche Ziel dieser Doktorarbeit ist daher die Zuverlässigkeit verschiedener Muschelarten mit ihren Proxies als Umweltarchive zu prüfen. Untersucht wurden die langlebigen Muscheln *Eurhomalea exalbida* (Dillwyn), die kurzlebige und schnell wachsende Muschel *Paphia undulata* (Born 1778) und die Süßwassermuschel *Margaritifera falcata* (Gould 1850).

Der erste Teil dieser Arbeit (Kapitel 2) beschäftigt sich mit der Sauerstoffisotopie ($\delta^{18}O_{schale}$) und dem Schalenwachstum von lebend gesammelten *E. exalbida* von den Falkland Inseln (Südwest Atlantik). Die Ergebnisse zeigen, dass *E. exalbida* voraussichtlich alle jahreszeitlichen Temperaturamplituden erfasst. Die Bildung der jährlichen Wachstumslinien ereignet sich zwischen Herbst und dem frühen Winter. Der auffallendste Befund ist jedoch, dass *E. exalbida* die Schale mit einem Offset von -0.48‰ bis -1.91‰ gegenüber der Sauerstoffisotopie des umgebenden Wassers bildet. Ohne Kenntnis dieses Offsets würden vergangene Temperaturen um 2.1-8.3°C überschätzt.

Mit steigendem ontogenetischen Alter steigt die Differenz zwischen gemessenen und rekonstruierten Temperaturen exponentiell, ungeachtet der jahreszeitlichen Variationen des Schalenwachstums. Diese Studie zeigt, dass unter Beachtung des Fraktionierungeffektes die Muschel *E. exalbida* als hochaufgelöstes Klimaarchiv für die mittleren und hohen Breiten der Südhemisphere dienen kann. Daher liefert diese Art quantifizierbare Temperaturabschätzungen, die Einblicke in die langzeitliche Paläoklimadynamik im südlichen Südamerika bieten.

Die stabile Kohlenstoffisotopie biogener Karbonate gilt allgemein als geeignet für die Rekonstruktion des im Meerwasser enthaltenen, gelösten inorganischen Kohlenstoffs. Die stabile Kohlenstoffisotopie ($\delta^{13}C_{schale}$) von *E. exalbida* wurde daher im zweiten Teil dieser Arbeit

(Kapitel 3) untersucht. Dieses Kapitel beschäftigt sich mit interannuellen (ontogenetisch) und intraannuellen (saisonal) Variationen im $\delta^{13}C$ der Schale. Sowohl ein Trend zu fallenden $\delta^{13}C_{schale}$ -Werten, als auch offensichtliche saisonale Zyklen wurden in allen untersuchten Individuen beobachtet. Dieser Trend zusammen mit den saisonalen Zyklen im $\delta^{13}C_{schale}$ scheinen in direktem Zusammenhang mit den Wachstumsraten der Schale zu stehen, die auf einer inversen Korrelation zwischen der metabolischen Mantelaktivität und der Schalenwachstumsraten beruhen. Umweltsignale im $\delta^{13}C$ der Schale sind durch Änderungen der Wachstumsraten der Schale überdeckt, auch bei Entfernen des ontogenetischen Trends. Dies deutet an, dass das $\delta^{13}C_{schale}$ der *E. exalbida* nicht sinnvoll als Umweltproxy, jedoch als potentielles Mittel für ökologische Untersuchungen genutzt werden kann.

Zusätzlich zu langlebigen Muschelarten, können auch kurzlebige Arten, die ihre Schale schnell absondern, für hochaufgelöste Umweltrekonstruktionen genutzt werden. Daher wurde *P. undulata* aus der Daya Bucht des Südchinesischen Meeres in Kapitel 4 genutzt, um vergangene Variationen des Ostasiatischen Monsuns auf kurzzeitigen Skalen zu bewerten und nachzuweisen. Die Ergebnisse zeigen, dass diese Art drei Jahre lebt und Schalenmaterial kontinuierlich zwischen März und November nahe des sauerstoffisotopischen Gleichgewichtes mit dem umgebendem Meerwasser bildet. Das $\delta^{18}O$ der Schale liefert eine qualitative Abschätzung der Menge des Monsunregens und des terrestrischen Abflusses und das $\delta^{13}C$ der Schale spiegelt die relative Menge des isotopisch leichten Kohlenstoffs wider, welches den Ozean während der Sommermonsun-Saison erreicht. Daher liefern Schalen der *P. undulata* nützliche Proxyarchive, um die Häufigkeit von außergewöhnlichen Sommermonsun-Zeiten in der Vergangenheit zu rekonstruieren. Die relative Stärke des mit dem Monsun verbundenen Niederschlags und die resultierenden Veränderungen des ozeanischen Salzgehaltes sowie der $\delta^{13}C$-Signatur kann somit durch Messungen des $\delta^{18}O_{schale}$ und $\delta^{13}C_{schale}$ und durch das Schalenwachstum ermittelt werden.

Der letzte Teil (Kapitel 5) dieser Arbeit befasst sich mit dem Schalenwachstum und der Lebensdauer der Süßwassermuschel *M. falcata* aus vier Flüssen in Britisch Kolumbien in Kanada. Zwei Gruppen, welche durch die Georgia Straße getrennt sind, können klar unterschieden werden. Die Arten der westlichen Gruppe (Piercy Creek River und Chase River) zeigen eine kurze Lebensdauer, während die Arten der östlichen Gruppe (Salmon River und Little Campbell River) länger leben. Zusätzlich scheint die mittlere Lebenserwartung von Süden nach Norden zu sinken. Die berechneten Wachstumsformeln (Körpergröße vs. Alter) zwischen der östlichen und westlichen Gruppe unterscheiden sich ebenfalls. Die Westgruppe zeigt eine geringere Wachstumsrate, während Muscheln der östlichen Gruppe schneller wachsen. Unterschiedliche Wachstumsraten werden durch unterschiedliche Wassertemperaturen oder Nahrungsverfügbarkeit

hervorgerufen. Das Schalenwachstum wird auch durch die Eutrophierung in den stärker urbanisierten Bereichen des Festlandes (östliche Gruppe) begünstigt. Jedoch sind diese Mutmaßungen aufgrund von mangelnden lokalen Wasserdaten noch nicht überprüft. Dies sollte zukünftig bearbeitet werden.

Insgesamt zeigt diese Studie eindeutig die artspezische Komplexität unterschiedlicher umweltbedingter Proxyarchive in marinen Muschelarten (*E. exalbida* und *P. undulata*), sowie in Süßwassermuscheln (*M. falcata*). Nützliche Proxies wie die stabile Sauerstoff- und Kohlenstoffisotopie wurden individuell für beide marine Muschelarten, sowie das Schalenwachstum für Meer- und Süßwassermuscheln bewertet. Die Ergebnisse zeigen, dass die Rekonstruktion von Paläo-Umweltbedingungen mit Hilfe oben genannter Proxies, vor allem der Kohlenstoffisotopie, nicht immer möglich ist. Es sollte betont werden, dass vor zukünftiger Anwendung biogener Archive in der palöoklimatologischen und ökologischen Forschung diese Kalibrierungsstudie daher nicht missachtet werden sollte.

ACKNOWLEDGEMENTS

Firstly, I would like to thank my thesis supervisor Prof. Dr. *** for offering me the opportunity to pursue this Ph.D. Deep gratitude to his constructive comments and plenty of time spent on corrections to improve my writing, and also his support and encouragement. I would further like to thank my thesis co-advisor Prof. Dr. *** for his helpful comments.

I would like to acknowledge the Chinese Scholarship Council (CSC) for providing financial support (2010-2012), which makes this study possible. And also, I would like to thank the Earth System Research Centre-Geocycles (Johannes Gutenberg-University of Mainz), who funded this work for the extension year (2012-2013).

This work would not have been possible without the bivalve shell samples and environmental data. I would like to acknowledge Prof. Dr. *** (China University of Geosciences, China) and Prof. Dr. *** (South China Sea Institute of Oceanology Chinese Academy of Sciences, China) for providing me living and fossil *Paphia undulata* material, Mr. *** (Fisheries Department, Falkland Islands) for collecting *Eurhomalea exalbida* shells, and Mr. *** (Raincoast Applied Ecology, British Columbia, Canada) for providing all *Margaritifera falcata* specimens for this work.

To all the excellent colleagues from the INCREMENTS Research Group at University of Mainz I would like to express my gratefulness. I would like to thank *** for her patience on my German study, helpful discussions on my thesis, all her encouragement and support, and to be a close friend. I am grateful to *** for his discussions on my thesis, *** for conducting the XRD analyses, and *** for his encouragement with his humorous body language. I thank my roommate, Dr. *** for her helpful discussions and suggestions on my work. I would like to thank our technical assistant *** for processing the isotope samples and general technical assistance. Ms. ***, our secretary from the paleontological department is kindly acknowledged for many things she has helped me with during my Ph.D. period. Thanks also go to the people in our group who I got to know in Mainz.

I would further like to thank my previous colleagues in this group, *** for picking me up from the airport at 01st Sep 2010, which making my first day easier, and for his kind help and warm-hearted words; Dr. ***, for helping me about my Ph.D. registration at the university and the instructions in the laboratory; Dr. ***, for his nice discussion and encouragement on my first presentation, and for his and his family's support, which cheered me up when I had homesick during the beginning months; *** for her instructions in the laboratory; and *** for his support and encouragement with funny and warm words. I would not have adapted German life and study

that fast without their helps. I am grateful to Dr. *** and Dr. *** for their useful comments and English improvement on my manuscripts. Thanks also go to the guest researchers of our group, Dr. *** (National University of La Plata, Argentina) and Dr. *** (University of Tokyo, Japan) for their supports.

Furthermore, I am sincerely indebted to my dear friends for proofreading the thesis, namely ***, ***, ***, ***, ***, and ***, as well as *** from University of Southampton, UK.

I am very grateful to all the awesome Chinese friends back in China and who I got to know in Germany. Although I have no enough room in this acknowledgement to name you all one by one, I have all your names in my heart. Thank you for all your encouragement and support and prayer. I would not have grown in progress and enjoyed the life that much without you guys.

Especially soft and warm appreciation is to my family. First to my husband, ***, who is the most amazing guy I've ever met, thank you for being there and waiting for me over years. Also to my parents, sister and parents in law, thank you for your support, understanding and encouragement. The life is wonderful indeed with all of you.

Signature: 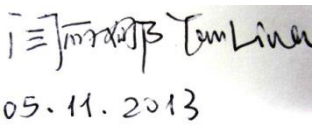

Date: 05.11.2013

Place: Mainz

TABLE OF CONTENTS

A. FRONT MATTER

B. THESIS

C. APPENDICES

LIST OF FIGURES

LIST OF TABLES

Chapter 1: INTRODUCTION

"Climate change is likely to be the predominant scientific, economic, political and moral issue of the 21st century" (Hansen and Sato, 2012). The estimation of future climate relies on the establishment of numerical climate models, which requires detailed information about climate variability in the past and further verification by placing the current climate change into context. Instrumental data of environmental parameters are spatiotemporally incomplete and extremely rare prior to the year 1860 (Smith and Reynolds, 2003). Therefore, almost the entire knowledge of paleoclimatic conditions and changes is obtained from climate proxy archives. Archives are sequentially accreted or deposited through time and thus record a time series of environmental information. Proxies are geochemical or physical signals recorded in biological or geological structures that reflect changes in the environment where the archive has been formed. Important environmental proxy archives are tree rings (e.g., Fritts, 1976; Becker et al., 1991), ice cores (e.g., Petit et al., 1990, 1999; Steig et al., 1994; Thompson et al., 1998; Vimeux et al., 2002), sclerosponges (e.g., Swart et al., 1998; Lazareth et al., 2000; Fallon et al., 2005; Rosenheim et al., 2004, 2005), foraminifers (e.g., Bemis et al., 1998; Kasemann et al., 2008; Cortina et al., 2011), speleothems (e.g., Lauritzen and Lundberg, 1999; McDermott, 2004), corals (e.g., Hudson, 1981; Beck et al., 1992; Ren et al., 2003; Lazareth et al., 2013), pollens (e.g., Alley, 1976; Hebda, 1995; Wang et al., 2011), fish otoliths (e.g., Kalish, 1991; Wurster and Patterson, 2001; Wang et al., 2013), laminated sediments (e.g., Schelske et al., 1988, 1991, 1995; Moore et al., 2001; Pérez-Cruz, 2006) and mollusk shells (e.g., Grossman and Ku, 1986; Goodwin et al., 2001; Schöne et al., 2004a, 2004b, 2011).

The shells of bivalve mollusks have been considered to be reliable archives providing high-resolution and chronologically aligned records of past environmental properties (e.g., Jones et al., 1989; Goodwin et al., 2001; Schöne et al., 2002, 2003a, 2004c; Chauvaud et al., 2005). Mollusks secrete calcium carbonate shells with successive annual, monthly, fortnightly, tidal, daily, and sub-daily layers (e.g., Lutz and Rhoads, 1980; Jones et al., 2007). The interaction between the environment and the physiology of the bivalve controls most of the features of the shell growth patterns and geochemical composition. Geochemical proxies from sequential sampling along the shell height can provide high-resolution records of the water geochemistry and can be used for interpreting spatial and temporal patterns in temperature, salinity, and hydrography.

Although most bivalve mollusks fulfill the prerequisites of environmental archives and record the environmental information during their growth (Epstein et al., 1953; Killingley and Berger, 1979; Jones et al., 1989; Goodwin et al., 2001; Schöne et al., 2003b, 2011), challenges

related to the use of bivalves as proxy archives still exist. The curse of physiology obscures the environmental signals (Schöne, 2008), e.g., species-specific geochemical compositions, such as stable carbon and oxygen isotopic equilibrium fractionation, that occurs in some but not at all species. Furthermore, the dependence of biological parameters, e.g., growth rates on various environmental variables, such as temperature, food availability and salinity.

Calibration studies using live-collected bivalves are therefore necessary because whether or not the shells of modern bivalves accurately record environmental information can be evaluated in light of measured oceanographic data. Calibrations allow to determine: (1) if the shell is precipitated in stable oxygen and carbon isotopic equilibrium; if not, is this disequilibrium fractionation accountable? (2) which variable(s) is/are the primary factor(s) controlling each proxy? and (3) if the studied species is a reliable archive for palaeoenvironmental reconstructions. Therefore, any considered proxy must be calibrated for each analysed species against instrumental information before it can be used with confidence and analogous fossil shells may then be studied in relation to their modern counterparts.

In the present study, the marine bivalves *Eurhomalea exalbida* from the South Atlantic, *Paphia undulata* from the South China Sea and the freshwater mussel *Margaritifera falcata* from the rivers in North America are investigated. It has been evaluated whether the marine shells faithfully record the environmental signals by comparing the reconstructed environmental parameters to the local instrumental data. *E. exalbida* has several prerequisites that are required for high-resolution paleoclimate proxy archive for South America, such as: longevity, broad biogeographic distribution and a high preservation potential. It is therefore significant to exploit the feasibility of *E. exalbida* as an archive for the southern hemisphere, where appropriate climate archives are scarce, particularly in marine environments. Long-lived bivalve species are generally considered beneficial as they record long-term environmental variability. In contrast, *P. undulata* is a short-lived and fast-growing species, which permits extractions of erratic monsoon signals by providing necessary temporal resolution. The results of the present study can help to improve and verify numerical models for predictions of future climates in areas dominated by the EAM. Modern microanalytical and microsampling techniques were employed in sclerochronology (the aquatic equivalent of dendrochronology) for both *E. exalbida* and *P. undulata* in this Ph.D. research in order to extract the potentially recorded environmental information from the shells. The approach used in this work provides a direct comparison of different proxies and specific environmental parameters, and thereby allows accurate paleoenvironmental reconstructions. Like many marine bivalves (e.g., Kennedy et al., 2001; Goodwin et al., 2001; Schöne et al., 2003b; Hallmann et al., 2013), the freshwater mussels also appear to be useful indicators for environmental variablity (Dunca and Mutvei, 2001; Schöne et al., 2004a, 2007; Howard and

Cuffey, 2006). The lifespans and shell growth rates of the western pearlshell *M. falcata* from different rivers with differenct land uses and river hydrology are analysed in this study. The preliminary findings could provide some environmental implications in relation to land use history, temperature, and water quality.

1.1. Sclerochronology

Sclerochronology is analogous to dendrochronology (Fritts, 1976), whereby both disciplines focus on the study of growth patterns and seek to trace organismal life history as well as to reconstruct environmental records. The term sclerochronology was introduced by Buddemeier and Maragos (1974) and Hudson et al (1976), and defined as the study of physicochemical variations in periodically growing hard parts of biogenic organisms (Oschmann, 2009). Sclerochronology is considered to be a powerful method applicable to various marine archives, such as corals (e.g., Mertz-Kraus et al., 2008; Maina et al., 2012) and mollusk shells (e.g., Radermacher et al., 2009; Wanamaker et al., 2009; Helama and Hood, 2011), which can help to decipher high-resolution marine archives for paleoclimate and paleoecology studies. Sclerochronology has been largely applied to tropical archives in order to reconstruct paleoceanic records by assessing the response of corals to environmental changes (e.g., Lough and Barnes, 1997; Cobb et al., 2003). By contrast, mollusk-based sclerochronological research has increasingly gained interest because mollusks are capable of providing complementary knowledge on paleoclimatic and paleoenvironmental variability in extratropical and coastal marine settings (e.g., Schöne et al., 2005a; Wanamaker et al., 2012), as well as on seasonal climatic fluctuations in the tropics (Nützel et al., 2010). Recently, bivalve sclerochronology is reviewed in detail (Schöne and Surge, 2012; Schöne and Gillikin, 2013). Sclerochronological techniques using bivalves have been applied with success to paleoclimatology, archeology, biology, evolution, and retrospective environmental biomonitoring based on a number of advantages of bivalves as environmental archives, such as unrivaled biogeographic distributions, extraordinary lifespans and a sensitive response to environmental changes (Butler et al., 2013; Schöne and Surge, 2012; Schöne and Gillikin, 2013; see chapter 1.3). The focus of bivalve sclerochronological research is principally on periodic growth patterns and geochemical properties of the shells.

The environmental-dependence of bivalve shell growth has been studied for many decades (Weymouth, 1922; Davenport, 1938). From the initial studies, it has been demonstrated that the accretion of shell material in bivalve mollusks is periodic (Evans et al., 1972; Richardson, 1988a, b). Shell formation, is on one hand controlled and maintained by biological clocks (Pittendrigh and Bruce, 1957; Rensing et al., 2001), for example: circadian rhythm (solar 24 h day, Clark II, 1975), tides (Evans, 1972), the seasons (Trutschler and Samtleben, 1988) and reproduction events (Jones, 1980). On the other hand, the timing and rate of shell growth is influenced by distinct environmental factors, such as temperature, food availability and salinity (Rhoads and Pannella, 1970; Chicharo and Chicharo, 2001). The growth lines of bivalve shells result from periodic growth breaks, which on an annual, monthly, fortnightly, daily and sub-daily time-scale (Pannella and McClintock, 1968; Jones, 1980; Lutz and Rhoads, 1980).

Typically, temperature is accepted to be dominant among the factors controlling shell growth rates of most species, i.e. growth rate increases with rising water temperatures (e.g., Kennish and Olsson, 1975; Koike, 1980; Goodwin et al., 2001; Schöne et al., 2002). Hallmann et al (2009) documented that intra-annual increment widths of *Saxidomus gigantea* showed clear seasonal oscillations with broadest increments in summer and very narrow increments or even no growth during the winter months. However, the slow-down of shell growth in summer was also found in some species, such as *Mesodesma donacium*, as suggested by Carré et al (2005). Jones (1980) and Mann (1982) suggested that growth line formation in *Arctica islandica* falls together with the time interval of most intense spawning. The annual temperature maximum could function as a stimulus for spawning and a concomitant reduction in shell growth (Jones, 1981; Mann, 1989). Yet, this conclusion is questionable. For example, Thorarinsdóttir (2000) observed that some *A.islandica* speciemens from Iceland spawned in all months during the year, suggesting that temperature is not the main factor controlling spawning and corresponding change in shell growth.

In addition to temperature, bivalve growth is also strongly regulated by food availability (Beukema et al., 1985; Jones et al., 1989; Nakaoka, 1992; Nakaoka and Matsui, 1994; Lewis and Cerrato, 1997; Dekker and Beukema, 1999; Carroll et al., 2009), as well as salinity (Sato, 1997; Schöne et al., 2003c; Marsden, 2004). For example, Carroll et al (2009, 2011) suggested that food availability could be the primary driver of bivalve growth of *Serripes groenlandicus* and *Clinocardium ciliatum* from the ice covered waters of the northwest Barents Sea and western Svalbard region. Both species cease growth in late fall due to limited food availability, despite warm water temperatures, and restarted to grow immediately after fresh food reaches the seafloor, although the water temperatures are still extremely low (Carroll et al., 2009, 2011). Moreover, Schöne et al (2003c) demonstrated that salinity played an important role on bivalve shell growth rates of *Chione cortezi* and *Chione fluctifraga* in the northern Gulf of California. The reduced freshwater influx to the Colorado River estuary was presented as the main factor for increased growth rates of both species. Conversely, reduced salinity (i.e. increased freshwater input with higher productivity) was the main reason for retarded growth rates, which means lowered salinity out-weighted the benefits of higher food supply for these bivalves (Schöne et al., 2003c). Nevertheless, the variation in bivalve shell growth is a controversial proxy for determining variations in ambient environments due to the varied and multiple dependences of different bivalve species.

Additionally, mollusk shells can preserve information on the life history and environment during their growth as variations in geochemistry, i.e. $\delta^{13}C_{shell}$, $\delta^{18}O_{shell}$ and trace elements, such as Mg/Ca, Sr/Ca, Ba/Ca and Pb/Ca (e.g., Pitts and Wallace, 1994; Lazareth et al., 2003; Freitas et al., 2005; Schöne et al., 2013; Goodwin et al., 2013). $\delta^{18}O_{shell}$ in bivalves is accepted to be a reliable

proxy for recording water temperature (e.g., Jones et al., 1983; Grossman and Ku, 1986; Goodwin et al., 2001; Schöne et al., 2004b; Chauvaud et al., 2005), and it also can reflect salinity variations (e.g., Davis and Calabrese, 1964; Müller-Lupp et al., 2003, 2004; Dettman et al., 2004). The $\delta^{13}C_{shell}$ in bivalves, however, has been somewhat contradictory, but it was proposed as a servable proxy for $\delta^{13}C_{DIC}$ (e.g., Mook and Vogel, 1968; Schöne et al., 2011), which is closely related to anthropogenic carbon inputs and primary productivity. In addition to isotopic proxies, trace elements were also investigated as proxies for temperature (Klein et al., 1996a; Takesue and van Geen, 2004), primary productivity (Stecher et al., 1996), and anthropogenic pollution (Bourgoin, 1990; Pitts and Wallace, 1994).

Sclerochronology can be considered to be a combined approach of growth pattern analyses and geochemistry studies. Growth patterns are used to determine growth rates and assign calendar years or even days to geochemical proxies if the date of the mollusk's death is known, allowing a direct comparison between environmental parameters and geochemical proxies in time series. Therefore, this approach is much more straightforward and interpretable than 'a distance series', i.e. 'an undated series'.

1.2. Stable isotopes

The use of stable isotope ratios in biogenetic carbonates (i.e. $\delta^{18}O$ and $\delta^{13}C$) as environmental proxies dates back to the late 1940s and 1950s (Urey, 1948; Epstein et al., 1953). Previous studies have discussed whether or not the investigated biogenetic carbonates biomineralise in isotopic equilibrium with the surrounding water, i.e. if they are formed similarly to inorganic carbonates that are precipitated in thermodynamic equilibrium with the ambient water, and record the environmental information faithfully (e.g., Graham et al., 1981; von Grafenstein et al., 1999; Wanamaker et al., 2006; Welsh et al., 2011). In the case of isotopic equilibrium precipitation, it is possible to establish a relation among carbonate $\delta^{18}O$, water temperature and water $\delta^{18}O$ (e.g., Schöne et al., 2004b; Ullmann et al., 2010; Welsh et al., 2011), and, to a certain degree, between carbonate $\delta^{13}C$ and $\delta^{13}C_{DIC}$ in the ambient water (Mook and Vogel, 1968; Fritz and Poplawski, 1974; Williams et al., 1977; Grossman, 1984). Notably, carbonate $\delta^{18}O$ is a dual proxy because it simultaneously records temperature changes and the water $\delta^{18}O$ signature (Urey, 1948). For calculating the water temperatures from the carbonate $\delta^{18}O$, the $\delta^{18}O$ value of the ambient water must be known which can be obtained from direct measurements (e.g., Hallmann et al., 2008; Yamamoto et al., 2010) or estimations based on the positive relationship between water $\delta^{18}O$ and salinity (e.g., Schöne et al., 2004b). However, it remains challenging to obtain quantifiable paleotemperature records from carbonate $\delta^{18}O$ since the water $\delta^{18}O$ data are unknown for ancient environments.

The non-equilibrium isotopic fractionation of biogenetic carbonates poses a significant problem for environmental reconstructions utilizing the isotopic proxy. Isotopic disequilibrium, i.e. in the presence of vital effects during the formation of carbonates (Urey et al., 1951; Adkins et al., 2003), can be explained by kinetic effects and metabolic effects (McConnaughey, 1989a, b). Kinetic effects are considered to result from slower reaction kinetics for molecules containing the heavy isotopes ^{18}O and ^{13}C during CO_2 hydration and hydroxylation, and thus it appears to be associated with fast $CaCO_3$ precipitation (McConnaughey, 1989b). Kinetic effects will act on both C and O isotopes due to CO_2 exchange equilibrating both isotopes with cell DIC, causing a simultaneous depletion in ^{18}O and ^{13}C, i.e. a linear correlations between $\delta^{18}O$ and $\delta^{13}C$ (McConnaughey, 1989b). Metabolic effects originate primarily from photosynthesis and respiration (McConnaughey, 1989a), causing changes in the dissolved inorganic carbon species (CO_2, H_2CO_3, HCO_3^-, and CO_3^{2-}) of the internal DIC. Early studies have demonstrated that the relative abundance of these dissolved inorganic carbon species is a function of pH (McCrea, 1950; Usdowski et al., 1991; Usdowski and Hoefs, 1993). McCrea (1950) noted that the $\delta^{18}O$ of the carbonate seems to be related to the proportion of HCO_3^- and CO_3^{2-} in the solution, i.e. $\delta^{18}O$ value of inorganically precipitated carbonates varied with pH. Later, Usdowski et al (1991) and

Usdowski and Hoefs (1993) experimentally demonstrated that the relationship was the result of equilibrium with the respective carbonate species, each of which has their own fractionation factor with water (Usdowski et al., 1991; Usdowski and Hoefs, 1993). The different fractionation factors, i.e. $\delta^{18}O_{VSMOW}$ [the water $\delta^{18}O$ is reported in per mil (‰) with respect to Vienna Standard Mean Ocean Water standard (VSMOW)] values at equilibrium with water being 41.2 ‰ for CO_2 (Kim and O'Neil, 1997), 34.3 ‰ for HCO_3^- (Zeebe and Wolf-Gladrow, 2001), 18.4 ‰ for CO_3^{2-} (Usdowski et al., 1991), and -41.1 ‰ for OH^- (McCrea, 1950), result in an overall depletion of ^{18}O in DIC at higher pHs (see detailed information in Rollion-Bard et al., 2003). Similarly, pH also drives the $\delta^{13}C$ value of $CaCO_3$, with more positive $\delta^{13}C$ at low pH and more negative $\delta^{13}C$ at high pH (Zhang et al., 1995). It seems more difficult to use stable isotopes of biogenetic carbonates for environmental reconstructions when the carbonates are precipitated out of stable isotopic equilibrium. Yet, it is still possible to determine a relationship between stable isotope ratios and environmental conditions, but the offset from isotopic equilibrium must be a constant and known value or accountable (e.g., Dudley et al., 1980; Smith et al., 2000).

1.2.1 $\delta^{18}O$ in bivalve shells - a reliable record of temperature?

Urey (1947) firstly recognized that the temperature coefficient of the equilibrium constant for oxygen isotope fractionation between $CaCO_3$ and water would potentially provide a paleothermometer for the ocean based on the exchange reaction. McCrea (1950) discussed the stable isotopic chemistry of inorganic carbonates precipitated from seawater and presented this temperature coefficient experimentally. The $\delta^{18}O$-thermometer was then calibrated by Epstein et al (1951, 1953) on the basis of marine shells. Consequently, the oxygen isotopic temperature scale was applied for paleotemperature determinations by Lowenstam (1954).

Bivalve shells are an important source of palaeotemperature information (e.g., Elorza and García-Garmilla, 1998; Malchus and Steuber, 2002; Wanamaker et al., 2006). The interpretation of their stable isotope composition relies, however, on the existence of equilibrium isotopic fractionation. In fact, equilibrium fractionation of oxygen isotopes between bivalve mollusk shells and the surrounding seawater is historically acknowledged as a reasonable assumption for mollusks (e.g., Wefer and Berger, 1991). Yet, this assumption has been questioned by certain researchers (e.g., Mitchell et al., 1994). The relationship between the $\delta^{18}O$ of bivalve aragonite and the ambient temperature is well described by the thermometry equation of Grossman and Ku (1986) and has been utilized in a numerous studies for reconstructing sea surface temperature (SST) of the past (e.g., Jones et al., 1984; Grossman and Ku, 1986; Schöne et al., 2004b; Dettman et al., 2004; Chauvaud et al., 2005; Nützel et al., 2010; Trevisiol et al., 2012). Schöne et al (2004b) presented a high-resolution SST proxy record of the southern North Sea during the period 1884–

1983, which has been calculated from the $\delta^{18}O$ of *Arctica islandica*, a long-lived bivalve mollusk shell. They also demonstrated that no vital effects altered the stable isotope geochemistry of this species, so that shell $\delta^{18}O$ values reflected ambient water temperatures that occurred during shell growth (Schöne et al., 2004b). Trevisiol et al (2012) investigated the Antarctic bivalve *Adamussium colbecki* to evaluate its reliability as a suitable archive of water mass properties. They found that shell precipitation occurs close to stable isotopic equilibrium and suggested that the $\delta^{18}O$ of *A. colbecki* is potentially a good summer temperature proxy for Antarctic Shelf waters (Trevisiol et al., 2012).

However, the temperature dependence of the $\delta^{18}O$ fractionation in biogenic carbonates can vary significantly in some species, suggesting the prevalence of a biological factor in the isotopic fractionation during biomineralisation process, i.e. vital effect may be species-dependent (Rahimpour-Bonab et al., 1997; Bemis et al., 1998). For example, a disequilibrium effect in shells of the geoduck, *Panopea abrupta* from Puget Sound, Washington State, U.S.A. was documented by Hallmann et al (2008). Temperatures reconstructed from $\delta^{18}O_{shell}$ values of these geoducks overestimated actual water temperatures by up to ca. 4°C. Less severe disequilibrium effects have also been reported from various other bivalves (Goodwin et al., 2001; Gillikin et al., 2005). Some authors even provided species-specific paleotemperature equations (e.g., Carré et al., 2005). Therefore, to interpret oxygen isotopes of fossil bivalve shells, it is necessary to perform species-specific calibration studies in modern counterparts.

1.2.2 $\delta^{13}C$ in bivalve shells - a reliable record of $\delta^{13}C_{DIC}$?

The anthropogenic carbon dioxide (CO_2) concentration continues to increase due to the emission of CO_2 from the combustion of fossil fuels, which is strongly depleted in ^{13}C relatively to ^{12}C (Tans, 1981; Andres et al., 1996), thus resulting in a decrease in the $\delta^{13}C$ ratio of atmospheric CO_2. The increase of atmospheric CO_2 levels is an important factor forcing climate change (Mudelsee, 2001; Rundgren et al., 2005). Additionally, it has been predicted that higher atmospheric CO_2 concentrations have led to an increase in oceanic uptake of CO_2 (Siegenthaler and Sarmiento, 1993), which means a significant negative shift in the $\delta^{13}C$ ratios of the dissolved inorganic carbon ($\delta^{13}C_{DIC}$) in ambient seawater. The $\delta^{13}C_{DIC}$ changes permit an estimation of the oceanic uptake rate of atmospheric CO_2 (Gruber et al., 2002; Quay et al., 2003). Seawater DIC and $\delta^{13}C_{DIC}$ data collected from field observations are insufficient, since they represent only a short period of time. The stable carbon isotope data of foraminifera, corals, sclerosponges and bivalves have been employed to extend the $\delta^{13}C_{DIC}$ record further back in time (Mook and Vogel, 1968; Fritz and Poplawski, 1974; Nozaki et al., 1978; Graham et al., 1981; Grossman, 1984; Grossman and Ku, 1986; Druffel and Benavides, 1986; Böhm et al., 1996; Swart et al., 1998; Lazareth et al., 2000; Schöne et al., 2011). For example, Mook and Vogel (1968) observed that the $\delta^{13}C_{shell}$ values of

estuary bivalves were in isotopic equilibrium with the surrounding water and suggested that $\delta^{13}C_{DIC}$ could be potentially reconstructed by using shell $\delta^{13}C$. In addition, Schöne et al (2011) demonstrated that $\delta^{13}C$ values in shells of the bivalve mollusk *Arctica islandica*, provide a measure of the seawater $\delta^{13}C_{DIC}$ history by presenting absolutely dated, annually resolved shell $\delta^{13}C$ record from surface waters of the North Atlantic.

However, it has also been proposed that the $\delta^{13}C_{shell}$ ratios in bivalves vary extremely strong due to the influence of two carbon sources (ambient water DIC and metabolic DIC) available during the calcification process (Tanaka et al., 1986; McConnaughey et al., 1997). The dominance of either seawater DIC or metabolic DIC appears to vary from species to species (e.g., Gillikin et al., 2006, 2007; Lorrain et al., 2004) and over the lifetime or even among different shell portions of an individual (Klein et al., 1996b; Elliot et al., 2003; Lorrain et al., 2004; Butler et al., 2011). The incorporation of metabolic DIC into the shell may obscure the recorded signals of the ambient water $\delta^{13}C_{DIC}$. Gillikin et al (2006) measured $\delta^{13}C$ values of *Mytilus edulis* shells and mantle tissues, DIC and particulate organic carbon in the Scheldt estuary and concluded that shell $\delta^{13}C$ values of this bivalve species, could not be used as a robust proxy of environmental $\delta^{13}C_{DIC}$ because of the high variability in metabolic carbon incorporation.

Numerous of studies noted a general ontogenetic decreasing trend in $\delta^{13}C_{shell}$ in various mollusk species (e.g., Jones et al., 1986; Krantz et al., 1987; Kennedy et al., 2001; Keller et al., 2002; Lorrain et al., 2004; Gillikin et al., 2007; Foster et al., 2009). Keller et al (2002) attributed the more negative shell $\delta^{13}C$ values in the ontogenetically older part of the bivalve *Chamelea gallina* to the utilization of more negative $\delta^{13}C_{DIC}$ derived from ^{13}C-depleted pore waters as the bivalve moves deeper into the sediment. Other authors attributed the decreasing trend in $\delta^{13}C_{shell}$ to the effects of metabolic changes (e.g., Krantz et al., 1987; Lorrain et al., 2004; Gillikin et al., 2007; Foster et al., 2009), claiming that the highly variable contribution of metabolic carbon hampers the use of $\delta^{13}C_{shell}$ as a proxy for environmental conditions (Lorrain et al., 2004; Gillikin et al., 2006). For example, Lorrain et al (2004) observed this ontogenetic decrease in the $\delta^{13}C$ of *Pecten maximus* shells. They proposed a simple model, where this trend was caused by an increase in the amount of respiratory CO_2 produced by the bivalve as a function of metabolic rate and body size, i.e. the metabolism increases while shell growth rates are reduced.

1.3. Advantages of bivalve shells as a proxy archive

The growth and geochemistry of accretionary skeletons precipitated by marine organisms have proved to be valuable proxies, which facilitate the development of histories of environmental change in marine systems (Pannella, 1971; Andrews, 1972; Rhoads and Lutz, 1980; Jones, 1981; Weidman et al., 1994; Witbaard et al., 1999; Ambrose et al., 2006; Richardson, 2001). In contrast to other climate archives, bivalves have several advantages, including the capability to provide high-resolution records, the sensitivity for environmental changes, a long lifespan, a high preservation potential as fossils and a broad geographic distribution.

Bivalve mollusks sequentially secret their shells with internal growth lines, such as the annual, fortnightly, daily and sub-daily lines (Pannella and McClintock, 1968; Jones, 1980; Rhoads and Lutz, 1980; Dunca et al., 2005; Hallmann et al., 2009). The periodic growth patterns enable precise calendar dating of each shell portion and provide high-resolution records of life history traits, as well as records of environmental changes. For example, Hallmann et al (2009) found that the butter clam, *Saxidomus gigantean* from the intertidal zone in the Pacific Coast of North America produced distinct circatidal, circalunidian and fortnightly shell growth patterns. They thus presented that microgrowth patterns of this species can be used to estimate the time of collection of an archaeological shell to the nearest day, and also the approximate tidal location where the clams lived.

Bivalves sensitively record ambient environmental conditions in their shells during growth (e.g., Jones et al., 1986; Bauer, 1992; Wanamaker et al., 2009). In particular, temperature (Kennish and Olsson, 1975), food supply (Ansell, 1968; Page and Hubbard, 1987; Sato, 1997), salinity (Davis and Calabrese, 1964; Marsden, 2004), and water quality (Mutvei et al., 1996; Dunca et al., 2005) can be inferred from the changes in shell growth rates (Koike, 1980; Bauer, 1992; Dunca and Mutvei, 2001) and geochemical properties (Jones et al., 1986; Wefer and Berger, 1991; Gillikin et al., 2005). Faster shell growth occurs at optimal temperatures and under abundant food availability and growth may cease below or above certain temperatures (Ansell, 1968, Schöne et al., 2003b). The shell growth of the freshwater bivalves, *Margaritifera margaritifera* from Sweden, for instance, is limited to temperatures above 5°C (Dunca and Mutvei, 2001). Additionally, variations in bivalve geochemistry are also controlled by environmental factors. For example, the $\delta^{18}O$ profiles in shells of the bivalve species, *Spisula sachalinensis* and *Mactra chinensis* collected along the east coast of Korea (Sea of Japan) exhibit distinct annual cycles and are consistent with the seasonal temperature variations of each locality (Khim et al., 2000). The averaged $\delta^{13}C$ values of the shells decrease gradually northward along the east coast of Korea, reflecting changes of water mass DIC in the shallow coastal setting (Khim et al., 2000).

The authors therefore, suggested that the bivalve shells could be useful to monitor the environmental conditions in coastal waters.

Bivalve mollusks are among the longest lived animals (e.g., Skrecky, 1996; Schöne et al., 2005a; Butler et al., 2013), and thus, they are suited as long-term paleoclimate archives. Although most bivalves typically live less than 10 years, some may live up to 50 years (Peterson, 1986) and some species attain ages far over 100–200 years (Jones, 1983) and potentially record the ambient environmental conditions during their entire life. For instance, the ocean quahog *Arctica islandica* can live more than 500 years (Butler et al., 2013), a record of longevity for non-colonial animals Dog cockles *Glycymeris glycymeris* live up to 200 years in populations off the west coast of Scotland (Brocas et al., 2013), and similar ages are observed for European freshwater mussels, *Margaritifera margaritifera (*Schöne et al., 2004a). Therefore, in addition to high-resolution palaeoenvironmental reconstructions, bivalve shells can provide very long records of past climatic and environmental variability. It should be noted that the individual's lifespan is not the limiting factor for long-term environmental reconstructions. It is possible to establsih a master-chronology of environmental history by using even short-lived bivalve species (Schöne et al., 2003d). Contemporaneous specimens with overlapping lifespans can be strung together to form mean and master chronologies, similar to tree-ring chronologies (Jones et al., 1989). Such multi-specimen records spanning many mollusk generations thereby can stretch over centuries to millennia and contain precise environmental data for the covered period (Marchitto et al., 2000; Schöne et al., 2003d).

Additionally, bivalve shells are often found in archeological middens and sediment cores as fossils (Hallmann et al., 2013; Burchell et al., 2013; Müller-Lupp et al., 2004), which potentially enable to reconstruct the environmental conditions of the past. Moreover, bivalves are beneficial in that they have a wide geographic distribution, which covers nearly all aquatic environments, i.e. freshwater, estuary and marine environment from the low to high latitudes (near the equator and the poles), and from shallow water to the deep sea (e.g., Müller-Lupp et al., 2004; Nützel et al., 2010; Kennish and Lutz, 1999), whereas many other organisms, such as corals, are limited in their latitudinal extent.

1.4. The bivalves *Eurhomalea exalbida*, *Paphia undulata* and *Margaritifera falcata*

The focus of this thesis is on shells of two marine veneroid bivalve species and one freshwater mussel species: the long-lived *Eurhomalea exalbida* from the Falkland Islands (South Atlantic), the short-lived *Paphia undulata* from the South China Sea, and the western pearlshell *Margaritifera falcata* from the British Columbia, Canada.

The bivalve mollusk *E. exalbida* is a long-lived species with individuals reaching over 70 years (Lomovasky et al., 2002). This species inhabits shallow waters along the eastern and western coasts of South America, including the Falkland Islands. It also occurs in numerous archaeological shell middens and sedimentary deposits in South America (e.g., Stilwell and Zinsmeister, 2009; Chiesa et al., 1995). The knowledge of regional paleoclimate dynamics of the southern hemisphere is very limited due to the lack of long-term and high-resolution proxy records (e.g., Vimeux et al. 2009; Neukom et al., 2011). *E. exalbida* is therefore a potential candidate for paleoclimatic reconstructions on the southern hemisphere, that is capable of dealing with both long term climate oscillations, e.g., on an annual scale, and short term changes on a (sub)seasonal scale. However, this species has received remarkably little attention as a climatic archive. Lomovasky et al (2002) observed decadal variability in the growth increment widths of *E. exalbida* and assumed that environmental parameters might be the main factors controlling these changes. Ivany et al (2008) used shells of fossil *Eurhomalea* spp. and *Cucullaea raea* from the La Meseta Formation of Seymour Island, Antarctica, to reconstruct seasonal temperature ranges during the Eocene. On average, $\delta^{18}O$-derived temperatures of *Eurhomalea* spp. shells yielded 2°C higher temperatures than shells of *C. raea* from the same stratigraphic level. They suggested that this 2°C temperature offset might be caused by differences in the growing season of the two species (Ivany et al., 2008). In this dissertation, extant *E. exalbida* is studied to examine the reliability of this species as a climate archive for paleoclimate reconstructions on the southern hemisphere.

The bivalve mollusk *P. undulata*, is also known as the short-necked clam or the undulated surf clam. This very short-lived and fast-growing species (individuals get about two years-old; the typical shell length of adults is 5 cm; Winckworth, 1931) exhibits a broad biogeographic distribution in the Indo-West Pacific, including the South China Sea (Poutiers, 1998) and well-preserved fossils of this species are frequently found in sedimentary strata. *P. undulata* is therefore a potential archive for high-resolution paleoclimate reconstructions in regions affected by the EAM. Climate archives, such as sediments (Wan et al., 2006; Wang et al., 1999), planktonic foraminifera (Chen et al., 2003; Steinke et al., 2011) and pollen (Li et al., 2010)

provide longer-term variations of the EAM since the Late Pleistocene. In contrast, corals (e.g., Sun et al., 2005; Yu et al., 2005) and bivalve mollusk shells (e.g., Marwick and Gagan, 2011; Schöne et al., 2004c; Stephens et al., 2008; Yan et al., 2013) offer an better insight into (sub)seasonally and inter-annually resolved EAM reconstructions, which are still rather rare. Since tropical corals (e.g., Sun et al., 2005; Yu et al., 2005) typically are not well preserved as fossils or tend to be diagenetically altered due to their large porosity, studies on bivalve shells from EAM-related regions are increasingly crucial. Marwick and Gagan (2011) presented a record of paleomonsoon activity extending back to 35,000 BP (years before present), based on the analysis of oxygen isotope ratios of freshwater bivalve excavated from the northwest Thailand. In the present study, marine bivalve, *P. undulata* is analysed to evaluate the feasibility of this species as a proxy archive of the EAM and the capability of providing the necessary temporal resolution needed for the extraction of peculiar monsoon signals in the Indo-West Pacific.

The freshwater pearl mussel *M. falcata* is a common species in the Pacific Northwest of North America, which prefers cold and clean creeks and rivers with sand, gravel and cobble streambeds (Vannote and Minshall, 1982; Nedeau et al., 2005). *M. falcata* has been documented as an ideal indicator of the ambient aquatic ecosystems due to its sedentary habits, the extreme longevity, the sensitivity to environmental changes, and the distinct annal periodicity of the shell growth (Howard et al., 2005; Howard and Cuffey, 2006; Schöne et al., 2007; Webb et al., 2008; Limm and Power, 2011). Adult *M. falcata* individuals are largely sedentary with limited mobility during their entire lives (Coker et al., 1921; Watters, 1992), and this species is one of the longest-lived animals in the world and its sister species *Margaritifera margaritifera* has been estimated to be in excess of a century (Hastie et al., 2000; Schöne et al., 2004a). Thus, they can record cumulative information of long-term environmental conditions (Nystrom et al. 1996). Furthermore, *M. falcata* is recognized to be sensitive to various environmental changes, thus the environmental conditions can be reflected in terms of reproduction, growth rates, and age structures (Howard et al., 2005; Webb et al., 2008; Limm and Power, 2011). Additionaly, *M. falcata* shells are precipitated by clear annual growth increments (Schöne et al., 2007), which enables the age and shell growth rates to be estimated. In this study, the pearlshell *M. falcata* speciemens collected from different rivers in British Columbia, Canada were analysed with a focus on the age structures and shell growth characteristics, which may provide insights into the riverine environmental conditions.

1.5. Sclerochronological methods

1.6.1 Shell cross-section preparation

For sclerochronological and stable isotope analyses, the right valve of each specimen was mounted on plexiglass cubes and coated with WIKO metal epoxy resin to avoid shell fracture during sectioning. After the epoxy had cured, two 2-3 millimeter thick sections were cut from the shells perpendicular to the growth lines along the axis of maximum growth from the umbo to the ventral margin. For this purpose, a low-speed precision saw (Buehler IsoMet 1000) with a 0.4mm thick low-concentration diamond-coated saw blade was used. Both slabs of each shell were mounted on glass slides, ground on glass plates using 800 and 1200 grit powder, respectively, and polished with 1µm Al_2O_3 powder on a Buehler G-cloth. After each grinding and polishing step, shell cross-sections were ultrasonically cleaned. One unstained cross-section was subsequently used for isotope analysis, whereas the second cut was Mutvei-stained and used for growth pattern analysis.

1.6.2 Shell growth pattern analyses

One polished section of each specimen was immersed in Mutvei's solution for 20min under constant stirring at 37-40°C (Schöne et al., 2005b). This agent simultaneously etches the carbonate of the shell, preserves organic matrices and stains acid mucopolysaccharides and glucosaminoglycans (acid mucosubstances and acetic mucins) blue (Steedman 1950). Since the growth lines are richer in organics, they stain darker blue and are more etch-resistant than the carbonate dominated portions between adjacent growth lines. Immersion in Mutvei's solution therefore facilitates the recognition and analysis of shell growth patterns under reflected-light microscopy.

To analyze shell growth patterns, digital images were taken from the stained cross-sections using a Nikon Coolpix 995 camera attached to a Wild Heerbrugg MZ3 binocular microscope equipped with sectoral dark field illumination (Schott VisiLED MC 1000). Growth increment widths were measured in the outer sublayer of the outer shell layer in the direction of growth to the nearest 2 µm using the image analysis software Panopea (© Peinl & Schöne).For annual growth line analysis, serial photographs of each specimen were stitched together with the Microsoft Image Composite Editor.

1.6.3 Stable isotope analyses

The remaining unetched, polished cross-sections were used for stable carbon and oxygen isotope analysis of the shell carbonate. In fast-growing juvenile shell portions of *E. exalbida*, shell material was obtained by drilling consecutive holes with a cylindrical SiC drill bit (300 µm

diameter at the tip). High-resolution sampling, however, required a micromilling technique, conducted parallel to the growth lines and perpendicular to the direction of growth, for which a cylindrical SiC drill bit (700 µm diameter) provided excellent results in the slower growing shell portion. Powder carbonate material of *P.undulata* were obtained by milling using a diamond-coated mill bit with 1mm diameter, because the outer shell layer in umbonal shell portions was only a few tens to hundreds of µm thick. In the remaining shell portions, powder samples were obtained by drilling (Figure 5.3) using the 300 µm SiC drill bit.

Each sample weighed between 50 and 120 µg. Samples were processed in a Thermo Finnigan MAT 253 continuous flow – isotope ratio mass spectrometer coupled to a GasBench II. Results are reported in δ-notation, and $\delta^{13}C$ and $\delta^{18}O$ values are given as parts per mil (‰). Isotope data were calibrated against NBS-19 and IVA-Carrara ($\delta^{13}C$ = 1.95‰; $\delta^{18}O$ = -2.20‰ (NBS-19); $\delta^{13}C$ = 2.01‰; $\delta^{18}O$ = -1.91‰ (NBS 19-calibrated IVA Carrara)) with 1σ replicated precision of 0.03‰ for $\delta^{13}C$ and 0.07‰ for $\delta^{18}O$ (NBS-19) and 0.04‰ for $\delta^{13}C$ and 0.06‰ for $\delta^{18}O$ (NBS 19-calibrated IVA Carrara). According to the empirically determined paleothermometry equation of Grossman and Ku (1986), shell $\delta^{18}O$ values can be used to calculate water temperatures. However, a small modification of this equation was required because Grossman and Ku (1986) reported the water $\delta^{18}O$ as VSMOW (correction by –0.27‰; Dettman et al., 1999). The corrected function is as follows:

$$T_{\delta^{18}O}(°C) = 20.60 - 4.34 \cdot (\delta^{18}O_{shell} - (\delta^{18}O_{water} - 0.27))$$

where $\delta^{18}O_{shell}$ is measured relative to the Vienna Pee Dee Belemnite (Vienna PDB) scale and $\delta^{18}O_{water}$ is relative to the VSMOW scale. Thus, assuming no change in the $\delta^{18}O_{water}$, a shift in $\delta^{18}O_{shell}$ by 1‰ reflects a temperature change of the ambient seawater of 4.34°C.

1.6. Objectives of research

The major objective of this Ph.D dissertation is the sclerochronological analyses of two marine bivalve mollusk species, *Eurhomalea exalbida* and *Paphia undulata*, and one freshwater bivalve species *Margaritifera falcata*.

Significant advancements have been made in paleoclimatic reconstructions for the northern hemisphere (Mann et al., 1999, Luterbacher et al., 2004, Lee et al., 2008; Rutherford et al., 2008). The regional paleoclimate dynamics of the southern hemisphere, by constrast, are still largely unknown (e.g., Vimeux et al. 2009; Neukom et al., 2011) and the lack of knowledge hampers the establishment of global paleoclimatic models. Southern South America is a particularly important climatic region, which is primarily influenced by the El Nino-Southern Oscillation, the Pacific Decadal Oscillation and the Southern Annular Mode (Garreaud et al. 2009). Apparently, there is a strong need for quantifiable paleoclimate proxy archives of annual or higher resolution from southern South America to better understand the decadal climate modes. *E.exalbida* has a great potential to act as an archive to reconstruct paleoclimate of southern hemisphere, and thus, the focus of Chapter 2 and Chapter 3 is on the evaluation of this species as an environmental archive.

In addition to climatic changes in mid-high latitude regions, the tropical climate system is also important for understanding global paleoclimatic changes. In the tropical climate system, the climate of the northern South China Sea realm is primarily dominated by the EAM system. The longer-term variations of the EAM have been studied based on proxy archives, such as sediments (Wang et al. 1999; Wan et al. 2006), planktonic foraminifera (Chen et al. 2003; Steinke et al. 2011) and pollen (Li et al. 2010). However, the long-term records fail to provide information about the frequency and strength of EAM extremes within individual years of the past, which is essential to predict the erratic monsoons in future. In fact, appropriate paleoclimate archives at an adequate quality (i.e., well-calibrated and (sub)seasonal resolution) from regions affected by the EAM are rather rare. *P. undulata* is a potential archive for reconstructions of erratic EAM signals in the Indo-West Pacific. Therefore, the focus of Chapter 4 is on assessing the suitability of this species as a proxy archive of peculiar monsoon extremes in this low latitude region related to EAM.

Besides marine bivalve species (Jones et al., 1989; Goodwin et al., 2001; Schöne et al., 2005c; Hallmann et al., 2008), the freshwater mussels have also been recognized to be a useful archive for studying environmental changes (Howard and Cuffey, 2006; Schöne et al., 2007). The western pearlshell *Margaritifera falcata* is one of the most common species in North America, which was originally widespread from Alaska and British Columbia south to central California and east to Montana, Wyoming, and northern Utah (Taylor 1981). This freshwater species has

been extirpated from some watersheds of United States in recent decades (Brim Box et al. 2003, 2006; Howard and Cuffey 2006; Stagliano et al. 2007). However, *M. falcata* is still abundant in many areas, particularly in a number of rivers of British Columbia, Canada. Since much effort has been primarily focused on the declining *M. falcata* populations of the United States, research on this species of British Columbia is rather sparse (Schöne et al., 2007; Rodland et al., 2009). The water environments of British Columbia are documented to be suitable and secure for *M. falcata* (NatureServe Explorer, 2012, http://www.natureserve.org/explorer/; The Xerces Society for Invertebrate Conservation, http://www.xerces.org/western-pearlshell/), yet the age distributions and growth rates may differ between rivers due to various land use activities and different river hydrology (Howard et al., 2005; Howard and Cuffey, 2006). Therefore, there is a crucial need to analyze the variations in the life history and growth characteristics of *M. falcata* from different rivers of British Columbia. The preliminary investigation will be presented in Chapter 5, which may provide insights into the riverine environmental conditions.

The principal attention is focused on the calibration of measured sclerochronological and geochemical data, since potential proxies must be calibrated individually for each species of interest before it can be used for further paleoenvrionmental reconstruction with analogous fossil shells. Accordingly, the following objectives are addressed in the present study:

For *Eurhomalea exalbida*:

- During which season of the year do the shells of *E.exalbida* grow? Does the rate of shell growth differ during different seasons?
- Are the shells of *E.exalbida* formed in stable carbon and oxygen isotopic equilibrium with the ambient water?
- Can the $\delta^{18}O_{shell}$ values be used to reliably reconstruct past water temperatures?
- Is there an ontogenetic trend in the $\delta^{13}C_{shell}$? If there is an ontogenetic trend, which factor(s) control the decrease trend in $\delta^{13}C_{shell}$ values?
- Are there seasonal variations in $\delta^{13}C_{shell}$ values? If there are seasonal variations in $\delta^{13}C_{shell}$, which factors controlled the variations?

For *Paphia undulata*:

- How old are the *P. undulata* specimens? During which season of the year do the shells grow? What is the growth rate of the shells during different seasons?
- Are shells of *P. undulata* reliable proxy archives which serve to reconstruct the frequency of exceptional summer monsoons in the past?
- Can the $\delta^{18}O_{shell}$ and $\delta^{13}C_{shell}$ values as well as shell growth patterns of *P. undulata* be used to estimate the relative strength of monsoon-related precipitation and associated changes in ocean salinity and the $\delta^{13}C_{DIC}$ signature?

For *Margaritifera falcata*:

- Are there any differences and similarities in shell lifespans of *M. falcata* between four rivers in southwestern British Columbia?
- Are there any differences and similarities in shell growth equations (height versus age) of this species between four rivers in southwestern British Columbia?
- Can the preliminary results give any implications on the effects of riverine environments on the shell growth of the freshwater mussels?

The $\delta^{13}C_{shell}$ and $\delta^{18}O_{shell}$, as well as shell growth patterns were analysed and discussed to investigate the reliability of bivalve shells as indicators of environmental parameters and species-specific discrepancies. The results of this dissertation are presented in chapters two, three, four and five. By integrating all the results and conclusions of the four chapters, this study will improve the understanding of bivalve proxy archives as providers of environmental information.

Chapter 2: *Eurhomalea exalbida* (Bivalvia): a reliable recorder of climate in southern South America?

Lina Yan[1], Bernd R. Schöne[1] and Alexander Arkhipkin[2]

1 Institute of Geosciences, Earth System Science Research Center, University of Mainz, Becherweg 21, 55127 Mainz, Germany

2 Fisheries Department, Falkland Islands Government, P.O. Box 598, Stanley, Falkland Islands

Yan, L., Schöne, B.R., and Arkhipkin, A., 2012. *Eurhomalea exalbida* (Bivalvia): A reliable recorder of climate in southern South America? Palaeogeography, Palaeoclimatology, Palaeoecology 350–352: 91–100.

Foreword

The present chapter aims at determining if $\delta^{18}O_{shell}$ of long-lived marine bivalve *Eurhomalea exalbida* can serve as a temperature proxy in southern South America. The key objects are as follows: firstly, to trait shell growth history and to determine growth rates of the shells during different seasons; secondly, to test whether the shells of *E. exalbida* formed in oxygen isotopic equilibrium with the ambient water and can the $\delta^{18}O_{shell}$ values be used to reliably reconstruct past water temperatures.

ABSTRACT

Due to the lack of suitable high-resolution archives, regional and continental-scale climate dynamics of southern South America are not well understood. Shells of the long-lived, shallow-marine bivalve mollusk, *Eurhomalea exalbida* (Dillwyn) are likely to contain information on the past water temperatures. As yet, however, no rigorous calibration study has been presented so that growth history traits and the reliability of shell oxygen isotope-based temperature estimates remain unknown. Shell growth patterns and oxygen isotope ratios of four young specimens of *E. exalbida* from the Falkland Islands (Southwest Atlantic) were analyzed and cross-calibrated with environmental parameters. Results indicate that *E. exalbida* likely captured the full seasonal temperature amplitude in its shell. Annual growth line formation occurred between fall and early winter. The most remarkable finding, however, was that *E. exalbida* formed its shell with an offset of -0.48‰ to -1.91‰ from expected oxygen isotopic equilibrium with the ambient water. If this remained unnoticed, paleotemperature estimates would overestimate actual water temperatures by 2.1°-8.3°C. With increasing ontogenetic age, the discrepancy between measured and reconstructed temperatures increases exponentially, irrespective of the seasonally varying shell growth rates. We attribute this finding to a pH increase in the extrapallial fluid during ontogeny favoring a dominance of the (isotopically lighter) carbonate ions over (isotopically heavier) bicarbonate ions. When this disequilibrium fractionation effect is taken into account, *E. exalbida* can serve as a high-resolution paleoclimate archive for mid to high latitudes of southern South America providing quantifiable temperature estimates, even from single fossil specimens.

Key words

Oxygen isotopes; Bivalve sclerochronology; Temperature; Disequilibrium; Paleoclimate

2.1. Introduction

Well-constrained numerical climate models require a detailed understanding of the forcing and feedback mechanisms operating within the Earth system. For this purpose, it is necessary to document the dynamics of key aspects of climate, such as temperature, at high spatiotemporal resolution, i.e., on inter-annual to seasonal and regional to global scales. Such data can be used to assess the human impact on climate and ecosystems and, in turn, to evaluate how regional climates and seasonal extremes might have influenced migration, mobility and subsistence practices of past human populations.

Instrumental data of environmental parameters are extremely scarce prior to about AD 1860 and often only cover the few most recent decades, namely the remote sensing era. Therefore, our knowledge of the pre-industrial (= natural) variability of environmental parameters is almost entirely based on climate proxy archives such as tree rings, speleothems or varved sediments (e.g., Jones et al., 2001). Specifically, the dense dendrochronological network of the northern hemisphere has provided a profound insight into changing frequencies and amplitudes of natural climate modes as well as inter-annual temperature and precipitation patterns on various spatial scales during the last two thousand years (e.g., Schweingruber et al 1991; Briffa et al 1994; Büntgen et al., 2011).

However, due to the limited number of appropriate high-resolution proxy records, much less is known about regional paleoclimate dynamics of the southern hemisphere (e.g., Vimeux et al. 2009; Neukom et al., 2011). This is particularly true for southern South America, a key climatic region that is affected by decadal climate modes of global significance, including the El Nino-Southern Oscillation, the Pacific Decadal Oscillation and the Southern Annular Mode (Garreaud et al. 2009). The few existing well-dated, annually resolved paleotemperature data from this region largely come from Andean trees (Neukom et al 2009). Naturally, dendrochronological records are strongly biased toward summer, i.e., the main vegetation period. Clearly, there is a strong need for additional quantifiable paleoclimate proxy archives of annual resolution or better from southern South America.

The long-lived bivalve mollusk *Eurhomalea* spp. is a potential candidate for high-resolution paleoclimate reconstructions of southern South America. This genus inhabits shallow waters along both coasts of South America (south of 36° [Buenos Aires] along the Atlantic coast and south of 42° [Chiloe Island] along the Pacific coast; e.g., Keen, 1954; Powell, 1960; Ríos, 1994; Lomovasky et al., 2002 and references therein) including the Falkland Islands. It also occurs in numerous archaeological shell middens and sedimentary deposits (e.g., Stilwell and Zinsmeister, 2009; Chiesa et al., 1995). Dextraze and Zinsmeister (1987) claimed that the distinct

internal growth lines in this genus form during winter and thus represent annual growth lines. This was later confirmed by shell oxygen isotope analyses of living *Eurhomalea exalbida* (Dillwyn) from Argentina (Lomovasky et al., 2002) and *Eurhomalea* spp. from the Eocene of Antarctica (Ivany et al 2008). In the Beagle Channel (54° S), individuals of *E. exalbida* live for more than 70 years (Lomovasky et al., 2002). For climate reconstructions, this species has received remarkably little attention. Lomovasky et al (2002) observed decadal variability in growth increment widths of *E. exalbida* and assumed that these might be caused by environmental parameters. Ivany et al (2008) used shells of fossil *Eurhomalea* spp. and *Cucullaea raea* from the La Meseta Formation of Seymour Island, Antarctica, to reconstruct seasonal temperature ranges during the Eocene. On average, $\delta^{18}O$-derived temperatures of *Eurhomalea* spp. shells yielded 2°C higher temperatures than shells of *C. raea* from the same stratigraphic level. Ivany et al (2008) attributed this finding to differences in the growing season of the two species.

In the present study, we conduct the first detailed calibration of extant *E. exalbida* shells with environmental variables. In particular, we focus on growth history traits and the potential use of oxygen isotope values of shells of this species as an indicator of temperature. Are the shells of this species formed in oxygen isotopic equilibrium with the ambient water? Can the shell $\delta^{18}O$ values be used to reliably reconstruct past water temperatures? During which season of the year do the shells grow? What is the growth rate of the shells during different seasons? Results of this study provide the basis for paleoclimate reconstructions of the southern hemisphere using *E. exalbida*.

2.2. Material and methods

A total of four young (four to ten years-old) specimens of *E. exalbida* were collected alive from the upper sublittoral (shallow subtidal; 2m water depth) zone near Stanley, Falkland Islands (Figure 2.1; Table 2.1). Two specimens were obtained on 21st February 2009 and the remaining two on 5th April 2009 (Table 2.1). Soft tissues were removed from each specimen immediately after collection, and shells were kept dry until further studies.

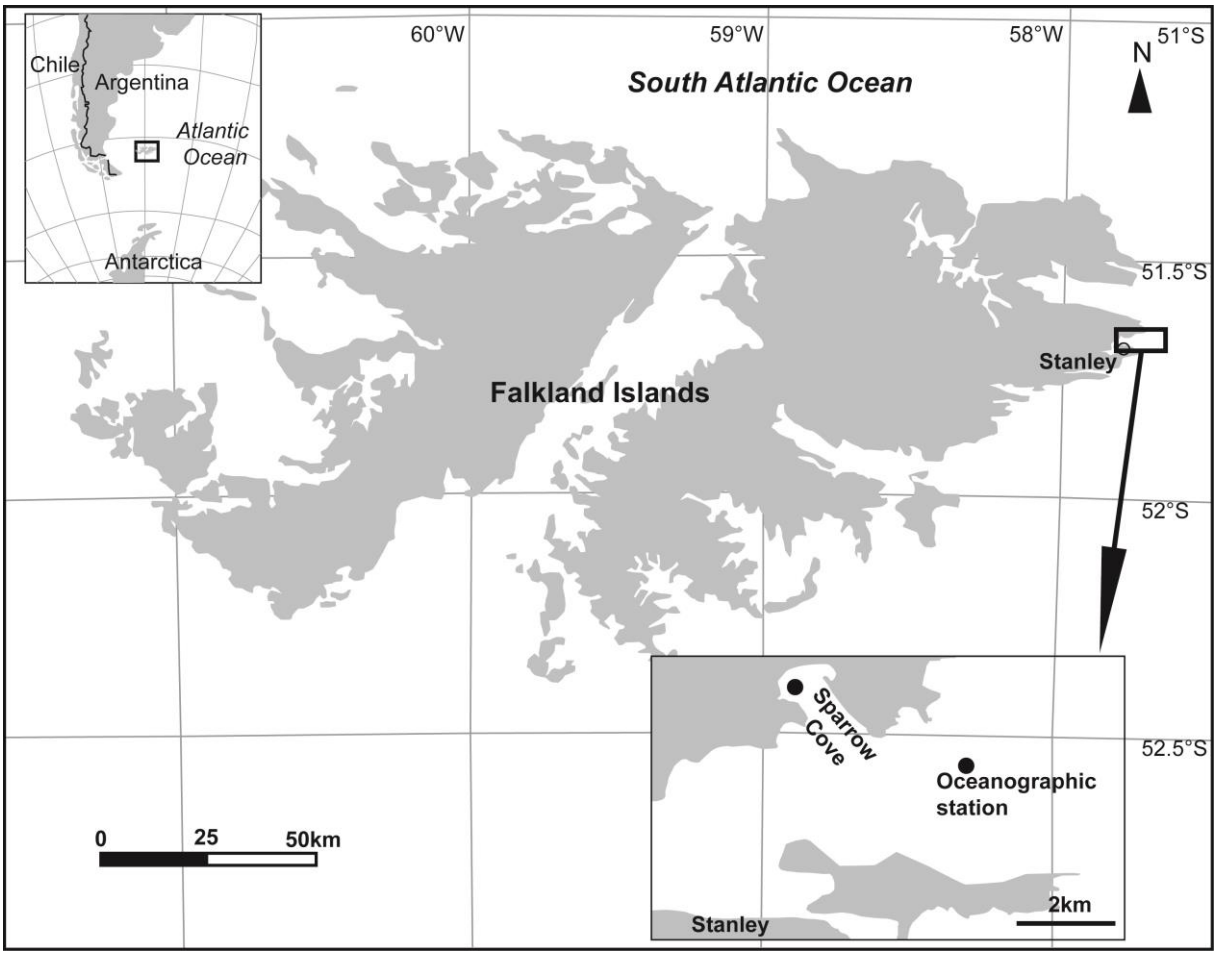

Figure 2. 1. Map showing the sample locality at Sparrow Cove (51°39'S, 57°48'W) NE Stanley, Falkland Islands, and the nearby oceanographic station (51°40'S, 57°45'W).

2.2.1. Preparation of cross-sections

The right valve of each specimen was mounted on plexiglass cubes and coated with WIKO metal epoxy resin to avoid shell fracture during sectioning. After the epoxy had cured, two three-millimeter thick sections were cut from the shells perpendicular to the growth lines along the axis of maximum growth from the umbo to the ventral margin (Figures 2.2A, B). For this purpose, a low-speed precision saw (Buehler IsoMet 1000) with a 0.4mm thick low-concentration diamond-coated saw blade was used. Both slabs of each shell were mounted on glass slides (Figure 2.2B), ground on glass plates using 800 and 1200 grit powder, respectively, and polished with 1µm Al_2O_3 powder on a Buehler G-cloth. After each grinding and polishing step, shell cross-sections were ultrasonically cleaned. One unstained cross-section was later used for isotope analysis (Figure 2.2C-E), whereas the second Mutvei-stained sample was used for growth pattern analysis (Figure 2.3).

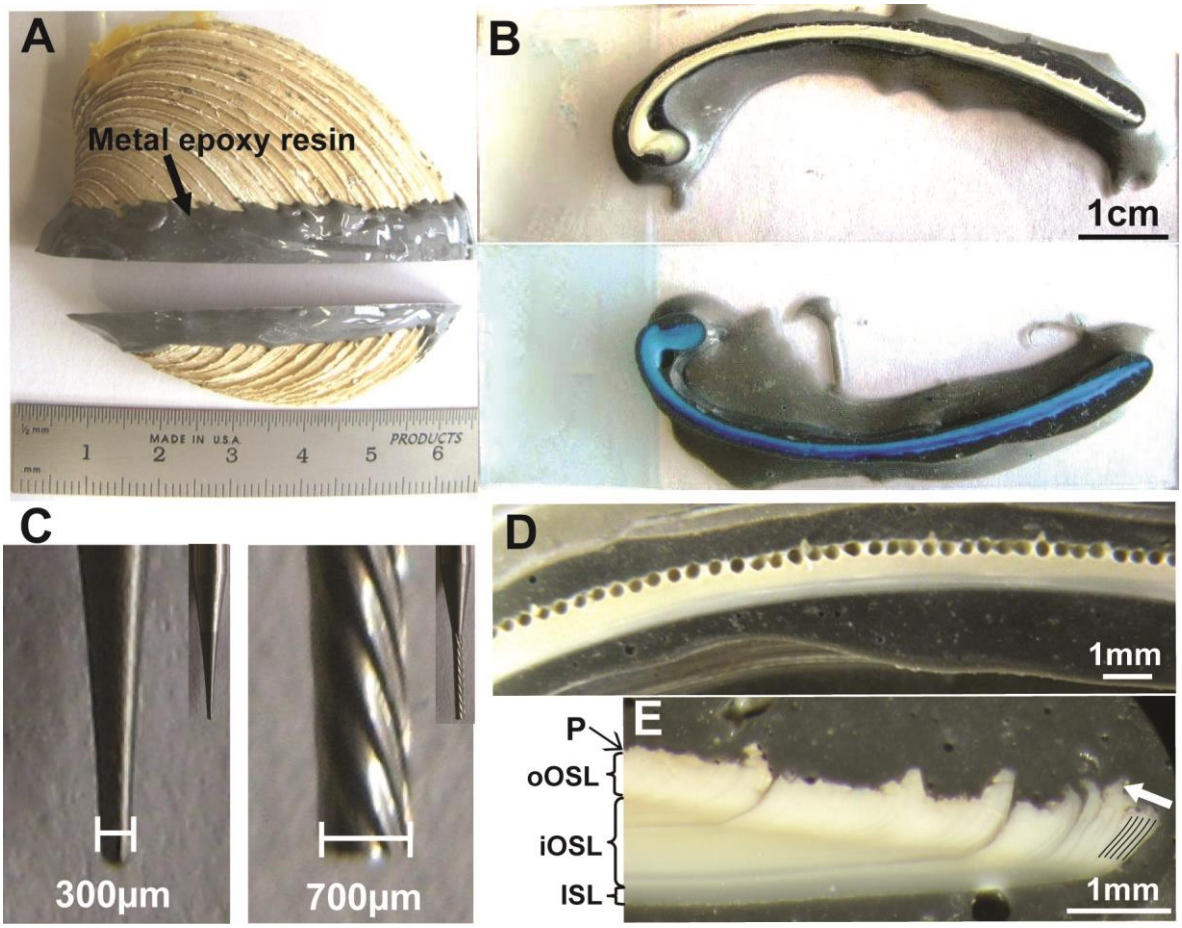

Figure 2. 2. Sample preparation of *Eurhomalea exalbida* shells. (A) Cross-sectioned right valve. (B) Thick-sections mounted on glass slides used for isotope sampling (upper panel) and growth pattern analyses (lower panel; immersed in Mutvei's solution), respectively. (C) Drill bits (left) and mill bits (right) used for isotope sampling. (D) Faster growing shell portions were microdrilled. (E) Higher resolution was achieved by micromilling shell powder (thin black lines) from the oOSL. White arrow indicates direction of sampling. P = periostracum; oOSL/iOSL = outer/inner sublayer of the outer shell layer. Inner shell layer starts only at the pallial line and is not shown here.

2.2.2. Sclerochronological analyses

In preparation for shell growth pattern analyses, one polished section of each specimen was immersed in Mutvei's solution (Figures 2.2B, 2.3) for 20min under constant stirring at 37-40°C (Schöne et al., 2005a). This agent simultaneously etches the carbonate of the shell, preserves organic matrices and stains acid mucopolysaccharides and glucosaminoglycans (acid mucosubstances and acetic mucins) blue (Steedman 1950). Since the growth lines are richer in organics, they stain darker blue and are more etch-resistant than the carbonate dominated portions

between adjacent growth lines. Immersion in Mutvei's solution therefore facilitates the recognition and analysis of shell growth patterns under reflected-light microscopy (Figure 2.3).

To analyze shell growth patterns, digital images were taken from the stained cross-sections using a Nikon Coolpix 995 camera attached to a Wild Heerbrugg MZ3 binocular microscope equipped with sectoral dark field illumination (Schott VisiLED MC 1000). Growth increment widths were measured in the outer sublayer of the outer shell layer[1] (Figure 2.3B) in the direction of growth to the nearest 2 µm using the image analysis software Panopea (© Peinl & Schöne).

[1] In previous studies, the outer sublayer of the outer shell layer of bivalve shells was referred to as ‚outer (shell) layer', and the inner sublayer of the outer shell layer as ‚middle (shell) layer'. However, these mere descriptive terms have no bearing on shell formation, because both sublayers of the outer shell layer are formed by the same (outer) extrapallial fluid. In addition, they are distinctly separated from the inner shell layer (which is precipitated from the inner extrapallial fluid) by the myostracum. The revised terminology herein follows Schöne et al. (2012).

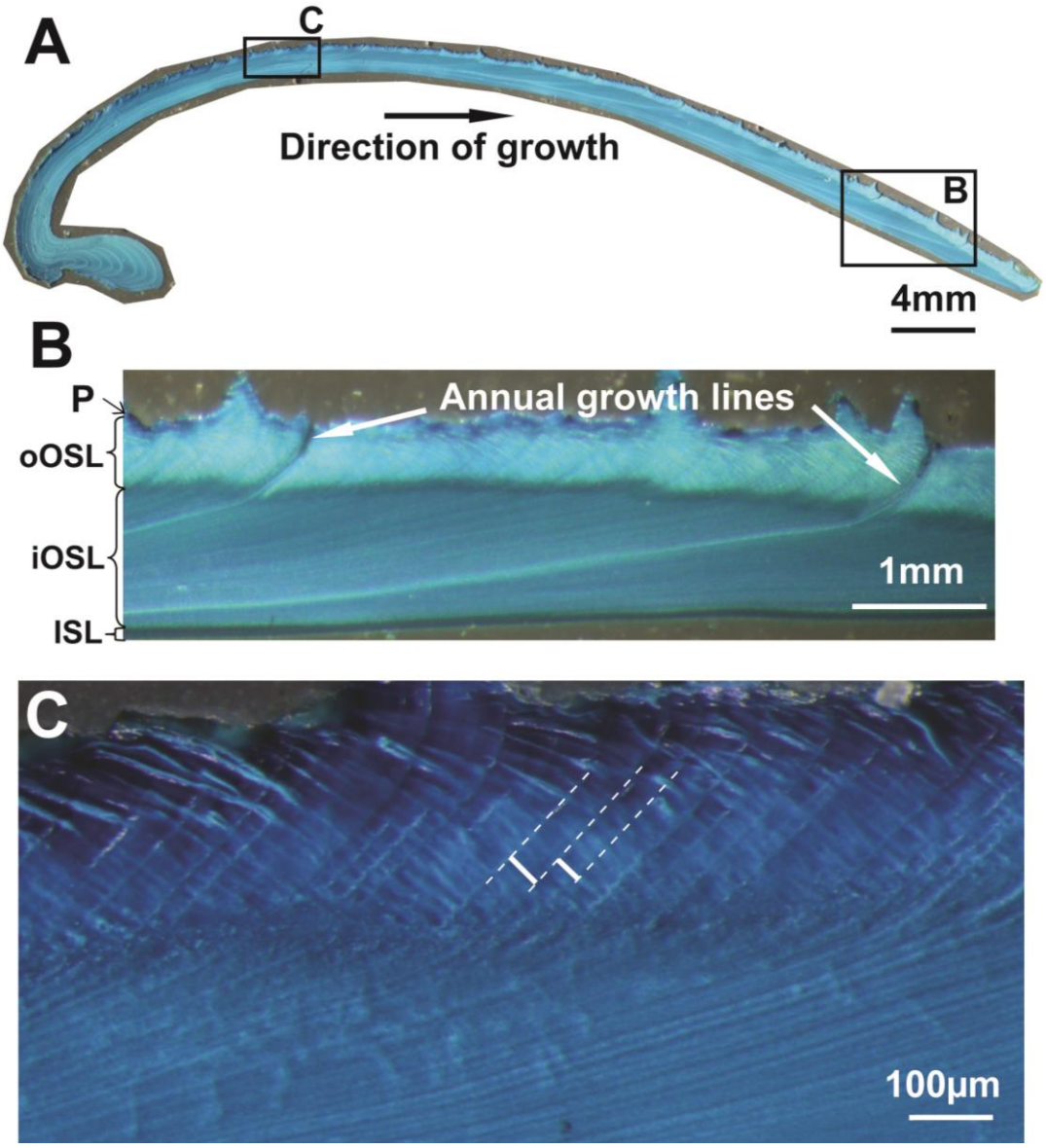

Figure 2. 3. Growth patterns in cross-sectioned valves of *Eurhomalea exalbida*. (A) Overview showing major annual growth lines in the outer shell layer of the umbo and the ventral margin separating annual growth increments. (B) Annual growth lines separate annual growth increments. (C) Daily growth increments and lines in the outer shell layer. Increment widths were measured perpendicular to the direction of growth. Legend see captions of Figure 2.2 ISL = inner shell layer.

2.2.3. Stable oxygen isotope analyses

For stable oxygen isotope analyses of shell carbonate ($\delta^{18}O_{shell}$), a total of 708 powder samples (Table 2.1) were taken from the outer sublayer of the outer shell layer of unstained cross-sections (Figures 2D+E). In fast-growing, juvenile shell portions, shell material was obtained by drilling holes with a cylindrical SiC drill bit (300 µm diameter at the tip; Komet/Gebr. Brasseler GmbH & Co. KG, model no. H52 104 003; Figures 2.2C+D). High-resolution sampling, however, required

a micromilling technique, for which a cylindrical SiC drill bit (700 µm diameter; model no. H364S 103 007; Figure 2.2C) provided excellent results. Each sample weighed between 50 and 120 µg. Samples were processed in a Thermo Finnigan MAT 253 continuous flow – isotope ratio mass spectrometer coupled to a GasBench II. Results are reported in δ-notation, and $\delta^{18}O$ values are given as parts per mil (‰). Samples were calibrated against NBS-19 ($\delta^{18}O$ = -2.20‰). On average, replicated internal precision (1σ) and the accuracy (1σ) were better than 0.07‰.

Table 2. 1. List of *Eurhomalea exalbida* specimens sampled for oxygen isotopes.

Specimen ID	Date of collection	Ontogenetic age /years sampled	No. of isotope samples	Highest resolution (days / sample)
AA-FL-A11R	21 Feb 2009	4 / 2005-2009	286	3
AA-FL-A23R	21 Feb 2009	10 / 1999-2009	141	6
AA-FL-A17R	05 Apr 2009	4 / 2005-2009	163	3
AA-FL-A18R	05 Apr 2009	9 / 2001-2009	116	4

Typically, the $\delta^{18}O_{shell}$ values reflect changes in temperature and the oxygen isotope signature of the ambient water ($\delta^{18}O_{water}$). Due to the close correlation of $\delta^{18}O_{water}$ and salinity (freshwater mixing line), the $\delta^{18}O_{shell}$ values also reflect changes in ambient salinity (Figure 2.4). If the $\delta^{18}O_{water}$ value is known and if the shells were formed in oxygen isotopic equilibrium with the fluid in which they lived, the temperature of the water can be reliably reconstructed from $\delta^{18}O_{shell}$ (Epstein et al., 1953). For the reconstruction of temperatures from $\delta^{18}O_{shell}$ values ($T_{\delta^{18}O}$) of *E. exalbida* (aragonite according to XRD analysis), we used the paleothermometry equation of Grossman and Ku (1986). However, a small modification of their equation was required because they report $\delta^{18}O_{water}$ values in SMOW-0.27% (see footnote 1 in Dettman et al. 1999). The corrected function is:

$$(1) \qquad T_{\delta^{18}O}(°C) = 20.60 - 4.34 \cdot (\delta^{18}O_{shell} - (\delta^{18}O_{water} - 0.27))$$

where $\delta^{18}O_{shell}$ is measured relative to the Vienna PDB scale and $\delta^{18}O_{water}$ is relative to the V-SMOW scale. Therefore, a 1‰ change in $\delta^{18}O_{shell}$ or $\delta^{18}O_{water}$ indicates a temperature change of 4.34°C if $\delta^{18}O_{water}$ remains unchanged.

In shallow water environments, salinity and, hence, the $\delta^{18}O_{water}$ signature can underlie seasonal and inter-annual variations that can hamper precise temperature estimates based on $\delta^{18}O_{shell}$ values unless the $\delta^{18}O_{water}$ value is closely monitored. Since no long-term observations were available for the study area, the $\delta^{18}O_{water}$ signature was reconstructed from sea surface salinity (SSS) from a nearby oceanographic station (see next section; Figure 2.1). To do so, a local freshwater mixing line was constructed for this area based on the NASA Goddard Institute for Space Studies (GISS) dataset (Schmidt, 1999; Bigg and Rohling, 1999; Global Seawater Oxygen-18 Database - v1.21; http://data.giss.nasa.gov/o18data/) as well as data provided in Colonese et al (2012) and Rozanski et al (1993) (Figure 2.4):

(2) $$\delta^{18}O_{water}(‰) = 0.30 \cdot SSS - 10.52 .$$

Salinity and the $\delta^{18}O_{water}$ value of a single water sample obtained in September 2011 from the exact same locality at which the shells lived fitted perfectly on the local freshwater mixing line introduced in equation 2 (SSS = 34.82 PSU; $\delta^{18}O_{water}$ = -0.06‰; Figure 2.4; salinity was computed from Na^+ concentration via ICP-OES using the equation given by DOE 1994, and $\delta^{18}O_{water}$ was determined via equilibration method on the GasBench II).

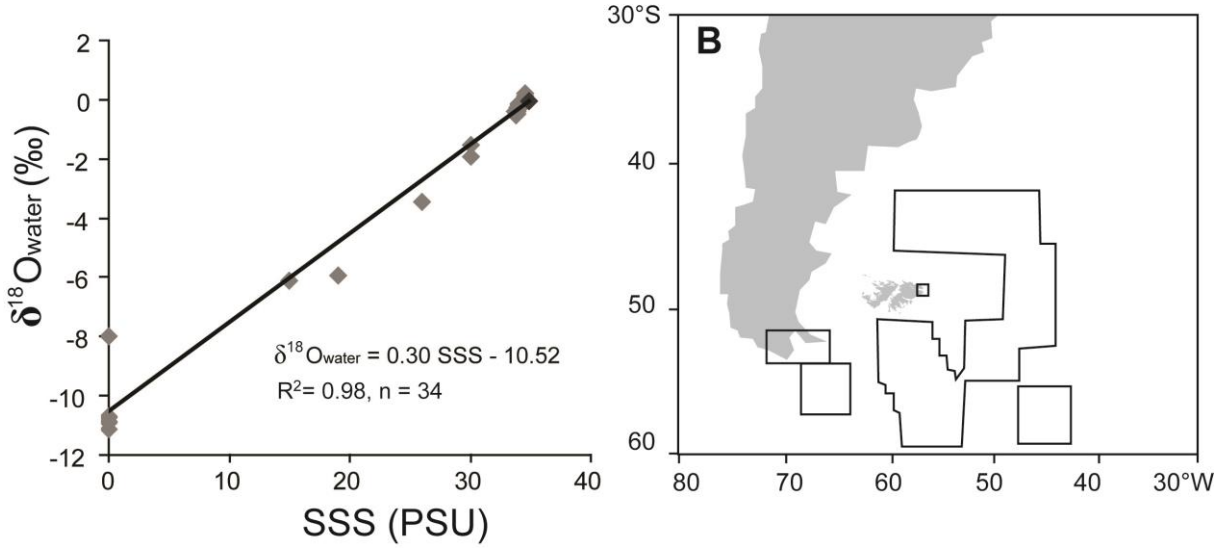

Figure 2. 4. (A) Freshwater mixing line constructed from regional $\delta^{18}O_{water}$ and sea surface salinity (SSS) data (GISS dataset; Colonese et al., 2012; Rozanski et al., 1993). Black diamond showing $\delta^{18}O_{water}$ and salinity of a water sample from the locality where the shells lived taken in September 2011. (B) Region from which the aforementioned data came.

2.2.4. Instrumental records of environmental parameters

Monthly records of sea surface salinity and sea surface temperature were obtained from an oceanographic station near the site of shell collection (Figures 2.1, 2.5). Between 1999 and 2009, monthly average salinity in 2m water depth ranged from 33.55 to 33.75 PSU with an average value of 33.68±0.12 PSU (1σ; n=70; data from some months were missing; Figure 2.5). Using equation 2, this translates into a long-term $\delta^{18}O_{water}$ value of -0.42±0.10 ‰. Freshest conditions and the largest inter-annual 1σ variability (33.55±0.26 PSU) occurred in July (Figure 2.5) which translates into a $\delta^{18}O_{water}$ value of -0.46±0.15‰. For temperature reconstructions, we used the long-term average value of -0.42‰ and the maximum observed monthly 1σ variability of 0.15‰.

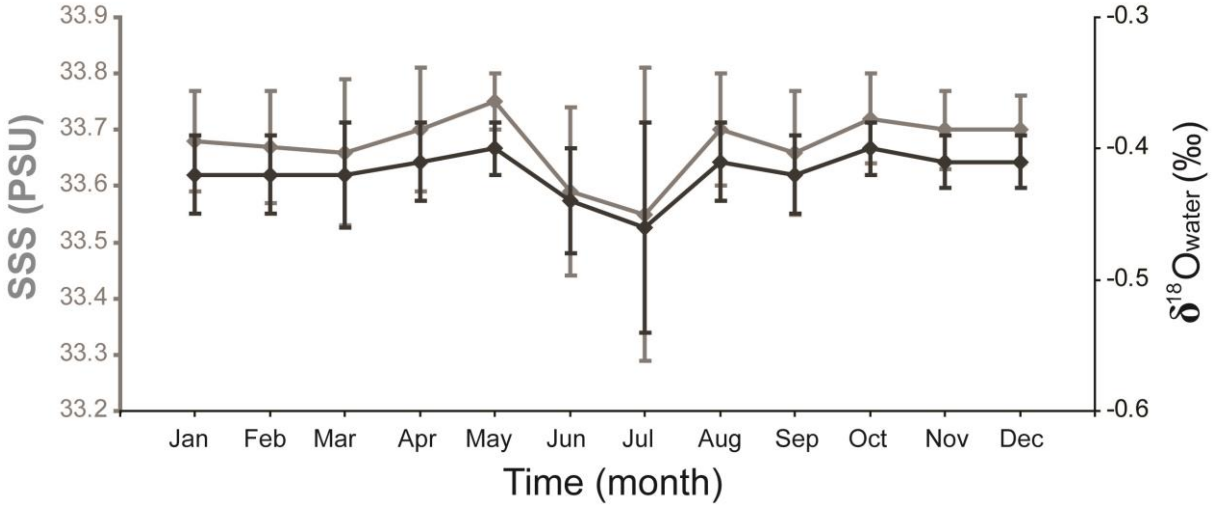

Figure 2. 5. Inter-annual (1σ error bars) variability of monthly sea surface salinity (SSS) and $\delta^{18}O_{water}$ reconstructed thereof using the regional freshwater mixing line (Figure 2.4).

During the time interval of 1999 to 2011, SST ranged from 3.19° to 12.76°C (Figure 2.6). Missing SST data of the oceanographic station record were reconstructed from remote sensing data. For this purpose, a linear regression model was computed from the oceanographic station SST and satellite SST (NOAA_OI_SST_V2 data provided by the NOAA/OAR/ESRL PSD, Boulder, Colorado, USA, from their Web site at http://www.esrl.noaa.gov/psd/). At the study locality, coldest and warmest temperatures typically occurred during August/September (austral winter) and February/March (austral summer), respectively (Figure 2.6).

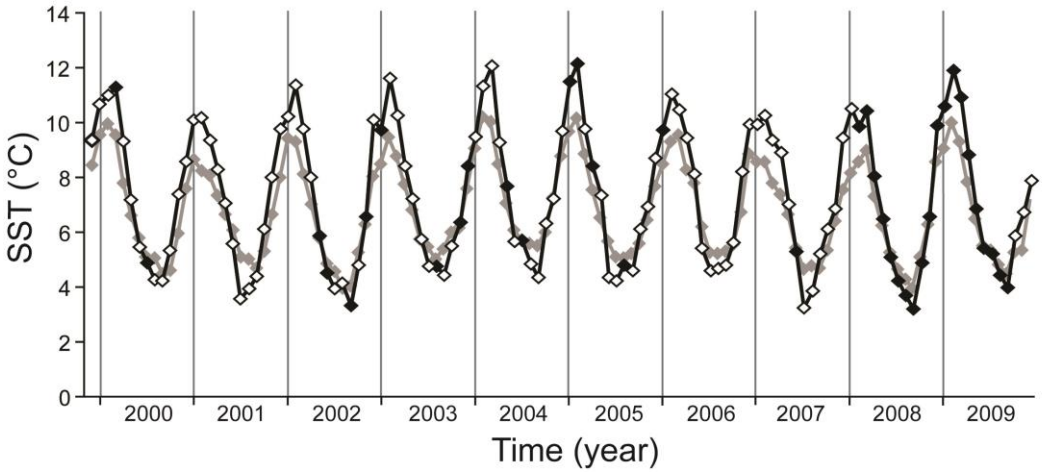

Figure 2. 6. Monthly sea surface temperature (SST) data from the oceanographic station NE Stanley (Figure 2.1) (open diamonds) and from satellite measurements (NOAA_OI_SST_V2) (grey solid diamonds). Missing data in the oceanographic station data were reconstructed (black solid diamonds) from linear regression model using remote sensing data and oceanographic data.

2.3. Results

2.3.1. Major growth patterns

In the outer shell layer (ventral margin and cardinal tooth) of all studied specimens of *Eurhomalea exalbida*, distinct major growth lines were observed (Figures 2.3A+B) which were interpreted as annual growth lines in previous studies (Lomovasky et al. 2002, Dextraze and Zinsmeister 1987, Ivany et al. 2008). These annual growth lines formed etch-resistant ridges and stood out significantly from the remaining more deeply etched shell portions, i.e. the annual growth increments (Figure 2.3B). Specimens collected in late February showed ca. 80% of the newly formed annual growth increment, whereas the annual increment formation was nearly completed and the annual growth line about to form in shells collected in early April. Before the very first annual growth line of each specimen, we observed ca. 20% (estimation based on the width of the preceding annual growth increment and the ontogenetically decreasing growth rate) of an annual growth increment.

2.3.2. Daily growth patterns

Higher magnification (100X) revealed finer-scale growth patterns that were oriented parallel to the annual growth lines (Figure 2.3C). In shell portions formed during early ontogeny (years two and three), ca. 200 micrometer-scale growth increments were detected between consecutive annual growth lines. Examples are depicted in Figure 2.7. Narrowest discernable microgrowth increments occurred near annual growth lines and measured ca. 6 µm. Microincrement widths

increased toward the middle of the annual increment, reached a maximum of ca. 60-70 µm at around increment number 155 and then gradually decreased toward the following annual growth line (Figure 2.7). Annual growth lines were typically ca. 50 µm broad and consisted of an indistinguishable number of very narrow microgrowth increments.

In many previously studied subtidal bivalve species, these microgrowth increments were shown to form on a daily basis and can be used to assign precise calendar dates to each shell portion if at least one date (e.g., the date of death) is known. Consequently, the annual increment formation (= main growing season) of *E. exalbida* at the study locality starts ca. 230 days before early April, i.e., during mid to late August (= ca. one month before the winter temperature minimum). Fastest growth would occur ca. 70 to 85 days before April, i.e., during mid to late January (= late spring/early summer) and slowest or no growth between early fall and early winter (= time of annual growth line formation) (Figure 2.7).

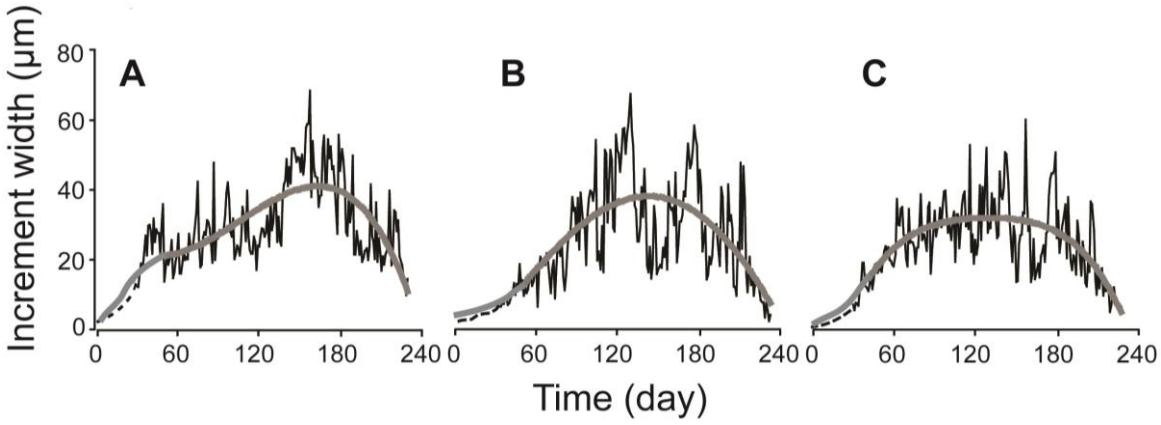

Figure 2. 7. Daily growth increment width curves in juvenile shell portions of AA-FL-A23R (A), AA-FL-A17R (B) and AA-FL-A18R (C). Higher-order polynomials have been computed to illustrate the seasonal growth trends. At the beginning of the annual increment, individual daily increments were too narrow to confidently measure their widths.

2.3.3. Shell oxygen isotopes

Intra-annual $\delta^{18}O_{shell}$ curves (Figure 2.8) of all studied shells showed distinct seasonal oscillations, but were left-skewed and strongly asymmetric. Most positive values of +1.80 to +2.22 ‰ occurred shortly after, but not directly at the annual growth lines. After a slow, gradual decline, most negative $\delta^{18}O_{shell}$ values of -0.55 to -0.97 ‰ were observed shortly before the following annual growth line (Figure 2.8). Seasonal $\delta^{18}O_{shell}$ amplitudes ranged from 2.35 to 3.13 ‰. The largest range was detected in the annual increment that was sampled with the highest spatial resolution (specimen AA-FL-A17R; Table 2.2).

Table 2. 2. Shell oxygen isotope-derived temperature extremes and ranges between 1999 and 2009. For comparison, during the same time interval instrumental winter and summer temperatures were 4.3°±1.0°C and 11.5°±1.2°C (seasonal range: 7.0°±1.0°C).

Specimen ID	$T_{\delta 18O}$ (°C)		
	Summer	Winter	Seasonal amplitude
AA-FL-A11R	17.5±2.5	9.6±0.6	7.9±2.6
AA-FL-A23R	17.0±2.4	11.1±1.5	6.0±1.6
AA-FL-A17R	16.6±3.6	8.7±0.7	7.9±3.0
AA-FL-A18R	16.6±1.8	11.2±0.8	5.4±1.5

2.3.4. Shell oxygen isotope-derived water temperatures

To compute water temperatures from $\delta^{18}O_{shell}$ values ($T_{\delta 18O}$), we assumed a $\delta^{18}O_{water}$ value of -0.42±0.15‰ based on a long-term average salinity (see section 2.4) and equation 2. The 1σ error represents the maximum observed monthly variability which occurred during July (Figure 2.5). The data were temporally aligned so that the reconstructed temperatures were in best agreement (tested by linear regression analysis) with the instrumentally determined temperatures (Figure 2.9). According to this temporal alignment, the annual growth increments formed between mid-August and early April of the following year and captured the annual minimum and maximum temperatures in most cases (Figure 2.9). Furthermore, annual growth lines (= shell portion representing the time interval of strongly reduced or even halted shell growth) were deposited between early April and mid-August of the following year (Figure 2.9).

In Figure 2.9 (upper panel), an independent dating technique was applied. In the first step, presumed daily increments were used to estimate the time represented by each $T_{\delta 18O}$ value. Then, this (floating, not yet calendar aligned) $T_{\delta 18O}$ chronology was compared with the weekly satellite SST data and so arranged that the shapes of the floating $T_{\delta 18O}$ chronology and the satellite time-series closely matched (shape matching technique). This procedure enabled the identification of the timing of seasonal shell growth, i.e., mid-August to early April of the following year.

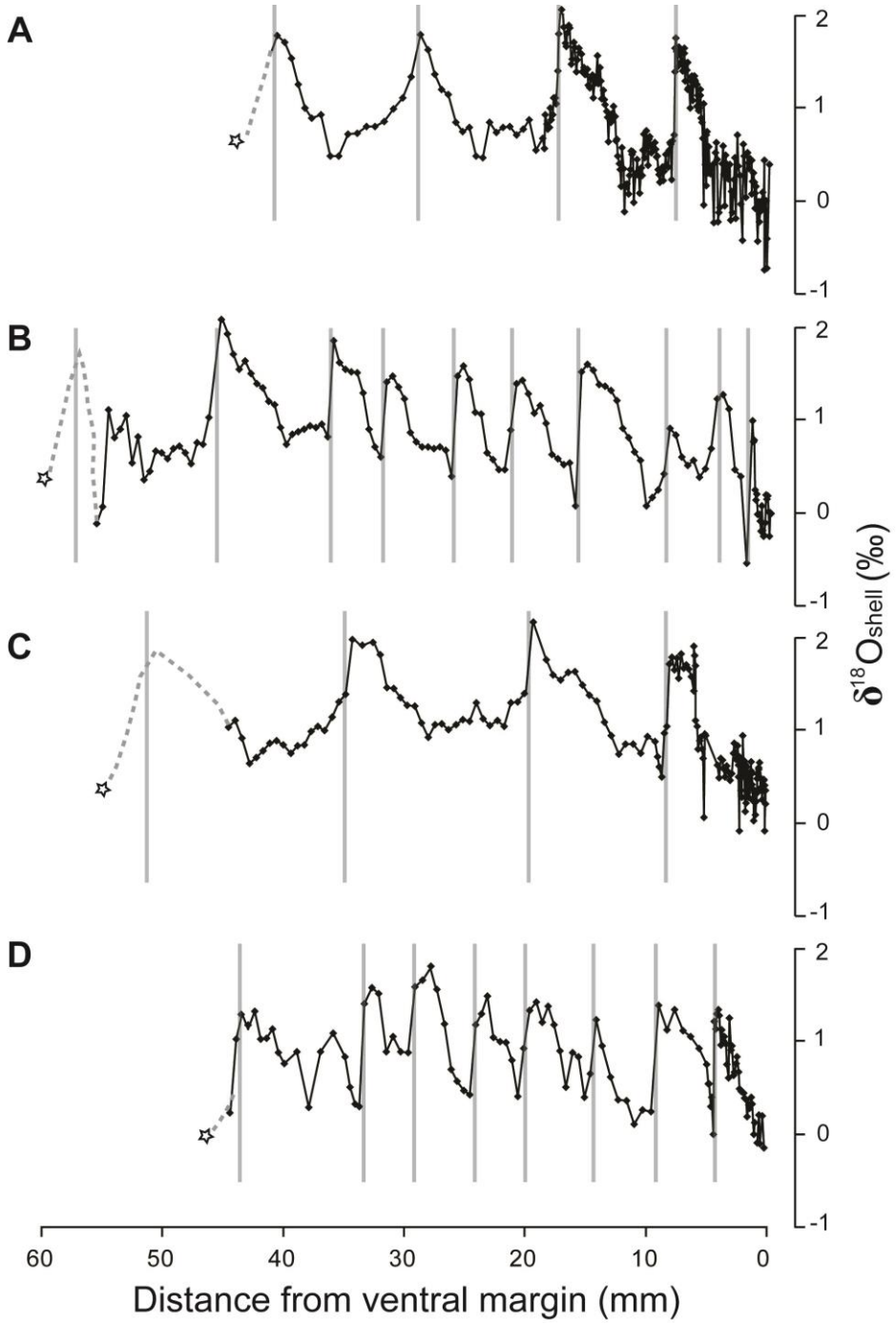

Figure 2. 8. $\delta^{18}O_{shell}$ records of four specimens of *Eurhomalea exalbida* collected on 21st February 2009 (A: AA-FL-A11R, B: AA-FL-A23R) and 5th April 2009 (C: AA-FL-A17R, D: AA-FL-A18R) respectively. Asterisks denote first shell formation; vertical grey lines.

In addition, the (presumed) daily increment widths were depicted in this figure to illustrate how shell growth and temperature are related to each other. As described in section 3.2., maximum shell growth did not fall together with the highest summer temperature and annual growth lines were not formed during winter, but between early April and mid-August of the following year. Furthermore, the number of microgrowth increments counted between the

minimum and maximum oxygen isotope-derived water temperatures (~170) coincided very well with the number of days that elapsed during the time interval between the observed winter and summer extremes (~180) (Figure 2.9).

Although reconstructed (6.8±1.3°C) and instrumentally determined (7±1.0°C) seasonal temperature ranges were largely the same, the $T_{\delta 18O}$ overestimated instrumental data by 2.1°-8.3°C (on average, ca. 6°C; corresponding to a $\delta^{18}O_{shell}$ shift of -0.48‰ to -1.91‰; on average, -1.39‰) (Figure 2.9). When shifted by the average computed offset of 6°C, $T_{\delta 18O}$ of the first few years of growth underestimated actual temperatures, while those of ontogenetic years eight to ten, or so, overestimated instrumental temperatures. In other words, with increasing ontogenetic age, the discrepancy between measured and reconstructed temperatures increased exponentially, no matter if summer or winter extremes were compared (Figure 2.10).

2.4. Discussion

According to the results of this calibration study, the long-lived bivalve, *Eurhomalea exalbida* is a highly suitable candidate for detailed paleoclimate reconstructions of mid to high latitude settings of the southern hemisphere. Specifically, this species likely grows during the coldest and warmest part of the year and is, thus, capable of providing information on nearly the full seasonal temperature amplitude of the past. Other than tree ring data, which only contain data on the austral summer, shells of *E. exalbida* can also be used to estimate winter temperatures. Winter proxies are highly relevant for paleoclimate models, because many natural climate phenomena occur during the cold season. However, absolute temperature reconstructions based on shell oxygen isotopes of this species are not as straightforward and simple as in the case of many other bivalve mollusks.

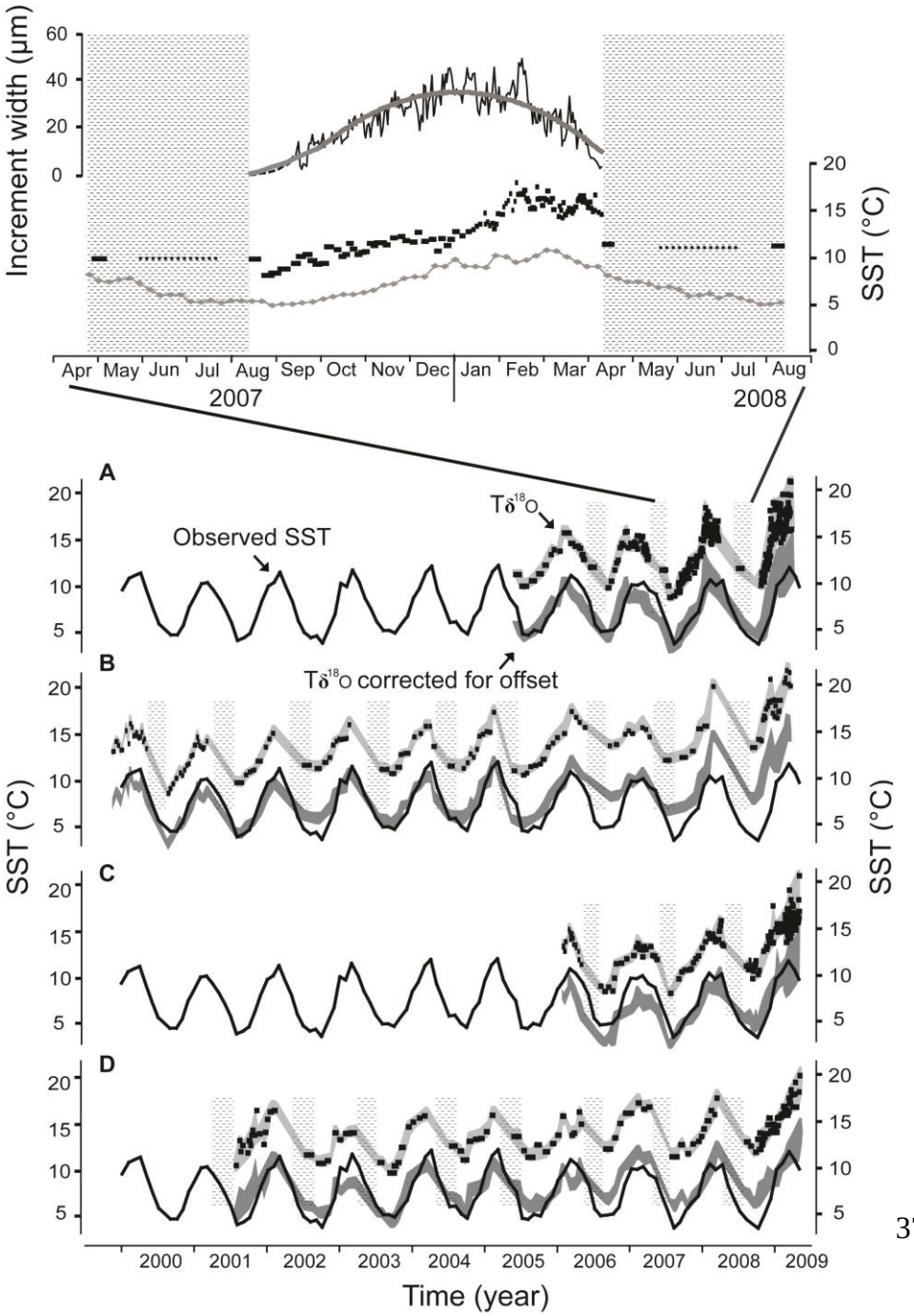

Figure 2. 9. Temporal alignment of $\delta^{18}O_{shell}$ and $T_{\delta 18O}$ data. Upper panel: $\delta^{18}O_{shell}$ values were first temporally arranged by daily increments and then, the constructed floating $\delta^{18}O_{shell}$ chronology cross-matched with weekly satellite SST data. The main growing season started in mid-August and ended in early April of the following year. Little to no growth occurred during the remainder of the year resulting in the formation of an annual growth line. Average daily increment width chronology (computed from three curves in Figure 2.8) is shown for direct comparison with temperature data. Note that shell growth is not always coupled to temperature. For example, maximum growth occurred during late spring/early summer, but not when the maximum temperatures prevailed. Despite similar temperatures in austral spring and fall, shell growth is strongly reduced in fall. Lower panel: Temporally aligned $T_{\delta 18O}$ (small dark dots) and 1σ error (indicated by grey envelope; envelope is also shown for times during growth line formation when shell was growing very slowly or not at all). Apparently, oxygen isotope-derived temperatures overestimated instrumental temperatures by 2.1°-8.3°C. When shifted by the average offset (6°C; dark grey envelope), reconstructed and measured temperatures fitted well, but not perfectly, because offset increased during ontogeny. Vertical grey bars denote annual growth lines.

2.4.1. Disequilibrium fractionation

The most surprising result of this study was that *E. exalbida* did not form its shell in oxygen isotopic equilibrium with the ambient water, but ca. -0.48‰ to -1.91‰ away from it depending on ontogenetic age. With increasing age, the offset seemed to increase exponentially (Figure 2.10; see also discussion in section 4.1.2). Accordingly, $T_{\delta 18O}$ of one to ten year-old specimens overestimated actual temperatures by ca. 2.1°-8.3°C. If this offset

(3) $\delta^{18}O_{offset} = 4.20 \cdot e^{0.07 \cdot age}$ (Figure 2.10)

is taken into account, however, shell oxygen isotope-derived temperatures can provide instrumental temperature estimates to approximately the nearest 0.9°C (95% confidence interval of data from the four studied shells depicted in Figure 2.10).

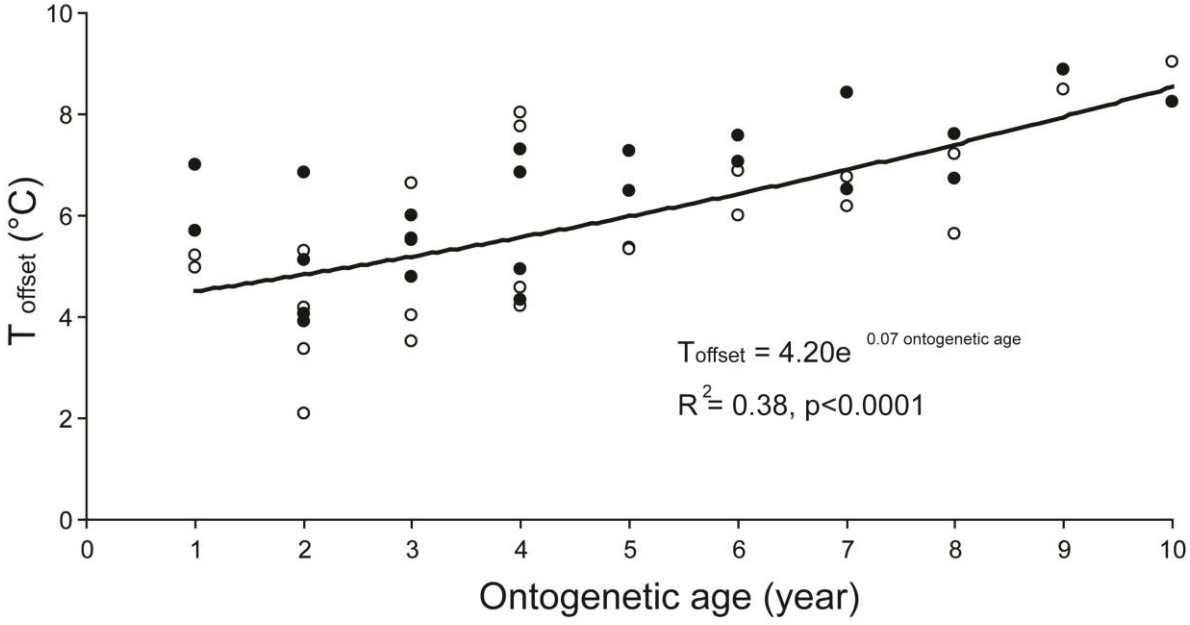

Figure 2. 10. Discrepancy (T_{offset}) between instrumentally determined and shell oxygen isotope-derived temperatures increased exponentially during ontogeny. Filled circles = winter values; open circles = summer values.

2.4.1.1 Reliability of environmental data used for calibration

It is not very common for a sclerochronologist to find bivalves precipitating their shells out of equilibrium. The first question that arises is about the reliability of the environmental data used for calibration. Despite the fact that salinity (and hence the reconstructed $\delta^{18}O_{water}$ value) was not monitored at Sparrow Cove, where the shells lived (Figure 2.1), but rather at an oceanographic station less than 4km away, their close proximity and the well-mixed surface ocean water in this region makes it unlikely that $\delta^{18}O_{water}$ at Sparrow Cove differed significantly from that measured at the oceanographic station. Moreover, the constant offset observed between measured and $\delta^{18}O_{shell}$-based temperatures could only be reduced if the $\delta^{18}O_{water}$ values at Sparrow were 1‰ more negative than those measured at the nearby station. This seems very unlikely, because the oxygen isotope signature of water collected from Sparrow Cove in September 2011 was nearly the same as the long-term average station value. Furthermore, if the $\delta^{18}O_{water}$ variability at Sparrow Cove would have been larger on seasonal and inter-annual time-scales, the measured and reconstructed temperatures would likely not have matched each other so well and seasonal ranges would have been significantly different. Therefore, the oceanographic station data should reflect the conditions at Sparrow Cove very closely, and the observed isotopic offset in *E. exalbida* is real.

2.4.1.2 Vital effects

The observed departures from oxygen isotopic equilibrium in shells of *E. exalbida* were probably caused by vital effects (Urey et al. 1951; Epstein et al., 1951), i.e., kinetic and/or metabolic isotope effects that affected the ion sources for oxygen reaching the site of calcification. In bivalves the common ion source for oxygen is HCO_3^- which moves across ion channels of the mantle epithelium (Wheeler, 1992).

Due to kinetic isotope effects, faster shell growth would increase the relative amount of ^{16}O (Erez, 1978; McConnaughey, 1989) in the newly formed shell and result in more negative $\delta^{18}O_{shell}$ values than expected for equilibrium. However, despite significantly changing rates of shell growth during the growing season, we did not observe a larger oxygen isotopic offset in shell portions formed during summer (fast growth) than during winter (slow growth) (Figure 2.10). More importantly, slower growing shell portions of *E. exalbida* exhibited a larger offset than faster growing youth portions (Figure 2.10). Therefore, kinetic effects cannot explain the observed offset.

Metabolic isotope effects include the incorporation into the shell of isotopically light CO_2 originating from respiration (Swart, 1983). Respired CO_2 can likely be ruled out, because bivalves utilize the oxygen of the ambient water (in marine systems: oxygen from HCO_3^-) and not that of ingested food to secrete its shell (Epstein et al., 1953; McConnaughey, 1989; McConnaughey and

Gillikin, 2008). Moreover, the availability of metabolic CO_2 fluctuates seasonally (higher during times of increased ingestion and seasonally available food) and would, therefore, result in seasonally varying oxygen isotopic offsets. However, this has not been observed.

Another kind of metabolic effects involve changes in pH affecting the oxygen isotope exchange between dissolved inorganic carbon species (CO_2, H_2CO_3, HCO_3^-, CO_3^{2-}) and H_2O (McConnaughey, 1989). At intermediate pH, bicarbonate ions dominate in the solution, whereas carbonate ions are most abundant at high pH (Spero et al., 1997; Zeebe, 1999). Since CO_3^{2-} is isotopically lighter than the bicarbonate ion, a more alkaline solution will be more depleted in ^{18}O and, thus, the $CaCO_3$ forming from that solution will have a lower $\delta^{18}O$ value (Zeebe, 1999). Typically, the extrapallial fluid (EPF) of bivalves has the same pH as the ambient seawater, i.e., around 8 in living oceans. We hypothesize here that the progressive depletion in ^{18}O in the shell of *E. exalbida* during ontogeny resulted from an ontogenetic increase in pH of the EPF. Support for this assumption comes from reports on ontogenetic changes in the amount and composition of amino acids in some bivalve species. For example, in *Arctica islandica*, the relative abundance of less acidic amino acids increase during ontogeny (Goodfriend and Weidman, 2001). This may shift the pH of the EPF toward higher values and result in more negative $\delta^{18}O_{shell}$ values than expected for equilibrium with seawater.

Additional future research is certainly needed to understand in more detail the actual mechanisms behind the observed ontogenetic changes of the oxygen isotope fractionation in this species. This is particularly relevant because more recent studies have suggested that the EPF may not be the agent of the shell precipitation process (e.g., Jacob et al., 2008). Therefore, the hypotheses discussed in the previous section may not hold true. Subsequent studies should also analyze how large the $\delta^{18}O_{offset}$ value becomes in gerontic specimens of *E. exalbida*. As extrapolation using equation 3 would result in an unrealistically large offset at the maximum recorded age for this species (564‰ at age 70), it is likely that the offset is not an exponential function throughout the life of the organism. Rather, the $\delta^{18}O_{offset}$ may be better described by linear equation or a logistic function in which the offset is approximately exponential in the early growth phase (observed here), and approaches a stable value during the later stages of growth. However, this has to be subject of subsequent studies.

2.4.1.3 Oxygen isotopic disequlibrium fractionation in other bivalves

The present paper is not the first to report on bivalve shells which do not precipitate their shells in oxygen isotopic equilibrium with the ambient environment as suggested by the equation by Grossman and Ku (1986). For example, Hallmann et al (2008) documented such disequilibrium effects in shells of the geoduck, *Panopea abrupta* from Puget Sound, Washington State, U.S.A.

Temperatures reconstructed from $\delta^{18}O_{shell}$ values of these geoducks overestimated actual water temperatures by up to ca. 4°C. Less severe disequilibrium effects have also been reported from various other bivalves (Goodwin et al., 2001; Gillikin et al., 2005). Some authors even provided species-specific paleotemperature equations (e.g., Carré et al 2005). It should be noted that *E. exalbida* does not simply form its shell with a constant offset from expected equilibrium, but this offset changes through lifetime. Therefore, we used the term "disequilibrium" rather than 'shifted equilibrium'.

It is likely that disequilibrium fractionation effects existed in fossil relatives of *E. exalbida* as well. For example, $T_{\delta 18O}$ of *Eurhomalea* spp. from the Eocene of Antarctica exceeded those of coeval *Cucullaea raea* specimens, on average, by 2°C (Ivany et al., 2008). According to the authors, *C. raea* preferred the colder temperature range, whereas *Eurhomalea* spp. did not grow shell during winter. However, if the physiological tolerances of *Eurhomalea* spp. have not changed through time and if they remain the same in different species of this genus, the Eocene *Eurhomalea* spp. specimens might have grown during the warmest and coldest part of the year and formed their shells away from oxygen isotopic equilibrium with the ambient water like living *E. exalbida*.

2.4.2. Annual growth lines, but no winter lines

Like all other hitherto studied bivalve species, *E. exalbida* does not grow continuously and at the same rate throughout the year, but shell formation slows down periodically to form an annual growth line (Figure 2.9). However, the exact timing of the annual growth line formation in *E. exalbida* has been misinterpreted in previous studies. According to Dextraze and Zinsmeister (1987), Lomovasky et al (2002) and Ivany et al (2008), annual growth lines in *Eurhomalea* spp. form during winter. Whereas Dextraze and Zinsmeister (1987) merely assumed that *Eurhomalea* spp. form winter lines "analogous to tree rings" and other bivalve species, Lomovasky et al (2002) and Ivany et al (2008) based their interpretation on geochemical data. Shell oxygen isotope curves exhibited seasonal oscillations with most positive $\delta^{18}O_{shell}$ values occurring near annual growth lines. However, the coarse sampling resolution and missing information on seasonal growth rates did not permit a more precise analysis of the exact timing and duration of shell growth.

As demonstrated by high-resolution $\delta^{18}O_{shell}$ and growth pattern analyses in the present study (Figure 2.9), shell growth of *E. exalbida* is not exclusively controlled by temperature, and at the studied locality this species does not form winter lines. (1) Maximum shell growth does not occur at the highest temperatures in February/March, but ca. one month before that time during mid/late January (Figure 2.9). Likely, this is because food availability is highest during this time of the year (Signorini et al., 2006). The importance of food availability for bivalve shell growth

has long been known and has been described in detail, for example, by Ansell (1968) for *Mercenaria mercenaria*. (2) The onset of the annual growing season of *E. exalbida* occurs around mid-August, before the seasonal temperature minimum (August/September). Therefore, this species closely captures environmental conditions in its shell that occur during the coldest part of the year. (3) Despite similar temperatures during September to December and May to July/August, very little or no shell material is formed between early fall and early winter (Figure 2.9). As a consequence, the seasonal $T_{\delta 18O}$ curve is strongly asymmetric (left-skewed) and exhibits a saw-tooth shaped pattern (Figure 2.9).

In summary, at the study site, *E. exalbida* did not form winter lines. Instead, annual growth line formation took place between early fall and early winter (Figure 2.9). During this time interval, shell growth was at minimum or even halted. Similar findings have previously been reported for other long-lived cold-water species such as *Arctica islandica* from the northern North Atlantic (Jones, 1980; Schöne et al., 2005b). Jones (1980) suggested that growth line formation in *A. islandica* falls together with the time interval of most intense spawning (Mann, 1982). The annual temperature maximum could function as a stimulus for spawning and a concomitant reduction in shell growth (Jones, 1981; Mann, 1989). However, the spawning peak in *E. exalbida* typically occurs during November (Morriconi et al., 2002). Taking the amount of shell that formed before the very first annual growth line (~20% of an annual growth increment) into account, *E. exalbida* probably started forming the first shell material during January/February, about three months after spawning/hatching. Therefore, the timing of the annual cessation of shell growth in this species does not seem to be linked to reproduction, and further research is required to understand its actual cause(s).

2.4.3. Microgrowth patterns: daily periods of shell growth

In conjunction with microincrement counts, cross-matching of observed and oxygen isotope-derived temperature curves suggested that shell growth occurred on a daily basis. For example, the number of microgrowth increments between the lowest and highest $T_{\delta 18O}$ corresponded nearly perfectly to the number of days that had elapsed between the instrumentally determined seasonal temperature extremes.

2.5. Summary and conclusions

This paper highlighted the need for rigorous calibration studies prior to using stable oxygen isotope values of bivalve shells for paleoclimate reconstructions. Specifically, it is required to test whether the shells are formed in isotopic equilibrium with the ambient water, i.e., whether shell oxygen isotope-derived temperatures given by the Grossman and Ku (1986) equation equal instrumental temperature data.

Specimens of *Eurhomalea exalbida* from a shallow subtidal setting in the NE of the Falkland Islands show distinct annual and daily growth patterns in their shells. The main growing season starts in mid-August about one month before the seasonal temperature minimum and ends in early April about one month after the summer temperature maximum. Fastest growth occurs during late spring and early summer. Annual growth lines are laid down between later summer and early winter. This species forms its shell with a negative offset of -0.48‰ to -1.91‰ from the expected oxygen isotopic equilibrium with the ambient water, resulting in an overestimation of actual temperatures by 2.1°-8.3°C. With increasing ontogenetic age, the discrepancy between measured and reconstructed temperatures increased exponentially, no matter if summer or winter extremes were compared.

If this disequilibrium fractionation effect is taken into account, *E. exalbida* represents a unique high-resolution paleotemperature archive for mid to high latitude settings of southern South America providing robust and reliable winter and summer temperature estimates, even from single specimens. Such data can elucidate regional and continental-scale climate patterns and provide an insight into land-sea interactions. The importance of such a high-resolution marine recorder from southern South America becomes apparent when considering the well-known role of the Southern Ocean in regulating the global climate (e.g., Emile-Geay et al., 2007). Future studies should investigate how the observed disequilibrium fractionation effect changes through lifetime of older specimens. Given the longevity of this species and its potential to record decadal climate variations (Lomovasky et al., 2002), future studies should combine the construction of long, uninterrupted master chronologies with geochemical studies similar to current efforts in the northern North Atlantic and north Pacific (Schöne et al., 2003; Black et al., 2008; Butler et al., 2013).

2.6. Acknowledgments

We are grateful to divers of the Shallow Marine Survey Group (SMSG) from the Falkland Islands for collection of specimens of bivalves, and water samples from Sparrow Cove, Port William, East Falkland. Special thanks go to *** for processing the isotope samples and general technical assistance. We thank *** for information on the biogeographic distribution of *E. exalbida*. *** is kindly acknowledged for comments on a former draft of this manuscript. Satellite SST (NOAA_OI_SST_V2) data were obtained from NOAA/OAR/ESRL PSD, Boulder, Colorado, USA, from their Web site at http://www.esrl.noaa.gov/psd/. Salinity and $\delta^{18}O_{water}$ values for the northwest Pacific came from the NASA-Goddard Institute for Space Studies (http://data.giss.nasa.gov/o18data/). Two anonymous reviewers provided very helpful comments; we are grateful for their assistance. This study was made possible by PhD scholarship to LY

awarded by the China Research Council and a research grant to BRS by the German Research Foundation, DFG (SCHO 793/4).

2.7. References

Ansell, A.D., 1968. The rate of growth of the hard clam *Mercenaria mercenaria* (L) throughout the geographic range. Journal du Conseil Permanent International pour l'Exploration de la Mer 31, 364–409.

Bigg, G.R., and Rohling, E.J., 2000. An oxygen isotope data set for marine water. Journal of Geophysical Research 105, 8527–8535.

Black, B.A., Gillespie, D.C., MacLellan, S.E., and Hand, C.M., 2008. Establishing highly accurate production-age data using the tree-ring technique of crossdating: a case study for Pacific geoduck (*Panopea abrupta*). Canadian Journal of Fisheries and Aquatic Science 65, 2572–2578.

Briffa, K.R., Jones, P.D., and Schweingruber, F.H., 1994. Summer temperatures across northern North America: Regional reconstructions from 1760 using tree-ring densities. Journal of Geophysical Research 99, 25835–25844.

Büntgen, U., Tegel, W., Nicolussi, K., McCormick, M., Frank, D., Trouet, V., Kaplan, J.O., Herzig, F., Heussner, K.-U., Wanner, H., Luterbacher, J., and Esper, J., 2011. 2500 years of European climate variability and human susceptibility. Science 331, 578–582.

Butler, P.G., Wanamaker, Jr, A.D., Scourse, J.D., Richardson, C.A., and Reynolds, D.J., 2013. Variability of marine climate on the North Icelandic Shelf in a 1,357-year proxy archive based on growth increments in the bivalve *Arctica islandica*. Palaeogeography, Palaeoclimatology, Palaeoecology 373, 141–151.

Carré, M., Bentaleb, I., Blamart, D., Ogle, N., Cardenas, F., Zevallos, S., Kalin, R.M., Ortlieb, L., and Fontugne, M., 2005. Stable isotopes and sclerochronology of the bivalve *Mesodesma donacium*: Potential application to Peruvian paleoceanographic reconstructions. Palaeogeography, Palaeoclimatology, Palaeoecology 228, 4–25.

Chiesa, J.O., Parma, S.G., and Camacho, H.H., 1995. Observaciones estratigraficas en el Paleogeno del noroeste de la Provincia de Santa Cruz (Republica Argentina). Parte II: Invertebrados marinos de la Formacion El Chacy (Eoceno), Provincia de Santa Cruz, Argentina. Systematica y bioestratigrafia. Monografias de la Acadamia Nacional de Ciencias Exactas, Fisicas Y Naturales 11, 17–68.

Colonese, A.C., Verdun-Castello, E., Alvarez, M., Godino, I.B., Zueeo, D., and Salvatelli, L., 2012. Oxygen isotopic composition of limpet shells from the Beagle Channel: implications for seasonal studies in shell middens of Tierra del Fuego. Journal of Archaeological Science, doi:10.1016/j.jas.2012.01.012.

Dettman, D.L., Reische, A.K., and Lohmann, K.C., 1999. Controls on the stable isotope composition of seasonal growth bands in aragonitic fresh-water bivalves (unionidae). Geochimica et Cosmochimica Acta 63, 1049–1057.

Dextraze, B.L., and Zinsmeister, W.J., 1987. A study of the internal annual growth lines of the late Eocene mollusk *Eurhomalea* Antarctica. Antarctic Journal of the United States 22, 14–15.

DOE, 1994. Handbook of methods for the analysis of the various parameters of the carbon dioxide system in sea water; version 2, Dickson, A.G., and Goyet, C., (eds.) ORNL/CDIAC-74.

Emile-Geay, J., Cane, M., Seager, R., Kaplan, A., and Almasi, P., 2007. El Niño as a mediator of the solar influence on climate. Paleoceanography 22, PA3210, doi:10.1029/2006PA001304.

Epstein, S., Buchsbaum, R., Lowenstam, H., and Urey, H.C., 1951. Carbonate-water isotopic temperature scale. Bulletin of the Geological Society of America 62, 417–426.

Epstein, S., Buchsbaum, R., Lowenstam, H.A., and Urey, H.C., 1953. Revised carbonate-water isotopic temperature scale. Bulletin of the Geological Society of America 64, 1315–1326.

Erez, J., 1978. Vital effect on stable-isotope composition seen in foraminifera and coral skeletons. Nature 273, 199–202.

Garreaud, R.D., Vuille, M., Compagnucci, R., and Marengo, J., 2009. Present-day South American climate. Palaeogeography, Palaeoclimatology, Palaeoecology 281, 180–195.

Gillikin, D.P., De Ridder, F., Ulens, H., Elskens, M., Keppens, E., Baeyens, W., and Dehairs, F., 2005. Assessing the reproducibility and reliability of estuarine bivalve shells (*Saxidomus giganteus*) for sea surface temperature reconstruction: implications for paleoclimate studies. Palaeogeography, Palaeoclimatology, Palaeoecology 228, 70–85.

Goodfriend, G.A., and Weidman, C.R., 2001. Ontogenetic trends in aspartic acid racemization and amino acid composition within living and fossil shells of the bivalve Arctica. Geochimica et Cosmochimica Acta 65, 1921–1932.

Goodwin, D.H., Flessa, K.W., Schöne, B.R., and Dettman, D.L., 2001. Cross-calibration of daily growth increments, stable isotope variation, and temperature in the Gulf of California bivalve mollusk *Chione cortezi*: implications for paleoenvironmental analysis. Palaios 16, 387–398.

Grossman, E.L., and Ku, T.-L., 1986. Oxygen and carbon isotope fractionation in biogenic aragonite; temperature effects. Chemical Geology (Isotope Geoscience Section) 59, 59–74.

Hallmann, N., Schöne, B.R., Strom, A., and Fiebig, J., 2008. An intractable climate archive - Sclerochronological and shell oxygen isotope analyses of the Pacific geoduck, *Panopea abrupta* (bivalve mollusk) from Protection Island (Washington State, USA). Palaeogeography, Palaeoclimatology, Palaeoecology 269, 115–126.

Ivany, L.C., Lohmann, K.C., Hasiuk, F., Blake, D.B., Glass, A., Aronson, R.B., and Moody, R.M., 2008. Eocene climate record of a high southern latitude continental shelf: Seymour Island, Antarctica. Bulletin of the Geological Society of America 120, 659–678.

Jacob, D.E., Soldati, A.L., Wirth, H., Huth, J., Wehrmeister, U., and Hofmeister, W., 2008. Nanostructure, composition and mechanisms of bivalve shell growth. Geochimica et Cosmochimica Acta 72, 5401–5415.

Jones, D.S., 1980. Annual cycle of shell growth increment formation in two continental shelf bivalves and its paleoecologic significance. Paleobiology 6, 331–340.

Jones, D.S., 1981. Reproductive cycles of the Atlantic surf clam *Spisula solidissima*, and the ocean quahog *Arctica islandica* off New Jersey. Journal of Shellfish Research 1, 23–32.

Jones, P.D., Osborn, T.J., and Briffa, K.R., 2001. The evolution of climate over the last millennium. Science 292, 662–667.

Keen, M., 1954. Nomenclatural notes on the pelecypod Family Veneridae. Minutes of the Conchological Club of Southern California 139, 50–55.

Lomovasky, B.J., Brey, T., Morriconi, E., and Calvo, J., 2002. Growth and production of the venerid bivalve *Eurhomalea exalbida* in the Beagle Channel, Tierra del Fuego. Journal of Sea Research 48, 209–216.

Mann, R., 1982. The seasonal cycle of gonadal development in *Arctica islandica* from the southern New England shelf. Fishery Bulletin (U.S.) 80, 315–326.

Mann, R., 1989. Larval ecology of *Arctica islandica* on the inner continental shelf of the eastern United States. Journal of Shellfish Research 8, 464.

McConnaughey, T. 1989. ^{13}C and ^{18}O isotopic disequilibrium in biological carbonates: II. In vitro simulation of kinetic isotope effects. Geochimica et Cosmochimica Acta 53, 163–171.

McConnaughey, T.A., and Gillikin, D.P., 2008. Carbon isotopes in mollusk shell carbonate. Geo-Marine Letters 28, 287–299.

Morriconi, E., Lomovasky, B.J., Calvo, J., and Brey, T., 2002. The reproductive cycle of *Eurhomalea exalbid*a (Chemnitz, 1795) (Bivalvia: Veneridae) in Ushuaia Bay (54°50' S), Beagle Channel (Argentina). Invertebrate Reproduction and Development 42, 61–68.

Neukom, R., del Rosario Prieto, M., Moyano, R., Luterbacher, J., Pfister, C., Villalba, R., Jones, P.D., and Wanner, H., 2009. An extended network of documentary data from South America and its potential for quantitative precipitation reconstructions back to the 16th century. Geophysical Research Letters 36, L12703, doi:10.1029/2009GL038351.

Neukom, R., Luterbacher, J., Villalba, R., Kuttel, M., Frank, D., Jones, P.D., Grosjean, M., Wanner, H., Aravena, J.-C., Black, D.E., Christie, D.A., D'Arrigo, R., Lara, A., Morales, M., Soliz-Gamboa, C., Srur, A., Urritia, R., and von Gunten, L. 2011. Multiproxy summer and winter surface air temperature field reconstructions for southern South America covering the past centuries. Climate Dynamics 37, 35–51.

Powell, A.W., 1960. Antarctic and Subantarctic Mollusca. Records of the Auckland Institute and Museum 5, 117–193.

Ríos, E., 1994. Seashells of Brazil. 2nd edition. Editora da Fundação Universidade do Rio Grande, Rio Grande, USA, pp. 368.

Rozanski K., Araguas-Araguas L., and Gonfiantini R., 1993. Isotopic patterns in modern global precipitation. Geophysical Monograph Series78, 1–36.

Schmidt, G.A., 1999. Forward modeling of carbonate proxy data from planktonic foraminifera using oxygen isotope tracers in a global ocean model. Paleoceanography 14, 482–497.

Schöne, B.R., Dunca, E., Fiebig, J., and Pfeiffer, M., 2005a. Mutvei's solution: an ideal agent for resolving microgrowth structures of biogenic carbonates. Palaeogeography, Palaeoclimatology, Palaeoecology 228, 149–166.

Schöne, B.R., Houk, S.D., Freyre Castro, A.D., Fiebig, J., Kröncke, I., Dreyer, W., and Oschmann, W., 2005b. Daily growth rates in shells of *Arctica islandica*: Assessing sub-seasonal environmental controls on a long-lived bivalve mollusk. Palaios 20, 78–92.

Schöne, B.R., Oschmann, W., Kröncke, I., Dreyer, W., Janssen, R., Rumohr, H., Houk, S.D., Freyre Castro, A.D., Dunca, E., and Rössler, J., 2003. North Atlantic Oscillation dynamics recorded in shells of a long-lived bivalve mollusk. Geology 31, 1037–1040.

Schöne, B.R., Radermacher, P., Zhang, Z., and Jacob, D.E., 2012. Crystal fabrics and element impurities (Sr/Ca, Mg/Ca, and Ba/Ca) in shells of *Arctica islandica* – implications for paleoclimate reconstructions. Palaeogeography, Palaeoclimatology, Palaeoecology, in press, doi:10.1016/j.palaeo.2011.05.013.

Schweingruber, F.H., Briffa, K.R., and Jones, P.D., 1991. Yearly maps of summer temperatures in Western Europe from A.D. 1750 to 1975 and Western North America from 1600 to 1982: Results of a readiodensitometrical study on tree rings. Vegetatio 92, 5–71.

Signorini, S.R., Garcia, V.M.T., Piola, A.R., Garcia, C.A.E., Mata, M.M., and McClain, C.R., 2006. Seasonal and interannual variability of coccolithophore blooms in the vicinity of the Patagonian shelf break (38ºS – 52ºS). Geophysical Research Letters 33, L16610, doi:10.1029/2006GL026592.

Spero, H.J., Bijma J., Lea D.W., and Bemis B.E., 1997. Effect of seawater carbonate concentration on foraminiferal carbon and oxygen isotopes. Nature 390, 497–500.

Steedman, H.F., 1950. Alcian Blue 8GS: A new stain for mucin. Quarterly Journal of Microscopical Science 91, 477–479.

Stilwell, J.D., and Zinsmeister, W.J., 1992. Molluscan systematics and biostratigraphy, Lower Tertiary La Meseta Formation, Seymour Island, Antarctic Peninsula. American Geophysical Union, Washington D.C., pp. 1–192.

Swart, P.K., 1983. Carbon and oxygen isotope fractionation in scleractinian corals: A review. Earth-Science Reviews 19, 51–80.

Urey, H.C., Lowenstam, H.A., Epstein, S., and McKinney, C.R., 1951. Measurement of paleotemperatures and temperatures of the Upper Cretaceous of England, Denmark, and the southeastern United States. Bulletin of the Geolocial Society of America 62, 399–416.

Vimeux, F., Ginot, P., Schwikowski, M, Vuille, M., Hoffmann, G., Thompson, L.G., and Schotterer, U., 2009. Climate variability during the last 1000 years inferred from Andean ice cores: A review of methodology and recent results. Palaeogeography, Palaeoclimatology, Palaeoecology 281, 229–241.

Wheeler, A.P., 1992. Mechanisms of molluscan shell formation. In: Bonucci, E., (ed.) Calcification in Biological Systems. CRC Press, Boca Raton, Florida, USA, pp. 77–83.

Zeebe, R., 1999. An explanation of the effect of seawater carbonate concentration on foraminiferal oxygen isotopes. Geochimica et Cosmochimica Acta 63, 2001–2007.

Chapter 3: Interpretation of stable carbon isotope ratios of *Eurhomalea exalbida* shells: a proxy for environmental conditions or shell growth rates?

Foreword

In this Chapter, the controversial environmental proxy, $\delta^{13}C_{shell}$, is evaluated for the marine bivalve *Eurhomalea exalbida*. It is primarily focused on the relationship among the environmental parameters, shell growth patterns, variations in $\delta^{13}C_{shell}$ and $\delta^{13}C_{shell\text{-}detrended}$ after removing the ontogenetic trend associated with shell growth rates. Accordingly, both inter-annual and intra-annual $\delta^{13}C_{shell}$ values are assessed in this study in order to determine the factor(s) controlling the variations in $\delta^{13}C_{shell}$ and to investigate the possibility of unraveling the environmental signals from $\delta^{13}C_{shell}$.

Abstract

The reconstruction of paleoenvironmental dissolved inorganic carbon from bivalve shells is generally precluded by carbon disequilibrium fractionation as a result of vital effects. In this study, carbon isotope ratios of shells of the bivalve, *Eurhomalea exalbida* (Dillwyn) were analysed with a focus on inter-annual (ontogenetic) and intra-annual (seasonal) carbon isotopic variations, which were interpreted on the basis of environmental comparisons. A decrease in $\delta^{13}C_{shell}$ values through ontogeny and clear seasonal cycles were observed in all studied specimens. Both the $\delta^{13}C_{shell}$ decreasing trend and the seasonal cycles are closely associated with shell growth rates as indicated by statistically significant correlations. The inverse correlation between the mantle metabolic activity and shell growth rates might be responsible for the decreasing trend and the seasonal cycles in $\delta^{13}C_{shell}$. Furthermore, environmental signatures recorded in $\delta^{13}C_{shell}$ are largely complicated by variations in shell growth rates, and they are still obscured after removing the ontogenetic decreasing trend in shell growth. This suggests that $\delta^{13}C_{shell}$ in *E. exalbida* cannot serve as an environmental proxy, but it could be useful as a potential tool for ecological studies. Notably, the hypotheses in this study may only hold true in ontogenetic younger shells. Further research is needed for the older shells.

Keywords

Bivalve mollusk shell, Carbon isotopes, Phytoplankton, Metabolic carbon contribution, Shell growth rates, Ontogeny

3.1. Introduction

The oceanic uptake of atmospheric CO_2, which is strongly depleted in ^{13}C relative to ^{12}C due to the combustion of fossil fuels (Tans, 1981; Andres et al., 1996), would result in a negative shift in $\delta^{13}C_{DIC}$ of ambient seawater (e.g., Racapé et al., 2013). The knowledge of the spatiotemporal variability in $\delta^{13}C_{DIC}$ is of importance for understanding the past oceanic carbon cycles and the prediction of the future increase rate of the anthropogenic CO_2. With the construction of data sets of the World Ocean Circulation Experiment / Joint Global Ocean Flux Study, the total concentration of anthropogenic CO_2 in the global oceans has been estimated since the industrial revolution (e.g., Gruber, 1998; Sabine et al., 2002; Lee et al., 2003). However, very little is known about the variability in the oceanic carbon cycle of the past due to the lack of appropriate $\delta^{13}C_{DIC}$ data, especially for the South Atlantic, which is the major oceanic sink with high anthropogenic CO_2 storage rate (Ríos et al., 2012).

The $\delta^{13}C$ of biogenic carbonates is considered to be one of the effective tools for the measurement of the $\delta^{13}C_{DIC}$, since it has been suggested that the $\delta^{13}C$ of bivalve mollusks shells, corals and sclerosponges records the changes in $\delta^{13}C_{DIC}$ beyond the instrumental era (Mook and Vogel, 1968; Nozaki et al., 1978; Krantz et al., 1987; Böhm et al., 1996; Swart et al., 1998; Lazareth et al., 2000; Schöne et al., 2011). However, corals and sclerosponges are mostly limited to tropical settings. In contrast, bivalve mollusks have a broad geographic distribution and thereby they could be a potential archive for extending the $\delta^{13}C_{DIC}$ record in extratropical regions.

Unfortunately, for some marine mollusks, the shell carbon isotopic composition is more or less impacted by the proportion of metabolic carbon incorporated into the shell material (McConnaughey, 1989a, b; McConnaughey et al., 1997; McConnaughey and Gillikin, 2008). Therefore, some authors claimed that the variable contribution of metabolic carbon precludes the use of $\delta^{13}C_{shell}$ as a proxy for environmental conditions (e.g., Owen et al., 2002; Gillikin et al., 2006). Notably, a general ontogenetic decrease in $\delta^{13}C_{shell}$ has been found in some mollusk species (e.g., Jones et al., 1986; Krantz et al., 1987; Kennedy et al., 2001; Keller et al., 2002; Lorrain et al., 2004; Gillikin et al., 2007; Foster et al., 2009). Lorrain et al (2004) proposed a 'metabolic carbon availability' model, which shows a link between the deceasing $\delta^{13}C_{shell}$ trend and an increasing metabolic carbon contribution with body size, i.e. age. Similarly, Owen et al (2002) did not find a relationship between $\delta^{13}C_{shell}$ values in the scallop, *Pecten maximus* and environmental factors, but a strong correlation between intra-annual $\delta^{13}C_{shell}$ variations and shell growth rates. However, it is still poorly known if environmental factors exert an effect on $\delta^{13}C_{shell}$ variations through varied shell growth rates, since the timing and rate of shell growth is influenced by distinct

environmental factors, such as temperature, food availability and salinity (Rhoads and Pannella, 1970; Chicharo and Chicharo, 2001).

Furthermore, it is also speculated that seawater $\delta^{13}C_{DIC}$ could be reconstructed from $\delta^{13}C_{shell}$ if the metabolic contribution could be removed (e.g., Lorrain et al., 2004). This kind of study is rather rare. To our knowledge, only Chauvaud et al (2011) conducted a relevant investigation. They observed a linear decrease in $\delta^{13}C_{shell}$ with increasing shell height in three calcitic *Pecten maximus* specimens. Subsequently, they removed the linear drift by taking the residuals of the linear regression. By comparing the detrended $\delta^{13}C_{shell}$ values to the environmental variables, Chauvaud et al (2011) concluded that $\delta^{13}C_{shell}$ variations in *P. maximus* could not be used as a proxy for past $\delta^{13}C_{DIC}$ variations even after removing the linear trend. In fact, the residuals are the vertical distances (i.e., observed value minus predicted value) between the regression line and the recorded data. This method can be used to determine how well a line describes the data. However, using the residuals of a linear regression fails to remove the ontogenetic trend in $\delta^{13}C_{shell}$ variations. For a better understanding of the environmental implications behind the ontogenetic $\delta^{13}C_{shell}$ variations, it is essential to investigate how the $\delta^{13}C_{shell}$ values vary with shell growth rates and to remove the effects of ontogeny reasonably.

Therefore, the focus of the present study is on the relationship among the environmental parameters, $\delta^{13}C_{shell}$ variations and shell growth patterns of *Eurhomalea exalbida*, which is a long-lived bivalve mollusk in southern South America, with a wide geographic distribution in the South Atlantic. This species has been studied in terms of growth, reproduction and climate reconstructions utilizing shell oxygen isotopes (Dextraze and Zinsmeister, 1987; Lomovasky et al., 2002; Morriconi et al., 2002; Ivany et al 2008; Aguirre et al., 2009; Yan et al., 2012). We are aiming (1) to analyse ontogenetic (inter-annual) trends of $\delta^{13}C_{shell}$ values in *E. exalbida*; (2) to determine the factor(s) controlling the ontogenetic variability and how the factor(s) can be correctly removed; (3) to examine the seasonal (intra-annual) variations in $\delta^{13}C_{shell}$ values and the corresponding controlling factors; (4) to explore the relationship between environmental parameters and shell growth rates; and (5) to evaluate the feasibility of deciphering environmental records in $\delta^{13}C_{shell}$ variations of *E. exalbida*.

3.2. Materials and Methods

Four *Eurhomalea exalbida* specimens (FL-AA-A11R, -A17R, -A18R and -A23R) with an age of four to ten years were collected alive from Sparrow Cove, a shallow subtidal (2m water depth) zone near Stanley, Falkland Islands (Figure 3.1). Two of the specimens (A11R and A23R) were

obtained on 21st February 2009 and the other two shells (A17R and A18R) on 5th April 2009. Soft tissues were removed immediately after collection, and shells were kept dry until further studies.

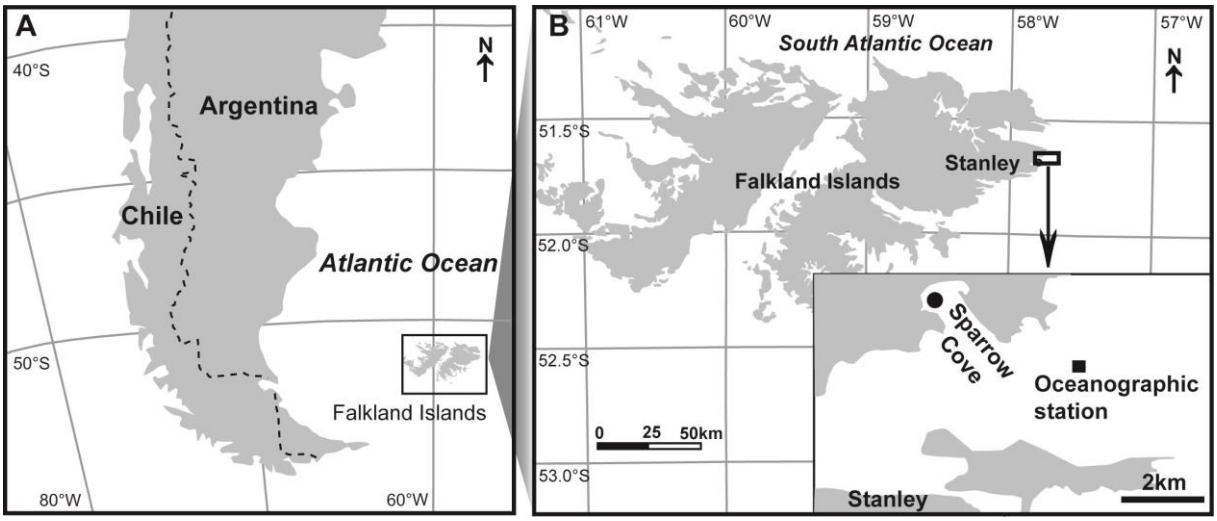

Figure 11. (A) Map showing locality in the south Atlantic where bivalve shells, *Eurhomalea exalbida*, have been live-collected and instrumental records were taken. (B) Sample locality at Sparrow Cove, Falkland Islands (filled circle) and nearby oceanographic station (filled square).

3.2.1. Stable isotope analyses

The right valve of each specimen was prepared for stable isotope analyses. Preparatory steps included coating with metal epoxy resin, sectioning, grinding, polishing and ultrasonically cleaning. Aragonite powder samples were taken from the outer sublayer of the outer shell layer of the shell cross-sections using microdrilling and micromilling techniques. Each sample was processed in a Thermo Finnigan MAT 253 continuous flow–isotope ratio mass spectrometer coupled to a GasBench II. Results are reported in δ-notation, and $\delta^{13}C$ and $\delta^{18}O$ values are given as parts per mil (‰). Isotope data were calibrated against NBS-19 ($\delta^{13}C$ = 1.95‰; $\delta^{18}O$ = -2.20‰) with 1σ replicated precision of 0.03‰ for $\delta^{13}C$ and 0.07‰ for $\delta^{18}O$. More details about the preparation of the cross-sections and the analyses of stable isotopes can be found in Chapter 2.

3.2.2. Environmental recordings

Water samples were collected from Sparrow Cove, Falkland Islands, in September 2011, June and July 2013. Subsequently, the $\delta^{18}O$ values of the seawater were measured. Monthly records of chlorophyll a, salinity (Figure 3.2) and sea surface temperature (SST) were obtained from the meteorological stations at the shell collection site. The chlorophyll a, the salinity and the SST data were recorded from February 2003 to December 2010 (the chlorophyll a and SST data in several months are missing), from January 2000 to December 2010 and from December 1999 to August 2011, respectively. Long term monthly precipitation data for Stanley, Falkland Islands were

derived from www.climatemps.com/graph/stanley-falkland-islands_files. In addition, data on the monthly precipitation from 2000 to 2009 in the Eastern Falkland Islands were obtained from the Global Precipitation Climatology Centre (Schneider et al., 2011; Figure 3.2). Missing chlorophyll a data of the oceanographic station record were filled with the monthly average data. Missing SST data were reconstructed from remote sensing data. For this purpose, a linear regression model was computed from the oceanographic station SST and satellite SST (NOAA_OI_SST_V2 data provided by the NOAA/OAR/ESRL PSD, Boulder, Colorado, USA, at http://www.esrl.noaa.gov/psd/). Daily chlorophyll a, salinity and SST data were then linearly interpolated from monthly values for further statistical analyses.

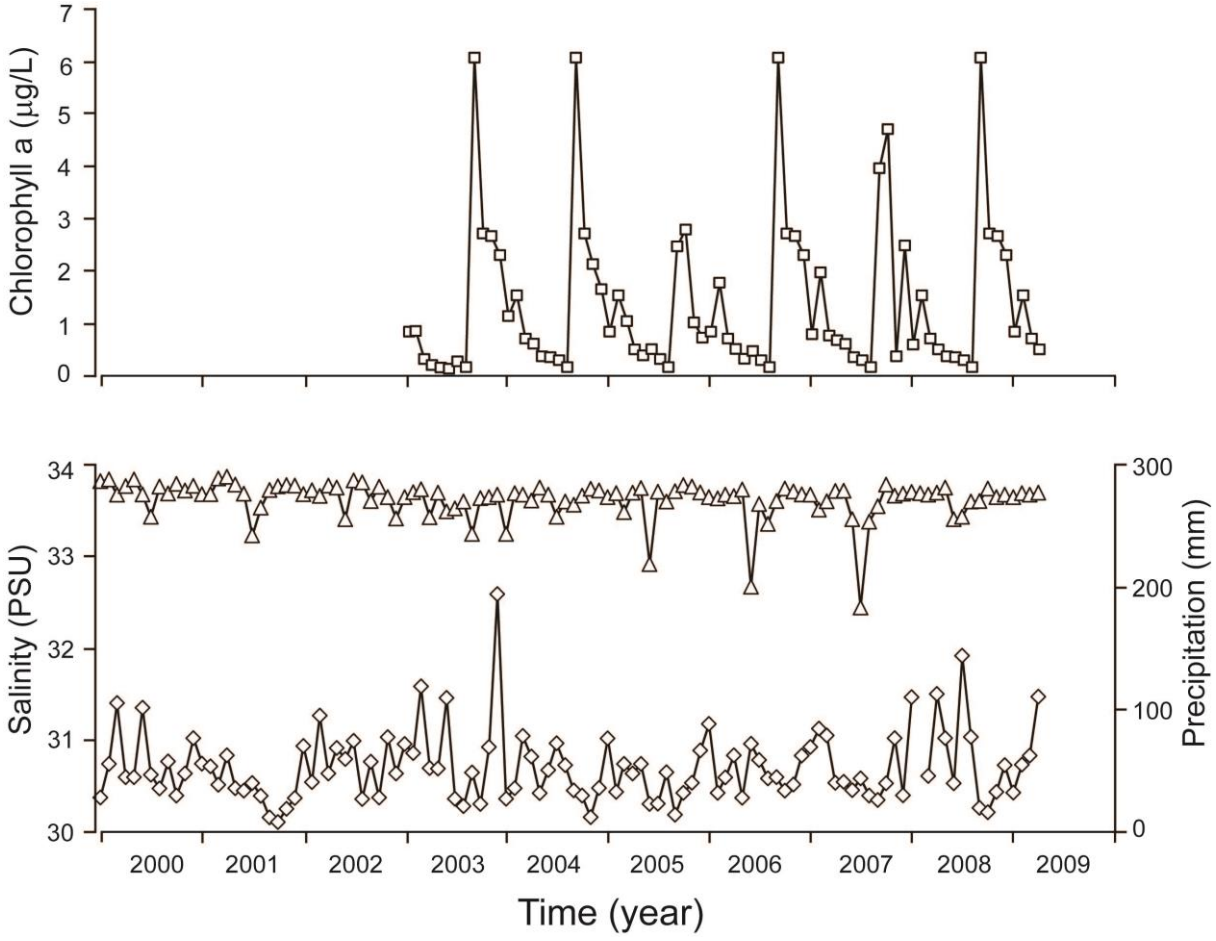

Figure 3. 2. Inter-annual variability of monthly chlorophyll a and salinity (empty triangle) from the meteorological stations at the shell collection site, and monthly precipitation (empty diamond) in the Eastern Falkland Islands.

3.2.3. Annual increment widths and daily growth rate model

For annual growth pattern analysis, one of the polished sections of each shell was immersed in Mutvei's solution (Schöne et al., 2005) and then photographed under reflected-light microscopy employing dark field illumination. Serial photographs of each specimen were stitched together with the Microsoft Image Composite Editor. Then annual increment widths were measured in the outer shell layer in the direction of growth using the image analysis software Panopea (© Peinl and Schöne).

Daily growth rates in ontogenetically younger parts of the shell have been measured and described for the studied specimens in Chapter 2, allowing the estimation of daily growth rates of each year by calculating the proportion to the annual increment widths. Thus, a daily growth rate model was established for each specimen.

3.2.4. Removing the ontogenetic trend

A new approach was developed to remove the ontogenetic trend in $\delta^{13}C_{shell}$ profiles. First, the least-squares fit to the $\delta^{13}C_{shell}$ data was computed and the maximum of calculated $\delta^{13}C_{shell}$ values was taken from the linear function as an anchor. Then this regression line was lifted up to a horizontal line (Figure 3.3). The corresponding equation is as follows:

$$\delta^{13}C_{shell\text{-}detrended} = \delta^{13}C_{shell} + \delta^{13}C_{shell\text{-}D\text{-}value}$$

where $\delta^{13}C_{shell\text{-}detrended}$ refers to the $\delta^{13}C_{shell}$ values after removing the ontogenetic trend and and $\delta^{13}C_{shell\text{-}D\text{-}value}$ is the difference between the regression line and the horizontal line of each $\delta^{13}C_{shell}$ value (Figure 3.3).

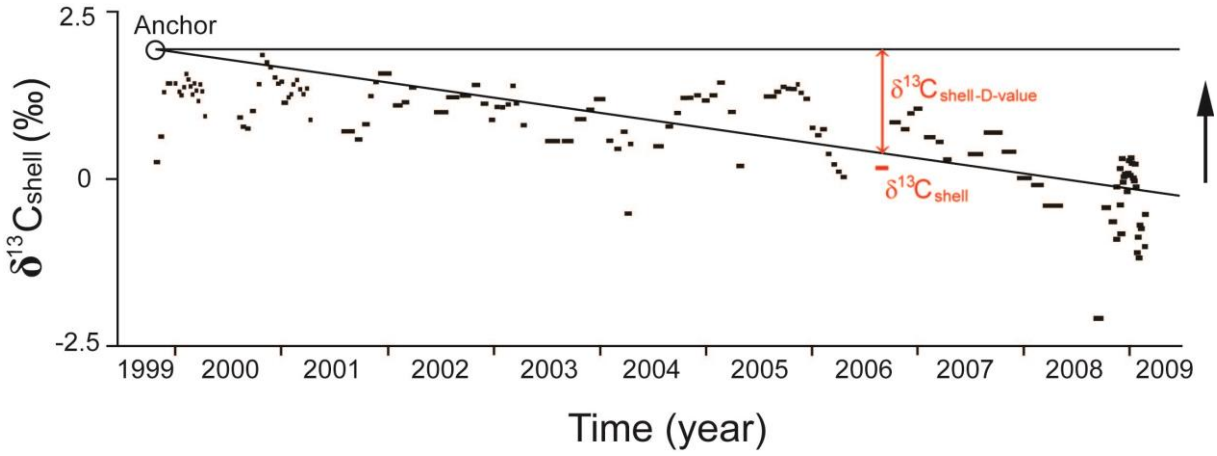

Figure 3. 3. The model of removing the ontogenetic trend in $\delta^{13}C_{shell}$ profiles (FL-AA-A23R as an example).

3.2.5. Temporal alignment of $\delta^{13}C_{shell}$ profiles

The temporal alignment of the $\delta^{13}C_{shell}$ and $\delta^{13}C_{shell\text{-}detrended}$ profiles was conducted for comparisons with shell growth rates on the time-series (Figure 3.4). The time-series has been well identified by combining sclerochronological and oxygen isotope analyses (in Chapter 2). Subsequently, the annual and monthly $\delta^{13}C_{shell}$ and $\delta^{13}C_{shell\text{-}detrended}$ values of each specimen were calculated by applying weighted arithmetic means.

3.3. Results

3.3.1. $\delta^{13}C_{shell}$ and $\delta^{13}C_{shell\text{-}detrended}$ profiles

A general decreasing trend in $\delta^{13}C_{shell}$ is observed in all specimens, with more positive values in the ontogenetically younger shell portions and more negative values in the ontogenetically older years. Annual $\delta^{13}C_{shell}$ values range from 0.97‰ to 0.87‰, 1.60‰ to 1.31‰, 0.84‰ to -0.09‰, and 1.25‰ to -0.38‰, for FL-AA-A11R, -A17R, -A18R, and -A23R, respectively (irrespective of the ontogenetically younger year with incomplete sampling). Apparently, $\delta^{13}C_{shell}$ values of the two ontogenetic younger shells exhibit slight changes from the umbo towards the ventral margin. The $\delta^{13}C_{shell\text{-}detrended}$ values of FL-AA-A11R and -A17R are almost equal to the corresponding $\delta^{13}C_{shell}$ values. However, the $\delta^{13}C_{shell\text{-}detrended}$ values of the two ontogenetic older shells (FL-AA-A18R and -A23R) are more positive than their corresponding $\delta^{13}C_{shell}$ values, in particular in the ontogenetic older shell portion (Figure 3.4).

Intra-annual cycles are evident in most of the $\delta^{13}C_{shell}$ profiles, with more positive values in December/January and the most negative values occurring in either April or August which is at or close to the annual growth line (Figure 3.4). The $\delta^{13}C_{shell\text{-}detrended}$ profile of each specimen displays a similar intra-annual variation to its corresponding $\delta^{13}C_{shell}$ profile.

3.3.2. $\delta^{13}C_{shell}$ and $\delta^{18}O_{shell}$

The $\delta^{13}C_{shell}$ values were computed with the $\delta^{18}O_{shell}$ values in each specimen. It appears that the $\delta^{13}C_{shell}$ values are non-linearly and positively correlated to the $\delta^{18}O_{shell}$ values. The relationship was best described by a logarithmic function (Figure 3.5). The most negative $\delta^{13}C_{shell}$ value of each year corresponded to or was extremely close to the most positive $\delta^{18}O_{shell}$ value.

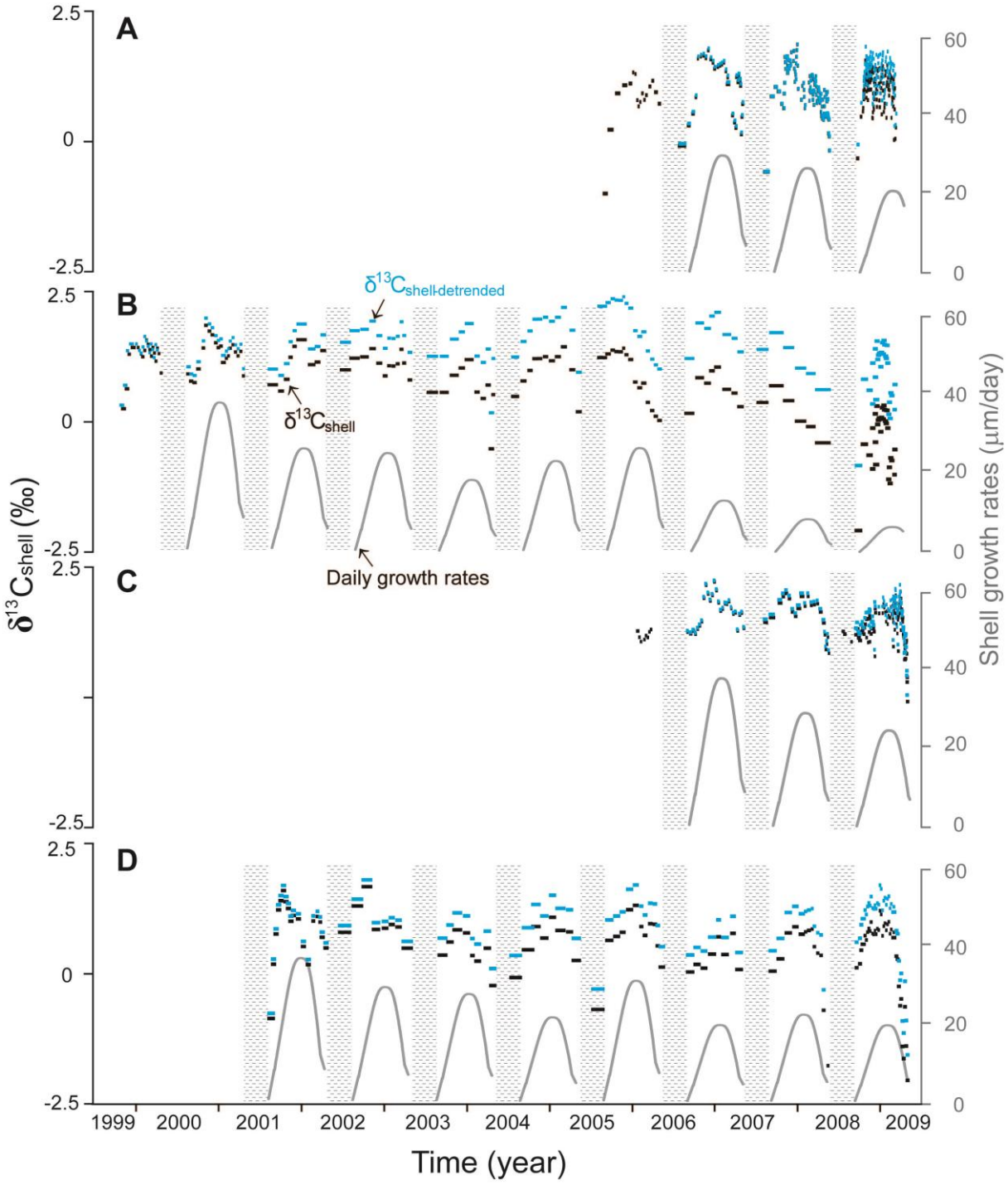

Figure 3. 4. Time series of $\delta^{13}C_{shell}$ (black-short bar) and $\delta^{13}C_{shell\text{-}detrended}$ (blue-short bar) and the daily growth rate model (grey curve). Vertical mottled bar = annual growth slowdown or growth cessation. (A): FL-AA-A11R, (B): FL-AA-A23R, (C): FL-AA-A17R, and (D): FL-AA-A18R.

3.3.3. Environmental parameters

The measured $\delta^{18}O$ values of the seawater in the site where *E. exalbida* was collected were 0.25‰ (September 2011), 0.26‰ (June 2013) and 0.25‰ (July 2013). According to field observations, the phytoplankton bloom occurred in spring (September, October and November) of each year

(Figure 3.2). The concentration of phytoplankton decreased to 1-2 μg/L in summer and kept decreasing until April. The overall variation in salinity is very low and ranges from 32.44 to 33.86 PSU throughout January 2000 to December 2010 (Figure 3.2). The minimum of monthly salinity is recorded in June or July, i.e. in the austral winter, and it was especially pronounced in the years 2005, 2006 and 2007 with the lowest salinity of 32.4 PSU. In contrast, salinity remains slightly higher in the other months and ranges from 33.2 to 33.9 PSU. In addition, the precipitation appears to be higher in the first half of the year with the maximum precipitation in December and January, i.e. in the austral summer. The SST ranged from 3.2 to 12.8°C during the time interval of 1999 to 2011.

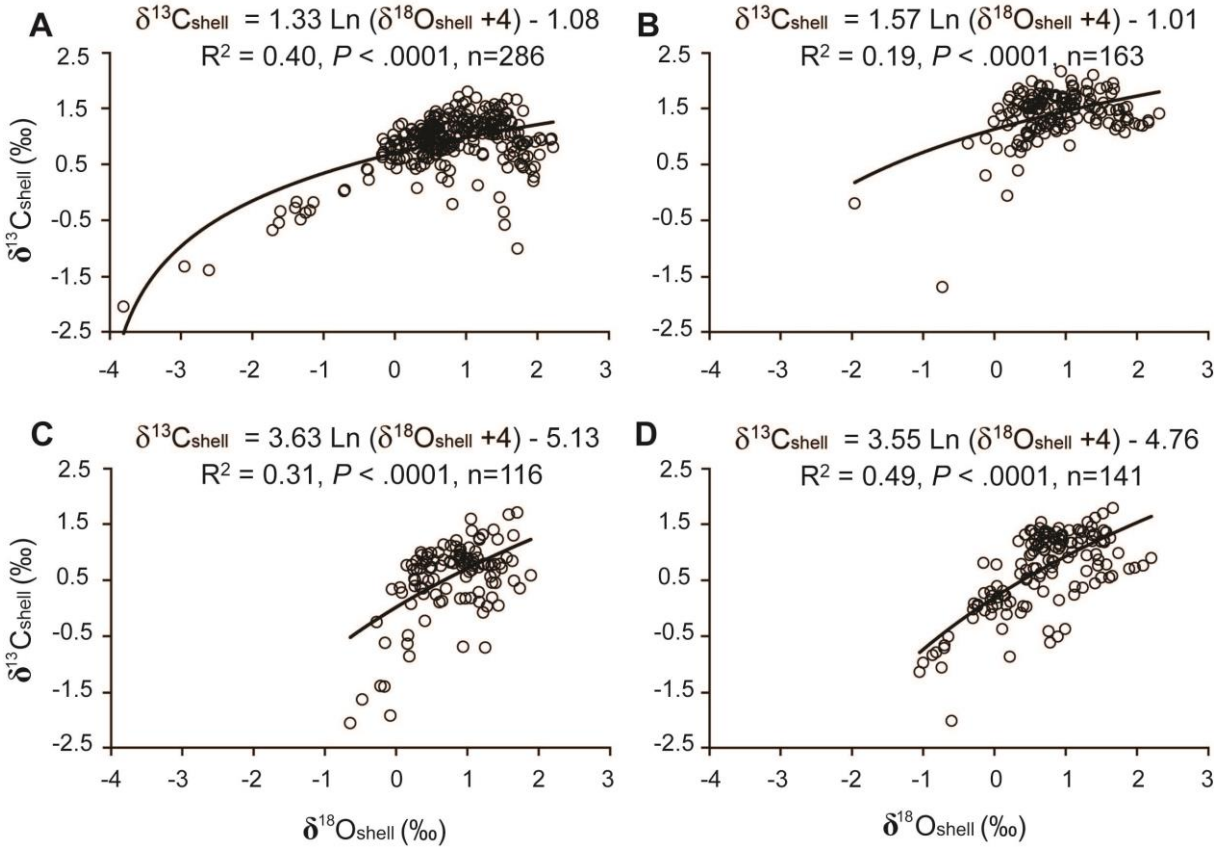

Figure 3. 5. $\delta^{13}C_{shell}$ versus $\delta^{18}O_{shell}$ in the four speciemens. (A): AA-FL-A11R, (B): AA-FL-A17R, (C): AA-FL-A18R, and (D): AA-FL-A23R.

3.3.4. $\delta^{13}C_{shell}$, $\delta^{13}C_{shell\text{-}detrended}$, shell growth rates and environmental parameters

The monthly average variations of $\delta^{13}C_{shell\text{-}detrended}$, the reconstructed daily growth rates, and the monthly averages of the environmental factors, i.e. chlorophyll a, salinity, precipitation and SST were compared (Figure 3.6). In addition, statistical analyses (simple and multiple regressions)

among these variables, i.e. $\delta^{13}C_{shell}$, $\delta^{13}C_{shell\text{-}detrended}$, shell growth rates and environmental parameters were performed (Table 3.1).

Table 3. 1. List of the regression analyses between $\delta^{13}C_{shell}$ and environmental variables, between $\delta^{13}C_{shell\text{-}detrended}$ and environmental variables, and between shell growth and environmental variables.

Regression analysis	AA-FL-A11R R^2, p	AA-FL-A17R R^2, p	AA-FL-A18R R^2, p	AA-FL-A23R R^2, p
simple regressions				
$\delta^{13}C_{shell}$ vs. Chl a	0.00; > 0.05	0.00; > 0.05	0.00; > 0.05	0.00; > 0.01
$\delta^{13}C_{shell}$ vs. S	0.12; <0.0001	0.06; <0.0001	0.04; <0.0001	0.08; <0.0001
$\delta^{13}C_{shell}$ vs. T	0.17; <0.0001	0.00; > 0.05	0.00; > 0.01	0.01; > 0.001
$\delta^{13}C_{shell\text{-}detrended}$ vs. Chl a	0.00; > 0.05	0.00; > 0.05	0.00; > 0.05	0.00; > 0.05
$\delta^{13}C_{shell\text{-}detrended}$ vs. S	0.12; <0.0001	0.06; <0.0001	0.05; <0.0001	0.03; <0.0001
$\delta^{13}C_{shell\text{-}detrended}$ vs. T	0.17; <0.0001	0.00; > 0.05	0.02; <0.0001	0.00; > 0.05
$\delta^{13}C_{shell}$ vs. SGR	0.53; <0.0001	0.36; <0.0001	0.37; <0.0001	0.44; <0.0001
SGR vs. T	0.46; <0.0001	0.31; <0.0001	0.31; <0.0001	0.28; <0.0001
SGR vs. Chl a	0.11; <0.0001	0.07; <0.0001	0.08; <0.0001	0.21; <0.0001
SGR vs. S	0.20; <0.0001	0.16; <0.0001	0.09; <0.0001	0.09; <0.0001
multiple regressions				
SGR vs. T, Chl a and S	0.49; <0.0001	0.35; <0.0001	0.34; <0.0001	0.55; <0.0001

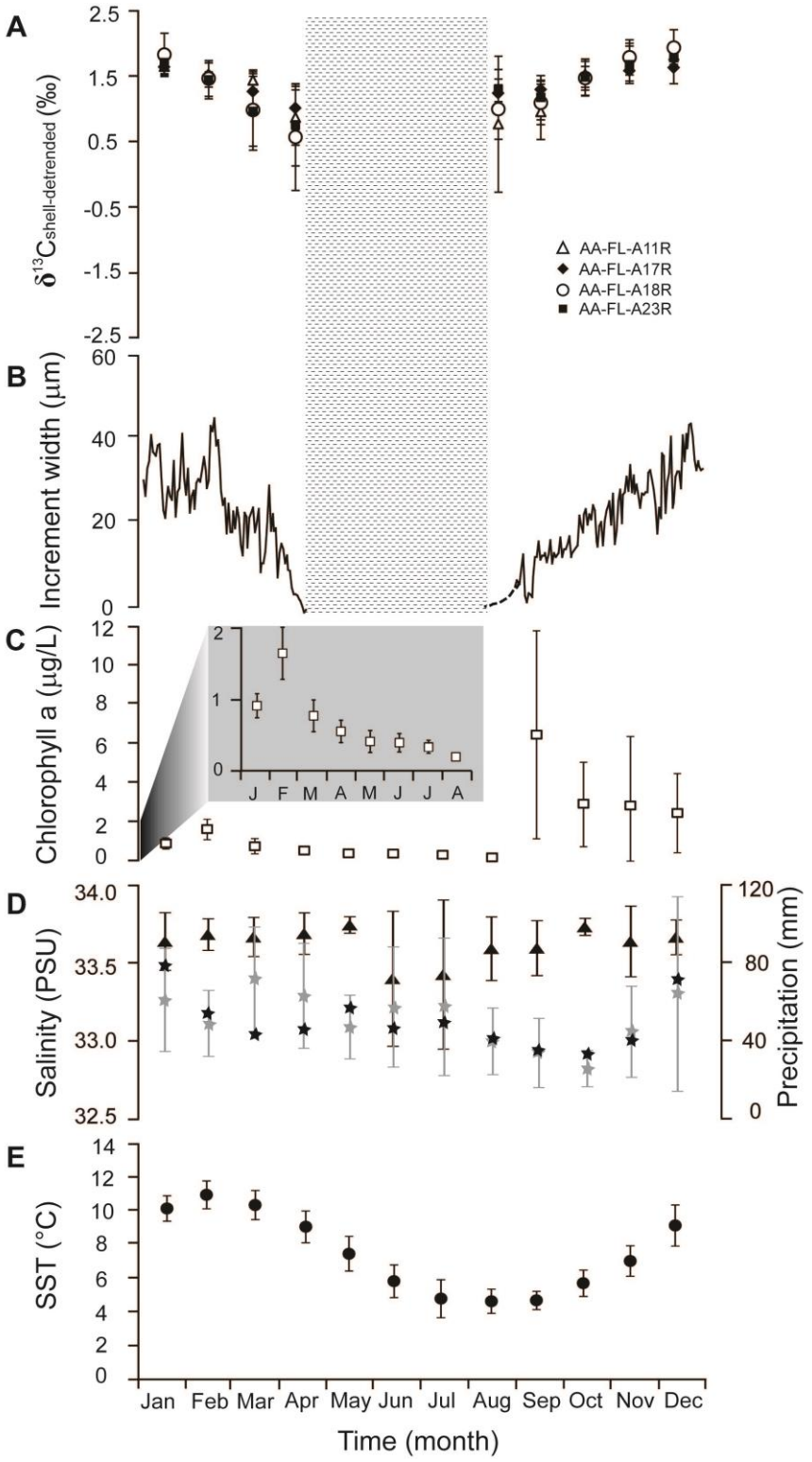

Figure 3. 6. Comparison between (A) monthly variations of detrended shell carbon isotopes ($\delta^{13}C_{shell\text{-}detrended}$), (B) daily growth rate model (unsmoothed), and the monthly average environmental factors, i.e. (C) chlorophyll a, (D) salinity and precipitation and (E) SST with 1σ standard deviation displayed as vertical bars. (A)(B): Vertical mottled bar = annual growth slowdown or growth cessation. (C): Enlarged graph from January to August is showing in grey background. (D): filled triangle denotes salinity data; stars denote precipitation data. Monthly precipitation data were derived from www.climatemps.com/graph/stanley-falkland-islands_files (black stars) and from Global Precipitation Climatology Centre (grey stars).

3.3.4.1. $\delta^{13}C_{shell}$ and shell growth rates

The annual increment widths of *E. exalbida* range from 11.36 to 8.01 mm, 14.21 to 9.27 mm, 11.89 to 3.64 mm, and 9.42 to 1.60 mm, for FL-AA-A11R, -A17R, -A18R, and -A23R, respectively, and display a decreasing trend throughout ontogeny. A significant and strong logarithmic correlation is observed between the annual increment widths and the $\delta^{13}C_{shell}$ values ($R^2 = 0.80$, $p < 0.0001$) (Figure 3.7).

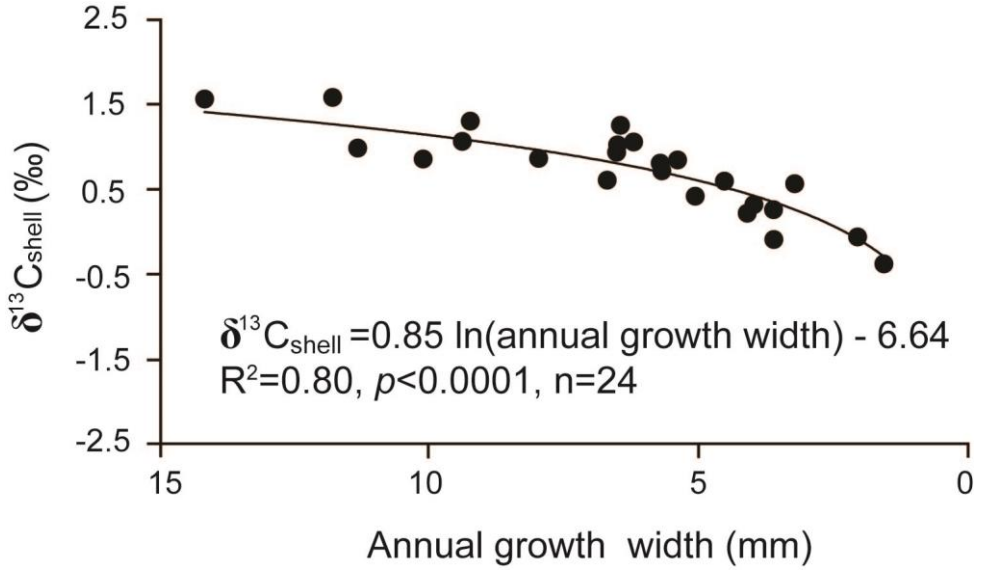

Figure 3. 7. A negative logarithmic relationship between annual $\delta^{13}C_{shell}$ values and annual growth increment widths.

The smoothed daily growth rate model was compared to the $\delta^{13}C_{shell}$ profiles (Figure 3.4). It appears that the year with more negative $\delta^{13}C_{shell}$ values corresponds to times of decreased shell growth rates, especially in FL-AA-A23R. Moreover, the intra-annual variation of the $\delta^{13}C_{shell}$ values shows similar seasonal cycles with shell growth rates of each year, i.e. more positive $\delta^{13}C_{shell}$ values correspond to higher shell growth rates and more negative $\delta^{13}C_{shell}$ values are in accordance with lower shell growth rates. Statistically, reconstructed daily shell growth rates can explain 36-53% of the $\delta^{13}C_{shell}$ variations (Table 3.1).

3.3.4.2. Shell growth rates and environmental parameters

For the purpose of clarifying the relationship between shell growth and environmental conditions, the reconstructed shell growth rates were statistically compared to environmental parameters, which are known as factors affecting bivalve shell growth, i.e. temperature, salinity and chlorophyll a values. A statistically significant positive relationship (stepwise multiple regression, $R^2 = 0.34\sim0.55$, $p < 0.0001$) was observed between the shell growth rates and all studied environmental variables. Temperature alone accounted for 28~46% of the variation in shell

growth (simple linear regression) (Table. 3.1). Summarizing, *E. exalbida* grows fastest at higher temperatures, at s higher primary productivity and under normal marine salinity conditions.

3.3.4.3. $\delta^{13}C_{shell}$, $\delta^{13}C_{shell\text{-}detrended}$ and environmental parameters

Comparing monthly average variations, it seems that there is no clear linkage between $\delta^{13}C_{shell\text{-}detrended}$ and chlorophyll a levels or salinity (Figure 3.6). The $\delta^{13}C_{shell\text{-}detrended}$ values of each specimen decrease in the first half of the year whereas the chlorophyll a and salinity values keep fairly constant during this period. In the second half of the year, the $\delta^{13}C_{shell\text{-}detrended}$ values increase towards more positive values while the salinity shows only slight variations. The chlorophyll a concentration in July and August is as low as in the first half of the year, and increases sharply to peak of ca. 6.5 µg/L in September, then decreases strongly from September to Decembe. Furthermore, in order to assess how environmental variables might have influenced carbon isotope variations in the shells of *E. exalbida*, $\delta^{13}C_{shell}$ and $\delta^{13}C_{shell\text{-}detrended}$ were statistically computed to temperature, salinity and chlorophyll a values (Table 3.1). The results indicate that all considered environmental parameters have effects neither on the $\delta^{13}C_{shell}$ variations, nor on the $\delta^{13}C_{shell\text{-}detrended}$ variations.

3.4. Discussion

3.4.1. Isotope fractionation in Eurhomalea exalbida

Assessments of the equilibrium geochemical relationships for isotopes are essential to reconstruct environmental parameters from stable carbon and oxygen isotopes in bivalve shells. Deviations from equilibrium result from either kinetic or metabolic effects (McConnaughey, 1989a). Metabolic effects are the result of the incorporation of ^{13}C-depleted carbon into the shells compared with the DIC of the surrounding seawater, caused by metabolism (McConnaughey, 1989a, 1989b, 1997). Kinetic effects occur due to the discrimination against the heavier isotopes of carbon and oxygen (^{13}C and ^{18}O) during hydration and hydroxylation of CO_2 (McConnaughey, 1989a, b).

In fact, *Eurhomalea exalbida* does not form its shell in oxygen isotopic equilibrium with the ambient water, but decreases exponentially (at least within the first ten years of age) depending on the ontogenetic age. It was speculated that the pH shift of the extrapallial fluid (EPF) toward higher values might result in more negative $\delta^{18}O_{shell}$ values than expected for equilibrium with the seawater (Chapter 2). To evaluate whether carbon isotopes of *E. exalbida* are precipitated in equilibrium, the carbon isotope composition of shells precipitated under equilibrium with South Atlantic seawater was calculated using the theoretical equilibrium value (Romanek et al., 1992). Expected aragonite equilibrium $\delta^{13}C$ values are ~2.7‰ more positive than the $\delta^{13}C_{DIC}$ of the

ambient seawater (Romanek et al., 1992). The $\delta^{13}C_{DIC}$ value was estimated to be approximately +1.81‰, based on data from the South Atlantic Ocean at a latitude of 50°S (Gruber et al., 1996), and equilibrium aragonite $\delta^{13}C$ values were calculated to be ~4.5‰. Observed $\delta^{13}C_{shell}$ values in *E. exalbida* varied from -1.7±0.5‰ to 1.9±0.2‰, which is obviously more negative than predicted under isotopic equilibrium. Both $\delta^{13}C$ and $\delta^{18}O$ in *E. exalbida* are depleted in heavier isotopes, i.e. ^{13}C and ^{18}O. Kinetic effects might have played a role during isotope fractionation, which would cause a simultaneous depletion of $\delta^{13}C$ and $\delta^{18}O$ with respect to the equilibrium. However, I did not observe a simultaneous negative offset in oxygen and carbon isotopes of *E. exalbida* shells, but a logarithmic correlation (Figure 3.5). Therefore, the isotope disequilibrium fractionation in *E. exalbida* does not seem to be attributable to the hypothesis of kinetic isotope effects. This conclusion is consistent with previous studies, which have determined that the kinetic isotope effects on mollusk shells are minimal (e.g., Owen et al., 2008). Alternatively, the offset from the carbon isotope equilibrium is likely due to the incorporation of ^{13}C-depleted metabolic carbon into the shell material (McConnaughey, 1989a, b).

3.4.2. Inter-annual variations of $\delta^{13}C_{shell}$

The $\delta^{13}C_{shell}$ profiles of the studied *E. exalbida* specimens exhibit a decreasing trend during ontogeny. There is a significant correlation ($p < 0.0001$) between the annual $\delta^{13}C_{shell}$ values and annual growth widths. The shell growth rate explains 80% of the annual $\delta^{13}C_{shell}$ variability (Figure 3.7). In a number of previous studies, the general decreasing trend of $\delta^{13}C_{shell}$ through ontogeny was observed and thought to be either caused by the influence of pore water $\delta^{13}C_{DIC}$ gradients, or effects of metabolic changes (e.g., Jones et al., 1986; Krantz et al., 1987; Owen et al., 2002; Elliot et al., 2003; Lorrain et al., 2004; Gillikin et al., 2007).

Is it possible that the decreasing trend in $\delta^{13}C_{shell}$ with increasing age is the result of more negative pore water $\delta^{13}C_{DIC}$ in deeper sediments? In fact, strong gradients in pore water $\delta^{13}C$ have been observed within the initial 5 cm of sediment due to the remineralisation of organic matter (McCorkle et al., 1985). Keller et al (2002) suggested that the pattern of decreasing $\delta^{13}C_{shell}$ was a result of the utilization of more negative pore water $\delta^{13}C_{DIC}$ related to a progressive deepening of the *Chamelea gallina*'s habitat into the sediment. This explanation is accepted by other authors, who suggested that infaunal bivalves are sometimes isotopically lighter than epifaunal bivalves (Krantz et al., 1987; Keller et al., 2002; Elliot et al., 2003). *E. exalbida* is a shallow infaunal species, i.e. they live below the sediment surface. It is still unstudied if they live in a constant depth or if they move deeper in the sediment with aging. If they live at the same depth in the sediment as they age, i.e. the depth where a bivalve lives is independent of the bivalve size, as suggested for *Mercenaria mercenaria* by Roberts (1989), then the possibility of influences of pore

water $\delta^{13}C_{DIC}$ gradients is minimal. Hypothetically, *E. exalbida* may live progressively deeper in the sediment with increasing age, thus whether they incorporate more negative pore water $\delta^{13}C_{DIC}$ depends primarily on how ambient seawater enters into bivalves. An infaunal bivalve needs to use these tube-like structures, paired siphons, including an inhalant and an exhalant siphon, to reach up to the surface of the sediment, so that the animal is able to respire, feed, and excrete, and also to reproduce (Zwarts, 1986; Coen and Heck, 1991). The siphons are long enough for reaching up to the sediment-water interface because they are longer with the increasing depth of a bivalve species living in the sediment (Zwarts, 1986; Coen and Heck, 1991). If the siphon is the only pathway for seawater entering into bivalves, it may be suggested that the depth of burial is not relevant for $\delta^{13}C_{shell}$ variability. However, since ambient water can also passively enter the mantle cavity and then interact with the inner epithelial cells and organs, molecules can be exchanged through the mantle epithelium between the hemolymph and the water in the mantle cavity (Marin et al., 2012). In this case, the pore water gradients might explain to some extent the decreasing trend in $\delta^{13}C_{shell}$ of *E. exalbida*. Nevertheless, the effects of the pore water gradients in the sediments cannot be ruled out, since it remains untested if *E. exalbida* lives always at the same depth or moves deeper into the sediment through its life history.

Alternatively, the most probable cause for a decreasing trend in $\delta^{13}C_{shell}$ during the lifetime of the bivalve is the metabolic change associated with shell growth rates. Prior to interpreting carbon isotopic variations linked to metabolic changes, it is essential to understand the incorporation of carbon into the shell material. Bivalve shell precipitation occurs in the extrapallial space by means of epithelial mantle activity, according to the equation of $Ca^{2+} + HCO_3^- \rightarrow CaCO_3 + H^+$. It is generally accepted that the sources of HCO_3^- ions follow two pathways: it may be taken up from the food, water filtration activity, or via passive diffusion from the external medium through the body; Alternately, HCO_3^- ions can result from the hydration of metabolic CO_2 (preferentially enriched in ^{12}C), which is accelerated by carbonic anhydrase (Marin et al., 2012). Assumedly, HCO_3^- ions provided by the hydration of metabolic CO_2 increases at slower shell growth portion in *E. exalbida*, which would result in a depletion of ^{13}C in the EPF, and thus more negative $\delta^{13}C_{shell}$ values. This hypothesis is supported from variations in the mantle metabolic activity (i.e. efficiencies of the metabolic pump) with changes of shell growth rates. Rosenberg and Hughes (1991) proposed metabolic gradients within the shell-secreting mantle and found that shell growth rates in *Mytilus edulis* were inversely proportional to the mantle metabolic activity (Rosenberg and Hughes, 1991), which means a higher mantle metabolic activity occurs in slower growing shell portions. If this holds true in *E. exalbida*, it provides an evidence for more metabolic CO_2 in the form of HCO_3^- in shell portions with reduced shell growth rates. During high mantle metabolic pumping, carbonic anhydrase catalyses the reaction $CO_2 + H_2O \leftrightarrow HCO_3^-$

+ H^+ in a more efficient manner, and thus the concentration of metabolically derived carbon in the EPF is higher in slow growing shell portions. Similarly, Lorrain et al (2004) also observed a significant correlation between daily growth increment widths and $\delta^{13}C$ variations in scallop shells, but only for one of six shells. Based on their data from scallops, they proposed a model, wherein the availability of metabolic carbon relative to the carbon requirements for calcification during mollusk shell growth, accounts for the ontogenetic variability in shell $\delta^{13}C$.

3.4.3. Intra-annual variations of $\delta^{13}C_{shell}$

The monthly average variations of $\delta^{13}C_{shell}$, the environmental parameters and the reconstructed daily shell growth rates show a complex relationship (Figure 3.6). One of the most interesting findings in this study is the distinct seasonal cycles in $\delta^{13}C_{shell}$, with more positive values in the spring/summer linked to higher shell growth rates and more negative $\delta^{13}C_{shell}$ values corresponding to lower shell growth rates. The most negative $\delta^{13}C$ values occur in April or August and are located at or close to the annual growth line (Figure 3.7). Apparently, the underlying cause of inter-annual variations in $\delta^{13}C_{shell}$, i.e. an inverse correlation between metabolic CO_2 into the EPF and shell growth rate, also explains the intra-annual $\delta^{13}C_{shell}$ variations, as manifested by the statistical results of reconstructed daily shell growth rates accounting for 36-53% of the intra-annual $\delta^{13}C_{shell}$ variations. This finding is consistent with observations of Owen et al (2002), who investigated the relationship between mollusk shell growth rate and skeletal $\delta^{13}C$ for the scallop, *Pecten maximus*. They found that seasonal variations in shell growth rates were the governing factor influencing shell carbon isotopes. Shell $\delta^{13}C$ values were more negative (by up to -2‰) at low shell growth rates as compared with predicted values for the precipitation of inorganic calcite in isotopic equilibrium with the seawater.

3.4.4. $\delta^{13}C_{shell}$, $\delta^{13}C_{shell\text{-}detrended}$ and environmental parameters

The $\delta^{13}C_{shell}$ variations are considered to be related to the $\delta^{13}C_{DIC}$ changes in the ambient water, as well as metabolic carbon derived from bivalve respiration (e.g., Lorrain et al., 2004). Although the contribution of metabolic carbon varies among species, it is generally thought to be relatively low (< 10%; McConnaughey et al., 1997) in aquatic shells. However, it is still questionable whether the metabolic effects overwhelm influences of environmental parameters completely.

3.4.4.1. $\delta^{13}C_{shell}$, $\delta^{13}C_{shell\text{-}detrended}$ and primary productivity

As a filter feeder, *E. exalbida* is closely linked with the activity of primary producers, which is evident since its shallow water habitat is strongly influenced by seasonal phytoplankton blooms. Photoautotrophs in the oceans are capable of changing the physical and chemical properties of the water column. In general, isotopically light ^{12}C is preferentially taken up by phytoplankton during photosynthesis and thus, removed from the ambient water, leaving the water more enriched in ^{13}C

(e.g., Fogel and Cifuentes, 1993; Gruber et al., 1999). *E. exalbida* ingests large quantities of phytoplankton and precipitates its shells in these chemically altered waters. Thus, the shells likely record changes in phytoplankton abundance in shallow water habitats. The most negative $\delta^{13}C_{shell}$ values (both $\delta^{13}C_{shell}$ and $\delta^{13}C_{shell\text{-}detrended}$) in *E. exalbida* shells occurred in April or August, which is at the lowest shell growth rate and the seasonal minimum of the phytoplankton concentration (Figures 3.2, 3.4, 3.6). It is thus possible that increased metabolic contribution related to decreased shell growth rates complicates the environmental signatures in $\delta^{13}C_{shell}$. Subsequently, phytoplankton blooms to the seasonal maximum of 6.5 μg/L in September (Figures 3.2, 3.6), and the corresponding $\delta^{13}C_{shell}$ values appear to increase slightly (Figures 3.4, 3.6). It seems most likely that $\delta^{13}C_{shell}$ values vary with shell growth rates, instead of ambient chlorophyll a levels. In contrast, from November to February, i.e. late Spring and early Summer, shell growth is faster and phytoplankton is abundant considering the time lag of the phytoplankton, since it takes some time from the phytoplankton bloom to the following depletion in ^{13}C of the seawater. It thus, can be speculated that the higher $\delta^{13}C_{shell}$ values during this period may reflect the seawater $\delta^{13}C_{DIC}$ records to a more extent than in other months of the year.

Furthermore, no significant correlation is observed between $\delta^{13}C_{shell}$ and chlorophyll a values based on statistical analyses, which likely confirms the observation of primary productivity of seawater might be obscured by the varied contribution of metabolic carbon through *E. exalbida* ontogeny. Since the metabolic contribution in $\delta^{13}C_{shell}$ is inferred to be connected to the variation of shell growth rates, it can thus be speculated that environmental signals might be revealed after the ontogenetic $\delta^{13}C_{shell}$ trends are removed. Unfortunately, the $\delta^{13}C_{shell\text{-}detrended}$ values are not statistically correlated to the chlorophyll a values, suggesting that the inter-annual effects associated with reduced shell growth rates are not the only factor hampering the environmental reconstruction from $\delta^{13}C_{shell}$.

3.4.4.2. $\delta^{13}C_{shell}$, $\delta^{13}C_{shell\text{-}detrended}$ and salinity

Salinity is determined to be linearly related to both $\delta^{13}C_{DIC}$ and $\delta^{18}O$ of the ambient water (Ingram et al., 1996; Surge et al., 2001; Gillikin et al., 2005). Therefore, it may be implied that the salinity information of the ambient water can be recorded in $\delta^{13}C_{shell}$. The salinity changes slightly during the whole year in Sparrow Cove (with an amplitude of ca. 0.7 PSU), except for June / July in 2005, 2006 and 2007 (Figure 3.2). Since the local precipitation data appear higher in summer months (Figure 3.2), it may not be the governing factor for the exceptional low salinity in winter. The relatively low winter salinity in these years may therefore be attributed to the input of intermediate waters as they flow into the South Atlantic as part of the Malvinas Current (Falkland Current) or mixing with the local winter freshwater through the sea surface (Piola and Gordon,

1989). However, this keeps untested yet and needs further investigation. The measured water $\delta^{18}O$ values of Sparrow Cove show little variability in 2011 and 2013, which confirms the slight changes in local salinity. Furthermore, it may indicate that the $\delta^{13}C_{DIC}$ of Sparrow Cove also varies slightly throughout the year. Therefore, the remarked intra-annual variations in $\delta^{13}C_{shell}$ (or $\delta^{13}C_{shell\text{-}detrended}$) do not result from $\delta^{13}C_{DIC}$ of the ambient water, but most likely from the variations in shell growth rates of *E. exalbida*.

3.4.5. Environmental effects on shell growth rates

It has been established that *E. exalbida* shell growth starts in mid-August and ends in early April with the fastest growth occurring during late spring and early summer. The annual growth lines form between later summer and early winter based on the daily growth pattern and high-resolution $\delta^{18}O_{shell}$ analyses in my previous work (Chapter 2). It has also been suggested that the shell growth of this species is not exclusively controlled by temperature, but also influenced by food availability (Chapter 2). This hypothesis is confirmed in this study by considering phytoplankton data. The higher shell growth rate, i.e. calcification rate, during late spring and early summer, corresponds to a higher rate of primary productivity at higher temperatures (Figure 3.6), which is an optimal environmental condition for bivalve growth (Jorgensen, 1990). Under such conditions, the filter-pump processes the ambient water at its full capacity, enabling the bivalve to more or less fully exploit its potential for growth (Jorgensen, 1990; 1996).

Based on the stepwise multiple regression analyses, salinity is another factor affecting the shell growth of *E. exalbida*. All three environmental variables (i.e. SST, chlorophyll a and salinity) account for 34~55% of the shell growth rates. Here, temperature alone explains 28~46% of the variation in shell growth (Table 3.1). It could be inferred that temperature is the most important driver for the shell growth, instead of chlorophyll a and salinity. The relationship between temperature and shell carbon isotopes has been discussed in depth by previous authors and it is generally accepted that $\delta^{13}C_{shell}$ is not significantly controlled by temperature (e.g., Romanek et al., 1987, 1992). It thus can be speculated that the chlorophyll a and the salinity information recorded in $\delta^{13}C_{shell}$ though impacting the shell growth rate might be rather little. However, further quantitative investigations are needed to test this speculation.

3.5. Conclusions

In this study, shell growth rates are found to have an important control on inter-annual (ontogenetic) and intra-annual (seasonal) $\delta^{13}C_{shell}$ variations in *Eurhomalea exalbida*. The metabolic contributions related to shell growth rates largely overwhelm the environmental signals in $\delta^{13}C_{shell}$, which hampers the use of $\delta^{13}C_{shell}$ variations as an indicator for variations of ambient seawater $\delta^{13}C_{DIC}$, but provides an implication for ecological studies. Furthermore, environmental

factors, i.e. SST, food supply and salinity, influence the timing and rate of shell growth of *E. exalbida*, but it seems like there is no further influence on $\delta^{13}C_{shell}$ variations through impacting the shell growth rates.

It should be noted that the results and discussions in this study are only based on the ontogenetic younger shells of the long-lived species *E. exalbida* (four to ten years old), which may attain an age of up to 70 years (Lomovasky et al., 2002). For example, the long-lived *Arctica islandica* exhibit little or no trend in shell $\delta^{13}C$ associated with shell growth rates after the first ca. 40 years of life in contrast to a decreasing trend in shell $\delta^{13}C$ during the first ca. 40 years of growth (Foster et al., 2007; Schöne et al., 2011; Butler et al., 2011). Therefore, the answer remains unknown whether the hypotheses here also hold true for shells throughout the life of *E. exalbida*. Subsequent studies should focus on the $\delta^{13}C_{shell}$ variations in ontogenetic older shells.

3.6. References

Aguirre, M.L., Richiano, S., Álvarez, M.F., and Eastoe, C., 2009. Quaternary molluscan fauna from the littoral area of northern Santa Cruz (Patagonia, Argentina). Geobios 42, 411–434.

Böhm, F., Joachmiski, M.M., Lehnert, H., Morgenroth, G., Kretschmer, W., Vacelet, J., and Dullo, W.C., 1996. Carbon isotope records from extant Caribbean and South Pacific sponges: evolution of $\delta^{13}C$ in surface water DIC. Earth and Planetary Science Letters 139, 291–303.

Butler, P.G., Wanamaker, Jr, A.D., Scoursea, J.D., and Richardsona, C.A., and Reynoldsa, D.J., 2011. Long-term stability of $\delta^{13}C$ with respect to biological age in the aragonite shell of mature specimens of the bivalve mollusk *Arctica islandica*. Palaeogeography, Palaeoclimatology, Palaeoecology 302, 21–30.

Carroll, M.L., Johnson, B.J., Henkes, G.A., McMahon,K.W., Voronkov, A., Ambrose, Jr, W.G., and Denisenko, S.G., 2009. Bivalves as indicators of environmental variation and potential anthropogenic impacts in the southern Barents Sea. Marine Pollution Bulletin 59, 193–206.

Chauvaud, L., Thébault, J., Clavier, J., Lorrain, A., and Strand, Q., 2011. What's hiding behind ontogenetic $\delta^{13}C$ variations in mollusk shells? new insights from the great scallop (*Pecten maximus*). Estuaries and Coasts 34, 211–220.

Chicharo, L., and Chicharo, M.A., 2001. Effects of environmental conditions on planktonic abundances, benthic recruitment and growth rates of the bivalve mollusc *Ruditapes decussatus* in a Portuguese coastal lagoon. Fisheries Research 53, 235–250.

Dextraze, B.L., and Zinsmeister, W.J., 1987. A study of the internal annual growth lines of the late Eocene mollusk *Eurhomalea Antarctica*. Antarctic Journal of the United States 22, 14–15.

Elliot, M., deMenocal, P.B., Linsley, B.K., and Howe, S.S., 2003. Environmental controls on the stable isotopic composition of *Mercenaria mercenaria*: potential application to paleoenvironmental studies. Geochemistry, Geophysics, Geosystems 4(7), 1056, doi:10.1029/2002GC000425.

Fogel, M.L., and Cifuentes, L.A., 1993. Isotope fractionation during primary production. In: Engel, M.H., and Macko, S.A., (eds.) Organic Geochemistry. Plenum Press, New York, USA, pp. 73-98.

Foster, L.C., Allison, N., Finch, A.A., Andersson, C., and Ninnemann, U.S., 2009. Controls on $\delta^{18}O$ and $\delta^{13}C$ profiles within the aragonite bivalve *Arctica islandica*. Holocene 19, 549–558.

Fritz, P., and Poplawski, S., 1974. ^{18}O and ^{13}C in the shells of freshwater molluscs and their environments. Earth and Planetary Science Letters 24, 91–98.

Gillikin, D.P., De Ridder, F., Ulens, H., Elskens, M., Keppens, E., Baeyens, W., and Dehairs, F., 2005. Assessing the reproducibility and reliability of estuarine bivalve shells (*Saxidomus giganteus*) for sea surface temperature reconstruction: implications for paleoclimate studies. Palaeogeography, Palaeoclimatology, Palaeoecology 228, 70–85.

Gillikin, D.P., Lorrain, A., Bouillon, S., Willenz, P., and Dehairs, F., 2006. Shell carbon isotopic composition of Mytilus edulis shells: relation to metabolism, salinity, $\delta^{13}C_{DIC}$ and phytoplankton. Organic Geochemistry 37, 1371–1382.

Gillikin, D.P., Lorrain, A., Meng, L., and Dehairs, F., 2007. A large metabolic carbon contribution to the $\delta^{13}C$ record in marine aragonitic bivalve shells. Geochimica et Cosmochimica Acta 71, 2936–2946.

Grossman, E.L., 1984. Carbon isotopic fractionation in live benthic foraminifera – comparison with inorganic precipitate studies. Geochimica et Cosmochimica Acta 48, 1505–1517.

Gruber, N., Keeling, C.D., Bacastow, R.B., Guenther, P.R., Lueker, T.J., Wahlen, M., Meijer, H.A., Mook, W.G., and Stocker, T.F., 1999. Spatiotemporal patterns of carbon-13 in the global surface oceans and the oceanic Suess effect. Global Biogeochemical Cycles 13, 307–335.

Gruber, N., 1998. Anthropogenic CO_2 in the Atlantic Ocean. Global Biogeochem Cycles 12, 165–191.

Ingram, B.L., Conrad, M.E., and Ingle, J.C., 1996. Stable isotope and salinity systematics in estuarine waters and carbonates: San Francisco Bay. Geochimica et Cosmochimica Acta, 60, 455–467.

Ivany, L.C., Lohmann, K.C., Hasiuk, F., Blake, D.B., Glass, A., Aronson, R.B., and Moody, R.M., 2008. Eocene climate record of a high southern latitude continental shelf: Seymour Island, Antarctica. Bulletin of the Geological Society of America 120, 659–678.

Jones, D.S., Williams, D.F., and Romanek, C.S., 1986. Life history of symbiont-bearing giant clams from stable isotope profiles. Science 231, 46–48.

Jorgensen, B.C., 1990. Bivalve filter feeding: hydrodynamics, bioenergetics, physiology and ecology. Olsen &Olsen, Fredensborg, Denmark, pp. 1–140.

Jorgensen, B.C., 1996. Bivalve filter feeding revisited. Marine Ecology Progress Series 142, 287–302.

Keller, N., Del Piero, D., and Longinelli, A., 2002. Isotopic composition, growth rates and biological behaviour of *Chamelea gallina* and *Callista chione* from the Gulf of Trieste (Italy). Marine Biology 140, 9–15.

Kennedy, H., Richardson, C.A., Duarte, C.M., and Kennedy, D.P., 2001. Oxygen and carbon stable isotopic profiles of the fan mussel, *Pinna nobilis*, and reconstruction of sea surface temperatures in the Mediterranean. Marine Biology 139, 1115–1124.

Krantz, D.E., Williams, D.F, and Jones, D.S., 1987. Ecological and paleoenvironmental information using stable isotope profiles from living and fossil mollusks. Palaeogeography, Palaeoclimatology, Palaeoecology 58, 249–266.

Lazareth, C.E., Willenz, P., Navez, J., Keppens, E., Dehairs, F., André, L., 2000. Sclerosponges as a new potential recorder of environmental changes: lead in *Ceratoporella nicholsoni*. Geology 28, 515–518.

Lee, K., Choi, S.-D., Park, G.-H., Wanninkhof, R., Peng, T.-H., Key, R.M., Sabine, C.L., Feely, R.A., Bullister, J.L., and Millero, F.J., 2003. An updated anthropogenic CO_2 inventory in the Atlantic Ocean. Global Biogeochem Cycles 17, 1116 http://dx.doi.org/10.1029/2003GB002067

Lomovasky, B.J., Brey, T., Morriconi, E., and Calvo, J., 2002. Growth and production of the venerid bivalve *Eurhomalea exalbida* in the Beagle Channel, Tierra del Fuego. Journal of Sea Research 48, 209–216.

Lorrain, A., Paulet, Y.M., Chauvaud, L., Dunbar, R., Mucciarone, D., and Fontugne, M., 2004b. $\delta^{13}C$ variation in scallop shells: increasing metabolic carbon contribution with body size? Geochimica et Cosmochimica Acta 68, 3509–3519.

Marin, F., Le Roy, N., and Marie, B., 2012. The formation and mineralization of mollusk shell. Frontiers in Bioscience 4, 1099–1125.

McConnaughey, T.A., 1989a. ^{13}C and ^{18}O isotopic disequilibrium in biological carbonates: I. Patterns. Geochim Cosmochim Acta 53, 151–162.

McConnaughey, T.A., 1989b. ^{13}C and ^{18}O isotopic disequilibrium in biological carbonates: II. In vitro simulation of kinetic isotope effects. Geochimica et Cosmochimica Acta 53, 163–171.

McConnaughey, T.A., and Gillikin, D.P., 2008. Carbon isotopes in mollusk shell carbonate. Geo-Marine Letters 28, 287–299.

McConnaughey, T.A., Burdett, J., Whelan, J.F., and Paull, C.K., 1997. Carbon isotopes in biological carbonates: respiration and photosynthesis. Geochimica et Cosmochimica Acta 61, 611–622.

McCorkle, D.C., Emerson, S.R., and Quay, P.D., 1985. Stable carbon isotopes in marine porewaters. Earth and Planetary Science Letters 74, 13–26.

Mook, W.G., and Vogel, J.C., 1968. Isotopic equilibrium between shells and their environment. Science 159, 874–875.

Morriconi, E., Lomovasky, B.J., Calvo, J., and Brey, T., 2002. The reproductive cycle of *Eurhomalea exalbida* (Chemnitz, 1795) (Bivalvia: Veneridae) in Ushuaia Bay (54°50' S), Beagle Channel (Argentina). Invertebrate Reproduction and Development 42, 61–68.

Nozaki, Y., Rye, D.M., Turekian, K.K., Dodge, R.E., 1978. A 200 year record of carbon-13 and carbon-14 variations in a Bermuda coral. Geophysical Research Letters 5, 826–828.

Owen, E.F., Wanamaker, A.D., Feindel, S.C., Schöne, B.R. and Rawson, P.D., 2008. Stable carbon and oxygen isotope fractionation in bivalve (*Placopecten magellanicus*) larval aragonite. Geochimica et Cosmochimica Acta 72, 4687–4698.

Owen, R., Kennedy, H., and Richardson, C., 2002. Isotopic partitioning between scallop shell calcite and seawater: effect of shell growth rate. Geochimica et Cosmochimica Acta 66, 1727–1737.

Piola, A.R., and Gordon, A.L., 1989. Intermediate waters in the southwest South Atlantic. Deep Sea Research 36, 1–16.

Racapé, V., Pierre, C., Metzl, N., Lo Monaco, C., Reverdin, G., Olsen, A., Morin, P., Rios, A.F., Vazquez-Rodriguez, M., and Perez, F.F., 2013. Anthropogenic carbon changes in the Irminger Basin (1981–2006): Coupling $\delta^{13}C_{DIC}$ and DIC observations. Journal of Marine System 126, 24–32.

Rhoads, D.C., and Pannella, G., 1970. The use of molluscan shell growth patterns in ecology and paleoecology. Lethaia 3, 143–161.

Ríos, A. F., Velo, A., Pardo, P. C., Hoppema, M., and Pérez, F. F., 2012. An update of anthropogenic CO_2 storage rates in the western South Atlantic basin and the role of Antarctic Bottom Water. Journal of Marine Systems 94, 197–203.

Roberts, D., Rittschof, D., Gerhart, D.J., Schmidt, A.R., and Hill, L.G., 1989. Vertical migration of the clam Mercenaria mercenaria (L.) (Mollusca, Bivalvia) – environmental correlates and ecological significance. Journal of Experimental Marine Biology and Ecology 126, 271–280.

Romanek, C.S., Grossman, E.L., and Morse, J.W., 1992. Carbon isotopic fractionation in synthetic aragonite and calcite: effects of temperature and precipitation rate. Geochimica et Cosmochimica Acta 56, 419–430.

Romanek, C.S., Jones, D.S., Williams, D.F., Krantz, D.E., and Radtke, R., 1987. Stable isotopic investigation of physiological and environmental changes recorded in shell carbonate from the giant clam *Tridacna maxima* Marine Biology 94, 385–393.

Rosenberg, G.D., and Hughes, W.W., 1991. A metabolic model for the detennination of shell composition in the bivalve mollusc, *Mytilus edulis*. Lethaia 24, 83–96.

Sabine, C.L., Feely, R.A., Key, R.M., Bullister, J.L., Millero, F.J., Lee, K., Peng, T.-H., Tilbrook, B., Ono, T., and Wang, C.S., 2002. Distribution of anthropogenic CO2 in the Pacific Ocean. Global Biogeochem Cycles 16, 1083 http://dx.doi.org/10.1029/2001GB001639

Schneider, U., Becker, A., Finger, P., Meyer-Christoffer, A., Rudolf, B., and Ziese, M., 2011. GPCC Full Data Reanalysis Version 6.0 at 1.0°: Monthly Land-Surface Precipitation from Rain-Gauges built on GTS-based and Historic Data. DOI: 10.5676/DWD_GPCC/FD_M_V6_100

Schöne, B.R., Dunca, E., Fiebig, J., and Pfeiffer, M., 2005. Mutvei's solution: an ideal agent for resolving microgrowth structures of biogenic carbonates. Palaeogeography, Palaeoclimatology, Palaeoecology 228, 149–166.

Schöne, B.R., Wanamaker, Jr, A.D., Fiebig, J., Thébault, J., and Kreutz ,K.J, 2011. Annually resolved $\delta^{13}C$ shell chronologies of long-lived bivalve mollusks (*Arctica islandica*) reveal oceanic carbon dynamics in the temperate North Atlantic during recent centuries. Palaeogeography, Palaeoclimatology, Palaeoecology 302, 31–42.

Surge, D., Lohmann, K.C., Dettman, D.L., 2001. Controls on isotopic chemistry of the American oyster, *Crassostrea virginica*: implications for growth patterns. Palaeogeography, Palaeoclimatology, Palaeoecology 172, 283–296.

Swart, P.K., Moore, M., Charles, C., Böhm, F., 1998. Sclerosponges may hold new keys to marine paleoclimate. EOS Transactions AGU 79, 636–638.

Yan, L., Schöne, B.R., and Arkhipkin, A., 2012. *Eurhomalea exalbida* (Bivalvia): a reliable recorder of climate in southern South America? Palaeogeography, Palaeoclimatology, Palaeoecology 350–352, 91–100.

Chapter 4: Shells of *Paphia undulata* (Bivalvia) from the South China Sea as potential proxy archives of the East Asian summer monsoon – a sclerochronological calibration study

Lina Yan[1,2], Bernd R. Schöne[1], Shengrong Li[2], Yan Yan[3]

1 Earth Science System Research Center, Department of Applied and Analytical Paleontology, Institute of Geosciences, University of Mainz, Germany

2 State Key Laboratory of Geological Processes and Mineral Resources, China University of Geosciences, China

3 South China Sea Institute of Oceanology Chinese Academy of Sciences, China

Yan, L., Schöne, B.R., Li, S., and Yan, Y., Shells of *Paphia undulata* (Bivalvia) from the South China Sea as potential proxy archives of the East Asian summer monsoon – a sclerochronological calibration study. Submitted to Journal of Oceanagraphy.

Foreword

A long lifespan is one of the advantages for bivalves that can serve as an ideal archive for long-term environmental changes. On the other hand, the short-lived bivalves can also be useful for providing details on sub-annual environmental changes including paleoseasonality and paleoweather. This chapter presents a high-resolution calibration study utilizing shells of the short-lived and fast growing marine bivalve mollusk, *Paphia undulata*. Shell growth patterns, stable carbon and oxygen isotopes are used to determine the life-history traits, to interpret the potential environmental controls on shell growth, and to investigate whether shells of *P. undulata* can be used as proxy archives to reconstruct the frequency of exceptional summer monsoons in the past.

Abstract

Climate of the northern South China Sea realm is dominated by the East Asian monsoon (EAM) system. Existing paleoclimate reconstructions offered an excellent insight into longer-term variations of the EAM. However, due to a lack of appropriate high-resolution paleoclimate data, relatively little is known about the frequency and strength of EAM extremes during the Holocene. To evaluate and establish a potential proxy archive for past variations of the EAM on shorter time-scales, we have carried out a calibration study on shells of the bivalve mollusk, *Paphia undulata* (Born 1778) from Daya Bay. This species lives for only three years. Shells of *P. undulata* grow uninterruptedly between March and mid November and are formed near oxygen isotopic equilibrium with the ambient environment. Shell stable carbon isotope values likely reflect the relative amount of isotopically light terrestrial carbon that reaches the ocean during the summer monsoon season. Therefore, shells of this species can provide reliable, sub-seasonally resolved data on past East Asian summer monsoon strengths, i.e. the relative amount of precipitation and associated salinity changes in the adjacent ocean. The feasibility of this method has been tested with two Holocene shells from sediment cores taken from nearby Beibu Gulf. If more detailed, (sub)seasonally resolved environmental data from the more distant past were available, predictions of future monsoon-related climate extremes in SE Asia could be significantly improved.

A rather peculiar finding is that shell growth of *P. undulata* seems to be largely uncoupled to measured local environmental variables. Although shell growth is limited to temperatures above ca. 15°C, growth rates appear to be negatively correlated to temperature and chlorophyll a levels and positively to salinity implying that shells grow faster at lower temperature, lower primary productivity and normal marine conditions. It is hypothesized here that extraordinary fast shell growth in early spring (March; low temperature and primary productivity) are facilitated by preserved energy resources and

ensure that the bivalve quickly reaches the predation window and the required size for reproduction. As previously reported, spawning occurs during summer, i.e. at times of maximum phytoplankton abundance.

Keywords

Bivalve mollusk shell · Sclerochronology · Light stable isotopes · Environmental variables · Shell growth rate · Erratic monsoon event · Terrestrial freshwater runoff

4.1. Introduction

To test and verify numerical models capable of predicting future climates in areas affected by the EAM, it is crucial to understand the temporal and spatial environmental variability in the anthropogenically less disturbed past. Existing reconstructions based on proxy records from sediments (Wan et al., 2006; Wang et al., 1999), planktonic foraminifera (Chen et al., 2003; Steinke et al., 2011) and palynology (Li et al., 2010) offer an excellent insight into longer-term variations of the EAM since the Late Pleistocene. However, (sub)seasonally and inter-annually resolved EAM reconstructions are much rarer and largely come from corals (e.g., Sun et al., 2005; Yu et al., 2005) and bivalve mollusk shells (e.g., Marwick and Gagan 2011; Schöne et al., 2004; Stephens et al., 2008; Yan et al., 2013). Accordingly, relatively little is known about the frequency and strength of EAM extremes within individual years of the past. In fact, the number of erratic monsoons, i.e. individual years of excessive or strongly reduced rainfall, appears to have increased recently and may continue to do so in a warmer world (Schewe and Levermann 2012). If more detailed, seasonally resolved environmental data from the more distant past were available, predictions of future climate extremes in SE Asia associated with the monsoon could be significantly improved.

To evaluate a potential proxy archive of the EAM in the Indo-West Pacific that is capable of providing the necessary temporal resolution, we have carried out a high-resolution calibration study utilizing shells of the veneroid bivalve mollusk, *Paphia undulata*, also known as short-necked clam or undulated surf clam. This very short-lived and fast-growing species (~ two years-old, typical shell length of 5 cm; Winckworth 1931) exhibits a broad biogeographic distribution in the Indo-West Pacific, including the South China Sea (Poutiers 1998) and is frequently found as well-preserved fossils in sedimentary strata. In the present study, we determine (1) the duration of the growing season, (2) the rate of shell growth during different seasons, (3) the longevity, and (4) the potential environmental controls on shell growth of *P. undulata* from Daya Bay, northern South China Sea. Knowing the life-history traits and environmental forcings of shell growth is prerequisite for the use of fossil shells of this species to reconstruct past changes of the EAM. In this study, we also applied the method presented herein to fossil shells (Holocene age) from sediment cores taken at nearby Beibu Gulf.

4.2. Material and methods

Two specimens of *Paphia undulata* (100% aragonite according to XRD analysis) were collected alive in ca. 6 m water depth at Daya Bay (Guangdong province; 22°42'N, 114°38'E), northern South China Sea on 13th May 2012. Shell lengths of specimens YY-DB-A01R and YY-DB-A04R were 4.7 cm and 4.4 cm, respectively. Daya Bay is a subtropical drowned valley bay located at the

southern coast of China (Figure 4.1). The area receives freshwater through some small seasonal streams (Chen et al., 2011), but no major perennial rivers are flowing into Daya Bay. In addition, two well-preserved (100% aragonite according to XRD analysis and Raman mapping) fossil shells (YL-BG-D03L = ca. AD 1400, YL-BG-D04L = ca. AD 280, age estimates based on sediment depth and $^{14}C_{AMS}$ dates of co-occurring mollusks) were obtained from two sediment cores taken at Beibu Gulf (Figure 4.1).

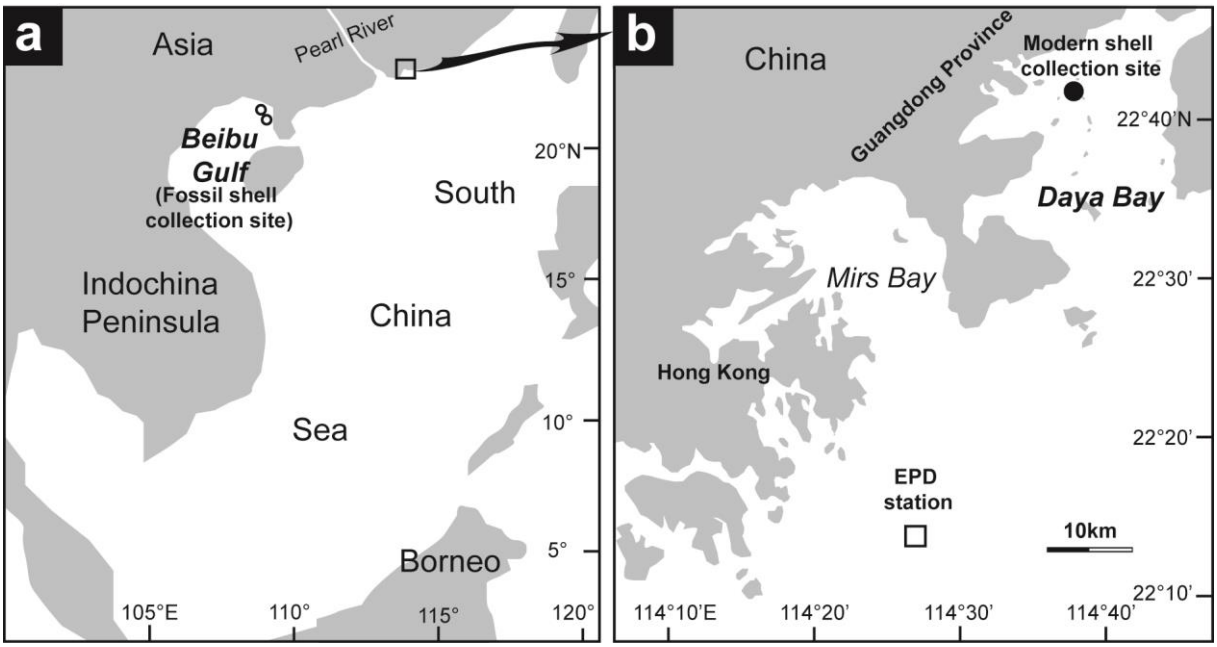

Figure 4. 1. Map showing localities in the South China Sea where bivalve shells, *Paphia undulata*, have been collected and instrumental records were taken. (a) Fossil shell collection site (sediment cores) at Beibu Gulf (open circles). (b) Sample locality of living specimens at Daya Bay (filled circle). Instrumental data were recorded at the Environmental Protection Department (EPD) station (open square).

4.2.1. Sample preparation

The shells were mounted on Plexiglas cubes with plastic welder (GlueTec Multipower) and coated with metal epoxy resin (WIKO) to avoid shell fracture during sectioning. Two 2mm-thick sections were cut from each shell perpendicular to the growth lines along the axis of maximum growth using a low-speed precision saw (Buehler IsoMet 1000) with a 0.4 mm-thick diamond-coated blade. The slabs were mounted on glass slides with metal epoxy resin, ground on glass plates with 800 and 1200 grit powder and polished with 1 μm Al_2O_3 powder on a Buehler G-cloth. After each grinding and polishing step, the cross-sections were ultrasonically rinsed.

4.2.2. Analysis of growth patterns and light stable isotopes

For growth pattern analysis, one of the polished sections was photographed, immersed in Mutvei's solution (Schöne et al., 2005) and then photographed again under reflected-light microscopy (Figure 4.2). Serial photographs of each specimen were stitched together (Figure 4.3) with the Microsoft Image Composite Editor.

For the determination of stable oxygen and carbon isotope values ($\delta^{18}O_{shell}$ and $\delta^{13}C_{shell}$), a total of 128 carbonate powder samples were taken from the outer shell layer of the remaining polished cross-sections (Table 4.1; Figures 4.3, 4.4). Since the outer shell layer in umbonal shell portions was only a few tens to hundreds of µm thick, samples were obtained by milling (Figure 4.3) using a diamond-coated mill bit with 1mm diameter (Komet/Gebr. Brasseler GmbH & Co. KG, model no. 835 104 010). Each milling step comprised 600 to 1000 µm width of shell growth. In the remaining shell portions, powder samples were obtained by drilling (Figure 4.3) using a 300 µm SiC drill bit (model no. H52 104 003). Unsampled shell portions between individual drill holes ranged from 120 to 150 µm. Each subsample weighed between 50 and 120 µg and was processed in a Thermo Finnigan MAT 253 continuous flow-isotope ratio mass spectrometer coupled to a GasBench II. Isotope data were reported in δ-notation and were given as parts per mil (‰). Samples were calibrated against a NBS 19-calibrated IVA Carrara marble ($\delta^{18}O$=-1.91‰, $\delta^{13}C$=2.01‰). On average, replicated internal precision (1σ) and the accuracy (1σ) were better than 0.06‰ and 0.04‰ for $\delta^{18}O$ and $\delta^{13}C$, respectively.

If the $\delta^{18}O_{water}$ value is known and if the shells were built in oxygen isotopic equilibrium with the ambient environment, $\delta^{18}O_{shell}$ values can provide reliable information on the ambient SST during growth (Epstein et al., 1953). To compute past water temperatures, the paleothermometry equation of Grossman and Ku (1986) with a scale correction of - 0.27‰ (Dettman et al., 1999) was used:

$$T_{\delta^{18}O}(°C) = 20.60 - 4.34 \cdot (\delta^{18}O_{shell} - (\delta^{18}O_{water} - 0.27)) \quad (1)$$

where $\delta^{18}O_{shell}$ is measured relative to Vienna PDB and $\delta^{18}O_{water}$ relative to SMOW. The $\delta^{18}O_{water}$ values were interpolated from instrumental salinity records (see below) using the local freshwater mixing line provided by Lin et al (2011):

$$\delta^{18}O_{water}(‰) = 0.24S - 8.33 \quad (2)$$

Between February 2011 and May 2012, reconstructed seasonal $\delta^{18}O_{water}$ values varied between -0.9 ‰ and -0.1 ‰. For temperature error estimates, the 1σ variation of $\delta^{18}O_{water}$ (0.2 ‰ ~ 0.9°C)

and the 1σ analytical error of the mass spectrometer (0.06 ‰ ~ 0.3°C) were both considered. Thus, the cumulative average error of $\delta^{18}O_{shell}$-derived temperatures equaled 1.2°C.

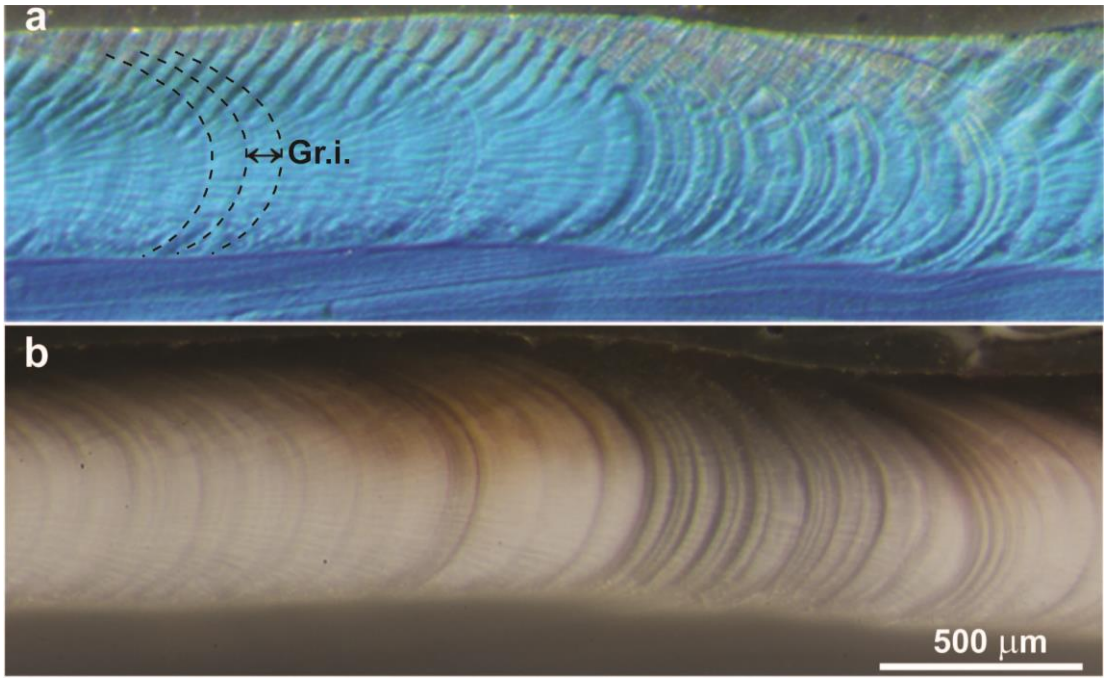

Figure 4. 2. Micrometer-scale shell growth patterns of *Paphia undulata* (specimen YY-DB-A04R) viewed under reflected-light microcopy. Note dark bundles of narrow increments. (a) Polished cross-section immersed in Mutvei's solution, (b) polished cross-section.

4.2.3. Instrumental records

Monthly records of water temperature, chlorophyll a levels and salinity were provided by the Environmental Protection Department (EPD) of the Government of the Hong Kong Special Administrative Region (Figure 4.1; EPD station at 22°13'N, 114°27'E). Data came from sea surface, 14 m and 28 m water depth. Temperature, chlorophyll a and salinity changed non-linearly with increasing water depth. Since the living shells lived in 6 m water depth, a model was computed to reconstruct the environmental variables at that depth. Daily environmental data were linearly interpolated from monthly values (Figure 4.5).

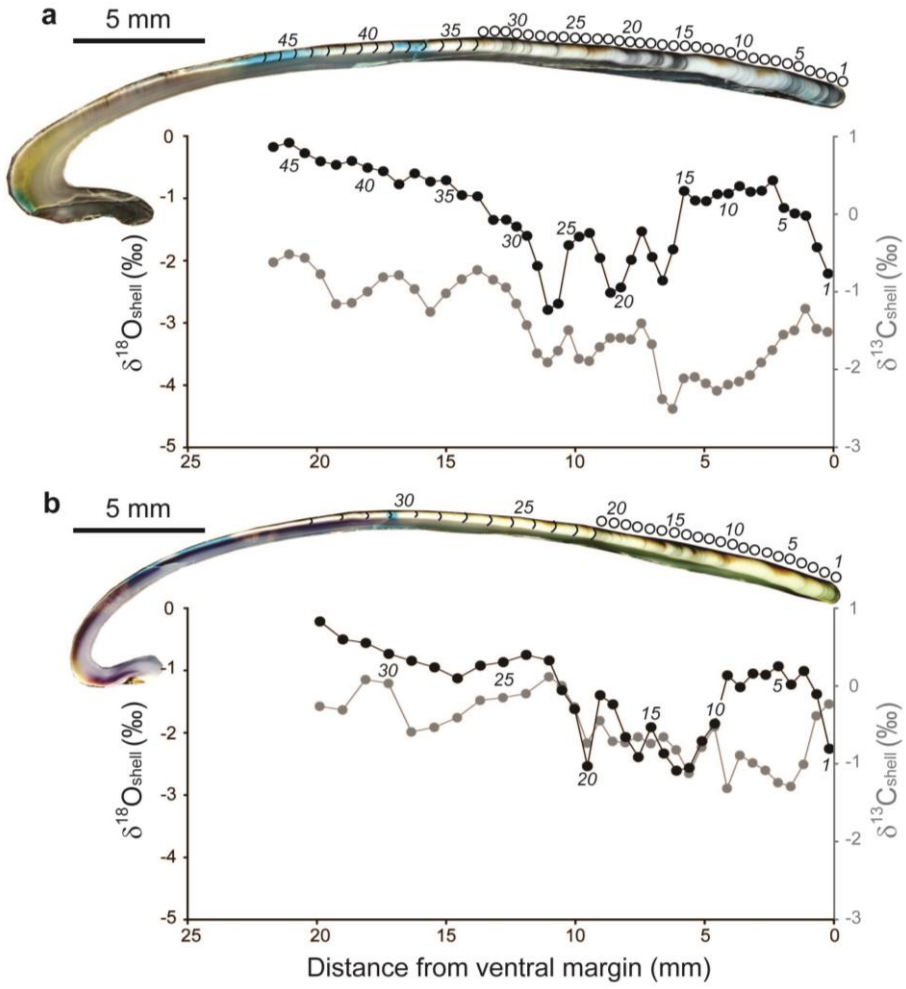

Figure 4. 3. Polished shell cross-sections of live-collected (13 May 2012) specimens of *Paphia undulata* and light stable isotope values. Open circles denote samples taken by drilling. Samples closer to the umbo were taken by milling (milling steps indicated by round lines). (a) Specimen YY-DB-A01R, (b) specimen YY-DB-A04R.

4.3. Results

4.3.1. Shell growth patterns

Growth patterns in the outer shell layer of *Paphia undulata* were difficult to discern, even after immersion in Mutvei's solution (Figure 4.2), and therefore not measured. Polished cross-sections of the living specimens revealed several darker bands ca. 1 to 2 mm and ca. 4 to 8 mm away from the ventral margin and about 1 cm away from the umbo (Figure 4.3). These dark bands consisted of bundles of narrow micrometer-scale growth increments (Figure 4.2).

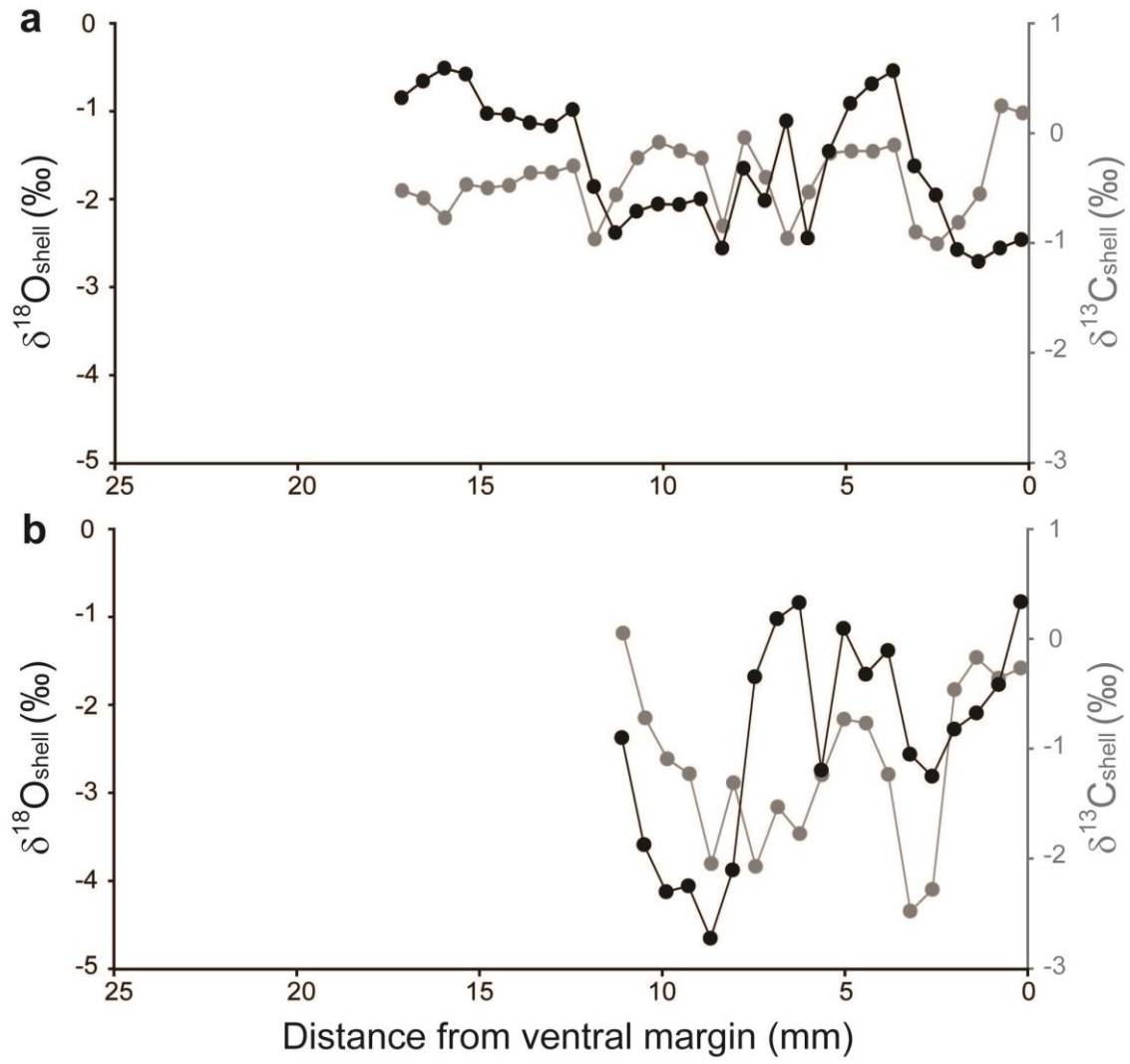

Figure 4. 4. Light stable isotope values of fossil specimens of *Paphia undulata*. (a) Specimen YL-DB-D03L, (b) specimen YL-DB-D04L.

4.3.2. Stable oxygen and carbon isotope values

Shell oxygen isotope curves of the two sampled living shells were fairly similar. The $\delta^{18}O_{shell}$ values ranged from -0.12‰ to -2.77‰ in specimen YY-DB-A01R and from -0.19‰ to -2.58‰ in specimen YY-DB-A04R (Figure 4.3). The most negative $\delta^{18}O_{shell}$ values, i.e. pronounced negative peaks of less than ca. -1.5‰, occurred near major dark growth bands, whereas whitish shell portions with less distinct microgrowth lines and broader microgrowth increments were enriched in ^{18}O and exhibited more gradually changing $\delta^{18}O_{shell}$ values (Figure 4.3). Stable carbon isotope values decreased from ca. -1‰ in the ontogenetically youngest sampled shell portions (~1.5 cm away from the umbo) to ca. -2.5‰ approximately 5 mm away from the ventral margin. Directly at the ventral margin, however, $\delta^{13}C_{shell}$ values shifted toward less negative values. No obvious agreement was observed between $\delta^{13}C_{shell}$ excursions and dark growth bands (Figure 4.3).

In the two fossil shells, $\delta^{18}O_{shell}$ values fluctuated between -0.49 and -2.69‰ and -0.84 and -4.64‰ in specimens YL-BG-D03L and YL-BG-D04L, respectively (Figure 4.4). Stable carbon isotope values of the shell from the Little Ice Age were up to 1.5 ‰ more positive than at present, whereas those of the specimen from the Roman Optimum were in the range of living shells. The $\delta^{13}C_{shell}$ values did not show directed trends toward more positive or more negative values through lifetime.

4.3.3. $\delta^{18}O_{shell}$ - derived water temperature and reconstructed growth rate

Isotope data were so arranged that the reconstructed and instrumental temperatures were in best agreement (Figure 4.5; YY-DB-A01R: $R = 0.92$, $R^2 = 0.84$, $p<0.0001$; YY-DB-A04R: $R = 0.93$, $R^2 = 0.87$, $p<0.0001$; forced through the origin). According to this temporal alignment, shells grew between early March and mid November at temperatures between 18° and 29°C and salinities of 34.3 and 31.8 PSU. Little or no shell was deposited between mid November of age two and mid March of age three. Taking into account that the instrumental data only came with monthly resolution, the temperatures reconstructed from $\delta^{18}O_{shell}$ values resembled instrumental temperatures reasonably well (Figure 4.5).

In conjunction with the known spatial sampling resolution, the temporal alignment of the isotope data also enabled the reconstruction of seasonal shell growth rates. Dark growth bands coincided with periods of reduced shell growth and were formed between May and mid November. Extremely fast shell growth, however, occurred during March. Within less than two weeks the shell grew more than 7 mm. Noteworthy, chlorophyll a levels were still at minimum during this time of the year. Shell growth rates largely remained below ca. 100 µm per day after April (Figure 4.5).

Since the first 1.5 cm of the shells could not be sampled, it remains unknown when exactly the seasonal shell growth started and during which month of the year the prodissoconch formed. Given that only ca. 5 mm of whitish shell portion has remained unsampled between the dark growth bands close to the umbo and the first isotope sample (~ 1.5 cm away from the umbo) and assuming that shells grew at similar high rates after the dark bands, seasonal growth at age two likely started during mid February at temperatures of ca. 15°C. Interestingly, at age three, shell growth only started in mid March at water temperatures above 20°C. Dark colors in the umbonal shell portions suggest that shell formation of the newborn started during summer.

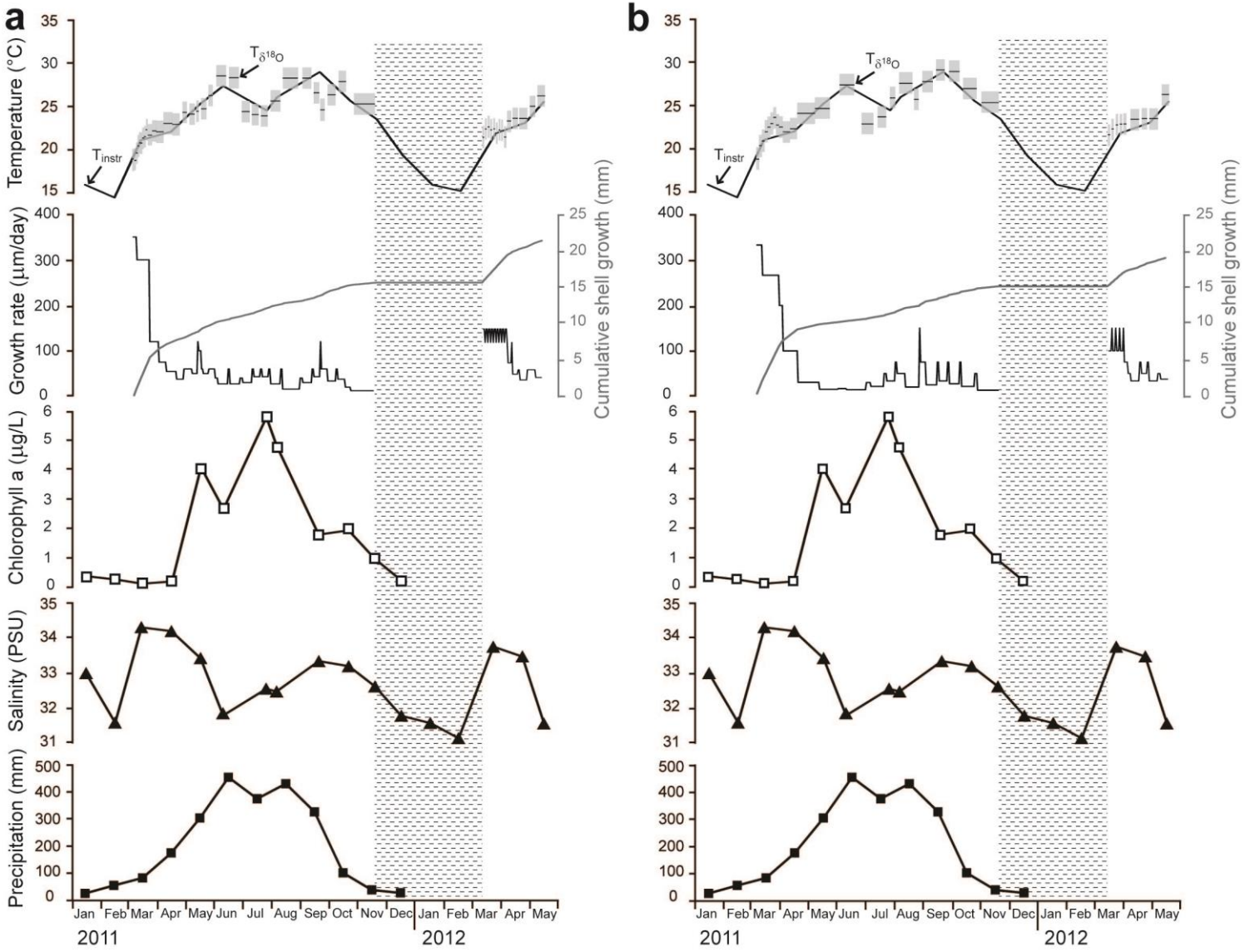

Figure 4. 5. Shell oxygen-isotope-derived temperatures ($T_{\delta 18O}$) and growth rates of live-collected (13 May 2012) *Paphia undulata* specimens from Daya Bay, South China Sea and environmental variables. $T_{\delta 18O}$ and shell growth rates during ontogenetic years two and three are depicted (see Figure 4.3). Grey bars around $T_{\delta 18O}$ denote temperature error of 1.2°C. Note good agreement between $T_{\delta 18O}$ and instrumental water temperature (T_{instr}). Vertical mottled bar = annual growth slowdown or growth cessation. (a) Specimen YY-DB-A01R, (b) specimen YY-DB-A04R.

4.3.4. Regression analyses: shell growth and environmental variables

To identify how environmental variables might have influenced *P. undulata*, reconstructed shell growth rates of live-collected specimens were compared to temperature, salinity and chlorophyll a values (Table 4.1), i.e. factors that are known to affect shell growth of bivalves. Shell growth was negatively correlated to temperature and chlorophyll a levels), but positively to salinity (Table 4.1). Accordingly, *P. undulata* grew faster at lower temperatures (43 to 50% explained variability; Table 4.1), lower primary productivity (16 to 25% explained variability; Table 4.1) and at normal marine conditions (22 to 39% explained variability; Table 4.1).

Table 4. 1. List of shells used in the present study, number of isotope samples and regression analyses between shell growth and environmental variables. YY-DB-A… = *Paphia undulata* collected alive at Daya Bay, South China Sea; YL-BG-D… = *P. undulata* dead-collected at Beibu Gulf, South China Sea. *R* = correlation coefficient, R^2 = coefficient of determination, All *p*-values <0.001, L = linear regression model, E = exponential regression model.

Sample ID	#isotope samples	Regression analysis (R, R^2): Shell growth versus			Date of death /Age
		T_{instr}	Chl a	S_{instr}	
Modern shells					
YY-DB-A01R	46	L, -0.71, 0.50	E, -0.40, 0.16	E, 0.47, 0.22	† 13 May 2012
YY-DB-A04R	33	L, -0.66, 0.43	E, -0.50, 0.25	E, 0.63, 0.39	† 13 May 2012
Fossil shells					
YL-BG-D03L	30				AD 1400
YL-BG-D04L	19				AD 280

4.4. Discussion

(Sub)seasonally resolved paleoclimate data from regions affected by the EAM are still very rare, and existing high-resolution proxy archives come with considerable limitations. For example, tropical corals (e.g., Sun et al., 2005; Yu et al., 2005) typically do not preserve well as fossils or tend to be diagenetically altered due to their large porosity. Likewise, shells of freshwater bivalves (Marwick and Gagan 2011) tend to decay within a few years after burial in humid regions (own

observations). Furthermore, *Tridacna* (Yan et al., 2013) is often bioeroded (Elliot et al 2009) and not frequently found in sedimentary strata. The bivalve, *Paphia undulata* outcompetes corals and other studied bivalves as high-resolution monsoon recorders for the following reasons. *P. undulata* exhibits a broad biogeographic distribution (Poutiers 1998) and occurs with pristine preservation in the fossil record (this study). Its shells are small and can therefore occur in sediment cores (this study). Fossil shells are often well-preserved which enables isotope geochemical analyses. As demonstrated in the present study, shells of *P. undulata* grow extremely rapidly which is prerequisite for a high-resolution archive. The shells faithfully record ambient environmental conditions between March and mid November, i.e. during the summer monsoon season, in the form of variable growth rates and isotope geochemical properties. The major disadvantage of this species is its short life span of only three years. It will be largely impossible to study seasonal precipitation rates over several consecutive years. As a consequence, a large number of shells are required to characterize the frequency of EAM extremes of a certain time interval.

4.4.1. Life-history traits

Despite its potential use as a high-resolution recorder of past environmental variability and its commercial importance in many South East Asian countries (Cesar et al., 2003; del Norte-Campos et al., 2010; Leethochavalit et al., 2004; Nabuab et al., 2010; Thomas and Nasser, 2009), the life-history traits of the genus *Paphia* and, in particular, of the overexploited *P. undulata* are not well known and have never been studied by means of sclerochronology. Only a single previous study (Winckworth, 1931) addressed the growth rates of this genus. Our findings on longevity as well as timing and rate of seasonal shell growth of *P. undulata* are in good agreement with observations of Winckworth (1931). Based on seasonal collections of specimens from Madras Harbor, southern India, Winckworth (1931) concluded that the lifespan of *P. undulata* does not exceed two years. Present results, however, suggested that specimens from the South China Sea grew for at least three years (Figure 4.5). Shells collected in fall measured less than 15 mm in length, and those from July were about 2 mm long (Winckworth 1931). Spawning likely occurred in June (Winckworth 1931). This finding is corroborated by cytological analyses (Zhao et al., 1991) and our study according to which first shell material formed during summer. Furthermore, Winckworth (1931) observed extremely rapid shell growth during late spring and summer, sharply reduced rates in fall, and a growth cessation during winter. At Daya Bay, shell growth at age two started ca. three months earlier than at Madras Harbor, but likewise at very rapid rates. These differences in the timing of seasonal shell growth may be attributed to habitat differences.

4.4.2. Environmental factors affecting shell growth

Winckworth (1931) identified temperature as the main environmental factor for shell growth of *P. undulata*. According to his study, shell growth is positively correlated to water temperature with maximum growth rates occurring at temperatures of ca. 31°C. The complete opposite was found in the present study for *P. undulata* from the South China Sea. Here, specimens grew slower with increasing temperature (Figure 4.5; Table 4.1).

The negative correlation between shell growth and temperature (Table 4.1) is rather peculiar, the more so as fastest shell growth occurred during times of lowest phytoplankton concentrations (Figure 4.5; Table 4.1). In fact, shell growth is strongly reduced in summer when both chlorophyll a levels and monsoon-related precipitation rates attain the annual maximum (Figure 4.5). According to many previous studies, shell growth increases when temperature rises unless optimum growth temperatures are not exceeded (e.g., Goodwin et al., 2001; Jones et al., 1989; Miyaji et al., 2010; Schöne et al., 2004b). In cases where temperature is less important for shell growth or exhibits a negative correlation with shell growth rate, food supply is typically the driving factor for growth of bivalves (e.g., Carroll et al., 2009).

Yet, the extraordinary fast shell growth rates in early spring may result from a biological necessity rather than a changing physical environment alone. The fast shell growth not only ensures that the bivalve quickly escapes the predation window, but also rapidly and timely reaches the required size for reproduction. In fact, the newborns are around in summer when phytoplankton levels are at maximum. Presumably, preserved energy resources from the previous year ensure that growth can start early in the year despite environmental conditions are not optimal for shell formation. The present study demonstrates that temperature and food supply may not always be the primary drivers of shell growth as postulated in numerous previous papers (e.g., Goodwin et al., 2001; Jones et al., 1989; Miyaji et al., 2010; Schöne et al., 2004).

Of course, we cannot preclude that extremely fast shell growth in early spring was attributed to stronger bottom currents and associated higher amounts of re-suspended organic matter at the sea floor that nourished the bivalves. This hypothesis remains untested because current strength has not been measured. Likewise, stable carbon isotope values of the shells likely do not yield information on food availability. The $\delta^{13}C_{shell}$ values decreased gradually during the growing season of year two. This may either indicate an incorporation of increasing amounts of isotopically light respiratory CO_2 with increasing ontogenetic age or, more likely, monsoon-related freshwater runoff from land with isotopically very light, plant-derived carbon which drove $\delta^{13}C_{DIC}$ and $\delta^{13}C_{shell}$ toward more negative values. It seems at least unlikely that the $\delta^{13}C_{shell}$ values

recorded changes in primary productivity, because changing chlorophyll a values did not have any notable effect on the stable carbon isotope signature of the shells (Figure 4.5).

4.4.3. Shell-based reconstructions of the relative monsoon strength

If $\delta^{13}C_{DIC}$ values were indeed influenced by terrestrial runoff during the summer monsoon season, $\delta^{13}C_{shell}$ values of specimens from the same locality and water depth could potentially serve as a proxy of the relative monsoon strength. Stronger precipitation and terrestrial runoff should then result in more negative $\delta^{13}C_{shell}$ values. Microgrowth patterns can function as an additional proxy of the relative monsoon-related precipitation and freshwater runoff into the ocean. During stronger monsoons and more frequent extreme rains, shell growth rates are slower and bundles of microgrowth increments and lines may appear darker and may be more numerous.

Furthermore, shell oxygen isotope values can provide qualitative estimates of the amount of monsoonal rain and terrestrial runoff. However, it needs to be considered that the fractionation of shell oxygen isotopes is also controlled by temperature, i.e., warmer water will be reflected by more negative $\delta^{18}O_{shell}$ values. Yet, a minimum estimate on the relative summer monsoon strength can be given, because bivalve shells (and skeletons of many other invertebrates) typically do not grow at temperatures higher than 31°C (Ansell, 1968; Schöne, 2008). Assuming such temperatures prevailed while the shell recorded monsoon-related freshwater discharge during summer, differences in the most negative $\delta^{18}O_{shell}$ values of different specimens can be indicative of erratic monsoons. For example, more negative $\delta^{18}O_{shell}$ values than measured in shells of this study would indicate higher precipitation rates and a stronger summer monsoon.

As indicated by one of the two fossil samples (YL-BG-D04L) from Beibu Gulf, the summer monsoon was much stronger when this specimen was alive. Based on the $\delta^{18}O_{shell}$ data, ocean salinity can be computed by solving equation 1 for $\delta^{18}O_{water}$, equation 2 for salinity and assuming the highest possible growth temperature of 31°C: 26.2 PSU. This result also suggests that *P. undulata* can grow shell even at lower salinities than 31.8 PSU which underscores the usefulness of this species as a proxy archive for the summer monsoon.

4.5. Summary and conclusions

Shells of *Paphia undulata* provide serviceable proxy archives to reconstruct the frequency of exceptional summer monsoons in the past. The relative strength of monsoon-related precipitation and associated changes in ocean salinity and the $\delta^{13}C_{DIC}$ signature can be estimated from the $\delta^{18}O_{shell}$ and $\delta^{13}C_{shell}$ values as well as shell growth patterns. Fast growth rates in early spring are likely facilitated by preserved energy resources from the previous year and not primarily

controlled by actual temperature and primary productivity, because the shells grew at fastest rates when temperature and chlorophyll a concentrations were near the seasonal minimum.

Fossil shells used in this study suggest that climatic warm intervals were characterized by more intense summer precipitation than at present, while colder periods were slightly drier. Future studies should focus on additional fossil material and apply the techniques presented herein to identify if the number of excessive monsoon-related precipitation events is indeed associated with climate change.

4.6. Acknowledgements

We are grateful to *** and ***, University of Mainz for conducting the XRD analyses and ***, AWI Bremerhaven for conducting Raman mapping. We are indebted to *** for processing the isotope samples. The Environmental Protection Department, Government of the Hong Kong Special Administrative Region is kindly acknowledged for providing instrumental data. This work has been made possible by a PhD scholarship provided by Earth System Science Research Center Geocycles, University of Mainz (2012-2013) and the Chinese Scholarship council (2010-2012).

4.7. References

Ansell, A.D., 1968. The rate of growth of the hard clam *Mercenaria mercenaria* (L) throughout the geographic range. Journal du Conseil Permanent International pour l'Exploration de la Mer 31, 364–409.

Carroll, M.L., Johnson, B.J., Henkes, G.A., McMahon,K.W., Voronkov, A., Ambrose, Jr, W.G., and Denisenko, S.G., 2009. Bivalves as indicators of environmental variation and potential anthropogenic impacts in the southern Barents Sea. Marine Pollution Bulletin 59, 193–206.

Cesar, S.A., Germano, B.P., and Melgo, J.F., 2003. Preliminary results on the population, reproductive and fishery biology of the nylon shell, *Paphia textile* (Gmelin 1790) in Leyte. UPV Journal of Natural Science 8, 83–95.

Chen, M., Shiau, L., Yu, P., Chiu, T., Chen, Y., and Wei, K., 2003. 500000-year records of carbonate, organic carbon, and foraminiferal sea–surface temperature from the southeastern South China Sea (near Palawan Island). Palaeogeography, Palaeoclimatology, Palaeoecology 197, 113–131.

Chen, S., Li,Y., Hu, J., Zhen, A., Huang, L., and Lin, Y., 2011. Multiparameter cluster analysis of seasonal variation of water masses in the eastern Beibu Gulf. Journal of Oceanography 67, 709–718.

del Norte-Campos, A.G.C., Nabuab, F.M., Palla, R.Q., and Burlas, M.R., 2010. The early development of the short-necked clam, *Paphia undulata* (Born 1778) (Mollusca, Pelecypoda: Veneridae) in the laboratory. Science Diliman 22, 13–20.

Dettman, D.L., Reische, A.K., and Lohmann, K.C., 1999. Controls on the stable isotope composition of seasonal growth bands in aragonitic fresh-water bivalves (Unionidae). Geochimica et Cosmochimica Acta 63, 1049–1057.

Elliot, M., Welsh, K., Chilcott, C., McCulloch, M., Chappell, J., and Ayling, B., 2009. Profiles of trace elements and stable isotopes derived from giant long-lived *Tridacna gigas* bivalves: Potential applications in paleoclimate studies. Palaeogeography, Palaeoclimatology, Palaeoecology 280, 132–142.

Epstein, S., Buchsbaum, R., Lowenstam, H.A., and Urey, H.C., 1953. Revised carbonate-water isotopic temperature scale. Geological Society of America Bulletin 64, 1315–1326.

Goodwin, D.H., Flessa, K.W., Schöne, B.R., and Dettman, D.L., 2001. Cross-calibration of daily growth increments, stable isotope variation, and temperature in the Gulf of California bivalve mollusk *Chione cortezi*: implications for paleoenvironmental analysis. Palaios 16, 387–398.

Grossman, E.L., and Ku, T.-L., 1986. Oxygen and carbon isotope fractionation in biogenic aragonite; temperature effects. Chemical Geology (Isotope Geoscience Section) 59, 59–74.

Jones, D.S., Arthus, M.A., and Allard, D.J., 1989. Sclerochronological records of temperature and growth from shells of *Mercenaria mercenaria* from Narragansett Bay, Rhode Island. Marine Biology 102, 225–234.

Leethochavalit, S., Chalermwat, K., Upatham, E.S., Choi, K.S., Sawangwong, P., and Kruatrachue, M., 2004. Occurrence of *Perkinsus* sp. in undulated surf clams *Paphia undulata* from the Gulf of Thailand. Diseases of Aquatic Organisms 60, 165–171.

Li, Z., Zhang, Y., Li, Y., and Zhao, J., 2010. Palynological records of Holocene monsoon change from the Gulf of Tonkin (Beibuwan), northwestern South China Sea. Quaternary Research 74, 8–14.

Lin, I., Wang, C., Lin, S., and Chen, Y., 2011. Groundwater-seawater interactions off the coast of southern Taiwan: Evidence from environmental isotopes. Journal of Asian Earth Sciences 41, 250–262.

Marwick, B., and Gagan, M.K., 2011. Late Pleistocene monsoon variability in northwest Thailand: an oxygen isotope sequence from the bivalve *Margaritanopsis laosensis* excavated in Mae Hong Son provinceQuaternary Science Reviews 30, 3088–3098.

Miyaji, T., Tanabe, K., Matsushima, Sato, Y. S., Yokoyama, Y., and Matsuzaki, H., 2010. Response of daily and annual shell growth patterns of the intertidal bivalve *Phacosoma japonicum* to Holocene coastal climate change in Japan. Palaeogeography, Palaeoclimatology, Palaeoecology 286, 107–120.

Nabuab, F.M., Ledesma-Fernandez, L., and del Norte-Campos, A., 2010. Reproductive biology of the short-necked clam, *Paphia undulata* (Born 1778) from southern Negros Occidental, Central Philippines. Science Diliman 22, 31–40.

Poutiers, J.M., 1998. Bivalves. In: Carpenter, K.E., and Niem, V.H., (eds.) FAO species identification guide for fishery purposes. The living marine resources of the Western Central Pacific, Volume 1, FAO, Rome, Italy, pp. 328–344.

Schewe, J., and Levermann, A., 2012. A statistically predictive model for future monsoon failure in India. Environmental Research Letters 7044023, doi:10.1088/1748-9326/7/4/044023

Schöne, B.R., 2008. The curse of physiology – Challenges and opportunities in the interpretation of geochemical data from mollusk shells. Geo-Marine Letters 28, 269–285.

Schöne, B.R., Houk, S.D., Freyre Castro, A.D., Fiebig, J., Kröncke, I., Dreyer, W., and Oschmann, W., 2005. Daily growth rates in shells of *Arctica islandica*: Assessing sub-seasonal environmental controls on a long-lived bivalve mollusk. Palaios 20, 78–92.

Schöne, B.R., Oschmann, W., Tanabe, K., Dettman, D., Fiebig, J., Houk, S.D., and Kanie, Y., 2004. Holocene seasonal environmental trends at Tokyo Bay, Japan, reconstructed from bivalve mollusk shells – implications for changes in the East Asian monsoon and latitudinal shifts of the Polar Front. Quaternary Science Reviews 23, 1137–1150.

Steinke, S., Glatz, C., Mohtadi, M., Groeneveld, J., Li, Q., and Jian, Z., 2011. Past dynamics of the East Asian monsoon: No inverse behavior between the summer and winter monsoon during the Holocene. Global and Planetary Change 78, 170–177.

Stephens, M., Mattey, D., Gilbertson, D.D., and Murray-Wallace, C.V., 2008. Shell-gathering from mangroves and the seasonality of the Southeast Asian Monsoon using high-resolution stable isotopic analysis of the tropical estuarine bivalve (*Geloina erosa*) from the Great Cave of Niah, Sarawak: methods and reconnaissance of molluscs of early Holocene and living times. Journal of Archaeological Science 35, 2686–2697.

Sun, D., Gagan, M.K., Cheng, H., Scott-Gagan, H., Dykoski, C.A., Edwards, R. L., and Su, R., 2005. Seasonal and interannual variability of the Mid-Holocene East Asian monsoon in coral $\delta^{18}O$ records from the South China Sea. Earth and Planetary Science Letters 237, 69–84.

Thomas, S., and Nasser, M., 2009. Growth and population dynamics of short-neck clam *Paphia malabarica* from Dharmadom estuary, North Kerala, southwest coast of India. Journal of the Marine Biological Association of India 51, 87–92.

Wan, S., Li, A., Clift, P.D., and Jiang, H., 2006. Development of the East Asian summer monsoon: evidence from the sediment record in the South China Sea since 8.5 Ma. Palaeogeography, Palaeoclimatology, Palaeoecology 241, 139–159.

Wang, L., Sarnthein, M., Erlenkeuser, H., Grimalt, J.O., Grootes, P., Heilig, S., Ivanova, E., Kienast, M., Pelejero, C., and Pflaumann, U., 1999. East Asian monsoon climate during the late Pleistocene: high-resolution sediment records from the South China Sea. Marine Geology 156, 245–284.

Winckworth, R., 1931. On the growth of *Paphia undulata* (Veneridae). Proceedings of the Malacological Society of London 19, 171–174.

Yan, H., Shao, D., Wang, Y., and Sun, L., 2013. Sr/Ca profile of long-lived *Tridacna gigas* bivalves from South China Sea: A new high-resolution SST proxy. Geochimica et Cosmochimica Acta 112, 52–65.

Yu, K., Zhao, J., Wei, G., Cheng, X., and Wang, P., 2005. Mid-late Holocene monsoon climate retrieved from seasonal Sr/Ca and $\delta^{18}O$ records of *Porites lutea* corals at Leizhou Peninsula, northern coast of South China Sea. Global and Planetary Change 47, 301–316.

Zhao, Z., Li, F., and Ke, C., 1991. On the sex gonad development and reproductive cycle of clam *Paphia undulata*. Journal of Fisheries of China 15, 1–8.

Chapter 5: A preliminary investigation of shell growth of *Margaritifera falcata* in rivers of British Columbia, Canada

Foreword

Life history traits and shell growth patterns of the marine bivalves can provide valuable environmental information. Likewise, shell growth characteristics of the freshwater mussels are also useful indicators for ambient environmental changes. In this chapter, population age structures and shell growth rates are analyzed in the western pearlshell, *Margaritifera falcata* from different river environments. The aim is to infer the effects of environmental parameters on the shell growth characteristics of the freshwater mussels.

5.1. Introduction

The western pearlshell, *Margaritifera falcata* (Gould 1850) is a common freshwater species in the Pacific Northwest. The range of this species extended from Alaska and British Columbia south to central California and east to Montana, Wyoming, and northern Utah (Taylor 1981), but the geographical area occupied and local abundance of *M. falcata* have declined substantially during the past decades (e.g., Stagliano et al., 2007; Hastie and Toy, 2008). The factors attributed to its decline include poor water quality, river habitat degradation and host fish impacts (Frest and Johannes 1995; Hovingh 2004; Brim Box et al., 2006; Howard and Cuffey 2006). *M. falcata* has been of main concern to biologists and environmentalists for conservation biology, particularly in a number of rivers of United States, due to a recent decline and even the potential extirpation of this species (e.g., Brim Box et al., 2003, 2006; Howard and Cuffey 2006; Stagliano et al., 2007). *M. falcata* is still widely distributed and considered secure in British Columbia (BC), Canada (NatureServe Explorer, 2012, http://www.natureserve.org/explorer/; The Xerces Society for Invertebrate Conservation, http://www.xerces.org/western-pearlshell/), yet the age distributions and growth rates could differ significantly between rivers due to variations in land use and river hydrology (Howard et al., 2005; Howard and Cuffey, 2006). However, there are rather few studies on *M. falcata* in this region (Schöne et al., 2007; Rodland et al., 2009).

As many other bivalve mollusks (e.g., Jones et al., 1989; Goodwin et al., 2001; Schöne et al., 2005; Hallmann et al., 2008), freshwater pearl mussels hold the potential to be used as ideal indicators of environmental variability (Howard and Cuffey, 2006; Schöne et al., 2007). This is especially due to the high-sensitivity of this species to environmental changes (Howard et al., 2005; Webb et al., 2008; Limm and Power, 2011). In addition, *M. falcata* is a long-lived bivalve species that belongs to a family with maximum lifespans of >100 years (e.g., Hastie et al., 2000; Schöne et al., 2004), which allows long-term reconstructions of environmental conditions. Importantly, *M. falcata* forms distinct annual growth lines and increments, which provide reliable evidences for age determinations and shell growth pattern analyses, and thus allow the direct comparisons of age and size.

In order to unravel the effects of environmental factors on growth rates of western pearlshells, population age structures and the relationship between shell height and ontogenetic ages were investigated in *M. falcata* specimens collected from four rivers in southwestern BC. The preliminary objective is to examine the differences and similarities in lifespans, as well as in growth equations (inferred from the relationship of shell height versus age) of individuals from the different rivers, and further to decipher the effects of environmental parameters on the shell growth of the western pearlshells.

5.2. Material and methods

Thirty-eight living and two hundred fifty-eight dead specimens of *M. falcata* were collected between April 2005 and April 2008 from Piercy Creek, Chase River, Salmon River and Little Campbell River of BC, Canada (Figure 5.1, Table 5.1). After removal of the soft parts, all shells were measured with vernier callipers to the nearest 0.1 mm by their height, i.e. the distance from the umbo to the ventral margin (Figure 5.2). Subsequently, the shells were cleaned in de-ionized water and 99.5% Ethanol and air-dried for further analysis.

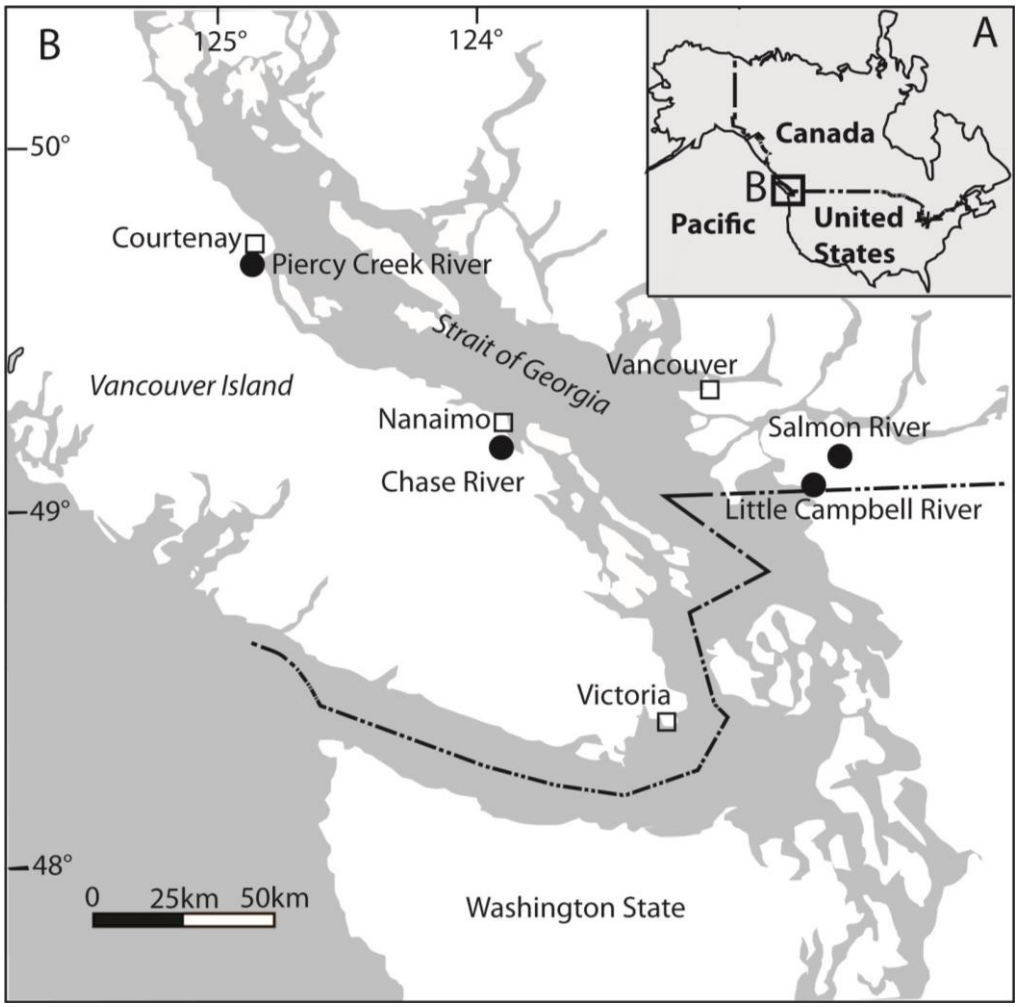

Figure 5. 1. Map displaying the four sampling localities (Little Campbell River, Salmon River, Chase River and Piercy Creek River from South to North, respectively) in British Columbia, Canada.

One value of each specimen was mounted on plexiglass cubes, and shell surfaces were coated with a protective layer of a WIKO metal epoxy resin prior to cutting. After the epoxy had cured, two ca. 2–3mm thick slabs were cross-sectioned along the axis of minimum growth and perpendicular to the growth lines. All cross-sections were mounted on glass slides, ground (800

and 1,200 grit SiC powder) on glass plates and polished (1µm Al_2O_3 powder) on a Buehler G-cloth. After polishing, one slab of each specimen was immersed in Mutvei's solution for 20-25 min under constant stirring at 37-40°C (Schöne et al., 2005). This treatment facilitates the estimation of ontogenetic ages of bivalves by revealing distinct annual growth lines and increments. For *M. falcata,* annual growth lines were visible in both stained and unstained slabs, and therefore, age determination were double checked on both slabs (Figure 5.2).

Table 5. 1. List of *Margaritifera falcata* shells used in this study.

Locality	Collected date	Number of specimens		Estimated age (years)	
		Alive	Dead	Range	Average
Little Campbell River	01 Jun; 01 Sep; 29 Oct 2005;01 Apr 2008	8	172	2-81	26±3
Salmon River	01 May 2005	6	32	3-53	23±3
Chase River	15 May; 28 Oct 2005	16	39	3-22	15±1
Piercy Creek River	20 April 2005	8	15	4-37	14±5
Total		38	258		

The erosion of considerable parts around the umbo in ontogenetically older shells precludes the age estimation of *M. falcata* (Figure 5.2). For solving this problem, the distance from each annual growth line to the umbo was measured in intact young shells and a regression curve was established between the age and the corresponding distance (Figure 5.3), which was then applied to estimate the number of annuli lost in the eroded portions of shells.

To evaluate the shell growth characteristics quantitatively, a regression function was computed between shell height and age for each river. The relationships were best described by natural logarithmic functions with an intercept of 13, which corresponds to the average shell height of one-year-old specimens of the four rivers determined on the shell cross-sections (Figure 5.4).

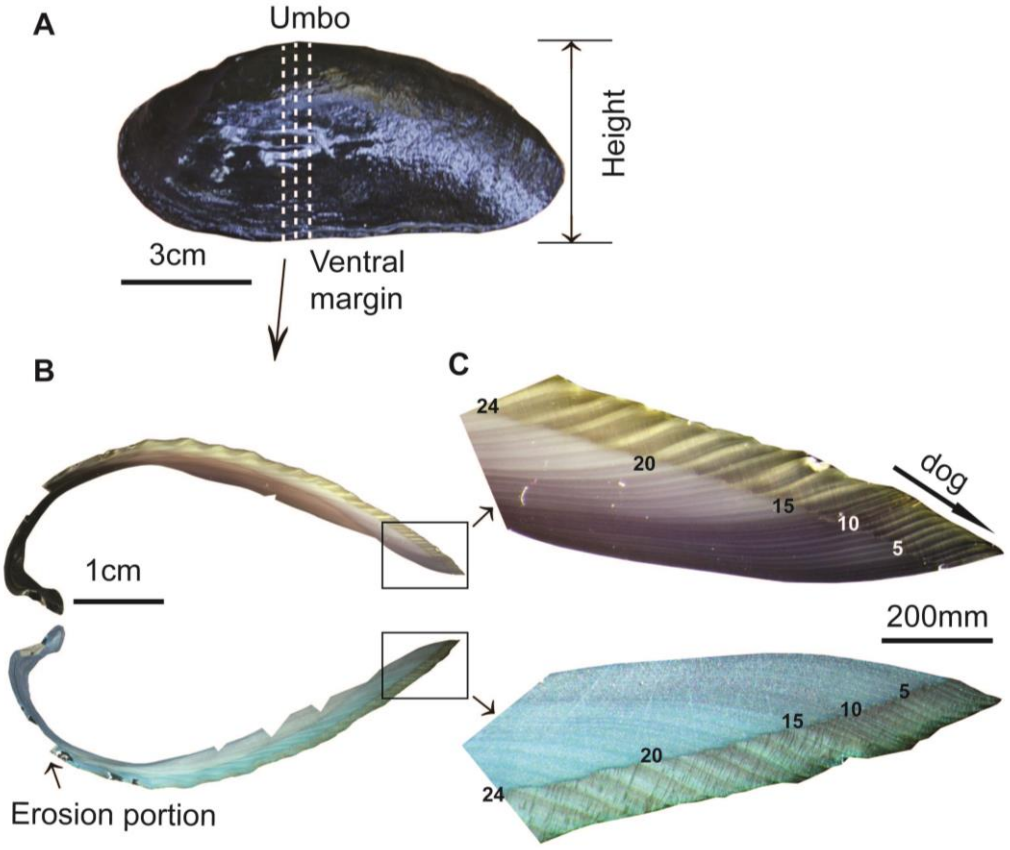

Figure 5. 2. Sample preparation of *Margaritifera falcata* shells. (A) The shell height was measured along the vertical distance from the umbo to the ventral margin. Dashed lines indicate the cross-sectioned slabs. (B) Both etched and unetched slabs reveal annual growth lines and increments in the outermost shell layers. The shell portion close to the umbo been eroded in ontogenetically older specimens (arrow). (C) An example of annual growth lines in the stained and unstained slab of each shell. dog = direction of growth.

5.3. Results

5.3.1. Shell lifespans

The maximum lifespan of individual *M. falcata* differs considerably among populations from the four rivers, with 81 years, 53 years, 37 years and 24 years for Little Campbell River, Salmon River, Piercy Creek River and Chase River populations, respectively. Two groups, i.e. a western group and an eastern group can be clearly distinguished, and are separated by the Georgia Strait, stretching in a NW-SE direction between Vancouver Island and the BC mainland (Figure 5.1). Specimens from the western group (Piercy Creek River and Chase River) exhibit generally shorter lifespans, whereas the eastern group (Salmon River and Little Campbell River) achieve a longer

life (Figure 5.5). Moreover, the average lifespan seems to decrease from southeast to northwest (Table 5.1).

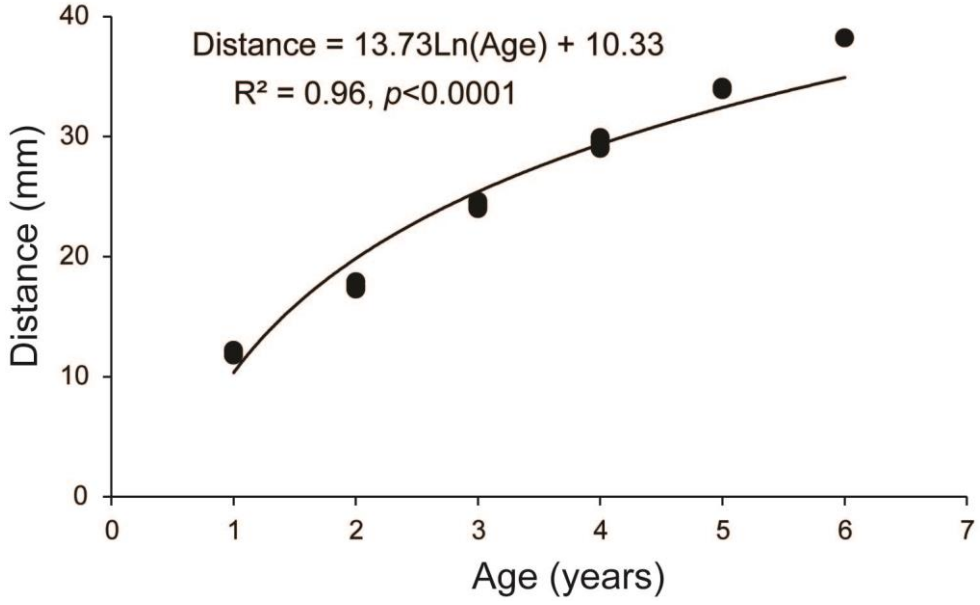

Figure 5. 3. The regression function applied for the age estimation in shells with eroded portions.

5.3.2. Growth equations

For each river locality, a growth equation has been computed based on the relationship between shell height and ontogenetic age of the local *M. falcata* specimens (Figure 5.4). The growth equations inferred from specimens of Salmon River and Little Campbell River (i.e. the eastern group) are very similar. The same holds true for the two equations derived from *M. falcata* of Piercy Creek River and Chase River (the western group; Figure 5.4). Overall, the western group exhibits a lower growth rate with a slope of ca. 7.7~7.8, while bivalves from the eastern group grow faster with a slope of ca. 9.1.

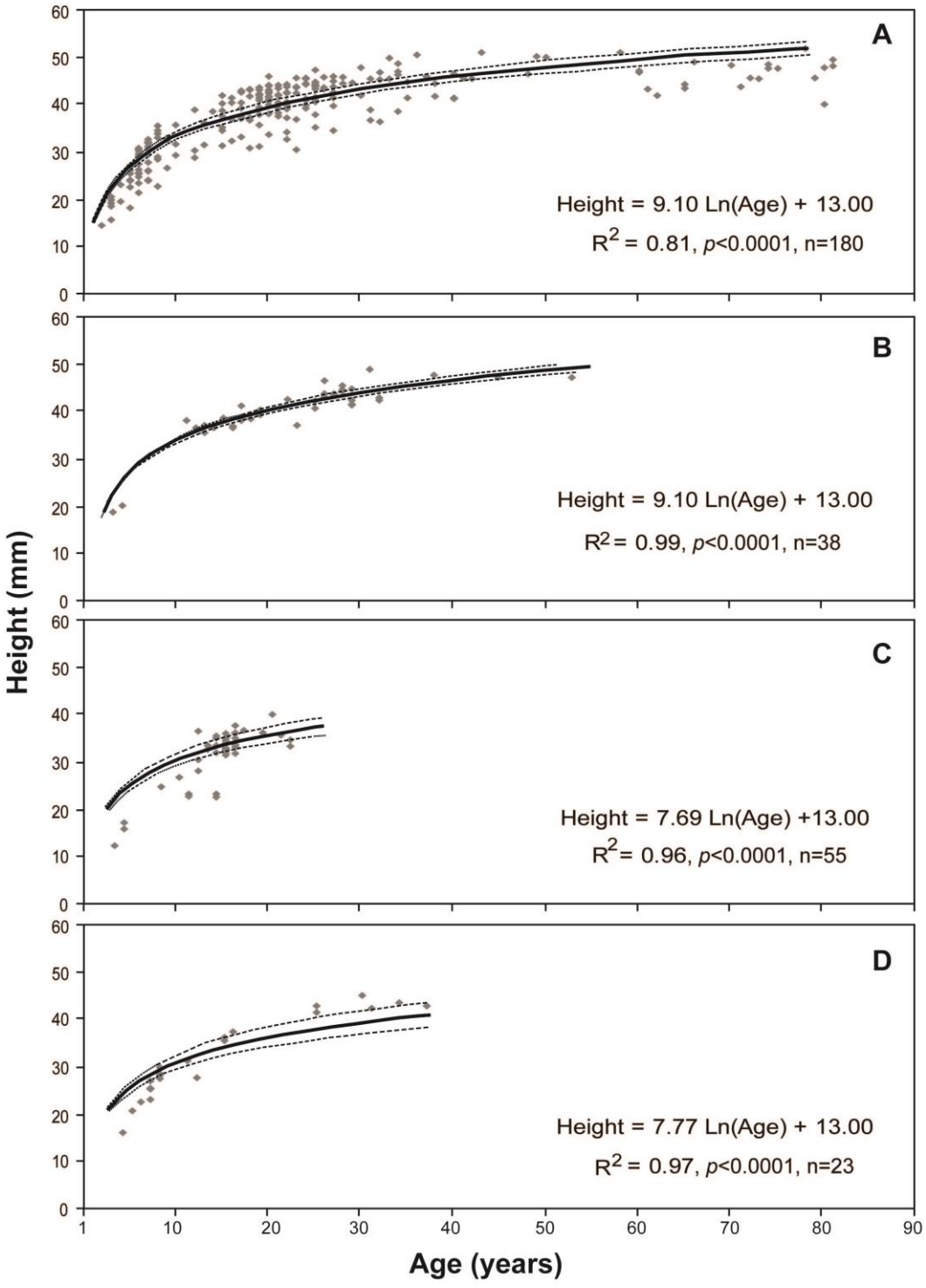

Figure 5. 4. The relationship between shell height and estimated ontogenetic age of the freshwater pearlshell *Margaritifera falcata* in the four different rivers is best described by a logarithmic function (black curve). The 95% confidence interval is indicated by a dotted curve. A: Little Campbell River. B: Salmon River. C: Piercy Creek River. D: Chase River.

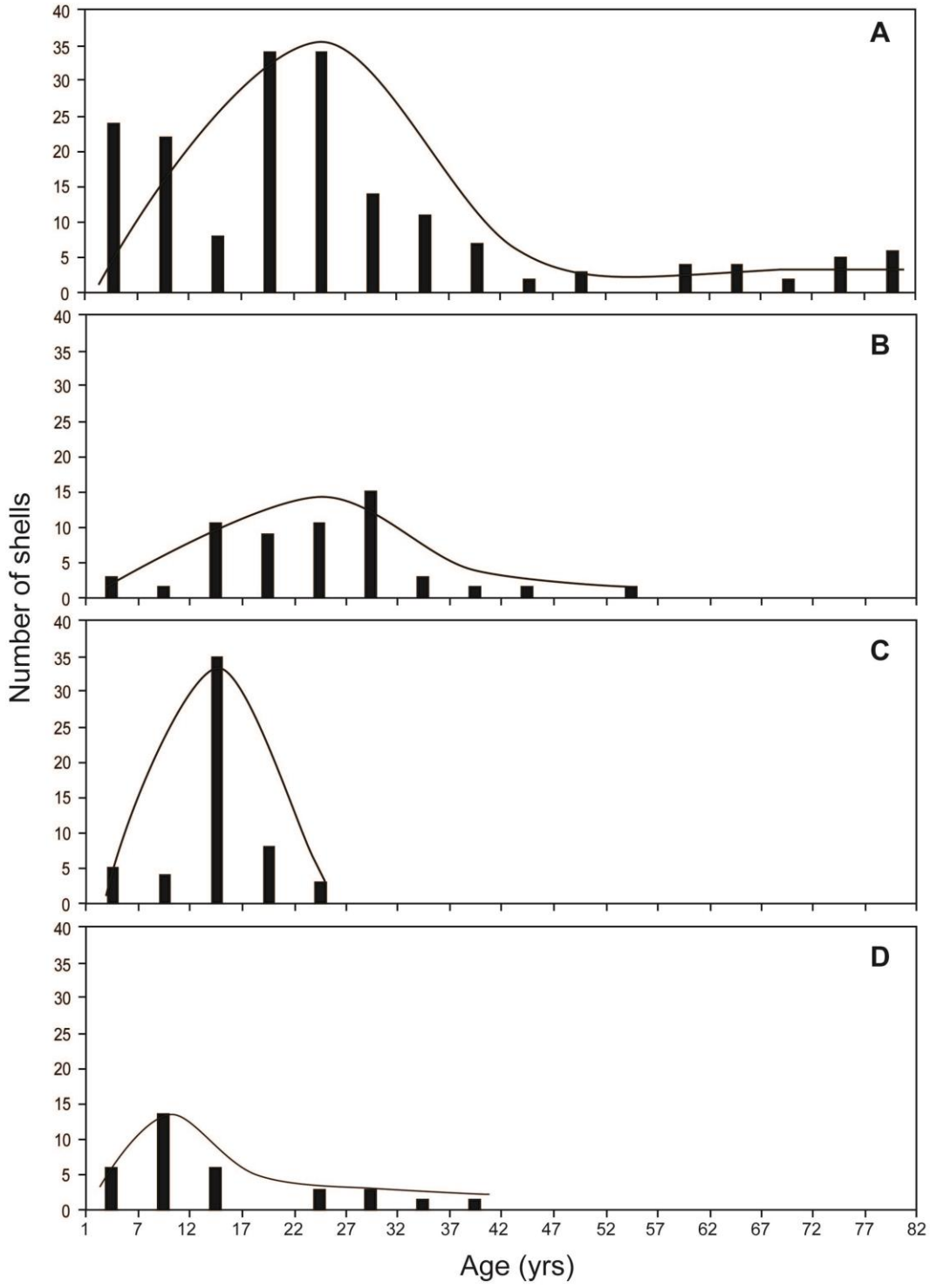

Figure 5. 5. Age distributions and running means of *Margaritifera falcata* in four different rivers. A: Little Campbell River. B: Salmon River. C: Piercy Creek River. D: Chase River.

5.4. Discussion

5.4.1. Land use impacts on lifespans

It has been well investigated that land use practices can affect freshwater mussel populations and age structures (e.g., Brim Box and Mossa, 1999; Howard and Cuffey, 2006; Arbuckle and Downing, 2008; Shea et al., 2013). Howard and Cuffey (2006) analyzed population age structures of *M. falcata* in two northern California Coast Range rivers, the South Fork Eel and the Navarro. They observed considerable differences in mortality rates and recruitment rates between rivers and demonstrated that land use history may be one of the controlling factors. In this study, *M. falcata* specimens from four rivers, in BC, may also record some valuable information on land use histories. The Little Campbell River is located 35 km south of Vancouver with most watersheds within BC and a small part extending into Washington State, US. Land cover in the river watershed is dominated by agricultural land use in the upper reaches with heavy urbanization occurring in the lower reaches (Juteau, 2008). Similarly, the Salmon River watershed is located southeast of Vancouver and has a drainage area of 49 km^2, which has a predominant agricultural and urban land uses, as it flows through the urban-rural fringe (Wernick, 1996). Therefore, the longer life spans of *M. falcata* in eastern populations may be induced by the elevated nutrient input from agricultural land use. On the other hand, water quality can likely be degraded by heavy metals from urban and industrial runoff, as well as by pesticides and fertilizers from agricultural fields. Thus, river pollution may play an adverse role on the age distribution of the investigated species. Nevertheless, it is speculated that the current river environments of the eastern group are favorable for the pearlshell survival and growth. Unlike the eastern group, the rivers in the western group are not dominated by agricultural land uses. The Piercy creek is part of the Millard/Piercy watershed which is located on the edge of Courtenay, BC. The watershed has more or less been influenced by the increased urban development during the past decade, which is characterized by multi land uses, such as forest, rural residential, urban and agricultural land uses (LeBlanc et al., 2009). Chase River is one of Nanaimo's most productive urban waterways with a watershed area of roughly 25 km^2. Its land is mainly used for park, residential and commercial use, since it flows through Colliery Dam Park and the city of Nanaimo (City of Nanaimo, Engineering and Environment, http://www.nanaimo.ca/). The shorter life spans of *M. falcata* in western populations seem to be more greatly affected by urbanization, resulting in more industrial runoff with heavy metals that might inhibit physiological functions of the bivalves. However, these speculations have not been proven yet, since testing them would require continuous water monitoring of these four river watersheds.

It should be noted that the differing lifespans of *M. falcata* might also be a sampling artifact, i.e. due to the different number of specimens collected from each river. This effect might be especially severe for Little Campbell River, where the most specimens have been collected (n = 172). The larger amount of shells coming from this site may be one of the reasons for the longer lifespans of specimens in this river when compared to samples from the other three rivers. It is thus necessary to combine the analysis of the population densities in the four rivers for an improved understanding of age structures and the effects of the ambient environment on shell growth.

5.4.2. Influencing factors on shell growth rates: temperature, nutrient supply, or others?

A number of previous studies have demonstrated that temperature is one of the major influence factors controlling shell growth rates of the freshwater mussels (e.g., Mutvei et al., 1996; Schöne et al., 2004; Dunca et al., 2005). It is generally accepted that shells grow faster during warmer temperatures and that growth may cease below certain temperature thresholds (e.g., Dunca and Mutvei, 2001; Schöne et al., 2004). Dunca and Mutvei (2001), for instance, found that the shell growth of freshwater bivalves from Sweden stops when temperatures fall below 5°C. Temperature may therefore be responsible for the higher slope of the regression curves in the eastern *M. falcata* populations, implying faster shell growth rates or a longer growing season in each year. Since Piercy Creek River is located in the northernmost region among these four rivers, it might thus be possible that the shell growth rates of *M. falcata* are lower as a result of the relatively high latitude. Yet, this hypothesis cannot be tested in detail, because water temperatures have not been monitored and it is unknown whether the temperature is truly lower than that in rivers of the eastern group. Nevertheless, the similarly low shell growth rates of specimens from Chase River, which lies on a similar latitude of the Little Campbell River and Salmon River (Figure 5.1), likely imply that temperature may not be the exclusive factor for controlling shell growth. In addition, previous investigations of the growth rates and chemistry in shells of freshwater mussels have shown that bivalve shell growth may also have benefited from increased food availability (Mutvei et al., 1996). The nutrient influx into the rivers which are fed from the agricultural lands may be higher than those which are fed from the forest lands or parklands due to the impacts of fertilizers and other chemical compounds. Presumably, the high nutrient environment is likely favorable for faster shell growth of *M. falcata*. This speculation can therefore, explain the higher shell growth rates in Little Campbell River and Salmon River which flow through areas that are mainly dominated by agricultural land use, comparing to the two western rivers. However, future work should incorporate field measurements of river hydrology and water chemistry to test these hypotheses.

5.4. Summary and further work

The lifespans and growth characteristics of the western pearlshell, *Margaritifera falcata* were preliminarily investigated in this study. The results indicate that age distributions and shell growth rates differ considerably between rivers, which are inadequate for a reliable and convincing evaluation of environments, but can provide some implications on the role of environmental factors, such as land use history, river hydrology and water chemistry, on longevity and shell growth rates of pearl shells. Further investigations are needed to obtain local environmental data by situ monitoring in order to determine the environmental factors that contribute to shell growth characteristics of the mussels.

5.5. References

Arbuckle, K., and Downing, J., 2008. Freshwater mussel abundance and species richness: GIS relationships with watershed land use and geology. Canadian Journal of Fisheries and Aquatic Sciences 59, 310–316.

Brim Box, J., and Mossa, J., 1999. Sediment, land use, and freshwater mussels: prospects and problems. Journal of the North American Benthological Society 18, 99–117.

Brim Box, J., Howard, J., Wolf, D., O'Brien, C., Nez, D., and Close, D., 2006. Freshwater mussels (Bivalvia: Unionoida) of the Umatilla and Middle Fork John Day Rivers in eastern Oregon. Northwest Science 80(2), 95–107.

Brim Box, J., Wolf, D., Howard, J., O'Brien, C., Nez, D., and Close, D., 2004. Distribution and Status of Freshwater Mussels in the Umatilla River System, 2002-2003. Annual Report, BPA Report DOE/BP-00011402-1, pp. 1–74.

Dunca, E., and Mutvei, H., 2001. Comparison of microgrowth pattern in *Margaritifera margaritifera* shells from south and north Sweden. American Malacological Bulletin 16, 239–250.

Frest, T.J. and Johannes, E.J., 1995. Interior Columbia Basin mollusk species of special concern. Final report to the Interior Columbia Basin Ecosystem Management Project, Walla Walla, WA. Contract #43-0E00-4-9112, pp. 1–274.

Goodwin, D.H., Flessa, K.W., Schöne, B.R., and Dettman, D.L., 2001. Cross-calibration of daily growth increments, stable isotope variation, and temperature in the Gulf of California bivalve mollusk *Chione cortezi*: implications for paleoenvironmental analysis. Palaios 16, 387–398.

Hallmann, N., Schöne, B.R., Strom, A., and Fiebig, J., 2008. An intractable climate archive - Sclerochronological and shell oxygen isotope analyses of the Pacific geoduck, *Panopea abrupta* (bivalve mollusk) from Protection Island (Washington State, USA). Palaeogeography, Palaeoclimatology, Palaeoecology 269, 115–126.

Hastie, L.C., Young, M.R., Boon, P.J., Cosgrove, P.J., and Henninger, B., 2000. Sizes, densities, and age structures of Scottish *Margaritifera margaritifera* (L.) populations. Aquatic Conservation: Marine and Freshwater Ecosystems 10, 229–247.

Hastie, L.C., and Toy, K.A., 2008. Changes in density, age structure and age-specific mortality in two western pearlshell (*Margaritifera falcata*) populations in Washington (1995-2006). Aquatic Conservation: Marine and Freshwater Ecosystems 18, 671–678.

Hovingh, P., 2004. Intermountain freshwater mollusks, USA (*Margaritifera*, *Anodonta*, *Gonidea*, *Valvata*, *Ferrissia*): geography, conservation, and fish management implications. Monographs of the Western North American Naturalist 2(1), 109–135.

Howard, J.K., Cuffey, K.M., and Solomon, M., 2005. Toward using *Margaritifera falcata* as an indicator of base level nitrogen and carbon isotope ratios: insights from two California Coast Range rivers. Hydrobiologia 541, 229–236.

Howard, J.K. and K.M. Cuffey. 2006. Factors controlling the age structure of *Margaritifera falcata* in 2 northern California streams. Journal of the North American Benthological Society 25(3), 677–690.

Jones, D.S., Arthus, M.A., and Allard, D.J., 1989. Sclerochronological records of temperature and growth from shells of Mercenaria mercenaria from Narragansett Bay, Rhode Island. Marine Biology 102, 225–234.

Juteau, C., 2008. Little Campbell River watershed water quality monitoring 2005–2007. Ministry of Environment Environmental Quality Section, pp. 1–75.

LeBlanc, G.V., Chamberlain, D., Holbrook, C., Minard, J., and Dawson, K., 2009. A Report for the Comox Valley Conservation Strategy: Millard-Piercy watershed gap analysis, towards a watershed-based planning framework for the Comox Valley, pp. 1–79.

Limm, M.P., and Power, M.E., 2011. Effect of the western pearlshell mussel *Margaritifera falcata* on Pacifi c lamprey Lampetra tridentata and ecosystem processes. Oikos 120, 1076–1082.

Mutvei, H., Dunca, E., Timm, H., and Slepukhina, T., 1996. Structure and growth rates of bivalve shells as indicators of environmental changes and pollution. Bulletin de l'Institut Océanographique Monaco 14, 65–72.

Pellett, K., 2008. Salmon River nutrient enrichment for fish habitat restoration, 2007. Report prepared by BCCF for BC Ministry of Environment Fisheries Section, Nanaimo, BC; BC Hydro Bridge Coastal Restoration Program, Burnaby, BC; Western Forest Products Forest Investment Account; and Georgia Basin/Vancouver Island Living Rivers, pp. 1–49.

Rodland, D.L., Schöne, B.R., Baier, S., Zhang, Z., Dreyer, W., and Page, N.A., 2009. Changes in gape frequency and thermal tolerance in the freshwater bivalves Anodonta cygnea and *Margaritifera falcata*. Journal of Molluscan Studies 75, 51–57.

Schöne B.R., Page N.A., Rodland D.L., Fiebig J., Baier S.M., Helama, S.O. and Oschmann, W. 2007. ENSO-coupled precipitation records (1959-2004) based on shells of freshwater bivalve mollusks (*Margaritifera falcata*) from British Columbia. International Journal of Earth Sciences 96(3), 525 –540.

Schöne, B.R., Dunca, E., Mutvei, H., and Norlund, U., 2004. A 217-year record of summer air temperature reconstructed from freshwater pearl mussels (*M. margaritifera*, Sweden) Quaternary Science Reviews 24, 1803–1816.

Schöne, B.R., Houk, S.D., Freyre Castro, A.D., Fiebig, J., Kröncke, I., Dreyer, W., and Oschmann, W., 2005. Daily growth rates in shells of *Arctica islandica*: Assessing sub-seasonal environmental controls on a long-lived bivalve mollusk. Palaios 20, 78–92.

Shea, C.P., Peterson, J.T., Conroy, M.J., and Wisniewski, J.M., 2013. Evaluating the influence of land use, drought and reach isolation on the occurrence of freshwater mussel species in the lower Flint River Basin, Georgia (U.S.A.). Freshwater Biology 58, 382–395.

Stagliano, D.M., Stephens, G.M., and Bosworth, W.R., 2007. Aquatic invertebrate species of concern on USFS northern region lands. Report to USDA Forest Service, Northern Region. Montana Natural Heritage Program, Helena, Montana and Idaho Conservation Data Center, Boise, Idaho, pp. 1–95.

Taylor, D.W., 1981. Freshwater mollusks of California: a distributional checklist. California Fish and Game 67, 140–163.

Webb, K., Craft, C., and Elswick, E., 2008. The evaluation of the freshwater western pearl mussel, *Margaritifera falcata* (Gould, 1850), as a bioindicator through the analysis of metal partitioning and bioaccumulation. Northwest Science 82(3), 163–173.

Wernick, B. 1996. Land use and water quality dynamics on the urban-rural fringe: A GIS evaluation of the Salmon River watershed, Langley, B.C. Mater Thesis, Institute for Resources and Environment, University of British Columbia, pp. 1–217.

Chapter 6: CONCLUSIONS AND FUTURE PERSPECTIVES

Shell characteristics of many bivalves are affected by environmental conditions. In turn, this environmental variability could be recorded in bivalve shells. If the environmental characteristics in modern shells could be recognized by means of calibrated investigations, they would be of great significance in paleoenvironmental reconstructions by applying to fossil shells. Generally, the environmental variability is recorded in the form of changes in shell growth rates, $\delta^{18}O_{shell}$ and $\delta^{13}C_{shell}$. $\delta^{18}O_{shell}$ is considered to be the most well-studied parameter and is a reliable proxy of SST (e.g., Jones et al., 1984; Grossman and Ku, 1986; Schöne et al., 2004b; Nützel et al., 2010; Trevisiol et al., 2012). This Ph.D. research supports previous observations that $\delta^{18}O_{shell}$ values of bivalves provide a good proxy for temperatures if the $\delta^{18}O_{seawater}$ is known or can be accurately estimated (Marsh et al., 1999, Weidman et al., 1994 and Schöne et al., 2004b), but has improved the state of understanding by considering both conditions of isotope equilibrium and disequilibrium fractionation (Chapter 2, 4). $\delta^{13}C_{shell}$ is thought to be a controversial proxy of environmental conditions so far (e.g., Krantz et al., 1987; Keller et al., 2002; Lorrain et al., 2004; Gillikin et al., 2007; Foster et al., 2009). In this study, it is demonstrated that factors determining carbon isotopes in shells, including environmental parameters and metabolic effects, are strongly species-specific (Chapter 3, 4). Controls on shell growth rates are inferred to include other parameters in addition to temperature, food availability and salinity in marine bivalve shells (Chapter 2, 3), such as biological necessity (Chapter 4). Furthermore, the lifespans and shell growth rates of the freshwater mussels may record the river land use history and river hydrology information (Chapter 5).

The sclerochronological studies on the marine bivalves, *Eurhomalea exalbida* from South Atlantic and *Paphia undulata* from South China Sea have proven species-specific discrepancy in tracking environmental controls on shell growth patterns, stable carbon and oxygen isotope proxies. In addition, the freshwater pearlshells, *Margaritifera falcata* from different river environments imply the potential influence of environmental variability in terms of variations in age structures and shell growth rates.

6.1. *Eurhomalea exalbida*

Temperature reconstructions based on the $\delta^{18}O_{shell}$ values of *E. exalbida* are not as straightforward and simple as in the case of many other bivalve species (e.g., Grossman and Ku, 1986; Schöne et al., 2004b). The disequilibrium offset of *E. exalbida* increases exponentially with increasing ontogenetic age. Accordingly, $T_{\delta 18O}$ of one to ten year-old specimens overestimates observed temperatures by ca. 2.1°-8.3°C. It can thus be concluded that $\delta^{18}O_{shell}$ of *E. exalbida* should only

be considered as a faithful archive for paleotemperature reconstructions, where, the $\delta^{18}O_{shell}$ disequilibrium is accounted for. When this disequilibrium offset is calculated reasonably, *E. exalbida* can provide reliable temperature estimates, including seasonal maximum and minimum temperatures. Robust temperature estimates are of considerable importance for interpretations of regional and continental-scale climate patterns from southern South America as the Southern Ocean has an important influence on the global climate.

The $\delta^{13}C_{shell}$ ratio incorporated into the shell of *E. exalbida* is not in carbon isotopic equilibrium with the ambient seawater. The observed $\delta^{13}C_{shell}$ ratios are more negative than the predicted $\delta^{13}C_{shell}$ ratios in equilibrium. Even if the ontogenetic decreasing trend is removed, the signal of environmental variability recorded in $\delta^{13}C_{shell}$ is strongly complicated by changes in shell growth rates. It could therefore, be suggested that $\delta^{13}C_{shell}$ in *E. exalbida* is better served as a tool for ecological investigations, rather than a proxy for environmental changes.

In addition, shell growth of *E. exalbida* is demonstrated to be controlled by temperature, as well as by food availability and salinity. All three environmental variables account for 34~55% of the shell growth rates. Temperature is the most important driver and alone explains 28~46% of the variation in shell growth of *E. exalbida*.

6.2. *Paphia undulata*

The $\delta^{18}O_{shell}$ ratios from *P. undulata* shells can provide not only temperature estimates, but also qualitative estimates of the amount of monsoonal rain and terrestrial runoff. This is because oxygen isotopes incorporated into the shell are in approximate isotopic equilibrium with the ambient seawater. The extremely negative $\delta^{18}O_{shell}$ ratios are hypothesized to be a consequence of erratic summer monsoon-related freshwater discharge, rather than extremes of temperatures, as bivalve shells typically do not grow at temperatures higher than 31°C (Ansell, 1968; Schöne, 2008).

The more negative $\delta^{13}C_{shell}$ values in *P. undulata* observed during the growing season of year two are concluded to be indicators for either an increased incorporation of isotopically light respiratory CO_2 through ontogeny or an enhanced input of terrestrial (plant-derived) isotopically light $\delta^{13}C_{DIC}$ through monsoon-related freshwater runoff. Furthermore, this study concludes that, although variability in primary productivity affects $\delta^{13}C_{DIC}$, this may have little effect on the stable carbon isotope signature of the shells.

Analysis of *P. undulata* shell growth rates demonstrates that temperature and food supply may not always be the primary drivers of shell growth. A negative correlation is found between *P. undulata* shell growth and temperature. Fastest shell growth rates correspond to the time intervals

with lowest phytoplankton concentrations in early spring. In contrast, reduced shell growth rates occur in summer when both chlorophyll-a levels and monsoon-related precipitation rates are at their annual maximum. Therefore, it is most likely that fastest shell growth rates in early spring are primarily the result of biological necessity rather than from a changing environment.

6.3. *Margaritifera falcata*

The preliminary investigations on lifespans and growth characteristics of the freshwater mussel, *Margaritifera falcata* demonstrate that age distributions and shell growth rates differ substantially between the studied four rivers. The specimens collected from Little Campbell River and Salmon River in the eastern Georgia Strait have longer average lifespans than specimens from Chase River and Piercy Creek River both located in the western Georgia Strait. Land use history is speculated to be the controlling factor for differences in lifespans of *M. falcata*. Eastern rivers near to Vancouver are predominantly surrounded by agricultural land, whereas the land surrounding western rivers is characterized by various uses, such as parkland, forestland and residential land uses. Furthermore, the shells from the rivers of the eastern group grow faster than those in western rivers, which is possibly in relation to variations in temperature and nutrient supply. These findings suggest that land use impacts on local river hydrology and water chemistry have the potential to affect shell growth in this freshwater mussel species, although supporting observations and measurements are required to verify the potential link between land use and bivalve shell growth in these rivers.

6.4. Future research

The results of the present study show that further studies are required to fully characterize *E. exalbida*, *P. undulata* and *M. falcata* shells as quantifiable and faithful paleoenvironmental archives.

***Eurhomalea exalbida*:**

- Future research is needed to fully understand the actual mechanisms behind the observed ontogenetic changes of the stable carbon and oxygen isotope fractionations in *E.exalbida*. Here, a crucial first step would be to investigate if and to what extent the observed disequilibrium fractionation changes through lifetime of ontogenetic older specimens.
- Given the longevity of this species and its potential to record decadal climate variations (Lomovasky et al., 2002), future studies should combine the construction of long, uninterrupted master chronologies with geochemical studies similar to current efforts in the northern North Atlantic and North Pacific (Schöne et al., 2003d; Black et al., 2008; Butler et al., 2013).

- Additional measurements and observations of local and seasonal marine $\delta^{13}C_{DIC}$ variability are required to improve the understanding of measured $\delta^{13}C_{shell}$ ratios and observed environmental signals.

***Paphia undulata*:**

- Considering its short life span of about three years future studies will require a large number of shells to characterize the frequency of EAM extremes of a certain time interval, which allows the study of seasonal precipitation rates over several consecutive years.
- Preliminary results from fossil shells of this study provide certain implications on wet and dry conditions of the past. In order to identify if the number of excessive monsoon-related precipitation events is truly associated with climate change, additional fossil material of *P. undulata* is needed. It is highly recommended that future studies focus onto this aspect.

***Margaritifera falcata*:**

- To test if the speculations on the age structures and shell growth rates of the freshwater mussels are related to river environmental parameters, such as land use and water temperature, additional measurements and analyses of local river water hydrology and water chemistry are required.

In summary, knowledge about present natural environmental variation is essential for the reliable reconstruction of past environmental change and for accurate prediction of future environmental change. Calibration studies are a prerequisite for paleoenvironmental reconstructions. To successfully reconstruct past environmental and climatic changes, future research will need to extend these studies by applying modern sclerochronological and geochemical techniques.

REFERENCES

Adkins, J.F., Boyle, E.A., Curry, W.B., and Lutringer, A., 2003. Stable isotopes in deep-sea corals and a new mechanism for "vital effects". Geochimica et Cosmochimica Acta 67, 1129–1143.

Aguirre, M.L., Richiano, S., Álvarez, M.F., and Eastoe, C., 2009. Quaternary molluscan fauna from the littoral area of northern Santa Cruz (Patagonia, Argentina). Geobios 42, 411–434.

Alley, N.F., 1976. The palynology and palaeoclimatic significance of a dated core of Holocene peat, Okanagan Valley, southern British Columbia. Canadian Journal of Earth Sciences 13, 1131–1144.

Ambrose, Jr, W.G., Carroll, M.L., Greenacre, M., Thorrold, S., and McMahon, K., 2006. Variation in *Serripes groenlandicus* (Bivalvia) growth in a Norwegian high-Arctic fjord: Evidence for local- and large-scale climatic forcing. Global Change Biology 12, 1595–1607.

Andres, R.J., Maxland, G., and Bischoff, S., 1996. Global and latitudinal estimates of $\delta^{13}C$ from fossil fuel consumption and cement manufacture. Carbon Dioxide Information Analysis Center, CDIAC Communications 22, Oak Ridge National Laboratory, Oak Ridge, Tennessee, USA.

Andrews, J.T., 1972. Recent and fossil growth rates of marine bivalves, Canadian Arctic, and Late-Quaternary arctic Marine environments. Paleogeography, Paleoclimatology, Paleoecology 11, 157–176.

Ansell, A.D., 1968. The rate of growth of the hard clam *Mercenaria mercenaria* (L) throughout the geographic range. Journal du Conseil Permanent International pour I'Exploration de la Mer 31, 364–409.

Arbuckle, K., and Downing, J., 2008. Freshwater mussel abundance and species richness: GIS relationships with watershed land use and geology. Canadian Journal of Fisheries and Aquatic Sciences 59, 310–316.

Bauer, G., 1992. Variation in the life span and size of the freshwater pearl mussel. Journal of Animal Ecology 61, 425–436.

Beck, J.W., Edwards, R.L., Ito, E., Taylor, F.W., Recy, J., Rougerie, F., Joannot, P., and Henin, C., 1992. Sea surface temperature from coral skeletal strontium/calcium ratios. Science 257, 644–647.

Becker, B., Kroner, B., and Trimborn, P., 1991. A stable isotope tree-ring timescale of the Late Glacial/Holocene boundary. Nature 353, 647–649.

Bemis, B.E., Spero, H.J., Bijma, J., and Lea, D.W., 1998. Reevaluation of the oxygen isotopic composition of planktonic foraminifera: experimental results and revised paleotemperature equations. Paleoceanography 13, 150–160.

Beukema, J.J., Knoll, E., and Cadée, G.C., 1985. Effects of temperature on the length of the annual growing season of the Tellinid bivalve *Macoma balthica* (L.) living on tidal flats in the Dutch Wadden Sea. Journal of Experimental Marine Biology and Ecology 90, 129–144.

Bigg, G.R., Rohling E.J., 2000. An oxygen isotope data set for marine water. Journal of Geophysical Research 105, 8527–8535.

Black, B.A., Gillespie, D.C., MacLellan, S.E., and Hand, C.M., 2008. Establishing highly accurate production-age data using the tree-ring technique of crossdating: a case study for Pacific geoduck (*Panopea abrupta*). Canadian Journal of Fisheries and Aquatic Science 65, 2572–2578.

Böhm, F., Joachimski, M.M., Dullo, W.C., Eisenhauer, A., Lehnert, H., Reitner, J., and Wörheide, G., 2000. Oxygen isotope of marine aragonite of coralline sponge. Geochimica et Cosmochimica Acta 64, 1695–1703.

Böhm, F., Joachmiski, M.M., Lehnert, H., Morgenroth, G., Kretschmer, W., Vacelet, J., and Dullo, W.C., 1996. Carbon isotope records from extant Caribbean and South Pacific sponges: evolution of $\delta^{13}C$ in surface water DIC. Earth and Planetary Science Letters 139, 291–303.

Bourgoin, B.P., 1990. *Mytilus edulis* shell as a bioindicator of lead pollution – considerations on bioavailability and variability. Marine Ecology Progress Series 61, 253–262.

Briffa, K.R., Jones, P.D., and Schweingruber, F.H., 1994. Summer temperatures across northern North America: Regional reconstructions from 1760 using tree-ring densities. Journal of Geophysical Research 99, 25835–25844.

Brim Box, J., and Mossa, J., 1999. Sediment, land use, and freshwater mussels: prospects and problems. Journal of the North American Benthological Society 18, 99–117.

Brim Box, J., Howard, J., Wolf, D., O'Brien, C., Nez, D., and Close, D., 2006. Freshwater mussels (Bivalvia: Unionoida) of the Umatilla and Middle Fork John Day Rivers in eastern Oregon. Northwest Science 80(2), 95–107.

Brim Box, J., Wolf, D., Howard, J., O'Brien, C., Nez, D., and Close, D., 2004. Distribution and Status of Freshwater Mussels in the Umatilla River System, 2002-2003. Annual Report, BPA Report DOE/BP-00011402-1, pp. 74.

Brocas, W.M., Reynolds, D.J., Butler, P.G., Richardson, C.A., Scourse, J.D., Ridgway, I.D., and Ramsay, K., 2013. The dog cockle, Glycymeris glycymeris (L.), a new annually-resolved sclerochronological archive for the Irish Sea. Palaeogeography, Palaeoclimatology, Palaeoecology 373, 133–140.

Buddemeier, R.W., and Maragos, J.E., 1974. Radiographic studies of reef coral exoskeletons: rates and patterns of coral growth. Journal of Experimental Marine Biology and Ecology 14, 179–200.

Burchell, M., Hallmann, N., Martindale, A., Cannon, A., and Schöne, B.R., 2013. Seasonality and Intensity of Shellfish Harvesting on the North Coast of British Columbia. The Journal of Island and Coastal Archaeology 8, 152–169.

Büntgen, U., Tegel, W., Nicolussi, K., McCormick, M., Frank, D., Trouet, V., Kaplan, J.O., Herzig, F., Heussner, K.U., Wanner, H., Luterbacher, J., and Esper, J., 2011. 2500 years of European climate variability and human susceptibility. Science 331, 578–582.

Butler, P.G., Wanamaker, Jr, A.D., Scourse, J.D., Richardson, C.A., and Reynolds, D.J., 2013. Variability of marine climate on the North Icelandic Shelf in a 1,357-year proxy archive based on growth increments in the bivalve *Arctica islandica*. Palaeogeography, Palaeoclimatology, Palaeoecology

Butler, P.G., Wanamaker, Jr, A.D., Scoursea, J.D., Richardsona, C.A., and Reynoldsa, D.J., 2011. Long-term stability of $\delta^{13}C$ with respect to biological age in the aragonite shell of mature specimens of the bivalve mollusk *Arctica islandica*. Palaeogeography, Palaeoclimatology, Palaeoecology 302, 21–30.

Carré, M., Bentaleb, I., Blamart, D., Ogle, N., Cardenas, F., Zevallos, S., Kalin, R.M., Ortlieb, L., and Fontugne, M., 2005. Stable isotopes and sclerochronology of the bivalve *Mesodesma donacium*: Potential application to Peruvian paleoceanographic reconstructions. Palaeogeography, Palaeoclimatology, Palaeoecology 228, 4–25.

Carroll, M.L., Ambrose Jr, W.G., Levin, B.S., Ratner, A.R., Ryan, S.K., and Henkes, G.A., 2011. Climatic Regulation of *Clinocardium ciliatum* (bivalvia) growth in the northwestern

Barents Sea. Journal of Marine Systems. Palaeogeography, Palaeoclimatology, Palaeoecology 302, 10–20.

Carroll, M.L., Johnson, B.J., Henkes, G.A., McMahon,K.W., Voronkov, A., Ambrose, Jr, W.G., and Denisenko, S.G., 2009. Bivalves as indicators of environmental variation and potential anthropogenic impacts in the southern Barents Sea. Marine Pollution Bulletin 59, 193–206.

Cesar, S.A., Germano, B.P., and Melgo, J.F., 2003. Preliminary results on the population, reproductive and fishery biology of the nylon shell, *Paphia textile* (Gmelin 1790) in Leyte. UPV Journal of Natural Science 8, 83–95.

Chauvaud, L., Lorrain, A., Dunbar, R.B., Paulet, Y-M., Thouzeau, G., Jean, F., Guarini, J-M., and Mucciarone, D., 2005. The shell of the Great Scallop *Pecten maximus* as a high frequency archive of paleoenvironmental change. Geochemistry, Geophysics, Geosystems 6(8), Q08001, doi:10.1029/2004GC000890.

Chauvaud, L., Thébault, J., Clavier, J., Lorrain, A., and Strand, Q., 2011. What's hiding behind ontogenetic $\delta^{13}C$ variations in mollusk shells? new insights from the great scallop (*Pecten maximus*). Estuaries and Coasts 34, 211–220.

Chen, M., Shiau, L., Yu, P., Chiu, T., Chen, Y., and Wei, K., 2003. 500000-year records of carbonate, organic carbon, and foraminiferal sea-surface temperature from the southeastern South China Sea (near Palawan Island). Palaeogeography, Palaeoclimatology, Palaeoecology 197, 113–131.

Chen, S., Li,Y., Hu, J., Zhen, A., Huang, L., and Lin, Y., 2011. Multiparameter cluster analysis of seasonal variation of water masses in the eastern Beibu Gulf. Journal of Oceanography 67, 709–718.

Chicharo, L., and Chicharo, M.A., 2001. Effects of environmental conditions on planktonic abundances, benthic recruitment and growth rates of the bivalve mollusc *Ruditapes decussatus* in a Portuguese coastal lagoon. Fisheries Research 53, 235–250.

Chiesa, J.O., Parma, S.G., and Camacho, H.H., 1995. Observaciones estratigraficas en el Paleogeno del noroeste de la Provincia de Santa Cruz (Republica Argentina). Parte II: Invertebrados marinos de la Formacion El Chacy (Eoceno), Provincia de Santa Cruz, Argentina. Systematica y bioestratigrafia. Monografias de la Acadamia Nacional de Ciencias Exactas, Fisicas Y Naturales 11, 17–68.

Clark II, G.R., 1975. Periodic growth and biological rhythms in experimentally grown bivalves. In: Rosenberg, G.D., and Runcorn, S.K., (eds.) Growth Rhythms and the History of the Earth's Rotation. Wiley, London, UK, pp. 103–117.

Cobb, K.M., Charles, C.D., Cheng, H., and Edwards, R.L., 2003. El Niño/Southern oscillation and tropical Pacific climate during the last millennium. Nature 424, 271–276.

Coen, L.D., and Heck, Jr, K.L.,1991. The interacting effects of siphon nipping and habitat on bivalve (*Mercenaria mercenaria* (L.)) growth in a subtropical seagrass (*Halodule wrightii Aschers*) meadow.

Coffin, R.B., and Cifuentes, L.A., 1999. Stable isotope analyses of carbon cycling in the Perdido Estuary, Florida. Estuaries 22, 917–926.

Coker, R.E., Shira, A.F, Clark, H.W., and Howard, A.D., 1921. Natural History and Propagation of Freshwater Mussels. Bulletin of the Bureau of Fisheries 37, 1-29.

Colonese, A.C., Verdun-Castello, E., Alvarez, M., Godino, I.B., Zueeo, D., and Salvatelli, L., 2012. Oxygen isotopic composition of limpet shells from the Beagle Channel: implications for seasonal studies in shell middens of Tierra del Fuego. Journal of Archaeological Science, doi:10.1016/j.jas.2012.01.012.

Cortina, A., Sierro, F.J., Gonzalez-Mora, B., Asioli, A., Flores, F.J., 2011. Impact of climate and sea level changes on the ventilation of intermediate water and benthic foraminifer assemblages in the Gulf of Lions, off South France, during MIS 6 and 7. Palaeogeography, Palaeoclimatology, Palaeoecology 309, 215–228.

Davenport, C.B., 1938. Growth lines in fossil pectens as indicators of past climates. Journal of Paleontology 12, 514–515.

Davis, H.C., and Calabrese, A., 1964. Combined effects of temperature and salinity on development of eggs and growth of larvae of *M. mercenaria* and *C. virginica*. Fishery Bulletin 63, 643–655.

Dekker, R., and Beukema, J., 1999. Relations of summer and winter temperatures with dynamics and growth of two bivalves, Tellina tenuis and Abra tenuis, on the northern edge of their intertidal distribution. Journal of Sea Research 42, 207–220.

del Norte-Campos, A.G.C., Nabuab, F.M., Palla, R.Q., and Burlas, M.R., 2010. The early development of the short-necked clam, *Paphia undulata* (Born 1778) (Mollusca, Pelecypoda: Veneridae) in the laboratory. Science Diliman 22, 13–20.

Dettman, D., Flessa, K.W., Roopnarine, P.D., Schöne, B.R., and Goodwin, D.H., 2004. The use of oxygen isotope variation in shells of estuarine mollusks as a quantitative record of seasonal and annual Colorado River discharged. Geochimica et Cosmochimica Acta 68, 1253–1263.

Dettman, D.L., Reische, A.K., and Lohmann, K.C., 1999. Controls on the stable isotope composition of seasonal growth bands in aragonitic fresh-water bivalves (Unionidae). Geochimica et Cosmochimica Acta 63, 1049–1057.

Dextraze, B.L., and Zinsmeister, W.J., 1987. A study of the internal annual growth lines of the late Eocene mollusk *Eurhomalea Antarctica*. Antarctic Journal of the United States 22, 14–15.

DOE, 1994. Handbook of methods for the analysis of the various parameters of the carbon dioxide system in sea water; version 2. Dickson, A.G., and Goyet, C., (eds.) ORNL/CDIAC-74.

Druffel, E.M., and Benavides, L.M., 1986. Input of excess CO_2 to the surface ocean based on $^{13}C/^{12}C$ ratios in a banded Jamaican sclerosponge. Nature 321, 58–61.

Dudley, W.C., Duplessy, J.C., Blackwelder, P.L., Brand, L.E., and Guillard, R.R.L., 1980. Coccoliths in the Pleistocene-Holocene nannofossil assemblages. Nature 285, 222–223.

Dunca, E., and Mutvei, H., 2001. Comparison of microgrowth pattern in *Margaritifera margaritifera* shells from south and north Sweden. American Malacological Bulletin 16, 239–250.

Dunca, E., Schöne, B.R., and Mutvei, H., 2005. Freshwater bivalves tell of past climates: But how clearly do shells from polluted rivers speak? Palaeogeography, Palaeoclimatology, Palaeoecology 228, 43–57.

Elliot, M., deMenocal, P.B., Linsley, B.K., and Howe, S.S., 2003. Environmental controls on the stable isotopic composition of *Mercenaria mercenaria*: potential application to paleoenvironmental studies. Geochemistry, Geophysics, Geosystems 4(7), 1056, doi:10.1029/2002GC000425.

Elliot, M., Welsh, K., Chilcott, C., McCulloch, M., Chappell, J., and Ayling, B., 2009. Profiles of trace elements and stable isotopes derived from giant long-lived *Tridacna gigas* bivalves: Potential applications in paleoclimate studies. Palaeogeography, Palaeoclimatology, Palaeoecology 280, 132–142.

Elorza, J., and García-Garmilla, F., 1998. Palaeoenvironmental implications and diagenesis of inoceramid shells (Bivalvia) in the mid-Maastrichtian beds of the Sopelana, Zumaya and Bidart sections (coast of the Bay of Biscay, Basque Country). Palaeogeography, Palaeoclimatology, Palaeoecology 141, 303–328.

Emile-Geay, J., Cane, M., Seager, R., Kaplan, A., and Almasi, P., 2007. El Niño as a mediator of the solar influence on climate. Paleoceanography 22, PA3210, doi:10.1029/2006PA001304.

Emrich, K., Enhalt, D.H., and Vogel, 1.C., 1970. Carbon isotope fractionation during the precipitation of calcium carbonate. Earth and Planetary Science Letters 8, 363- 371.

Epstein, S., Buchsbaum, R., Lowenstam, H., and Urey, H.C., 1951. Carbonate-water isotopic temperature scale. Bulletin of the Geological Society of America 62, 417–426.

Epstein, S., Buchsbaum, R., Lowenstam, H.A., and Urey, H.C., 1953. Revised carbonate-water isotopic temperature scale. Bulletin of the Geological Society of America 64, 1315–1326.

Erez, J., 1978. Vital effect on stable-isotope composition seen in foraminifera and coral skeletons. Nature 273, 199–202.

Evans, J.W., 1972. Tidal growth increments in the cockle *Clinocardium nuttalli*. Science 176, 416–417.

Fallon, S.J., McCulloch, M.T., and Guilderson, T.P., 2005. Interpreting environmental signals from the coralline sponge *Astrosclera willeyana*. Palaeogeography, Palaeoclimatology, Palaeoecology 228, 58–69.

Fogel, M.L., and Cifuentes, L.A., 1993. Isotope fractionation during primary production. In: Engel, M.H., and Macko, S.A., (eds.) Organic Geochemistry. Plenum Press, New York, USA, pp. 73–98.

Foster, L.C., Allison, N., Finch, A.A., Andersson, C., and Ninnemann, U.S., 2009. Controls on $\delta^{18}O$ and $\delta^{13}C$ profiles within the aragonite bivalve *Arctica islandica*. Holocene 19, 549–558.

Freitas, P., Clarke, L.J., Kennedy, H., Richardson, C.A., and Abrantes, F., 2005. Mg/Ca, Sr/Ca, and stable-isotope ($\delta^{18}O$ and $\delta^{13}C$) ratio profiles from the fan mussel *Pinna nobilis*: Seasonal records and temperature relationships. Geochemistry, Geophysics, Geosystems 6, Q04D14, doi:10.1029/2004GC000872.

Frest, T.J. and Johannes, E.J., 1995. Interior Columbia Basin mollusk species of special concern. Final report to the Interior Columbia Basin Ecosystem Management Project, Walla Walla, WA. Contract #43-0E00-4-9112, pp. 274.

Fritts, H.C., 1976. Tree rings and climate. Academic Press, London, UK, pp. 1–567.

Fritz, P., and Poplawski, S., 1974. ^{18}O and ^{13}C in the shells of freshwater molluscs and their environments. Earth and Planetary Science Letters 24, 91–98.

Garreaud, R.D., Vuille, M., Compagnucci, R., and Marengo, J., 2009. Present-day South American climate. Palaeogeography, Palaeoclimatology, Palaeoecology 281, 180–195.

Gillikin, D.P., De Ridder, F., Ulens, H., Elskens, M., Keppens, E., Baeyens, W., and Dehairs, F., 2005. Assessing the reproducibility and reliability of estuarine bivalve shells (*Saxidomus giganteus*) for sea surface temperature reconstruction: implications for paleoclimate studies. Palaeogeography, Palaeoclimatology, Palaeoecology 228, 70–85.

Gillikin, D.P., Lorrain, A., Bouillon, S., Willenz, P., and Dehairs, F., 2006. Shell carbon isotopic composition of Mytilus edulis shells: relation to metabolism, salinity, $\delta^{13}C_{DIC}$ and phytoplankton. Organic Geochemistry 37, 1371–1382.

Gillikin, D.P., Lorrain, A., Meng, L., and Dehairs, F., 2007. A large metabolic carbon contribution to the $\delta^{13}C$ record in marine aragonitic bivalve shells. Geochimica et Cosmochimica Acta 71, 2936–2946.

Goodfriend, G.A., and Weidman, C.R., 2001. Ontogenetic trends in aspartic acid racemization and amino acid composition within living and fossil shells of the bivalve Arctica. Geochimica et Cosmochimica Acta 65, 1921–1932.

Goodwin, D.H., Flessa, K.W., Schöne, B.R., and Dettman, D.L., 2001. Cross-calibration of daily growth increments, stable isotope variation, and temperature in the Gulf of California bivalve mollusk *Chione cortezi*: implications for paleoenvironmental analysis. Palaios 16, 387–398.

Goodwin, D.H., Flessa, K.W., Schöne, B.R., and Dettman, D.L., 2001. Cross-calibration of daily growth increments, stable isotope variation, and temperature in the Gulf of California bivalve mollusk *Chione cortezi*: implications for paleoenvironmental analysis. Palaios 16, 387–398.

Goodwin, D.H., Gillikin, D.P., and Roopnarine, P.D., 2013. Preliminary evaluation of potential stable isotope and trace element productivity proxies in the oyster *Crassostrea gigas*. Palaeogeography, Palaeoclimatology, Palaeoecology 373, 88–97.

Graham, D.W., Corliss, B.H., Bender, M.L. and Keigwin, Jr, L.D., 1981. Carbon and oxygen isotopic disequilibria of Recent deep-sea benthic foraminifera. Marine Micropaleontology 6, 483–497.

Grossman, E.L., 1984. Carbon isotopic fractionation in live benthic foraminifera – comparison with inorganic precipitate studies. Geochimica et Cosmochimica Acta 48, 1505–1517.

Grossman, E.L., and Ku, T.-L., 1986. Oxygen and carbon isotope fractionation in biogenic aragonite; temperature effects. Chemical Geology (Isotope Geoscience Section) 59, 59–74.

Gruber, N., Keeling, C.D., Bates, N.R., 2002. Interannual variability in the North Atlantic Ocean carbon sink. Science, 298, 2374–2378.

Gruber, N., Keeling, C.D., Bacastow, R.B., Guenther, P.R., Lueker, T.J., Wahlen, M., Meijer, H.A., Mook, W.G., and Stocker, T.F., 1999. Spatiotemporal patterns of carbon–13 in the global surface oceans and the oceanic Suess effect. Global Biogeochemical Cycles 13, 307–335.

Gruber, N., 1998. Anthropogenic CO_2 in the Atlantic Ocean. Global Biogeochem Cycles 12, 165–191.

Hallmann, N., Burchell, M., Brewster, N., Martindale, A., and Schöne, B.R., 2013. Holocene climate and seasonality of shell collection at the Dundas Islands Group, northern British Columbia, Canada—A bivalve sclerochronological approach. Palaeogeography, Palaeoclimatology, Palaeoecology 373, 163–172.

Hallmann, N., Burchell, M., Schöne, B.R., Irvine, G., and Maxwell, D., 2009. High-resolution sclerochronological analysis of the bivalve mollusk Saxidomus gigantea from Alaska and British Columbia: techniques for revealing environmental archives and archaeological seasonality. Journal of Archaeological Science, 36 (10), 2353–2364.

Hallmann, N., Schöne, B.R., Strom, A., and Fiebig, J., 2008. An intractable climate archive - Sclerochronological and shell oxygen isotope analyses of the Pacific geoduck, *Panopea abrupta* (bivalve mollusk) from Protection Island (Washington State, USA). Palaeogeography, Palaeoclimatology, Palaeoecology 269, 115–126.

Hansen, J.E., and Sato, M., 2012. Paleoclimate implications for human-made climate change. In: Berger, A., Mesinger, F., and Šijački, D., (eds.) Climate Change: Inferences from Paleoclimate and Regional Aspects. Springer, pp. 21-48, doi:10.1007/978-3-7091-0973-1_2.

Hastie, L.C., and Toy, K.A., 2008. Changes in density, age structure and age-specific mortality in two western pearlshell (*Margaritifera falcata*) populations in Washington (1995-2006). Aquatic Conservation: Marine and Freshwater Ecosystems 18, 671–678.

Hastie, L.C., Young, M.R., Boon, P.J., Cosgrove, P.J., and Henninger, B., 2000. Sizes, densities, and age structures of Scottish *Margaritifera margaritifera* (L.) populations. Aquatic Conservation: Marine and Freshwater Ecosystems 10, 229–247.

Hebda, R.J., 1995. British Columbia vegetation and climate history with a focus on 6 ka BP. Geographie physique et Quaternaire, 49, 55-79.

Helama, S., and Hood, B.C., 2011. Stone Age midden deposition assessed by bivalve sclerochronology and radiocarbon wiggle-matching of *Arctica islandica* shell increments. Journal of Archaeological Science 38, 452–460.

Hovingh, P., 2004. Intermountain freshwater mollusks, USA (*Margaritifera*, *Anodonta*, *Gonidea*, *Valvata*, *Ferrissia*): geography, conservation, and fish management implications. Monographs of the Western North American Naturalist 2(1), 109–135.

Howard, J.K. and K.M. Cuffey. 2006. Factors controlling the age structure of *Margaritifera falcata* in 2 northern California streams. Journal of the North American Benthological Society 25(3), 677–690.

Howard, J.K., Cuffey, K.M., and Solomon, M., 2005. Toward using *Margaritifera falcata* as an indicator of base level nitrogen and carbon isotope ratios: insights from two California Coast Range rivers. Hydrobiologia 541, 229–236.

Hudson, H.J., 1981. Growth rates in Montastrea annularis: a record of environmental change in Key Largo coral reef marine sanctuary, Florida. Bulletin of Marine Science 31(2), 444–459.

Hudson, J.H., Shinn, E., Halley, R., and Lidz, B., 1976. Sclerochronology: a new tool for interpreting past environments. Geology 4, 361–364.

Ingram, B.L., Conrad, M.E., and Ingle, J.C., 1996. Stable isotope and salinity systematics in estuarine waters and carbonates: San Francisco Bay. Geochimica et Cosmochimica Acta, 60, 455–467.

Ivany, L.C., Lohmann, K.C., Hasiuk, F., Blake, D.B., Glass, A., Aronson, R.B., and Moody, R.M., 2008. Eocene climate record of a high southern latitude continental shelf: Seymour Island, Antarctica. Bulletin of the Geological Society of America 120, 659–678.

Jacob, D.E., Soldati, A.L., Wirth, H., Huth, J., Wehrmeister, U., Hofmeister, W., 2008. Nanostructure, composition and mechanisms of bivalve shell growth. Geochimica et Cosmochimica Acta 72, 5401–5415.

Jones, D.S., 1980. Annual cycle of shell growth increment formation in two continental shelf bivalves and its paleoecologic significance. Paleobiology 6, 331–340.

Jones, D.S., 1981. Reproductive cycles of the Atlantic surf clam *Spisula solidissima*, and the ocean quahog *Arctica islandica* off New Jersey. Journal of Shellfish Research 1, 23–32.

Jones, D.S., Arthus, M.A., and Allard, D.J., 1989. Sclerochronological records of temperature and growth from shells of Mercenaria mercenaria from Narragansett Bay, Rhode Island. Marine Biology 102, 225–234.

Jones, D.S., Williams, D.F., and Arthus, M.A., 1983. Growth history and ecology of the Atlantic surf clam, *Spisula solidissima* (Dillwyn), as revealed by stable isotopes and annual shell increments. Journal of Experimental Marine Biology and Ecology 73, 225–242.

Jones, D.S., Williams, D.F., and Romanek, C.S., 1986. Life history of symbiont-bearing giant clams from stable isotope profiles. Science 231, 46–48.

Jones, D.S., Williams, D.F., Arthur, M.A., and Krantz, D.E., 1984. Interpreting the paleoenvironmental, paleoclimatic and life history records in mollusc shells. Geobios 17, 333–339.

Jones, P.D., Osborn, T.J., and Briffa, K.R., 2001. The evolution of climate over the last millennium. Science 292, 662–667.

Jorgensen, B.C., 1990. Bivalve filter feeding: hydrodynamics, bioenergetics, physiology and ecology. Olsen &Olsen, Fredensborg, Denmark, pp. 1–140.

Jorgensen, B.C., 1996. Bivalve filter feeding revisited. Marine Ecology Progress Series 142, 287–302.

Juteau, C., 2008. Little Campbell River watershed water quality monitoring 2005–2007. Ministry of Environment Environmental Quality Section, pp. 1–75.

Kalish, J.M., 1991. Determinants of otolith chemistry: seasonal variation in the composition of blood-plasma, endolymph and otoliths of bearded rock cod *Pseudophycis barbatus*. Marine Ecology Progress Series 74, 137-159.

Kasemann, S.A., Schmidt, D.N., Pearson, P.N., Hawkesworth, C.J., 2008. Biological and ecological insights into Ca isotopes in planktic foraminifers as a palaeotemperature proxy. Earth and Planetary Science Letters 271 (1–4), 292–302.

Keen, M., 1954. Nomenclatural notes on the pelecypod Family Veneridae. Minutes of the Conchological Club of Southern California 139, 50–55.

Keigwin, L.D., and Cook, M.S., 2007. A role for North Pacific salinity in stabilizing North Atlantic climate. Paleooceanography 22, PA3102, doi:10.1029/2007PA001420.

Keller, N., Del Piero, D., and Longinelli, A., 2002. Isotopic composition, growth rates and biological behaviour of *Chamelea gallina* and *Callista chione* from the Gulf of Trieste (Italy). Marine Biology 140, 9–15.

Kennedy, H., Richardson, C.A., Duarte, C.M., and Kennedy, D.P., 2001. Oxygen and carbon stable isotopic profiles of the fan mussel, *Pinna nobilis*, and reconstruction of sea surface temperatures in the Mediterranean. Marine Biology 139, 1115–1124.

Kennish, M.J, and Olsson, R.K., 1975. Effects of thermal discharges on the microstructural growth of *Mercenaria mercenaria*. Environmental Geology 1, 41–64.

Kennish, M.J., and Lutz, R.A., 1999. Calcium carbonate dissolution rates in deep-sea bivalve shells on the East Pacific Rise at 21°N: results of an 8-year in-situ experiment Palaeogeography, Palaeoclimatology, Palaeoecology 154, 293–299.

Khim, B.K., Woo, K. S., and Je, J.G., 2000. Stable isotope profiles of bivalve shells: seasonal temperature variations, latitudinal temperature gradients and biological carbon cycling along the east coast of Korea. Continental Shelf Research 20, 843–861.

Killingley, J.S., and Berger, W.H., 1979. Stable isotopes in a mollusc shell: Detection of upwelling events. Science 205, 186–188.

Kim, S.T., and O'Neil, J.R., 1997. Equilibrium and nonequilibrium oxygen isotope effects in synthetic carbonates. Geochimica et Cosmochimica Acta 61, 3461–3475.

Kingston, A.W., Gröcke, D.R., and Burchell M., 2008. A multi-axial growth analysis of stable isotopes in the modern shell of *Saxidomus gigantea*: implications for sclerochronology studies. Geochemistry, Geophysics, Geosystems 9, Q01007 doi:10.1029/2007GC001807

Klein, R.T., Lohmann, K.C., and Thayer, C.W., 1996a. Bivalve skeletons record sea-surface temperature and $\delta^{18}O$ via Mg/Ca and $^{18}O/^{16}O$ ratios. Geology 24, 415-418.

Klein, R.T., Lohmann, K.C., and Thayer, C.W., 1996b. Sr/Ca and $^{13}C/^{12}C$ ratios in skeletal calcite of *Mytilus trossulus*: covariation with metabolic rate, salinity, and carbon isotopic composition of seawater. Geochimica et Cosmochimica Acta 60, 4207–4221.

Koike, H., 1980. Seasonal dating by growth line counting of the bivalve, *Meretrix lusoria*. University of Tokyo Bulletin, Tokyo, Japan, pp. 1–104.

Krantz, D.E., Williams, D.F, and Jones, D.S., 1987. Ecological and paleoenvironmental information using stable isotope profiles from living and fossil mollusks. Palaeogeography, Palaeoclimatology, Palaeoecology 58, 249–266.

Lauritzen, S.E., and Lundberg, J. 1999. Speleothems and climate: a special issue of The Holocene. Holocene 9, 643–647.

Lazareth, C.E., Vander Putten E., André L., and Dehairsm, F., 2003. High-resolution trace element profiles in shells of the mangrove bivalve *Isognomon ephippium*: a record of environmental spatio-temporal variations? Estuarine, Coastal and Shelf Sciences 57, 1103–1114.

Lazareth, C.E., Bustamante Rosell1, M.G., Turcq, B., Le Cornec, F., Mandeng-Yogo, M., Caquineau, S., and Cabioch, G., 2013. Mid-Holocene climate in New Caledonia (southwest Pacific): coral and PMIP models monthly resolved results. Quaternary Science Reviews 69, 83–97.

Lazareth, C.E., Willenz, P., Navez, J., Keppens, E., Dehairs, F., André, L., 2000. Sclerosponges as a new potential recorder of environmental changes: lead in *Ceratoporella nicholsoni*. Geology 28, 515–518.

LeBlanc, G.V., Chamberlain, D., Holbrook, C., Minard, J., and Dawson, K., 2009. A Report for the Comox Valley Conservation Strategy: Millard-Piercy watershed gap analysis, towards a watershed-based planning framework for the Comox Valley, pp. 1–79.

Lee, K., Choi, S.-D., Park, G.-H., Wanninkhof, R., Peng, T.-H., Key, R.M., Sabine, C.L., Feely, R.A., Bullister, J.L., and Millero, F.J., 2003. An updated anthropogenic CO_2 inventory in

the Atlantic Ocean. Global Biogeochem Cycles 17, 1116 http://dx.doi.org/10.1029/2003GB002067

Lee, T.C.K., Zwiers, F.W., and Tsao, M., 2008. Evaluation of proxy-based millennial reconstruction methods. Climate Dynamics, 31, 263–281.

Leethochavalit, S., Chalermwat, K., Upatham, E.S., Choi, K.S., Sawangwong, P., and Kruatrachue, M., 2004. Occurrence of *Perkinsus* sp. in undulated surf clams *Paphia undulata* from the Gulf of Thailand. Diseases of Aquatic Organisms 60, 165–171.

Lewis, D.E., and Cerrato, R.M., 1997. Growth uncoupling and the relationship between shell growth and metabolism in the soft shell clam *Mya arenaria*. Marine Ecology Progress Series 158, 177–189.

Li, Z., Zhang, Y., Li, Y., and Zhao, J., 2010. Palynological records of Holocene monsoon change from the Gulf of Tonkin (Beibuwan), northwestern South China Sea. Quaternary Research 74, 8–14.

Limm, M.P., and Power, M.E., 2011. Effect of the western pearlshell mussel Margaritifera falcata on Pacifi c lamprey Lampetra tridentata and ecosystem processes. Oikos 120, 1076–1082.

Lin, I., Wang, C., Lin, S., and Chen, Y., 2011. Groundwater-seawater interactions off the coast of southern Taiwan: Evidence from environmental isotopes. Journal of Asian Earth Sciences 41, 250–262.

Lomovasky, B.J., Brey, T., Morriconi, E., and Calvo, J., 2002. Growth and production of the venerid bivalve *Eurhomalea exalbida* in the Beagle Channel, Tierra del Fuego. Journal of Sea Research 48, 209–216.

Lorrain, A., Paulet, Y.M., Chauvaud, L., Dunbar, R., Mucciarone, D., and Fontugne, M., 2004. $\delta^{13}C$ variation in scallop shells: increasing metabolic carbon contribution with body size? Geochimica et Cosmochimica Acta 68, 3509–3519.

Lough, J.M., and Barnes, D.J., 1997. Several centuries of variation in skeletal extension, density and calcification in massive porites colonies from the Great Barrier Reef: a proxy for seawater temperature and a background of variability against which to identify unnatural change. Journal of Experimental Marine Biology and Ecology 211, 29–67.

Lowenstam, H.A., 1954. Factors affecting the aragonite:calcite ratios in carbonate-secreting marine organisms. Journal of Geology 62, 284–322.

Luterbacher, J., Dietrich, D., Xoplaki, E., Grosjean, M., and Wanner, H., 2004. European seasonal and annual temperature variability, trends, and extremes since 1500. Science 303, 1499–1503.

Lutz, R., and Rhoads, D., 1980. Growth patterns in the molluscan shell: an overview. In: Rhoads, D.C., Lutz, R.A. (eds.), Skeletal Growth of Aquatic Organisms: Biological Records of Environmental Change. Plenum Press, New York, USA, pp. 203–254.

Maina, J., de Moel, Hans., Vermaat,J.E., Bruggemann, J. H., Guillaume, M.M.M., Grove, C.A., Madin, J.S., Mertz-Kraus, R., and Zinke, J., 2012. Linking coral river runoff proxies with climate variability, hydrology and land-use in Madagascar catchments. Marine Pollution Bulletin 64, 2047–2059.

Malchus, N., and Steuber, T., 2002. Stable isotope records (O, C) of Jurassic aragonitic shells from England and NW Poland: palaeoecologic and environmental implications. Geobios 35, 29–39.

Mann, M.E., Bradley, R.S., and Hughes, M.K., 1999. Northern hemisphere temperatures during the past millennium: inferences, uncertainties, and limitations. Geophysical Research Letters 26, 759–762.

Mann, R., 1982. The seasonal cycle of gonadal development in *Arctica islandica* from the southern New England shelf. Fishery Bulletin (U.S.) 80, 315–326.

Mann, R., 1989. Larval ecology of *Arctica islandica* on the inner continental shelf of the eastern United States. Journal of Shellfish Research 8, 464.

Marchitto, T.A., Jones, G.A., Goodfriend, G.A., and Weidman, C.R., 2000. Precise temporal correlation of Holocene mollusk shells using sclerochronology. Quaternary Research 53, 236–246.

Marin, F., Le Roy, N., and Marie, B., 2012. The formation and mineralization of mollusk shell. Frontiers in Bioscience 4, 1099–1125.

Marsden, I.D., 2004. Effects of reduced salinity and seston availability on growth of the New Zealand little-neck clam *Austrovenus stutchburyi*. Marine Ecology Progress Series 266, 157–171.

Marsh, R., Petrie, B., Weidman, C.R., Dickson, R.R., Loder, J.W., Hannah, C.G., Frank, K., and Drinkwater, K., 1999. The 1882 tilefish kill – a cold event in shelf waters off the north-eastern United States? Fisheries Oceanography 8(1), 39–49.

Marwick, B., and Gagan, M.K., 2011. Late Pleistocene monsoon variability in northwest Thailand: an oxygen isotope sequence from the bivalve *Margaritanopsis laosensis* excavated in Mae Hong Son provinceQuaternary Science Reviews 30, 3088–3098.

McConnaughey, T.A., 1989a. ^{13}C and ^{18}O isotopic disequilibrium in biological carbonates: I. Patterns. Geochim Cosmochim Acta 53, 151–162.

McConnaughey, T.A., 1989b. ^{13}C and ^{18}O isotopic disequilibrium in biological carbonates: II. In vitro simulation of kinetic isotope effects. Geochimica et Cosmochimica Acta 53, 163–171.

McConnaughey, T.A., 2003. Sub-equilibrium oxygen-18 and carbon-13 levels in biological carbonates: carbonate and kinetic models. Coral Reefs 22, 316–327.

McConnaughey, T.A., and Gillikin, D.P., 2008. Carbon isotopes in mollusk shell carbonate. Geo-Marine Letters 28, 287–299.

McConnaughey, T.A., Burdett, J., Whelan, J.F., and Paull, C.K., 1997. Carbon isotopes in biological carbonates: respiration and photosynthesis. Geochimica et Cosmochimica Acta 61, 611–622.

McCorkle, D.C., Emerson, S.R., and Quay, P.D., 1985. Stable carbon isotopes in marine porewaters. Earth and Planetary Science Letters 74, 13–26.

McCrea, J.M., 1950. On the isotopic chemistry of carbonates and a paleotemperature scale. Journal of Chemical Physics 18, 849–857.

McDermott, F., 2004. Palaeo-climate reconstruction from stable isotope variations in speleothems: a review. Quaternary Science Reviews 23, 901–918.

Mertz-Kraus, R., Brachert, T.C., Reuter, M., 2008. *Tarbellastraea* (Scleractinia): A new stable isotope archive for Late Miocene paleoenvironments in the Mediterranean. Palaeogeography, Palaeoclimatology, Palaeoecology 257, 294–307.

Mitchell, L., Fallick, A., and Curry, G., 1994. Stable carbon and oxygen isotope composition of mollusc shells from Britain and New Zealand. Palaeogeography, Palaeoclimatology, Palaeoecology 111, 207–216.

Miyaji, T., Tanabe, K., Matsushima, Sato, Y. S., Yokoyama, Y., and Matsuzaki, H., 2010. Response of daily and annual shell growth patterns of the intertidal bivalve *Phacosoma japonicum* to Holocene coastal climate change in Japan. Palaeogeography, Palaeoclimatology, Palaeoecology 286, 107–120.

Mook, W.G., and Vogel, J.C., 1968. Isotopic equilibrium between shells and their environment. Science 159, 874–875.

Moore, J.J., Hughen, K.A., Miller, G.H. and Overpeck, J.T., 2001. Little Ice Age recorded in summer temperature reconstruction from varved sediments of Donard Lake, Baffin Island, Canada. Journal of Paleolimnology 25, 503–517.

Morriconi, E., Lomovasky, B.J., Calvo, J., and Brey, T., 2002. The reproductive cycle of *Eurhomalea exalbida* (Chemnitz, 1795) (Bivalvia: Veneridae) in Ushuaia Bay (54°50' S), Beagle Channel (Argentina). Invertebrate Reproduction and Development 42, 61–68.

Mudelsee, M., 2001. The phase relations among atmospheric CO_2 content, temperature and global ice volume over the past 420 ka. Quaternary Science Reviews, 20, 583–589.

Müller-Lupp, T., Bauch, H.A., and Erlenkeuser, H., 2004. Holocene hydrographical changes of the eastern Laptev Sea (Siberian Arctic) recorded in $\delta^{18}O$ profiles of bivalve shells. Quaternary Research 61, 32–41.

Müller-Lupp, T., Erlenkeuser, H., and Bauch, H.A., 2003. Seasonal and interannual variability of Siberian river discharge in the Laptev Sea inferred from stable isotopes in modern bivalves. Boreas 32(2), 292–303.

Mutvei, H., Dunca, E., Timm, H., and Slepukhina, T., 1996. Structure and growth rates of bivalve shells as indicators of environmental changes and pollution. Bulletin de l'Institut Océanographique Monaco 14, 65–72.

Nabuab, F.M., Ledesma-Fernandez, L., and del Norte-Campos, A., 2010. Reproductive biology of the short-necked clam, *Paphia undulata* (Born 1778) from southern Negros Occidental, Central Philippines. Science Diliman 22, 31–40.

Nakaoka, M., 1992. Spatial and seasonal variation in growth rate and secondary production of Yoldia notabilis in Otsuchi Bay, Japan, with reference to the influence of food supply from the water column. Marine Ecology Progress Series 88, 215–223.

Nakaoka, M., and Matsui, S., 1994. Annual variation in the growth rate of *Yoldia notabilis* (Bivalvia: Nuculanidae) in Otsuchi Bay northeastern Japan analyzed using shell microgrowth patterns. Marine Biology 119, 397–404.

Nedeau, E., A.K. Smith, and J. Stone. 2005. Freshwater Mussels of the Pacific Northwest. Pacific Northwest Native Freshwater Mussel Workgroup, Vancouver, Washington. pp. 45.

Neukom, R., del Rosario Prieto, M., Moyano, R., Luterbacher, J., Pfister, C., Villalba, R., Jones, P.D., and Wanner, H., 2009. An extended network of documentary data from South America and its potential for quantitative precipitation reconstructions back to the 16th century. Geophysical Research Letters 36, L12703, doi:10.1029/2009GL038351.

Neukom, R., Luterbacher, J., Villalba, R., Kuttel, M., Frank, D., Jones, P.D., Grosjean, M., Wanner, H., Aravena, J.-C., Black, D.E., Christie, D.A., D'Arrigo, R., Lara, A., Morales, M., Soliz-Gamboa, C., Srur, A., Urritia, R., and von Gunten, L. 2011. Multiproxy summer and winter surface air temperature field reconstructions for southern South America covering the past centuries. Climate Dynamics 37, 35–51.

Nozaki, Y., Rye, D.M., Turekian, K.K., and Dodge, R.E., 1978. A 200 year record of carbon–13 and carbon–14 variations in a Bermuda coral. Geophysical Research Letters 5, 826–828.

Nützel, A., Joachimski, M., and López Correa, M., 2010. Seasonal climatic fluctuations in the Late Triassic tropics – High-resolution oxygen isotope records from aragonitic bivalve shells (Cassian Formation, Northern Italy). Palaeogeography, Palaeoclimatology, Palaeoecology 285, 194–204.

Oschmann, W., 2009. Sclerochronology: editorial. International Journal of Earth Sciences (Geologische Rundschau) 98, 1–2.

Owen, E.F., Wanamaker, A.D., Feindel, S.C., Schöne, B.R. and Rawson, P.D., 2008. Stable carbon and oxygen isotope fractionation in bivalve (*Placopecten magellanicus*) larval aragonite. Geochimica et Cosmochimica Acta 72, 4687–4698.

Owen, R., Kennedy, H., and Richardson, C., 2002. Isotopic partitioning between scallop shell calcite and seawater: effect of shell growth rate. Geochimica et Cosmochimica Acta 66, 1727–1737.

Page, H.M., and Hubbard, D.M., 1987. Temporal and spatial patterns of growth in mussels *Mytihs edulis* on an offshore platform: relationships to water temperature and food availability. Journal of Experimental Marine Biology and Ecology 111, 159–179.

Pannella, G., 1971. Fish Otoliths: Daily Growth Layers and Periodical Patterns. Science 173, 1124–1127.

Pannella, G., and McClintock, C., 1968. Biological and environmental rhythms reflected in molluscan shell growth. Paleontological Society Memoirs 42, 64–80.

Pellett, K., 2008. Salmon River nutrient enrichment for fish habitat restoration, 2007. Report prepared by BCCF for BC Ministry of Environment Fisheries Section, Nanaimo, BC; BC

Hydro Bridge Coastal Restoration Program, Burnaby, BC; Western Forest Products Forest Investment Account; and Georgia Basin/Vancouver Island Living Rivers. pp. 1–49.

Pérez-Cruz, L., 2006. Climate and ocean variability during the middle and late Holocene recorded in laminated sediments from Alfonso Basin, Gulf of California, Mexico. Quaternary Research 65, 401–410.

Peterson, C.H., 1986. Quantitative allometry of gamete production by *Mercenaria mercenaria* into old age. Marine Ecology Progress Series 29, 93–97.

Petit, J.R., Jouzel, J., Rayhaud, D., Barkov, N.I., Barnola, J.M., Basile, I., Bender, M., Chapellaz, J., Davis, J., Delaygue, G., Delmotte, M., Kotlyakov, V.M., Legrand, M., Lipenkov, V., Lorius, C., Pépin, L., Ritz, C., Saltzman, E., and Stievenard, M., 1999. Climate and atmospheric history of the past 420,000 years from the Vostok ice core, Antarctica. Nature 399, 429–436.

Petit, J.R., Mounier, L., Jouzel, J., Korotkevich, Y.S., Kotlyakov, V.I., and Lorius, C., 1990. Palaeoclimatological and chronological implications of the Vostok core dust record. Nature 343, 56–58.

Piola, A.R., and Gordon, A.L., 1989. Intermediate waters in the southwest South Atlantic. Deep Sea Research 36, 1–16.

Pittendrigh, C.S., and Bruce, C.G., 1957. An oscillator model for biological clocks. In: Rudnick, D., (ed.) Rhythmic and Synthetic Processes in Growth. Princeton University Press, Princeton, New Jersey, USA, pp. 75–109.

Pitts, L.C., and Wallace, G.T., 1994. Lead deposition in the shell of the bivalve, *Mya arenaria* – an indicator of dissolved lead in seawater. Estuarine, Coastal and Shelf Science 39, 93–104.

Poutiers, J.M., 1998. Bivalves. In: Carpenter, K.E., and Niem, V.H., (eds) FAO species identification guide for fishery purposes. The living marine resources of the Western Central Pacific, Volume 1, FAO, Rome, Italy, pp. 328–344.

Powell, A.W., 1960. Antarctic and Subantarctic Mollusca. Records of the Auckland Institute and Museum 5, 117–193.

Quay, P., Sommerup, R., Westby, T., Sutsman, J., and McNichol, A., 2003. Changes in the $^{13}C/^{12}C$ of dissolved inorganic carbon in the ocean as a tracer of anthropogenic CO_2 uptake. Global Biogeochem Cycles 17(1) http://dx.doi.org/10.1029/2001GB001817.

Racapé, V., Pierre, C., Metzl, N., Lo Monaco, C., Reverdin, G., Olsen, A., Morin, P., Rios, A.F., Vazquez-Rodriguez, M., and Perez, F.F., 2013. Anthropogenic carbon changes in the Irminger Basin (1981–2006): Coupling $\delta^{13}C_{DIC}$ and DIC observations. Journal of Marine System 126, 24–32.

Radermacher, P., Schöne, B.R., Gischler, E., Oschmann, W., Thébault, J., and Fiebig, J., 2009. Sclerochronology – a highly versatile tool for mariculture and reconstruction of life history traits of the queen conch, *Strombus gigas* (Gastropoda). Aquatic Living Resources 22, 307–318.

Rahimpour-Bonab, H., Bone, Y., and Moussavi-Harami, R., 1997. Stable isotope aspects of modern molluscs, brachiopods, and marine cements from cool-water carbonates, Lacepede Shelf, South Australia. Geochimica et Cosmochimica Acta 61, 207– 218.

Ren, L., Linsley, B.K., Wellington, G.M., Schrag, D.P., and Hoegh-Guldberg, O., 2003. Deconvolving the $\delta^{18}O$ and Sr/Ca at Rarotonga in the southwestern subtropical Pacific for the period 1726 to 1997. Geochimica et Cosmochimica Acta 67, 1609–1621.

Rensing, L., Meyer-Grahle, U., and Ruoff, P., 2001. Biological timing and the clock metaphor: oscillatory and hourglass mechanisms. Chronobiology International 18, 329–369.

Rhoads, D.C., and Pannella, G., 1970. The use of molluscan shell growth patterns in ecology and paleoecology. Lethaia 3, 143–161.

Richardson, C.A., 1988a. Exogenous and endogenous rhythms of band formation in the shell of the clam *Tapes philippinarum* (Adams et Reeve, 1850). Journal of Experimental Marine Biology and Ecology 122, 105–126.

Richardson, C.A., 1988b. Tidally produced growth bands in the subtidal bivalve *Spisula subtruncata* (da Costa). Journal of Molluscan Studies 54, 71–82.

Richardson, C.A., 2001. Molluscs as archives of environmental change. Oceanography and Marine Biology: An Annual Review 39, 103–164.

Ríos, A. F., Velo, A., Pardo, P. C., Hoppema, M., and Pérez, F. F., 2012. An update of anthropogenic CO_2 storage rates in the western South Atlantic basin and the role of Antarctic Bottom Water. Journal of Marine Systems 94, 197–203.

Ríos, E., 1994. Seashells of Brazil. 2nd edition. Editora da Fundação Universidade do Rio Grande, Rio Grande, USA, pp. 368.

Roberts, D., Rittschof, D., Gerhart, D.J., Schmidt, A.R., and Hill, L.G., 1989. Vertical migration of the clam *Mercenaria mercenaria* (L.) (Mollusca, Bivalvia) – environmental correlates and ecological significance. Journal of Experimental Marine Biology and Ecology 126, 271–280.

Rodland, D.L., Schöne, B.R., Baier, S., Zhang, Z., Dreyer, W., and Page, N.A., 2009. Changes in gape frequency and thermal tolerance in the freshwater bivalves *Anodonta cygnea* and *Margaritifera falcata*. Journal of Molluscan Studies 75, 51–57.

Rollion-Bard, C., Chaussidon, M., and France-Lanord, C., 2003. pH control on oxygen isotopic composition of symbiotic corals. Earth and Planetary Science Letters 215, 275–288.

Romanek, C.S., Grossman, E.L., and Morse, J.W., 1992. Carbon isotopic fractionation in synthetic aragonite and calcite: effects of temperature and precipitation rate. Geochimica et Cosmochimica Acta 56, 419–430.

Romanek, C.S., Jones, D.S., Williams, D.F., Krantz, D.E., and Radtke, R., 1987. Stable isotopic investigation of physiological and environmental changes recorded in shell carbonate from the giant clam *Tridacna maxima* Marine Biology 94, 385–393.

Rosenberg, G.D., and Hughes, W.W., 1991. A metabolic model for the detennination of shell composition in the bivalve mollusc, *Mytilus edulis*. Lethaia 24, 83–96.

Rosenheim, B.E., Swart, P.K., Thorrold, S.R., Eisenhauer, A., and Willenz, P., 2005. Salinity change in the subtropical Atlantic: Secular increase and teleconnections to the North Atlantic Oscillation. Geophysical Research Letters 32, L02603, doi:10.1029/2004GL021499.

Rosenheim, B.E., Swart, P.K., Thorrold, S.R., Willenz, P., Berry, L., and Latkoczy, C., 2004. High-resolution Sr/Ca records in sclerosponges calibrated to temperature in situ. Geology 32, 145–148.

Rozanski, K., Araguas-Araguas, L., and Gonfiantini, R., 1993. Isotopic patterns in modern global precipitation. Geophysical Monograph Series 78, 1–36.

Rundgren, M., Björck, S., and Hammarlund, D., 2005. Last interglacial atmospheric CO_2 changes from stomatal index data and their relation to climate variations. Global and Planetary Change 49, 47–62.

Rutherford, S., Mann, M.E., Wahl, E., and Ammann, C., 2008. Reply to comment by Jason E. Smerdon et al. on ‘‘Robustness of proxy-based climate field reconstruction methods’. Journal of Geophysical Research, 113, D18107 http://dx.doi.org/10.1029/2008JD009964

Sabine, C.L., Feely, R.A., Key, R.M., Bullister, J.L., Millero, F.J., Lee, K., Peng, T.-H., Tilbrook, B., Ono, T., and Wang, C.S., 2002. Distribution of anthropogenic CO_2 in the Pacific Ocean. Global Biogeochem Cycles 16, 1083 http://dx.doi.org/10.1029/2001GB001639

Sato, S., 1997. Shell microgrowth patterns of bivalves reflecting seasonal change of phytoplankton abundance. Paleontological Research 1, 260–266.

Schelske, C.L., and Hodell, D.A., 1991. Recent changes in productivity and climate of Lake Ontario detected by isotopic analysis of sediments. Limnology and Oceanography 36(5), 961–975.

Schelske, C.L., and Hodell, D.A., 1995. Using carbon isotopes of bulk sedimentary organic matter to reconstruct the history of nutrient loading and eutrophication in Lake Erie. Limnology and Oceanography 40(5), 918–929.

Schelske, C.L., Robbins, J.A., Gardner, W.S., Conley, D.J., and Bourbonniere, R.A., 1988. Sediment record of biogeochemical responses to anthropogenic perturbations of nutrient cycles in Lake Ontario. Canadian Journal of Fisheries and Aquatic Sciences 45, 1291–1303.

Schewe, J., and Levermann, A., 2012. A statistically predictive model for future monsoon failure in India. Environmental Research Letters 7044023, doi:10.1088/1748-9326/7/4/044023

Schmidt, G.A., 1999. Forward modeling of carbonate proxy data from planktonic foraminifera using oxygen isotope tracers in a global ocean model. Paleoceanography 14, 482–497.

Schneider, U., Becker, A., Finger, P., Meyer-Christoffer, A., Rudolf, B., and Ziese, M., 2011. GPCC Full Data Reanalysis Version 6.0 at 1.0°: Monthly Land-Surface Precipitation from Rain-Gauges built on GTS-based and Historic Data. DOI: 10.5676/DWD_GPCC/FD_M_V6_100

Schöne, B.R., 2008. The curse of physiology – Challenges and opportunities in the interpretation of geochemical data from mollusk shells. Geo-Marine Letters 28, 269–285.

Schöne, B.R., Goodwin, D.H., Flessa, K.W., Dettman, D.L., and Roopnarine, P.D., 2002. Sclerochronology and growth of the bivalve mollusks Chione (Chionista) fluctifraga and C. (Chionista) cortezi in the northern Gulf of California, Mexico. Veliger 45 (1): 45–54

Schöne, B.R., Oschmann, W., Kröncke, I., Dreyer, W., Janssen, R., Rumohr, H., Houk, S.D., Freyre Castro, A.D., Dunca, E., and Rössler, J., 2003a. North Atlantic Oscillation dynamics recorded in shells of a long-lived bivalve mollusk. Geology 31, 1037–1040.

Schöne BR, Tanabe K, Dettman DL and Sato S, 2003b. Environmental controls on shell growth rates and $\delta^{18}O$ of the shallow-marine bivalve mollusk *Phacosoma japonicum* in Japan. Marine Biology 142, 473–485.

Schöne BR, Flessa KW, Dettman DL and Goodwin DH, 2003c. Upstream dams and downstream clams: Growth rates of bivalve mollusks unveil impact of river management on estuarine ecosystems (Colorado River delta, Mexico). Estuarine, Coastal and Shelf Science 58, 715–726.

Schöne BR, 2003d. A 'clam-ring' master-chronology constructed from a short-lived bivalve mollusc from the northern Gulf of California, USA. The Holocene 13, 39–49.

Schöne, B.R., Dunca, E., Mutvei, H., and Norlund, U., 2004a. A 217-year record of summer air temperature reconstructed from freshwater pearl mussels (*M. margaritifera*, Sweden) Quaternary Science Reviews 24, 1803–1816.

Schöne, B.R., Freyre Castro, A.D., Fiebig, J., Houk, S.D., Oschmann, W., and Kröncke, I., 2004b. Sea surface water temperatures over the period 1884–1983 reconstructed from oxygen isotope ratios of a bivalve mollusk shell (*Arctica islan*dica, southern North Sea) Palaeogeography, Palaeoclimatology, Palaeoecology 212, 215–232.

Schöne, B.R., Oschmann, W., Tanabe, K., Dettman, D., Fiebig, J., Houk, S.D., and Kanie, Y., 2004c. Holocene seasonal environmental trends at Tokyo Bay, Japan, reconstructed from bivalve mollusk shells – implications for changes in the East Asian monsoon and latitudinal shifts of the Polar Front. Quaternary Science Reviews 23, 1137–1150.

Schöne, B.R., Houk, S.D., Freyre Castro, A.D., Fiebig, J., Kröncke, I., Dreyer, W., and Oschmann, W., 2005a. Daily growth rates in shells of *Arctica islandica*: Assessing sub-seasonal environmental controls on a long-lived bivalve mollusk. Palaios 20, 78–92.

Schöne, B.R., Dunca, E., Fiebig, J., and Pfeiffer, M., 2005b. Mutvei's solution: an ideal agent for resolving microgrowth structures of biogenic carbonates. Palaeogeography, Palaeoclimatology, Palaeoecology 228, 149–166.

Schöne, B.R., Fiebig, J., Pfeiffer, M., Gleß, R., Hickson, J., Johnson, A.L.A., Dreyer, W., and Oschmann, W., 2005c. Climate records from a bivalved Methuselah (*Arctica islandica*, Mollusca; Iceland). Palaeogeography, Palaeoclimatology, Palaeoecology 228, 130–148.

Schöne B.R., Page N.A., Rodland D.L., Fiebig J., Baier S.M., Helama, S.O. and Oschmann, W., 2007. ENSO-coupled precipitation records (1959-2004) based on shells of freshwater bivalve mollusks (*Margaritifera falcata*) from British Columbia. International Journal of Earth Sciences 96(3), 525 –540.

Schöne, B.R., Wanamaker, Jr, A.D., Fiebig, J., Thébault, J., and Kreutz ,K.J, 2011. Annually resolved $\delta^{13}C$ shell chronologies of long-lived bivalve mollusks (*Arctica islandica*) reveal oceanic carbon dynamics in the temperate North Atlantic during recent centuries. Palaeogeography, Palaeoclimatology, Palaeoecology 302, 31–42.

Schöne, B.R., and Gillikin, D.P., 2013. Unraveling environmental histories from skeletal diaries – Advances in sclerochronology. Palaeogeography, Palaeoclimatology, Palaeoecology 373, 1–5.

Schöne, B.R., and Surge, D.M., 2012. Bivalve sclerochronology and geochemistry. In: Selden, P.A., (ed.) Treatise of Invertebrate Paleontology. Treatise Online 46, 1–24, Part N (Mollusca, Bivalvia), Revised, Volume 1, Chapter 14.

Schöne, B.R., Radermacher, P., Zhang, Z., and Jacob, D.E., 2013. Crystal fabrics and element impurities (Sr/Ca, Mg/Ca, and Ba/Ca) in shells of *Arctica islandica* – implications for paleoclimate reconstructions. Palaeogeography, Palaeoclimatology, Palaeoecology 373, 50–59.

Schweingruber, F.H., Briffa, K.R., and Jones, P.D., 1991. Yearly maps of summer temperatures in Western Europe from A.D. 1750 to 1975 and Western North America from 1600 to 1982: Results of a readiodensitometrical study on tree rings. Vegetatio 92, 5–71.

Shea, C.P., Peterson, J.T., Conroy, M.J., and Wisniewski, J.M., 2013. Evaluating the influence of land use, drought and reach isolation on the occurrence of freshwater mussel species in the lower Flint River Basin, Georgia (USA). Freshwater Biology 58, 382–395.

Siegenthaler, U., and Sarmiento, J.L., 1993. Atmospheric carbon dioxide and the ocean. Nature, 365, 119–125.

Skrecky, D., 1996. Miscellaneous round-up. Longevity Report, 10(57). Available at: http://www.quantium.cwc.net/lr57.htm or http://rae.tnir.org/cryonics/lr57.htm

Smith, J.E., Schwarcz, H.P., Risk, M.J., McConnaughey, T., and Keller, N., 2000. Paleotemperatures from deep-sea corals: overcoming 'vital effects'. Palaios 15, 25–32.

Smith, T.M., and Reynolds, R.W., 2003. Extended reconstruction of global sea surface temperatures based on COADS data (1854–1997). Journal of Climate 16, 1495–1510.

Spero, H.J., Bijma J., Lea D.W., and Bemis B.E., 1997. Effect of seawater carbonate concentration on foraminiferal carbon and oxygen isotopes. Nature 390, 497–500.

Spiker, B.C., and Schemel, L.E., 1979. Distribution and stable isotope composition of carbon in San Francisco Bay. In: Conomos, T.L., (ed.) San Francisco Bay: the urbanized estury. Pacific Division American Association for the Advancement of Science, San Francisco, USA, pp. 195–212.

Stagliano, D.M., Stephens, G.M., and Bosworth, W.R., 2007. Aquatic invertebrate species of concern on USFS northern region lands. Report to USDA Forest Service, Northern Region. Montana Natural Heritage Program, Helena, Montana and Idaho Conservation Data Center, Boise, Idaho, pp. 1–95.

Stecher, H.A., Krantz, D.E., Lord, C.J., Luther, G.W., and Bock, K.W., 1996. Profiles of strontium and barium in *Mercenaria mercenaria* and *Spisula solidissima* shells. Geochimica et Cosmochimica Acta 60, 3445–3456.

Steedman, H.F., 1950. Alcian Blue 8GS: A new stain for mucin. Quarterly Journal of Microscopical Science 91, 477–479.

Steig, E.J., Grootes P.M., and Stuiver. M., 1994. Seasonal precipitation timing and ice core records. Science 266, 1885–1886.

Steinke, S., Glatz, C., Mohtadi, M., Groeneveld, J., Li, Q., and Jian, Z., 2011. Past dynamics of the East Asian monsoon: No inverse behavior between the summer and winter monsoon during the Holocene. Global and Planetary Change 78, 170–177.

Stephens, M., Mattey, D., Gilbertson, D.D., and Murray-Wallace, C.V., 2008. Shell-gathering from mangroves and the seasonality of the Southeast Asian Monsoon using high-resolution stable isotopic analysis of the tropical estuarine bivalve (*Geloina erosa*) from the Great Cave of Niah, Sarawak: methods and reconnaissance of molluscs of early Holocene and living times. Journal of Archaeological Science 35, 2686–2697.

Stilwell, J.D., and Zinsmeister, W.J., 1992. Molluscan systematics and biostratigraphy, Lower Tertiary La Meseta Formation, Seymour Island, Antarctic Peninsula. American Geophysical Union, Washington D.C., USA, pp. 1–192.

Sun, D., Gagan, M.K., Cheng, H., Scott-Gagan, H., Dykoski, C.A., Edwards, R. L., and Su, R., 2005. Seasonal and interannual variability of the Mid-Holocene East Asian monsoon in coral $\delta^{18}O$ records from the South China Sea. Earth and Planetary Science Letters 237, 69–84.

Surge, D., Lohmann, K.C., Dettman, D.L., 2001. Controls on isotopic chemistry of the American oyster, *Crassostrea virginica*: implications for growth patterns. Palaeogeography, Palaeoclimatology, Palaeoecology 172, 283–296.

Swart, P.K., 1983. Carbon and oxygen isotope fractionation in scleractinian corals: A review. Earth-Science Reviews 19, 51–80.

Swart, P.K., Moore, M., Charles, C., and Böhm, F., 1998. Sclerosponges may hold new keys to marine paleoclimate. EOS Transactions AGU 79, 636–638.

Takesue, R.K., and van Geen, A., 2004. Mg/Ca, Sr/Ca, and stable isotopes in modern and Holocene Protothaca staminea shells from a northern California coastal upwelling region. Geochimica et Cosmochimica Acta 68, 3845–3861.

Tanaka, N., Monaghan, M.C., and Rye, D.M., 1986. Contribution of metabolic carbon to mollusc and barnacle shell carbonate. Nature 320(10), 520–523.

Tans, P., 1981. A compilation of bomb ^{14}C data for use in global carbon model calculation. In Bolin, B., (ed.) Scope. Carbon Cycle Modelling, Volume 16, John Wiley, New York, USA, pp. 131–137.

Taylor, D.W., 1981. Freshwater mollusks of California: a distributional checklist. California Fish and Game 67, 140–163.

Thébault, J., Chauvaud, L., L'Helguen, S., Clavier, J., Barats, A., Jacquet, S., Pécheyran, C. and Amouroux, D., 2009. Barium and molybdenum records in bivalve shells: Geochemical proxies for phytoplankton dynamics in coastal environments? Limnology and Oceanography 54(3), 1002–1014.

Thomas, S., and Nasser, M., 2009. Growth and population dynamics of short-neck clam *Paphia malabarica* from Dharmadom estuary, North Kerala, southwest coast of India. Journal of the Marine Biological Association of India 51, 87–92.

Thompson, L.G., Davis, M.E., Mosley-Thompson, E., Sowers, T.A., Henderson, K.A., Zagorodnov, V.S., Lin, P., Mikhalenko, V.N., Campen, R.K., Bolzan, J.F., Cole-Dai, J., and Francou, B., 1998. A 25,000-year tropical climate history from Bolivian ice cores. Science 282, 1858–1864.

Thorarinsdóttir, G.G., 2000. Annual gametogenic cycle in ocean quahog, *Arctica islandica*, from northwestern Iceland. Journal of the Marine Biological Association of the United Kingdom 80, 661–666.

Trevisiol, A., Bergamasco, A., Montagna, P., Sprovieri, M., and Taviani, M., 2012. Antarctic seawater temperature evaluation based on stable isotope measurements on *Adamussium colbecki* shells: kinetic effects vs. isotopic equilibrium. Journal of Marine Systems. http://dx.doi.org/10.1016/j.jmarsys.2012.10.012

Trutschler, K., and Samtleben, C., 1988. Shell growth of *Astarte elliptica* (Bivalvia) from Kiel Bay (Western Baltic Sea). Marine Ecology Progress Series 42, 155–162.

Ullmann, C.V., Wiechert, U., and Korte, C., 2010. Oxygen isotope fluctuations in a modern North Sea oyster (*Crassostrea gigas*) compared with annual variations in seawater temperature: Implications for palaeoclimate studies. Chemical Geology 277, 160–166.

Urey, H.C., 1948. Oxygen isotopes in nature and in the laboratory. Science 108, 489–496.

Urey, H.C., Lowenstam, H.A., Epstein, S., and McKinney, C.R., 1951. Measurement of paleotemperatures and temperatures of the Upper Cretaceous of England, Denmark, and the southeastern United States. Bulletin of the Geolocial Society of America 62, 399–416.

Usdowski, E., and Hoefs, J., 1993. Oxygen isotope exchange between carbonic acid, bicarbonate, and water: A re-examination of the data of McCrea (1950) and an expression for the overall partitioning of oxygen isotopes between the carbonate species and water. Geochimica et Cosmochimica Acta 57, 3815–3818.

Usdowski, E., Michaelis, J., Bottcher, M.E., and Hoefs, J., 1991. Factors for the oxygen isotope equilibrium fractionation between aqueous and gaseous CO_2, carbonic acid, bicarbonate, carbonate, and water (19°C). Zeitschrift fur Physikalische Chemie 170, 237–249.

Vannote, R.L., and Minshall, G.W., 1982. Fluvial processes and local lithology controlling abundance, structure, and composition of mussel beds. Proceedings of the National Academy of Sciences 79, 4103-4107.

Vimeux, F., Cuffey, K.M., and Jouzel, J., 2002. New insights into Southern Hemisphere temperature changes from Vostok ice cores using deuterium excess correction. Earth and Planetary Science Letters 203, 829–843.

Vimeux, F., Ginot, P., Schwikowski, M, Vuille, M., Hoffmann, G., Thompson, L.G., and Schotterer, U., 2009. Climate variability during the last 1000 years inferred from Andean ice cores: A review of methodology and recent results. Palaeogeography, Palaeoclimatology, Palaeoecology 281, 229–241.

Von Grafenstein, U., Erlernkeuser, H., and Trimborn, P., 1999. Oxygen and carbon isotopes in modern fresh-water ostracod valves: assessing vital offsets and autecological effects of interest for palaeoclimate studies. Palaeogeography, Palaeoclimatology, Palaeoecology 148, 133–152.

Wan, S., Li, A., Clift, P.D., and Jiang, H., 2006. Development of the East Asian summer monsoon: evidence from the sediment record in the South China Sea since 8.5 Ma. Palaeogeography, Palaeoclimatology, Palaeoecology 241, 139–159.

Wanamaker Jr., A.D., Butler, P.G., Scourse, J.D., Heinemeier, J., Eiríksson, J., Knudsen, K.L., and Richardson, C.A., 2012. Surface changes in the North Atlantic meridional overturning circulation during the last millennium. Nature Communications 3, 899. http://dx.doi.org/10.1038/ncomms1901.

Wanamaker, Jr, A. D., Kreutz K. J., Borns Jr, H. W., Introne D. S., Feindel S., and Barber B. J., 2006. An aquaculture-based method for calibrated bivalve isotope paleothermometry. Geochemistry, Geophysics, Geosystems 7, Q09011, doi:10.1029/2005GC001189.

Wanamaker, Jr, A.D., Kreutz, K.J., Schone, B.R., Maasch, K.A., Pershing, A.J., Borns, H.W., Introne, D.S., and Feindel, S., 2009. A late Holocene paleoproductivity record in the western Gulf of Maine, USA, inferred from growth histories of the long-lived ocean quahog (*Arctica islandica*). International Journal of Earth Sciences (Geologische Rundschau) 98, 19–29.

Wang, L., Sarnthein, M., Erlenkeuser, H., Grimalt, J.O., Grootes, P., Heilig, S., Ivanova, E., Kienast, M., Pelejero, C., and Pflaumann, U., 1999. East Asian monsoon climate during

the late Pleistocene: high-resolution sediment records from the South China Sea. Marine Geology 156, 245–284.

Wang, L.C., Wu, J.T., Lee, T.Q., Lee, P.F., and Chen, S.H., 2011. Climate changes inferred from integrated multi-site pollen data in northern Taiwan. Journal of Asian Earth Sciences 40, 1164–1170.

Wang, T., Surge, D., and Walker, K.J., 2013. Seasonal climate change across the Roman Warm Period/Vandal Minimum transition using isotope sclerochronology in archaeological shells and otoliths, southwest Florida, USA. Quaternary International, 308–309, 230–241.

Watabe, N., and Kingsley, R.J., 1989. Extra-, inter-, and intracellular mineralization in invertebrates and algae. In: Crick, R.E., (ed.) Origin, Evolution, and Modern Aspects of Biomineralization in Plants and Animals. Plenum Press, New York, USA, pp. 209–223.

Watters, G.T., 1992. Unionids, fishes, and the species area curve. Journal of Biogeography 19, 481–490.

Webb, K., Craft, C., and Elswick, E., 2008. The evaluation of the freshwater western pearl mussel, *Margaritifera falcata* (Gould, 1850), as a bioindicator through the analysis of metal partitioning and bioaccumulation. Northwest Science 82(3), 163–173.

Wefer, G., and Berger, W.H., 1991. Isotope paleontology: growth and composition of extant calcareous species. Marine Geology 100, 207–248.

Weidman, C.R., Jones, G.A., and Lohmann K.C., 1994. The long-lived mollusk *A. islandica*: a new paleoceanographic tool for the reconstruction of bottom water temperatures for the continental shelves of the northern North Atlantic Ocean. Journal of Geophysical Research: Oceans 99, 18305–18314.

Welsh, K., Elliot, M., Tudhope, A., Ayling, B., and Chappell, J., 2011. Giant bivalves (*Tridacna gigas*) as recorders of ENSO variability. Earth and Planetary Science Letters 307, 266–270.

Wernick, B. 1996. Land use and water quality dynamics on the urban-rural fringe: A GIS evaluation of the Salmon River watershed, Langley, B.C. Mater Thesis, Institute for Resources and Environment, University of British Columbia, pp. 217.

Weymouth, F.W., 1922. The life-history and growth of the pismo clam (*Tivela stultorum* Mawe). UC San Diego: Scripps Institution of Oceanography Library. Fish Bulletin 7, 129. http://www.escholarship.org/uc/item/4p6617pp

Wheeler, A.P., 1992. Mechanisms of molluscan shell formation. In: Bonucci, E., (ed.) Calcification in Biological Systems. CRC Press, Boca Raton, Florida, USA, pp. 77–83.

Wilbur, K.M., and Saleuddin, A.S.M., 1983. Shell formation. In: Saleuddin, A.S.M., and Wilbur, K.M., (eds.) The Mollusca. Academic Press, Salt Lake City, USA, pp. 235–287.

Williams, D.F., Sommer, M.A. and Bender, M.L., 1977. Carbon isotopic compositions of recent planktonic foraminifera of the Indian Ocean. Earth Planet. Science Letters 36, 391–403.

Winckworth, R., 1931. On the growth of *Paphia undulata* (Veneridae). Proceedings of the Malacological Society of London 19, 171–174.

Witbaard, R., Duineveld, G.C.A., and de Wilde, P.A.W.J., 1999. Geographic differences in growth rates of *Arctica islandica* (Mollsuca: Bivalvia) from the North Sea and adjacent waters. Journal of the Marine Biological Association of the UK 79, 907–915.

Wurster, C.M., and Patterson, W.P., 2001. Late Holocene climate change for the eastern interior United States: evidence from high-resolution $\delta^{18}O$ values of sagittal otoliths Palaeogeography, Palaeoclimatology, Palaeoecology 170, 81–100.

Yamamoto, N., Kitamura, A., Irino, T., Kase, T., and Ohashi, S., 2010. Climatic and hydrologic variability in the East China Sea during the last 7000 years based on oxygen isotopic records of the submarine caverniculous micro-bivalve *Carditella iejimensis*. Global and Planetary Change 72 (3), 131–140.

Yan, H., Shao, D., Wang, Y., and Sun, L., 2013. Sr/Ca profile of long-lived *Tridacna gigas* bivalves from South China Sea: A new high-resolution SST proxy. Geochimica et Cosmochimica Acta 112, 52–65.

Yan, L., Schöne, B.R., and Arkhipkin, A., 2012. *Eurhomalea exalbida* (Bivalvia): a reliable recorder of climate in southern South America? Palaeogeography, Palaeoclimatology, Palaeoecology 350–352, 91–100.

Yu, K., Zhao, J., Wei, G., Cheng, X., and Wang, P., 2005. Mid-late Holocene monsoon climate retrieved from seasonal Sr/Ca and $\delta^{18}O$ records of *Porites lutea* corals at Leizhou Peninsula, northern coast of South China Sea. Global and Planetary Change 47, 301–316.

Zeebe, R., 1999. An explanation of the effect of seawater carbonate concentration on foraminiferal oxygen isotopes. Geochimica et Cosmochimica Acta 63, 2001–2007.

Zeebe, R.E., and Wolf-Gladrow, D., 2001. CO_2 in Seawater: Equilibrium, Kinetics, Isotopes. Elsevier Oceanography Series 65, pp. 1–346.

Zhao, Z., Li, F., and Ke, C., 1991. On the sex gonad development and reproductive cycle of clam *Paphia undulata*. Journal of Fisheries of China 15, 1–8.

Zhang. J., Quay, P.D., and Wilbur, D.O., 1995. Carbon-isotope fractionation during gas-water exchange and dissolution of CO_2. Geochimica et Cosmochimica Acta 59, 107-114.

Zwarts, L., 1986. Burying depth of the benthic bivalve *Scrobicularia plana* (da Costa) in relation to siphon-cropping. Journal of Experimental Marine Biology and Ecology 101, 25–39.

APPENDIX 1: CURRICULUM VITAE

Msc. Lina Yan

Born on 04th June 1984 in Heilongjiang, China

Voice: +49 (0) 6131 39 23798

Mobile: +49 (0) 015163370060

Email: yanl@uni-mainz.de

EDUCATION

Johannes Gutenberg University Mainz (JGU) 09/2010 – present

Doctor degree candidate, Major in Paleontology, Institute of Geosciences

China University of Geosciences, Beijing (CUGB) 09/2007 – 07/2009

Master Degree, Major in Mineralogy, Petrology, Metallogeny, School of the Earth Sciences and Resources

Shijiazhuang University of Economics 09/2003 – 07/2007

(Formerly: Hebei College of Geology)

Bachelor Degree, Major in Gemology and Materials TechnologyMetallogeny, School of the Earth Sciences and Resources

PRACTICE EXPERIENCE

As an assistant teacher in China University of Geosciences, course: Crystallography and Mineralogy	2008 – 2009
As a part-time teacher in China University of Geosciences (Great Wall College), courses: Optical Crystallography; Crystallography and Mineralogy; English in geology	2007 – 2009
Production Practice in Station of quality control on Gem in Hebei Province	May 2007
Field Practice on Gemology in Changle of Shandong Province	July 2005
Field Practice on geological knowledge in Qinghuangdao of Heibei Province	June 2004

HONORS AND AWARDS

Specialty scholarship to doctoral candidates	2009 – 2010
Excellent Student Leader	2008 – 2009
Excellent graduate of Hebei Province	2003 – 2007
Excellent Student of Hebei Province	2006 – 2007
The Prize of Academic Scholarship in Each Year	2003 – 2007

LANGUAGES

Chinese (native)

English (fluent)

German (basic)

APPENDIX 2: PUBLICATIONS

Yan, L., Schöne, B.R., and Arkhipkin, A., 2012. *Eurhomalea exalbida* (Bivalvia): a reliable recorder of climate in southern South America? Palaeogeogr Palaeoclimatol Palaeoecol 350-352: 91–100

Yan, L., Li, S., Du, F., Lv, W., Zhang, N., and Chen, X., 2012. Mineralogical and geochemical study of carp otoliths from Baiyangdian Lake and Miyun Water Reservoir in China, African Journal of Biotechnology 11, 6847–6856

Li, S., Du, F., **Yan, L.**, Cao, Y., Luo, J., Gao, Y., Yang, L., and Tong, J., 2011. The genetic mineralogical characteristics of fish otoliths and their environmental typomorphism, African Journal of Biotechnology 10, 4405–4411

Du, F., Li, S., **Yan, L.**, Lv, W., Lu, J., and Sun, W., 2011. Relationship of phosphorus content in carp otoliths with that in ambient water in Xiaoxi Port of the Taihu Lake, East China, African Journal of Biotechnology 10, 11206–11213

Yan, L., Li, S., Luo, J., Du, F., Ma, G., Wang, Y., and Wang, W., 2009. Tentative application of computed tomography to study of carp otoliths and their responses to environment variations, Frontiers of Materials Science in China 3(2), 187–193

Yan, L., Li, S., Luo, J., and Du, F., 2009. Study of the Coupling Relationship between Micro-CT Character of Carp Otolith and the Heavy Metals in Waters, Acta Petrologica Et Mineralogica 28, 599–604 (In Chinese with English abstract)

Yan, L., Li, S., Luo, J., Du, F., Ma, G., Wang, Y., and Wang, W., 2008. Preliminary application of Computed Tomography (CT) to the relationship of carp otoliths and the ambient environment, Frontiers of Geosciences 15, 25–31 (In Chinese with English abstract)

Yan, Y., Li, S., Jia, B., Zhang, N., and **Yan, L.,** 2012. Composition typomorphic characteristics and statistic analysis of pyrite in gold deposits of different genetic types, Frontiers of Geosciences 96(4), 216–228

IN REVIEW:

Yan, L., Schöne, B.R., Li, S., and Yan, Y., 2013. Shells of *Paphia undulata* (Bivalvia) from the South China Sea as potential proxy archives of the East Asian summer monsoon – a sclerochronological calibration study. Submitted to Journal of Oceanagraphy

IN PREPARATION:

Yan, L., and Schöne, B.R., Interpretation of stable carbon isotope ratios of *Eurhomalea exalbida* shells: a proxy for environmental conditions or shell growth rates?

APPENDIX 3: CONFERENCE CONTRIBUTIONS

Poster presentations with published abstracts

Yan, L., Schöne, B.R., Li, S., and Yan, Y., 2013. Calibration on short-lived bivalve shells (*Paphia undulata*) and its implication on East Asian summer monsoon (eds.) Program and Abstracts, 3rd International Sclerochronology Conference, ISC2013, May 18–22, 2013, Bangor, UK.

Yan, L., Schöne, B.R., Li, S., Yan, Y., and Zhang, N., 2012. Reconstructing the East Asian monsoon (EAM) during the mid-late Holocene by using bivalve shells. Geocycles Earth System Research Centre Symposium, Nov15, 2012, Mainz, Germany.

Yan, L., Schöne, B.R., Li, S., Yan, Y., and Zhang, N., 2012. An attempt of applying a short-lived bivalve, *Paphia undulata* to reconstruct the East Asian monsoon during the mid-late Holocene. Paläontologische Gesellschaft, Centenary Meeting, Sep 23–30, 2012, Berlin, Germany.

Oral presentations with published abstracts

Yan, L., Li, S., Luo, J., Du, F., and Lv, W., 2009. Detection of heavy metals of otoliths by use of LA-ICP-MS and the response to the water environment, Bulletin of Mineralogy, Petrology and Geochemistry, 12th Symposium of Mineralogy, Petrology and Geochemistry of China, Guiyang, China 28, 317

Yan, L., Li, S., Luo, J., and Du, F., 2009. Study of calcium carbonate crystal structure of Wild carp otoliths and the relationship with micro-chemistry, Annual Symposium of Geological society of China, Beijing, China.

APPENDIX 4: STABLE ISOTOPE DATA

I. *EURHOMALEA EXALBIDA*

FL-AA-A11R

FL-AA-A11R, continued (a)

# samples	∑Distance from ventral margin (mm)	$\delta^{13}C$ (‰)	$\delta^{18}O$ (‰)	# samples	∑Distance from ventral margin (mm)	$\delta^{13}C$ (‰)	$\delta^{18}O$ (‰)
1	0.06	-0.54	-1.60*	36	1.98	1.32	0.41
2	0.11	-0.31	-1.19*	37	2.04	1.44	0.52
3	0.17	-0.16	-1.14*	38	2.11	-0.16	-1.37*
4	0.22	0.99	0.40	39	2.19	1.27	0.04
5	0.28	-0.35	-1.25*	40	2.27	1.41	0.48
6	0.33	-1.40	-2.53*	41	2.35	1.21	0.62
7	0.39	0.06	-0.72	42	2.43	0.43	-0.42
8	0.44	0.25	-0.40	43	2.50	-0.27	-1.38*
9	0.50	0.62	0.01	44	2.58	0.62	-0.03
10	0.55	-0.48	-1.31*	45	2.66	1.09	0.28
11	0.61	0.04	-0.73	46	2.74	-0.33	-1.58*
12	0.66	1.15	0.44	47	2.82	1.17	0.38
13	0.72	0.68	-0.07	48	2.89	1.32	0.72
14	0.77	0.85	0.09	49	2.97	0.91	-0.18
15	0.83	0.81	-0.04	50	3.05	1.39	0.47
16	0.88	-0.67	-1.69*	51	3.13	0.82	0.23
17	0.94	0.89	0.00	52	3.21	0.65	0.06
18	0.99	0.86	-0.11	53	3.28	0.53	-0.12
19	1.05	0.99	-0.22	54	3.36	0.65	0.10
20	1.10	1.23	-0.01	55	3.44	0.76	-0.21
21	1.16	-2.06	-3.67*	56	3.52	1.14	0.40
22	1.21	0.44	-0.43	57	3.60	1.07	0.24
23	1.27	-1.33	-2.86*	58	3.67	1.19	0.40
24	1.32	1.17	0.16	59	3.75	1.17	0.30
25	1.38	1.09	0.09	60	3.83	1.16	0.49
26	1.43	1.07	-0.08	61	3.91	0.97	-0.05
27	1.49	1.08	0.21	62	3.99	1.23	0.29
28	1.54	1.18	0.30	63	4.06	1.36	0.60
29	1.60	1.12	0.22	64	4.14	1.41	0.41
30	1.65	0.92	0.07	65	4.22	missing	missing
31	1.71	1.22	0.44	66	4.30	0.95	-0.07
32	1.76	1.28	0.44	67	4.38	0.84	-0.12
33	1.82	1.18	0.46	68	4.45	0.66	-0.22
34	1.87	1.11	0.35	69	4.53	1.25	0.45
35	1.93	1.27	0.42	70	4.61	1.38	0.63

FL-AA-A11R, continued (b)

# samples	∑Distance from ventral margin (mm)	$\delta^{13}C$ (‰)	$\delta^{18}O$ (‰)
71	4.69	1.19	0.52
72	4.76	1.12	0.42
73	4.84	0.70	-0.23
74	4.92	1.16	0.39
75	5.00	1.03	0.34
76	5.08	1.00	0.30
77	5.13	0.91	0.34
78	5.19	0.97	0.36
79	5.24	1.05	0.59
80	5.30	0.70	0.31
81	5.35	1.02	0.75
82	5.41	0.93	0.71
83	5.46	0.53	0.17
84	5.52	0.63	0.39
85	5.57	1.05	0.66
86	5.63	1.30	1.05
87	5.68	0.46	-0.04
88	5.74	1.05	0.67
89	5.79	1.36	0.85
90	5.85	1.43	0.89
91	5.90	1.43	1.21
92	5.96	1.37	1.14
93	6.01	1.33	1.00
94	6.07	1.04	0.97
95	6.12	1.29	1.14
96	6.18	1.17	1.26
97	6.23	1.10	1.02
98	6.29	1.07	1.25
99	6.34	1.08	1.30
100	6.40	1.01	1.31
101	6.45	1.21	1.35
102	6.51	1.17	1.30
103	6.56	1.22	1.09
104	6.62	1.26	1.35
105	6.67	1.20	1.34
106	6.73	1.31	1.29
107	6.78	0.80	1.01
108	6.84	1.17	1.21
109	6.89	1.29	1.22
110	6.95	1.09	1.20
111	7.00	1.29	1.49
112	7.06	1.32	1.41

FL-AA-A11R, continued (c)

# samples	∑Distance from ventral margin (mm)	$\delta^{13}C$ (‰)	$\delta^{18}O$ (‰)
113	7.11	1.32	1.48
114	7.17	1.19	1.29
115	7.22	1.51	1.65
116	7.28	1.25	1.59
117	7.33	1.11	1.49
118	7.39	1.07	1.40
119	7.44	1.05	1.48
120	7.50	0.95	1.60
121	7.55	0.84	1.50
122	7.61	0.92	1.57
123	7.66	0.89	1.65
124	7.72	0.88	1.63
125	7.77	0.63	1.66
126	7.83	0.47	1.44
127	7.88	0.55	1.61
128	7.94	0.44	1.75
129	7.99	0.47	1.65
130	8.05	-0.34	1.39
131	8.13	-0.19	0.71
132	8.21	0.22	0.65
133	8.29	0.10	0.24
134	8.37	0.50	0.61
135	8.45	0.80	0.63
136	8.53	0.94	0.55
137	8.61	0.86	0.36
138	8.69	0.89	0.39
139	8.77	0.93	0.51
140	8.85	0.86	0.38
141	8.93	0.72	0.33
142	9.01	0.45	0.22
143	9.09	0.66	0.36
144	9.17	0.67	0.32
145	9.25	0.54	0.21
146	9.33	0.49	0.28
147	9.41	0.53	0.34
148	9.49	0.80	0.49
149	9.57	0.83	0.48
150	9.65	0.89	0.56
151	9.73	0.88	0.63
152	9.81	0.77	0.54
153	9.89	0.80	0.58
154	9.97	0.81	0.52

FL-AA-A11R, continued (d)

# samples	∑Distance from ventral margin (mm)	$\delta^{13}C$ (‰)	$\delta^{18}O$ (‰)
155	10.05	0.97	0.61
156	10.13	0.85	0.69
157	10.21	0.84	0.67
158	10.29	0.75	0.38
159	10.37	1.03	0.76
160	10.45	0.78	0.57
161	10.53	1.03	0.47
162	10.61	1.21	0.72
163	10.69	1.06	0.55
164	10.77	0.92	0.28
165	10.85	1.00	0.36
166	10.93	0.89	0.09
167	11.01	0.94	0.32
168	11.09	1.07	0.29
169	11.17	1.07	0.45
170	11.25	0.93	0.29
171	11.33	1.01	0.30
172	11.41	0.80	-0.01
173	11.49	1.24	0.53
174	11.57	1.19	0.50
175	11.65	1.18	0.54
176	11.73	1.13	0.34
177	11.81	1.07	0.28
178	11.89	1.06	0.08
179	11.97	1.07	0.18
180	12.05	1.18	0.16
181	12.13	0.88	0.18
182	12.22	0.64	-0.11
183	12.31	1.02	0.35
184	12.40	1.06	0.57
185	12.48	0.97	0.16
186	12.57	0.90	0.34
187	12.66	0.93	0.40
188	12.74	0.79	0.49
189	12.83	1.45	0.67
190	12.92	1.54	0.65
191	13.00	1.85	0.91
192	13.09	1.75	1.02
193	13.18	1.67	0.89
194	13.27	1.54	0.94
195	13.35	1.34	0.85
196	13.44	1.23	0.91

FL-AA-A11R, continued (e)

# samples	∑Distance from ventral margin (mm)	$\delta^{13}C$ (‰)	$\delta^{18}O$ (‰)
197	13.53	0.99	0.64
198	13.61	1.31	0.91
199	13.70	1.28	0.97
200	13.79	1.21	1.04
201	13.87	1.26	1.09
202	13.96	1.16	1.20
203	14.06	1.26	1.11
204	14.16	1.53	1.29
205	14.27	1.73	1.44
206	14.37	1.63	1.27
207	14.47	1.71	1.56
208	14.57	1.43	1.28
209	14.67	1.57	1.33
210	14.78	1.50	1.12
211	14.88	1.36	1.35
212	14.98	1.34	1.32
213	15.08	1.31	1.22
214	15.18	1.29	1.25
215	15.29	1.47	1.42
216	15.39	1.62	1.36
217	15.49	1.61	1.37
218	15.59	1.45	1.44
219	15.69	1.38	1.39
220	15.80	1.11	1.59
221	15.90	0.96	1.60
222	16.00	0.90	1.65
223	16.10	0.67	1.52
224	16.20	0.62	1.39
225	16.31	0.70	1.66
226	16.41	0.67	1.71
227	16.51	0.76	1.53
228	16.61	0.71	1.47
229	16.71	0.70	1.87
230	16.82	0.97	1.89
231	16.92	0.94	1.81
232	17.02	0.90	1.66
233	17.12	0.94	1.70
234	17.22	1.01	1.87
235	17.33	0.98	2.01
236	17.43	1.00	2.03
237	17.53	0.84	2.05
238	17.63	0.49	1.80

FL-AA-A11R, continued (f)

# samples	∑Distance from ventral margin (mm)	$\delta^{13}C$ (‰)	$\delta^{18}O$ (‰)
239	17.73	-0.57	1.40
240	17.84	0.15	1.05
241	17.94	0.70	1.12
242	18.04	1.09	1.11
243	18.14	1.19	0.93
244	18.24	1.25	0.88
245	18.35	1.15	1.00
246	18.45	1.22	0.80
247	18.55	1.20	0.77
248	18.65	1.19	0.83
249	18.75	1.18	0.93
250	18.86	0.29	0.57
251	18.96	0.42	0.67
252	19.51	0.52	0.55
253	20.06	1.13	0.87
254	20.61	1.19	0.77
255	21.16	1.32	0.71
256	21.71	1.49	0.80
257	22.27	1.41	0.79
258	22.82	1.41	0.74
259	23.37	1.34	0.85
260	23.92	1.42	0.47
261	24.47	1.49	0.49
262	25.02	1.76	0.79
263	25.60	1.61	0.75

FL-AA-A11R, continued (g)

# samples	∑Distance from ventral margin (mm)	$\delta^{13}C$ (‰)	$\delta^{18}O$ (‰)
264	26.18	1.64	0.85
265	26.76	1.59	1.15
266	27.34	1.57	1.20
267	27.92	0.85	1.37
268	28.50	0.50	1.63
269	29.08	0.30	1.79
270	29.83	-0.07	1.34
271	30.58	0.73	1.11
272	31.33	0.94	0.99
273	32.08	1.15	0.86
274	32.83	1.02	0.80
275	33.58	0.87	0.80
276	34.33	0.77	0.73
277	35.08	0.89	0.73
278	35.83	0.73	0.49
279	36.58	0.69	0.49
280	37.33	0.82	0.93
281	38.08	1.30	0.89
282	38.65	1.31	1.01
283	39.22	1.11	1.26
284	39.79	1.09	1.54
285	40.36	0.94	1.71
286	40.93	0.22	1.79
287	41.50	-1.01	1.58

FL-AA-A17R

FL-AA-A17R, continued (a)

# samples	∑Distance from ventral margin (mm)	$\delta^{13}C$ (‰)	$\delta^{18}O$ (‰)
1	0.02	-1.71	-0.67
2	0.04	-0.05	0.20
3	0.08	0.42	0.34
4	0.12	0.32	-0.09
5	0.16	0.86	0.39
6	0.20	1.11	0.45
7	0.24	1.08	0.46
8	0.28	0.87	0.44
9	0.32	0.88	0.33

# samples	∑Distance from ventral margin (mm)	$\delta^{13}C$ (‰)	$\delta^{18}O$ (‰)
10	0.36	0.77	0.24
11	0.40	1.10	0.46
12	0.44	0.97	0.35
13	0.48	0.75	0.37
14	0.52	1.04	0.47
15	0.56	1.24	0.64
16	0.60	1.20	0.59
17	0.64	1.16	0.57
18	0.68	1.20	0.51

FL-AA-A17R, continued (b)

# samples	∑Distance from ventral margin (mm)	$\delta^{13}C$ (‰)	$\delta^{18}O$ (‰)
19	0.72	1.24	0.53
20	0.76	1.55	0.47
21	0.80	1.51	0.32
22	0.84	1.46	0.22
23	0.88	-0.18	-1.84*
24	0.92	1.54	0.08
25	0.96	1.70	0.22
26	1.00	1.69	0.34
27	1.04	1.31	0.02
28	1.08	1.91	0.34
29	1.12	1.76	0.23
30	1.16	2.05	0.52
31	1.20	1.86	0.41
32	1.24	1.74	0.55
33	1.28	1.63	0.65
34	1.32	1.82	0.37
35	1.36	1.63	0.54
36	1.40	1.59	0.41
37	1.44	1.55	0.27
38	1.48	0.91	-0.33
39	1.52	1.50	0.31
40	1.56	1.57	0.48
41	1.60	1.54	0.59
42	1.64	1.24	0.20
43	1.68	1.69	0.51
44	1.72	1.82	0.62
45	1.76	1.42	0.12
46	1.80	1.62	0.49
47	1.84	1.94	0.66
48	1.88	1.97	0.63
49	1.92	1.74	0.93
50	1.96	1.80	0.51
51	2.00	1.82	0.61
52	2.04	1.32	0.27
53	2.08	1.63	0.34
54	2.12	1.76	0.68
55	2.16	1.68	0.65
56	2.20	1.83	0.70
57	2.24	1.00	-0.09
58	2.28	1.46	0.48
59	2.32	1.54	0.62
60	2.36	1.77	0.82

FL-AA-A17R, continued (c)

# samples	∑Distance from ventral margin (mm)	$\delta^{13}C$ (‰)	$\delta^{18}O$ (‰)
61	2.49	1.62	0.68
62	2.62	1.75	0.85
63	2.75	1.55	0.74
64	2.88	1.55	0.52
65	3.01	1.58	0.45
66	3.14	1.42	0.54
67	3.27	1.67	0.61
68	3.40	1.47	0.49
69	3.53	1.65	0.58
70	3.66	1.74	0.67
71	3.79	1.80	0.69
72	3.92	1.63	0.48
73	4.05	1.63	0.61
74	5.03	1.64	0.93
75	5.09	1.72	0.95
76	5.13	0.81	0.06
77	5.23	1.28	0.69
78	5.33	1.34	0.78
79	5.43	1.45	0.91
80	5.53	1.35	0.88
81	5.63	1.34	0.79
82	5.73	1.24	1.03
83	5.83	1.56	1.09
84	5.88	1.53	1.69
85	5.93	1.58	1.79
86	5.99	1.28	1.89
87	6.03	1.53	1.41
88	6.23	1.52	1.56
89	6.43	1.52	1.65
90	6.63	1.42	1.69
91	6.83	1.23	1.66
92	7.03	1.34	1.81
93	7.23	1.28	1.55
94	7.43	1.11	1.76
95	7.63	1.16	1.63
96	7.83	1.33	1.78
97	8.03	1.22	1.70
98	8.23	0.87	1.03
99	8.43	1.18	0.96
100	8.63	1.05	0.49
101	8.83	0.94	0.60
102	9.03	1.22	0.71

FL-AA-A17R, continued (d)

# samples	∑Distance from ventral margin (mm)	$\delta^{13}C$ (‰)	$\delta^{18}O$ (‰)
103	9.23	1.45	0.86
104	9.83	1.65	0.92
105	10.43	1.81	0.74
106	11.03	1.79	0.84
107	11.63	1.78	0.84
108	12.23	1.95	0.73
109	12.83	1.77	0.93
110	13.43	1.95	1.08
111	14.03	1.72	1.30
112	14.63	1.57	1.36
113	15.23	1.65	1.48
114	15.83	1.91	1.62
115	16.43	2.01	1.61
116	17.03	1.94	1.52
117	17.63	1.82	1.58
118	18.23	1.55	1.75
119	18.83	missing	missing
120	19.43	1.46	2.22
121	20.00	1.34	1.38
122	20.57	1.63	1.30
123	21.14	1.60	1.29
124	21.71	1.30	1.03
125	22.28	1.64	1.09
126	22.85	1.62	1.04
127	23.42	1.72	1.11
128	23.99	1.85	1.28
129	24.56	1.80	1.08
130	25.13	1.81	1.10
131	25.70	1.71	1.05
132	26.27	1.67	0.99
133	26.84	1.83	1.06

FL-AA-A17R, continued (e)

# samples	∑Distance from ventral margin (mm)	$\delta^{13}C$ (‰)	$\delta^{18}O$ (‰)
134	27.41	2.06	1.05
135	27.98	2.23	0.91
136	28.55	1.97	1.06
137	29.12	1.86	1.25
138	29.69	2.00	1.26
139	30.26	2.16	1.34
140	30.83	1.91	1.44
141	31.40	1.47	1.45
142	31.97	1.39	1.80
143	32.54	1.33	2.08
144	33.11	1.23	2.00
145	33.68	1.29	2.08
146	34.25	1.24	1.96
147	34.82	1.28	1.38
148	35.39	1.38	1.29
149	35.96	1.37	1.13
150	36.53	1.46	0.98
151	37.10	1.65	1.03
152	37.67	1.58	0.98
153	38.24	1.56	0.83
154	38.81	1.32	0.82
155	39.38	1.28	0.74
156	39.95	1.17	0.83
157	40.52	1.20	0.87
158	41.09	1.13	0.85
159	41.66	1.38	0.77
160	42.23	1.09	0.69
161	42.80	1.17	0.63
162	43.37	1.29	0.91
163	43.94	1.53	1.09
164	44.51	1.58	1.02

FL-AA-A18R

FL-AA-A18R, continued (a)

# samples	∑Distance from ventral margin (mm)	$\delta^{13}C$ (‰)	$\delta^{18}O$ (‰)	# samples	∑Distance from ventral margin (mm)	$\delta^{13}C$ (‰)	$\delta^{18}O$ (‰)
1	0.11	-2.05	-0.55	41	4.31	-0.71	1.21
2	0.21	-1.39	-0.15	42	4.41	-1.94	-0.01
3	0.32	-0.64	0.20	43	4.52	0.35	0.39
4	0.42	-1.63	-0.39	44	4.62	0.39	0.29
5	0.53	-1.40	-0.10	45	4.73	0.51	0.54
6	0.63	-0.49	0.21	46	4.83	0.85	0.54
7	0.74	-0.62	-0.09	47	4.94	0.82	0.75
8	0.84	-0.25	-0.20	48	5.60	0.79	0.92
9	0.95	0.27	0.13	49	6.27	0.75	1.05
10	1.05	0.33	0.00	50	6.93	0.89	1.11
11	1.16	0.68	0.32	51	7.60	0.77	1.33
12	1.26	0.79	0.40	52	8.26	0.28	1.13
13	1.37	0.68	0.28	53	8.93	0.04	1.38
14	1.47	0.84	0.32	54	9.59	0.07	0.24
15	1.58	0.76	0.19	55	10.26	0.77	0.26
16	1.68	0.98	0.37	56	10.92	0.36	0.10
17	1.79	0.94	0.39	57	11.59	0.70	0.36
18	1.89	0.82	0.44	58	12.25	0.37	0.37
19	2.00	0.96	0.46	59	12.92	0.10	0.61
20	2.10	0.90	0.46	60	13.58	0.17	0.95
21	2.21	0.72	0.49	61	14.08	0.03	1.23
22	2.31	1.13	0.67	62	14.58	0.12	0.65
23	2.42	1.20	0.83	63	15.08	0.53	0.40
24	2.52	0.83	0.76	64	15.58	0.94	0.83
25	2.63	0.86	0.67	65	16.08	0.95	0.88
26	2.73	0.75	0.63	66	16.58	0.73	0.51
27	2.84	0.82	0.94	67	17.08	0.89	0.89
28	2.94	0.75	0.91	68	17.58	1.30	1.18
29	3.05	0.76	1.25	69	18.08	1.22	1.37
30	3.15	0.98	0.60	70	18.58	0.78	1.20
31	3.26	0.81	0.75	71	19.08	0.71	1.42
32	3.36	0.86	0.97	72	19.58	0.63	1.33
33	3.47	0.79	1.05	73	20.08	-0.69	0.92
34	3.57	0.64	1.00	74	20.58	0.25	0.41
35	3.68	0.72	1.12	75	21.08	0.79	0.80
36	3.78	0.56	0.96	76	21.58	0.82	0.98
37	3.89	0.56	1.28	77	22.08	1.07	1.00
38	3.99	0.44	1.34	78	22.58	0.67	1.04
39	4.10	0.18	1.30	79	23.08	0.90	1.49
40	4.20	0.11	1.13	80	23.58	0.45	1.30

FL-AA-A18R, continued (b)

# samples	∑Distance from ventral margin (mm)	$\delta^{13}C$ (‰)	$\delta^{18}O$ (‰)
81	24.08	-0.08	1.18
82	24.58	-0.23	0.42
83	25.08	0.48	0.47
84	25.58	0.24	0.57
85	26.08	0.34	0.70
86	26.68	0.77	1.18
87	27.28	0.83	1.56
88	27.88	0.58	1.80
89	28.48	0.35	1.66
90	29.08	0.48	1.58
91	29.68	0.89	0.87
92	30.28	0.93	0.89
93	30.88	0.86	1.05
94	31.48	0.84	0.88
95	32.08	1.66	1.51
96	32.68	1.29	1.57
97	33.28	0.78	1.40
98	33.68	0.49	0.30

FL-AA-A18R, continued (c)

# samples	∑Distance from ventral margin (mm)	$\delta^{13}C$ (‰)	$\delta^{18}O$ (‰)
99	34.08	0.69	0.32
100	34.48	0.98	0.51
101	34.88	1.09	0.83
102	35.88	1.00	1.08
103	36.88	0.17	0.88
104	37.88	0.51	0.29
105	38.88	1.04	0.89
106	39.88	1.11	0.76
107	40.38	1.00	0.88
108	40.88	1.24	1.13
109	41.38	1.37	1.03
110	41.88	1.58	1.02
111	42.38	1.39	1.32
112	42.88	1.22	1.13
113	43.38	0.75	1.29
114	43.88	0.18	1.02
115	44.38	-0.86	0.22
116	44.88	1.70	1.62

FL-AA-A23R

FL-AA-A23R, continued (a)

# samples	∑Distance from ventral margin (mm)	$\delta^{13}C$ (‰)	$\delta^{18}O$ (‰)
1	0.00	-0.53	-0.58
2	0.07	-1.01	-0.92
3	0.14	-0.74	-0.64
4	0.21	-0.69	-0.63
5	0.28	-1.18	-0.97
6	0.35	-0.87	-0.79
7	0.41	-1.10	-0.67
8	0.48	-0.12	-0.01
9	0.55	0.22	0.01
10	0.62	-0.03	-0.25
11	0.69	0.01	0.01
12	0.76	0.23	0.19
13	0.83	0.31	0.15
14	0.90	0.05	0.20
15	0.97	0.27	-0.10
16	1.04	0.08	-0.24
17	1.10	-0.19	-0.25
18	1.17	0.06	-0.18
19	1.24	0.07	0.08
20	1.31	0.03	-0.19
21	1.38	-0.05	-0.09
22	1.45	0.30	-0.01
23	1.52	-0.82	-0.74
24	1.59	0.15	-0.01
25	1.66	-0.12	0.21
26	1.73	-0.39	0.15
27	1.79	-0.90	0.25
28	1.86	-0.64	0.79
29	1.93	-0.43	0.77
30	2.00	-0.39	0.99
31	2.49	-2.08	-0.54
32	2.98	-0.09	0.39

FL-AA-A23R, continued (b)

# samples	∑Distance from ventral margin (mm)	$\delta^{13}C$ (‰)	$\delta^{18}O$ (‰)
33	3.47	0.02	0.47
34	3.96	0.39	1.12
35	4.45	0.68	1.28
36	4.94	0.37	1.23
37	5.42	0.30	0.70
38	5.91	0.55	0.48
39	6.40	0.63	0.39
40	6.89	1.05	0.57
41	7.38	0.97	0.52
42	7.87	0.73	0.60
43	8.36	0.85	0.84
44	8.85	0.14	0.91
45	9.34	0.03	0.43
46	9.83	0.11	0.25
47	10.31	0.22	0.17
48	10.80	0.40	0.08
49	11.29	0.73	0.57
50	11.78	0.64	0.66
51	12.27	0.75	0.82
52	12.76	1.18	0.91
53	13.25	1.28	1.21
54	13.74	1.40	1.32
55	14.23	1.34	1.36
56	14.72	1.36	1.39
57	15.20	1.39	1.54
58	15.69	1.29	1.60
59	16.18	1.21	1.52
60	16.67	0.19	0.08
61	17.16	1.00	0.54
62	17.65	1.43	0.52
63	18.14	1.25	0.59
64	18.63	1.16	0.63
65	19.12	1.24	0.96
66	19.61	1.20	1.16
67	20.09	1.20	1.08
68	20.58	0.97	1.28
69	21.07	0.78	1.43
70	21.56	0.45	1.39
71	22.05	-0.53	0.89
72	22.54	0.52	0.47
73	23.03	0.70	0.46

FL-AA-A23R, continued (c)

# samples	∑Distance from ventral margin (mm)	$\delta^{13}C$ (‰)	$\delta^{18}O$ (‰)
74	23.52	0.44	0.57
75	24.01	0.58	0.65
76	24.50	1.20	1.06
77	24.98	1.03	1.08
78	25.47	0.89	1.44
79	25.96	0.56	1.58
80	26.45	0.56	1.48
81	26.94	0.81	0.40
82	27.43	1.12	0.68
83	27.92	1.39	0.71
84	28.41	1.12	0.69
85	28.90	1.06	0.71
86	29.39	1.07	0.71
87	29.87	0.88	0.77
88	30.36	1.12	0.87
89	30.85	1.40	1.23
90	31.34	1.23	1.36
91	31.83	1.22	1.47
92	32.32	0.99	1.41
93	32.81	1.14	0.61
94	33.30	1.36	0.71
95	33.79	1.09	0.91
96	34.28	1.58	1.29
97	34.76	1.43	1.51
98	35.25	1.24	1.52
99	35.74	0.80	1.55
100	36.23	0.59	1.62
101	36.72	0.72	1.85
102	37.21	0.87	0.82
103	37.70	1.35	0.95
104	38.19	1.26	0.92
105	38.68	1.33	0.94
106	39.17	1.47	0.91
107	39.65	1.40	0.87
108	40.14	1.26	0.85
109	40.63	1.21	0.74
110	41.12	1.14	0.93
111	41.61	1.44	1.17
112	42.10	1.42	1.20
113	42.59	1.50	1.35
114	43.08	1.66	1.39

FL-AA-A23R, continued (d)

# samples	∑Distance from ventral margin (mm)	$\delta^{13}C$ (‰)	$\delta^{18}O$ (‰)
115	43.57	1.74	1.50
116	44.06	1.84	1.63
117	44.54	1.40	1.54
118	45.03	1.01	1.71
119	45.52	0.74	1.93
120	46.01	0.78	2.04
121	46.50	0.92	2.15
122	46.99	0.93	1.03
123	47.48	1.30	0.74
124	47.97	1.39	0.76
125	48.46	1.17	0.53
126	48.95	1.31	0.65
127	49.43	1.42	0.72
128	49.92	1.26	0.69

FL-AA-A23R, continued (d)

# samples	∑Distance from ventral margin (mm)	$\delta^{13}C$ (‰)	$\delta^{18}O$ (‰)
129	50.41	1.37	0.59
130	50.90	1.47	0.65
131	51.39	1.58	0.67
132	51.88	1.35	0.45
133	52.37	1.23	0.36
134	52.86	1.31	0.82
135	53.35	1.42	0.54
136	53.84	1.43	1.04
137	54.32	1.29	0.90
138	54.81	0.64	0.82
139	55.30	0.24	1.11
140	55.79	0.80	0.07
141	56.28	0.83	-0.11

*denotes the negative $\delta^{18}O$ outlier.

II. *PAPHIA UNDULATA*

YY-DB-A01R

YY-DB-A01R, continued (a)

# samples	∑Distance from ventral margin (mm)	$\delta^{13}C$ (‰)	$\delta^{18}O$ (‰)
1	0.36	-1.47	-1.78
2	0.72	-1.22	-1.28
3	1.08	-1.49	-1.24
4	1.44	-1.55	-1.16
5	1.80	-1.74	-0.72
6	2.16	-1.90	-0.88
7	2.52	-2.06	-0.90
8	2.88	-2.14	-0.81
9	3.24	-2.18	-0.93
10	3.60	-2.26	-0.94
11	3.96	-2.16	-1.05
12	4.32	-2.08	-1.04
13	4.68	-2.10	-0.89
14	5.08	-2.48	-1.81
15	5.48	-2.36	-2.31
16	5.88	-1.67	-1.93
17	6.28	-1.41	-1.53
18	6.68	-1.61	-1.98

YY-DB-A01R, continued (a)

# samples	∑Distance from ventral margin (mm)	$\delta^{13}C$ (‰)	$\delta^{18}O$ (‰)
19	7.08	-1.59	-2.42
20	7.48	-1.59	-2.50
21	7.88	-1.70	-1.95
22	8.28	-1.88	-1.55
23	8.68	-1.85	-1.61
24	9.08	-1.49	-1.75
25	9.48	-1.75	-2.68
26	9.88	-1.90	-2.77
27	10.28	-1.78	-2.08
28	10.68	-1.43	-1.60
29	11.08	-1.16	-1.45
30	11.48	-0.95	-1.34
31	11.88	-0.85	-1.35
32	12.28	-0.73	-0.97
33	12.28	-0.85	-0.95
34	13.08	-1.03	-0.72
35	13.88	-1.26	-0.74
36	14.68	-0.97	-0.61

YY-DB-A01R, continued (b)

# samples	∑Distance from ventral margin (mm)	$\delta^{13}C$ (‰)	$\delta^{18}O$ (‰)
37	15.48	-0.80	-0.78
38	16.28	-0.82	-0.57
39	17.08	-1.00	-0.52
40	17.88	-1.15	-0.41
41	18.68	-1.16	-0.47

YY-DB-A01R, continued (c)

# samples	∑Distance from ventral margin (mm)	$\delta^{13}C$ (‰)	$\delta^{18}O$ (‰)
42	19.48	-0.78	-0.42
43	20.28	-0.58	-0.29
44	21.08	-0.53	-0.12
45	21.88	-0.63	-0.19

YY-DB-A04R

YY-DB-A01R, continued (a)

# samples	∑Distance from ventral margin (mm)	$\delta^{13}C$ (‰)	$\delta^{18}O$ (‰)
1	0.55	-1.27	-2.23
2	1.10	-1.42	-1.35
3	1.65	-2.05	-0.98
4	2.20	-2.34	-1.20
5	2.75	-2.29	-0.91
6	3.30	-2.13	-1.04
7	3.85	-2.04	-1.02
8	4.40	-1.94	-1.24
9	4.95	-2.37	-1.05
10	5.45	-1.57	-1.83
11	5.95	-1.83	-2.11
12	6.45	-2.17	-2.54
13	6.95	-1.87	-2.58
14	7.45	-1.70	-2.31
15	7.95	-1.78	-1.89
16	8.45	-1.70	-2.37
17	8.95	-1.77	-2.04

# samples	∑Distance from ventral margin (mm)	$\delta^{13}C$ (‰)	$\delta^{18}O$ (‰)
18	9.45	-1.75	-1.52
19	9.95	-1.49	-1.37
20	10.45	-1.78	-2.51
21	10.95	-1.31	-1.59
22	11.45	-1.03	-1.29
23	11.95	-0.91	-0.81
24	12.95	-1.13	-0.72
25	13.95	-1.19	-0.84
26	14.95	-1.22	-0.90
27	15.68	-1.45	-1.10
28	16.41	-1.57	-0.92
29	17.14	-1.63	-0.82
30	17.87	-1.00	-0.71
31	18.60	-0.95	-0.53
32	19.33	-1.35	-0.47
33	20.06	-1.30	-0.19